UNIVERSITEIT VAN PRETORIA
UNIVERSITY OF PRETORIA
YUNIBESITHI YA PRETORIA

The Phytochemistry of Selected *Ancistrocladus* and *Monsonia* Species and their Anti-Pancreatic Cancer and Nrf2 Activator Properties

by

Muyisa Kavatsurwa Séverin

Submitted in partial fulfillment of the requirements for the degree

***Philosophiae Doctor* Chemistry**

Department of Chemistry

In the Faculty of Natural and Agricultural Sciences

University of Pretoria

South Africa

December 2019

Submission Declaration

I, **Muyisa Kavatsurwa Séverin** declare that the thesis, which I hereby submit for the degree *Philosophiae Doctor* in the Department of Chemistry, at the University of Pretoria, is my own work and has not previously been submitted by me for a degree at this or any other tertiary institution.

Signature:  Date: 17 December 2019

Plagiarism Declaration

Full names of student: Muyisa Kavatsurwa Séverin

Student number: 16407378

Title of work: The Phytochemistry of Selected *Ancistrocladus* and *Monsonia* Species and their Anti-Pancreatic Cancer and Nrf2 Activator Properties

Declaration

1. I understand what plagiarism is and I am aware of the University's policy in this regard.

2. I declare that this thesis is my own original work. Where other people's work has been used (either from a printed source, internet or any other source), due acknowledgement was given and reference was made according to departmental requirements.

3. I did not make use of another student's previous work and submit it as my own.

4. I did not allow and will not allow anyone to copy my work with the intention of presenting it as his or her own work.

Signature:  Date: 17 December 2019

Acknowledgements

I would like to acknowledge with gratitude and appreciation my supervisors Prof. VJ Maharaj (University of Pretoria), Prof. G Bringmann (University of Würzburg), and Dr. D Naidoo-Maharaj (University of Pretoria), for their full support, patience, time, ideas, guidance and significant scientific contributions to make the present work a success. I highly appreciated that opportunity you gave me to learn from various aspects of your experience.

I would like to express my gratitude to the “Université Officielle de Bukavu” in general, and Prof. JBB Muhigwa in particular, for all the support and permissions I received during this program.

This work was financially supported by the Deutsche Forschungsgemeinschaft (Project Br 699/14-2; SFB 630 “Agents against Infectious Diseases”) through the Excellence Scholarship Program BEBUC (www. foerderverein-uni-kinshasa.de), the South African Department of Science and Technology (DST), and the National Research Foundation (NRF)/South Africa.

I thank the University of Würzburg for allowing me to undertake the first part of the work in the University’s laboratories, and also for providing me with experimental assistance, especially: Dr. D Feineis (NIQs library), Dr. M Grüne and Mrs. P Altenberger (NMR), Dr. M Büchner and Mrs. J Adelmann (MS), and Mrs. M Michel and Mrs. S Fayez (oxidative degradation).

I would like to express my special gratitude to Dr. Blaise Kimbadi Lombe for, not only the strong joint scientific collaboration and mentorship in isolation and identification of naphthylisoquinoline alkaloids but also for delightful moments spent together in Würzburg. I think Dr. A. Zillenbiller for organizing my trip and stay in Würzburg for laboratory works.

My thoughts of gratitude go to Prof. S. Awale of University of Toyama in Japan and his group for anti-cancer bioassays, and also to Prof. RT Kumar of JSS University in India and his group for Nrf2 activation screening.

I am grateful to Prof. V Mudogo who guided me in how to identify *Ancistrocladus* species in the forest. To Prof. KI Ndjoko, I present my gratitude for her scientific advice during the course of this work. Special thanks to Prof. VM Mbuyi of the University of Kisangani, who initiated me to the organic chemistry.

I thank INERA (Institut National pour les Études et Recherches Agronomiques) for the assistance during the collection of *Ancistrocladus* plant material and CSIR (The Council for Scientific and Industrial Research) for providing the *Monsonia* plants material.

I thank all the members of the Bioprospecting group (A. Thakur, B. Tembeni, B. Mzondo, N.K Khorommbi, L. Kruger, C. Ezeofor, F. Katele, S. Mianda) in the Department of Chemistry at the University of Pretoria for the time we spent together, many fruitful discussions, and unforgettable moments. Special thanks to Dr. S Mamoalosi for her helping with NMR and for providing me with the necessary training on the use of the equipment. I thank M Wooding for analysis of the samples on the UPLC-QTOF-MS. I thank Dr. M Phanankosi and Dr. S Tinotenda for assistance.

Grateful thoughts go to my beloved spouse Ivette L Kyakimwa and my children Ashley M Kavatsurwa, Alvin N Kavatsurwa and Axel N Kavatsurwa for the love, encouragement, and strong moral support; the same thoughts go to my father Amédée K Kavatsurwa and my mother Emmanuelle K Masumbuko and all my brothers and sisters. Very special thanks to the families Wolf, Vakaniaki, Wimba, Kasigwa, Mayaya, Murandia, Biringanine, and Ndombi for their support.

To crown all, I say thanks to the almighty God for life, health, and strength He provided me with to bring this work to completion.

Summary

Fifteen naphthylisoquinoline (NIQ) alkaloids including four new compounds, the 5,8'-coupled ancistroyafungines A-C, and the 5,1'-linked ancistroyafungine D, as well as eleven known NIQs were isolated from the stem bark of an unidentified *Ancistrocladus* (Ancistrocladaceae) liana recently discovered in the North-Central region of the Democratic Republic of the Congo.

Most of the isolated alkaloids were *S*-configured at C-3, and possessed an oxygen function at C-6 in the isoquinoline portion, which is characteristic to the subclass of “Ancistrocladaceae-type” alkaloids. This finding was geo- and chemotaxonomically interesting since, except for one other *Ancistrocladus* species found in the Central Congo Basin, only Southeast Asian and East African Ancistrocladaceae are known to exclusively produce naphthylisoquinolines with these structural features. Moreover, the alkaloid pattern of this Congolese liana clearly differentiates this plant from all other *Ancistrocladus* taxa that have so far been botanically described, which suggests that it might represent a new species or subspecies. The new ancistroyafungines displayed strong preferential cytotoxic activities (with PC_{50} 7.6 to 22.7 µM) towards human PANC-1 pancreatic cancer cells in nutrient-deprived medium, without showing toxicity in normal, nutrient-rich conditions.

Along with the above described naphthylisoquinoline alkaloids, nine other analytes including four flavonoids: quercetin, kaempferol, hyperoside, and isoquercetin, and five lignans: justicidins A and B, 6-methoxyjusticidin A, chinensinaphthol, and retrochinensinaphthol methyl ether were isolated from *Monsonia angustifolia* and *Monsonia glauca* plants collected in South Africa.

The extracts, the fractions, and compounds of *M. angustifolia and M. glauca* plants were screened for the first time for their Nrf2 activity*. M. angustifolia* sequential extracts exhibited superior Nrf2 activation with three active extracts, *n*-hexane, methanol, and aqueous extracts showing 169.0, 236.1, and 130.0% increase relative to the control. The methanol extract of *M. angustifolia* showed

the strongest increase, better than that of sulforaphane (170.0%) used as positive control.

Seven fractions collected from the column chromatography of the methanol extract of *M. angustifolia* exhibited a good Nrf2 activation with percentage increase ranging from 106.0 to 199.0% relative to the control. The isolated flavonoids from these fractions were screened for Nrf2 activity but the tests were inconclusive as the compounds may have decomposed in DMSO during the lengthy storage process, nevertheless, these compounds have been previously reported to be Nrf2 modulators. Based on this, they are in all likelihood responsible of the good activity of the methanol extracts of both *Monsonia* species. This study was the first to report the presence of isolated flavonoids in *M. angustifolia*.

The isolated lignans were inactive against the human PANC-1 pancreatic cancer cell but they displayed strong to moderate activities against the HeLa cervical cancer cell. Justicidin B was the most potent compound of the isolated lignans with the IC_{50} value of 1.2 μM.

The UPLC-MS chromatograms of the two species showed them to be different, as justicidin B was mainly found in *M. glauca* while justicidin A and 6-methoxyjusticidin A were predominant in *M. angustifolia.* To the best of our knowledge, this is the first report on the presence of justicidin B in *Monsonia glauca*, as well as its phytochemical properties and its bioactivities.

Table of Contents

List of Schemes

List of Figures

Chapter 1

Chapter 2

Chapter 3

List of Tables

Chapter 2

Chapter 3

List of Abbreviations

^{13}C NMR	Carbon 13 nuclear magnetic resonance
^{1}H NMR	Proton nuclear magnetic resonance
Abs.	Absorbance
AIDS	Acquired Immunnodeficiency Syndrome
BCA	Bicinchoninic acid
CC	Column chromatography
COSY	Correlation spectroscopy
CSIR	Council for Scientific and Industrial Research
DHMN	Dihydroxy methyl naphthalene
DM	Diabetes Mellitus
DMEM	Dulbecco's modified Eagle's medium
DNA	Deoxyribonucleic acid
DRC	the Democratic Republic of the Congo
e.g.	Example
ECD	Electronic circular dichroism
EDTA	Ethylenediamine tetraacetic acid
ESI	Electron spray ionization
FBS	Fetal bovine serum
FDA	Food and Drug Administration
G6PD	Glucose-6-phosphate dehydrogenase
GC-MSD	Gas chromatography coupled to a Mass Selective Detector
GPS	Global positioning system
Hax	Axial proton
Heq	Equatorial proton
Hepatic a.	Hepatic artery
HIV	Human Immunodeficience Virus
HMBC	Heteronuclear Multiple Quantum Correlation Spectroscopy
HO-1	Heme Oxygenase-1

HPLC	High-performance liquid chromatography
HPLC-MS	High-performance liquid chromatography mass spectrometry
HPLC-UV	High-performance liquid chromatography ultraviolet
HRMS	High-resolution mass spectrometry
HSQC	Heteronuclear Single Quantum Coherence Spectroscopy
IC_{50}	Half maximal inhibitory concentration
IR	Infra red
IVC	Inferior vena cava
IUPAC	International Union of Pure and Applied Chemistry
L. adrenal	Left adrena
L. kidney	Left kidney
LC-MS	Liquid chromatography - mass spectrometry
Maf.	Musculloaponeurotic fibrosarcoma
Me	Methyl
MS	Mass spectrometry
m/z	Mass to charge ratio
NAD(P)H	Nicotinamide adenine dinucleotide phosphate
NDM	Nutrient-deprived medium
NHEK	Normal human epidermal keratinocytes
NIQ	Naphthylisoquinoline
NMR	Nuclear magnetic resonance
NOE	Nuclear Overhauser effect
NOESY	Nuclear Overhauser effect spectrometry
NP	Natural product
NQO1	Quinone Oxydoreductase-1
Nrf2	Nuclear Factor (Erythroid 2-Related) Factor 2
PBS	Phosphate buffered saline
PC_{50}	Half maximal preferential cytotoxicity
PDA	Photodiode array
Portal v.	Portal vena
ppm	Parts per million

QTOF	Quadrupole time-of-flight
R. kidney	Right kidney
ROESY	Rotating-frame Overhauser enhancement spectrometry
ROS	Reactive oxygen species
SA	South Africa
SANBI	South African Biodiversity Institute
SAR	Structure-activity relationship
SF	Sub-fraction
Splenic a.	Splenic artery
TDR	Tropical Diseases Research
TFA	Trifluoroacetic acid
TLC	Thin layer chromatography
t_R	Retention time
UPLC	Ultra-performance liquid chromatography
UPLC-QTOF-MS	Ultra-performance liquid chromatography quadrupole time of flight mass spectrometry
UV	Ultraviolet
WHO	World Health Organization

Supplementary Information

Chapter 1: Introduction

1.1. Overview

1.1.1. Background on Medicinal Plant Uses

Historically, plants have been used since ancient times in traditional communities for the treatment of many diseases [1]. According to the World Health Organization (WHO), traditional medicine can be defined as the total sum of knowledge, skills, and practices based on the theories, beliefs, and experiences indigenous to different cultures that are used to maintain health, as well as to prevent, diagnose, improve, or treat physical and mental illnesses; and 80% of the emerging world's population relies on traditional medicine for therapy [1]. By herbal medicines the WHO infers to herbs, herbal materials, herbal preparations, and finished herbal products that contain parts of plants or other plant materials as active ingredients [1, 2]. It is obvious that the main knowledge of herbal drugs in folklore cultures, developed through trial and error over centuries, along with the most important cure schemes, was carefully transferred orally from one generation to another. Traditional knowledge and experiences will still provide the lead bioactive compounds from the African biodiversity for developing and commercializing many important new remedies since modern allopathic medicine has its roots in this ancient medicine [1-5].

According to a report from the WHO [1, 6], the extensive use of traditional medicine in Africa, composed mainly of medicinal plants, is mostly linked to cultural and economic reasons; reason why the WHO recommends to African States to promote and integrate traditional medical practices in their health system [6]. Of all therapeutic systems, African traditional medicine is probably the oldest. Africa is considered as the cradle of mankind, with a rich biodiversity and cultural complexity evidenced by regional differences in healing practices [2, 6]. Holistic African traditional medicine in its diversity involves both the body and the mind [6]. The traditional healer typically prescribes medicines, particularly medicinal plants, to treat the symptoms after diagnosing and treating the psychological effects of an illness [2, 6, 7].

Two major reasons justify the strong interest of the African healthcare system in traditional medicine: the inadequate access to allopathic medicines and western forms of treatments, whereby the majority of people in Africa cannot afford access to modern medical care, because of the high cost or because of their non-availability [6]. Another fact justifying that strong interest is a lack of effective modern curative medical treatment for some ailments such as HIV/AIDS, which, although global in distribution, disproportionately affect Africa more than other areas in the world [6].

In the major part of Africa, medicinal plants are the most easily accessible health resource available to the local communities [6]. In addition, the patients preferably adhere most often to their use by the fact that, according to most of these people, traditional healers offer information, counselling, and treatment to patients and their families in a personal manner as well as having an understanding of their patients' environment [2, 6, 7].

Medicinal plants are now universally recognised as the basis for a number of critical human health, social, and economic support systems and benefits [8, 9]. There has been a noticeable increase of both international and local initiatives actively focused on the exploration of botanical resources of Southern Africa with the intention to screen indigenous plants for their pharmacologically active compounds [8, 10]. The use and trade of medicinal plants in Africa has been recognised as providing important primary health care benefits, livelihood opportunities and as being culturally significant [9].

Although medicinal plants are still widely used to cure diseases nowadays [11, 12], their exact mechanism of action is, in most cases, not yet understood. Plants typically contain mixtures of different phytochemicals, also known as secondary metabolites, that may act individually, additively, or in synergy to improve health [6]. Traditional healers claim that secondary metabolites (e.g., alkaloids, quinones, flavonoids, terpenoids, steroids, carbohydrates, and others), produced by plants, are capable of working in synergy so that the curative effect of the whole herb is greater than the

summed effects of the individual components and the toxicity of the whole herb is lower than that of isolated active ingredients [13]; what is in discordance with conventional medical practice that recommend avoiding polypharmacy whenever possible. For the conventional practitioners, the efficacy of herbs used to treat illness results from the lead compounds (or active principles) contained in plants in a mixture of other compounds [13]; such compounds must be isolated and purified, and structurally elucidated, which provides the fundamental prerequisites for the subsequent series of validation steps. Hence, there is a pressing need for extensive research on the isolation, purification, structure elucidation and bioactivity evaluation of the active ingredients to fully benefit from the potential of medicinal plants in Africa and promote the regulation in the sector.

1.1.2. Natural-Product Chemistry

The use of natural products as medicines has been documented throughout history in various forms: traditional medicines, remedies, potions, and oils with several bioactive natural-products remaining unidentified [14]. The dominant source of knowledge on natural product uses from medicinal plants is a result of human experiments by trial and error for many centuries searching for available foods for the treatment of diseases [14-16]. The classical natural-product chemistry methodologies enabled the discovery of a wide range of bioactive secondary metabolites from terrestrial and marine sources, and many of these natural-products have been developed as current drug candidates [14].

The most famous and well known example to date is the synthesis of the anti-inflammatory agent, acetylsalicyclic acid (**1**) (aspirin®) (Figure 1.1) derived from the natural-product, salicin (**2**) (Figure 1.1) isolated from the bark of the willow tree *Salix alba* L. [17]. Morphine (**3**) (Figure 1.1), one of several alkaloids isolated from *Papaver somniferum* L. (opium poppy), is a commercially important drug, first reported by the German pharmacist F. Sertürner in 1803 [17]. In the 1870s, the crude morphine from the plant *P. somniferum* was boiled in acetic anhydride to yield diacetylmorphine (heroin)

and found to be readily converted to codeine (painkiller and cough remedy) [17]. Historically, the medicinal use of poppy extracts was reported by Sumerians and Ancient Greeks [14, 17]. In the 1700s the active constituent digitoxin (**4**) [17] (Figure 1.1), cardiotonic glycoside isolated from *Digitalis purpurea* L. (foxglove), was found to enhance cardiac conduction, thereby improving the strength of cardiac contractibility. Digitoxin (**4**) and its analogues have long been used to heal congestive heart failure but because of their possible long-term detrimental effects they are being replaced by other medicines in the treatment of “heart deficiency” [14, 17].

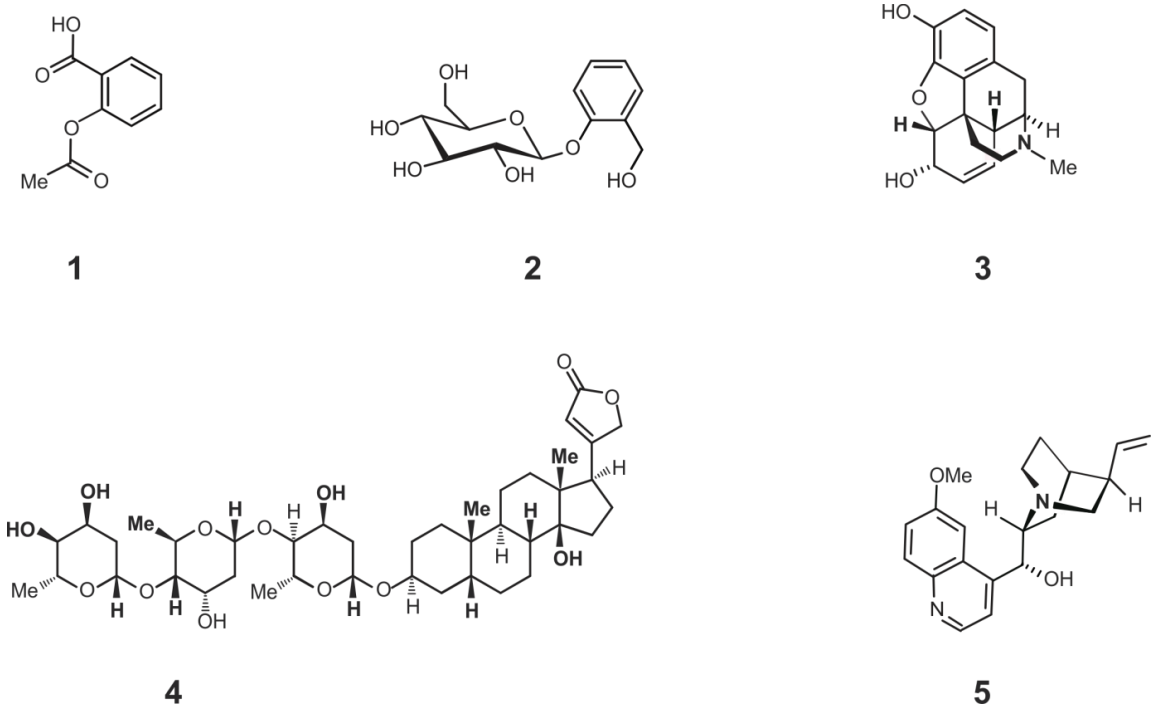

Figure 1.1: *Acetylsalicyclic acid (**1**), salicin (**2**), morphine (**3**), digitoxin (**4**), and quinine (**5**)*

Another great discovery is the anti-malarial drug quinine (**5**) (Figure 1.1) approved by the United States FDA in 2004, isolated for the first time in the 1820s from the bark of *Cinchona succirubra* Pav. ex Klotsch, which had been used for centuries to treat malaria, fever, indigestion, mouth and throat diseases, and cancer [14, 17, 18]. Formal use of the bark to treat malaria was established in the mid 1800’s, when the British began the worldwide cultivation of the plant [17, 18].

Given the fact that natural products have been historically considered as a source of many novel drugs, one can assume that they would still play a fundamental role in the current drug discovery strategies in the pharmaceutical industry [19, 20]. However, during the past 25-30 years it has been the trend for most big pharmaceutical companies to terminate or significantly scale down their natural-products operations [21, 22]. In fact, natural-products research is considerably time-consuming and purification technologies are often prohibitively expensive, *e.g.*, preparative HPLC, needed to eliminate undesirable compounds and to accumulate enough quantities of the targeted bioactive molecules for further biological evaluation [21, 22]. Furthermore, the complexity of some naturally occurring bioactive structures hinders the further lead optimization process [21, 22]. In contrast, combinatorial synthesis can efficiently provide large libraries of related compounds for modern high-throughput screening [23] [21, 24], but only with a small structural originality. Therefore, this rapidly growing area provides an enormous potential to accelerate drug discovery and development [25].

Nevertheless, natural-products derived from all sources or related to natural products have played and will continue to play a key role in the discovery of leads for the development of drugs to treat human diseases [26-32].

As shown in Figure 1.2, the number of naturally inspired agents (779, 49.9%) in the 1562 chemical entities from 1981−2014 is nearly equal to that of synthetic drugs (783, 50.1%) obtained by random screening [32].

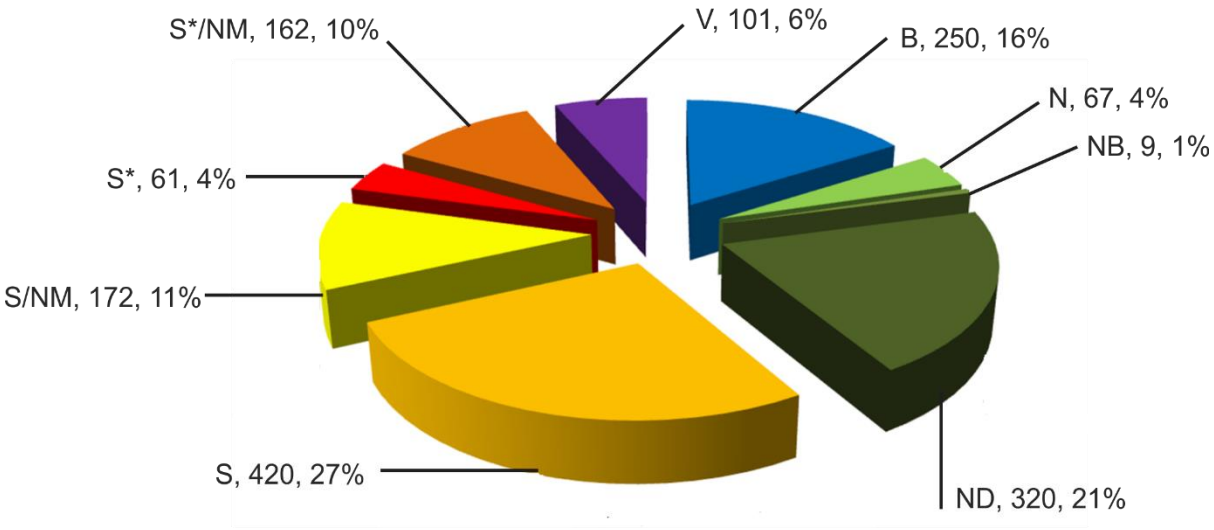

B: Biological macromolecule **N**: Unaltered natural-product **NB**: Botanical drug (defined mixture) **ND**: Natural-product derivative **S**: Synthetic drug **S***: Synthetic drug (pharmacophore from natural-product) **V**: Vaccine **S/NM**: Synthetic drug/Mimic of natural-product **S*/NM**: Synthetic drug (pharmacophore from natural-product)/Mimic of natural-product.

Figure 1.2: *All new approved drugs, 1981-2014, by source (N = 1562) (taken from DJ Newman et al. [32])*

The search for natural products through their isolation and their derivatization by partial or total synthesis still plays a key role in the search for best solutions to the current productivity crisis in drug discovery and development [33].

1.1.3. Pancreatic Cancer

The pancreas is a long, flat gland found in the abdomen behind the stomach (Figure 1.3) [34]. It consists of digestive enzyme-secreting acinar cells, bicarbonate-secreting ductal cells, centro-acinar cells that are the geographical transition between acinar and ductal cells, these enzymes are released into the small intestine to help with digestion; hormone-secreting endocrine islets whose cells produce amongst other hormones like insulin and glucagon, which help control the level of glucose (a type of sugar) in the blood [34-36].

Most often pancreatic cancer occurs from pancreatic intraepithelial neoplasia, the classic pre-neoplastic lesions, but it can also result from larger precursor lesions (intraductal papillary mucinous neoplasms and

mucinous cystic neoplasms); it exhibits abnormal autocrine and paracrine signaling cascades that provoke pancreatic cancer cell production, propagation, invasion, and metastasis [35]. The signaling in pancreatic cancer is complex, with multiple nodes and atypical crosstalk pathways [35].

The risk factors of pancreatic cancer are of three orders:

- Demographic factors: Old age (most reliable and important predictor), sex (more common in males than in females) and ethnic origin (mortality highest in black populations) [34-36].
- Genetic factors and medical conditions: Family history, hereditary pancreatitis, hereditary non-polyposis colorectal cancer, ataxia-telangiectasia, Peutz-Jeghers syndrome, familial breast cancer, familial atypical multiple mole melanoma, chronic pancreatitis, diabetic mellitus, gastrectomy, and deficiency in carcinogen metabolism and DNA repair [34-36].
- Environmental conditions and life style: Cigarette smoking, occupational exposures, low dietary intake of fruits and vegetables, food preparation and cooking methods (grilling or charring confers the highest risk) [34-36].

Pancreatic cancer has been reported as one of the most dreadful cancer types, with more than 95% of patients dying within the first five years after diagnosis [37-40]. According to investigations done by Wang *et al.,* 411,600 deaths have been reported worldwide in 2015 [23]. The strongly increasing incidence is even more alarming, with estimations predicting it to be among the top leading cancer diseases by 2030 [39, 41, 42].

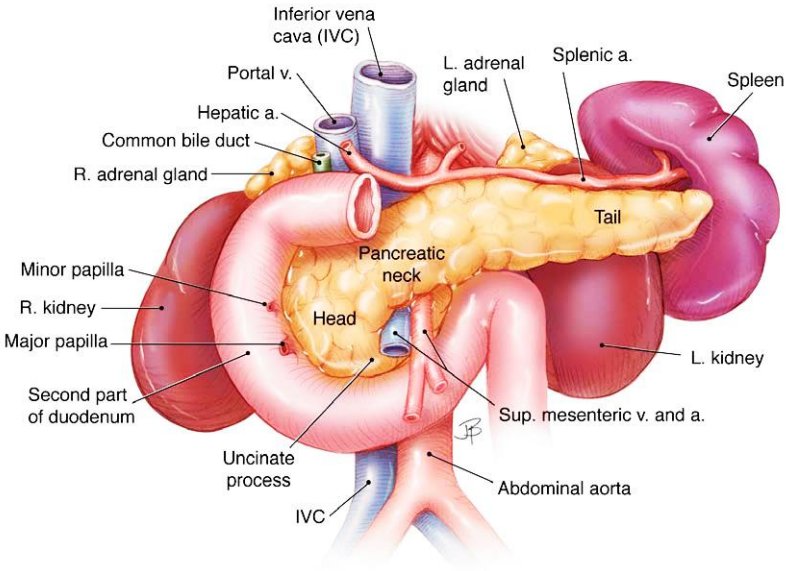

Figure 1.3: *The anatomy of the pancreas with its surrounding organs and structures (taken from D Longnecker [34])*

Surgery remains a potential cure, but it is in many cases not possible to have surgery as the disease may have been detected quite late, at a more advanced stage of an already rapidly progressing metastasis [36, 39, 43]. The rapid development of multidrug-resistance agents of the tumor cells observed in conventional chemotherapeutic treatment of this malignant cancer disorder is among the facts that reduce the efficacy of current therapeutic scheme [36, 44]. Added to that the fact that the pancreatic cancer cells have a remarkable inherent tolerance to extreme nutrition deprivation, enabling them to survive and proliferate aggressively under hypovascular and hypoxic conditions [45], there is a pressing need to develop new treatment strategies against pancreatic cancer.

1.1.4. Natural Products in Pancreatic Cancer Treatment

There are natural products and herbal medicines reported to possess beneficial effects in the fight against pancreatic cancer [46]. They can be used as a single compound (psorospermine, a natural-product occurring in the stembark and roots of the African plant *Psorospermum febrifugum* with inhibition properties against the growth of tumor *in vivo* in the MiaPaCa pancreatic xenograft model), as combination of natural-products with

conventional chemotherapeutic agents and also as combination among natural-products [46].

Methyl protodioscin, one of the main bioactive compounds isolated from the Dioscoreaceae plants, has been demonstrated to exhibit anti-pancreatic cancer activity by inhibiting the proliferation and promoting the apoptosis of pancreatic cancer cells [47].

Irofulven, a cytotoxic agent synthesized from the sesquiterpene mushroom metabolite of the natural-product illudin S, has been reported to enhance antitumor activity when combined with the known chemotherapeutic drug gemcitabine towards the MiaPaCa pancreatic xenograft model [46]. Psorospermin combined to gemcitabine was found to have additive effect in inhibiting the growth of tumor *in vivo* in the MiaPaCa pancreatic xenograft model [46].

The natural polyphenolic compound (-)-gossypol (found in cotton seeds) once combined with genistein (a prominent soy isoflavone) more significantly inhibited the growth of BxPC-3 pancreatic cancer cells, compared with either agent alone [46]. Sulforaphane, an active compound occurring in cruciferous vegetables, is reported to synergistically inhibit self-renewal capacity of pancreatic cancer stem cells with quercetin, a major polyphenol and flavonoid commonly detected in many fruits and vegetables [48].

Besides the above natural-products, naphthylisoquinoline alkaloids such as ancistrolikokines B and C [49] and E_3 [50], ancistroyafungines B and D [51], 6-*O*-methyl-4'-*O*-demethylhamatine [52] are also reported to display remarkable anti-pancreatic cancer activities (more details are given in chapter 2).

1.1.5. The Nuclear Factor (Erythroid 2-Related) Factor 2 (Nrf2)

Oxidative stress plays a promoting key role in several diseases including cancers, cardiovascular diseases, Alzheimer's disease, Parkinson's disease, Huntington's disease, atherosclerosis, chronic kidney diseases, skin disorder, and diabetes [53-58]. Oxidative stress is caused by a balance break between reactive species and the anti-oxidative stress defence systems in cells. These reactive species include reactive oxygen species (ROS), reactive nitrogen species, or reactive electrophilic species [58].

As reported by Nguyen *et al*. [59], the activation of the Nrf2-antioxidant response element signaling pathway is the major defensive mechanism against oxidative or electrophilic stress in the cell, which controls the expression of genes with protein products involved in the detoxication and elimination of reactive oxidants and electrophilic agents through conjugative reactions and by enhancing cellular antioxidant capacity. However, despite intensive research on Nrf2 activation, the regulatory mechanisms involved in mediating Nrf2 activation at the molecular level is still not fully understood [59]. It has been proven that Nrf2 activity is controlled, in part, by the cytosolic protein Keap1 (Figure 1.4), but the nature of this pathway and the mechanisms by which Keap1 acts to repress Nrf2 activity have not yet been fully described [59].

In its multiple protective roles, the Nrf2 cell defence pathway protects against oxidative stress and disorders including cancer and neurodegeneration [60]. Nrf2 is overexpressed in several types of human cancers, including lung, oesophagus, ovary, head and neck squamous cell carcinoma, gallbladder, and skin cancer [60].

One of the probable ways for preventing cancers is using natural products to induce cytoprotective enzymes including phase II and anti-oxidative enzymes that detoxify and eliminate harmful reactive intermediates formed from carcinogens [58]. Various natural compounds are reported to exert

chemopreventive activities against a wide range of cancer types by targeting the Nrf2 signaling pathway [61].

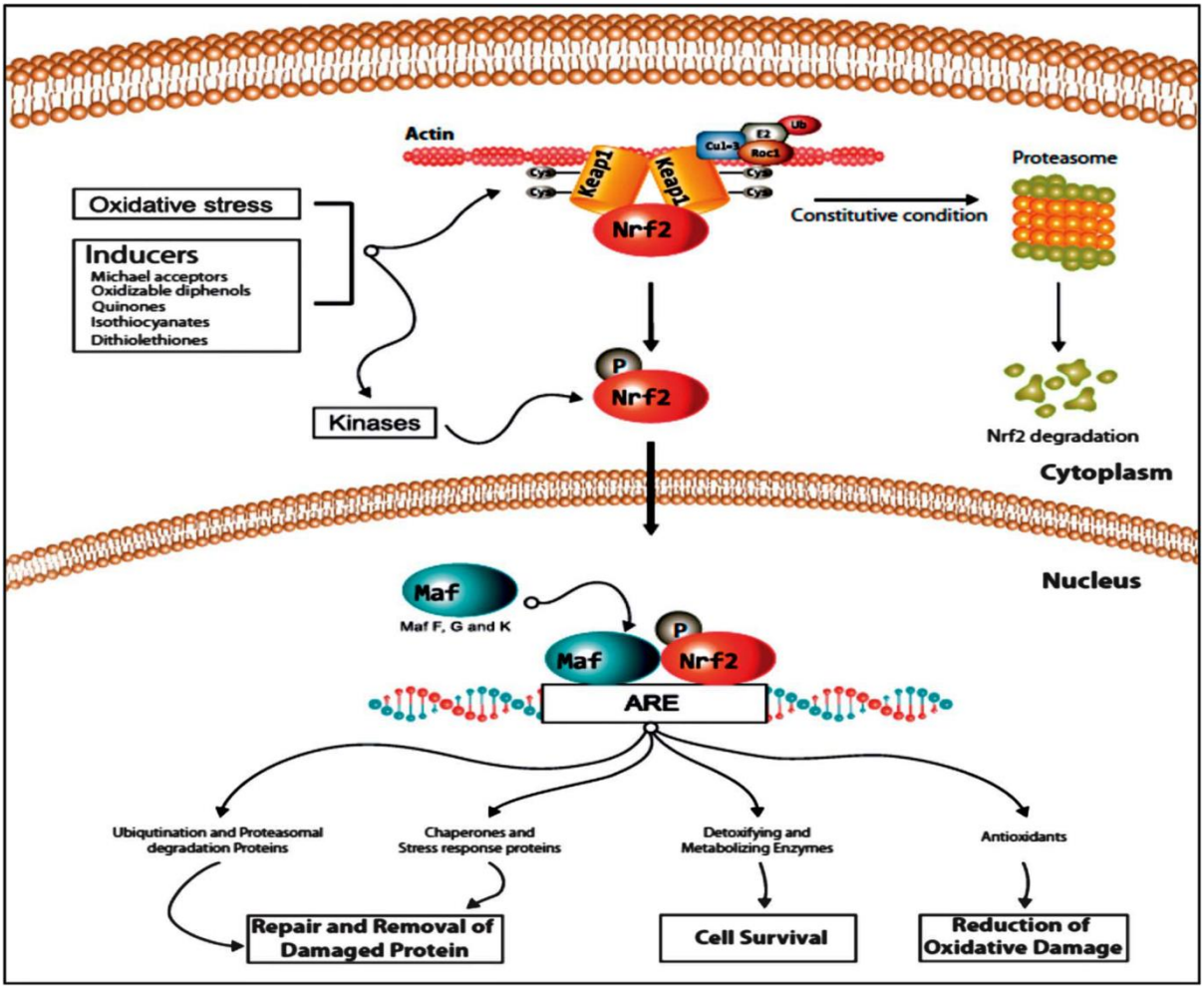

Figure 1.4: *Schematic illustration of the regulation of the Nrf2 pathway under constitutive and under stress conditions (taken from H Kumar et al. [58])*

However the risk is the possibility for tumor cells to exploit the cytoprotective properties of the Nrf2 pathway to promote their survival [58]. Mutational activation of Nrf2 might cause malignancy and increase chemoresistance [58]. Chemoresistance is a major problem during the successful treatment of many cancers [58, 62-81]. In this case, suppression of Nrf2 activity inhibits tumor growth and enhances the efficacy of cancer chemotherapeutic agents. Thus, Nrf2/ARE is somehow a double-edged sword in cancer biology with regards to the benefits and risks to cells [58, 62-80]. Activating

Nrf2 is important for cancer chemoprevention in normal and premalignant tissues; however, Nrf2 activity provides a growth advantage by increasing the cancer chemoresistance and enhancing the tumor cell growth in fully malignant cells [58, 62-80]. A controlled inhibition of Nrf2-dependent cytoprotection using Nrf2 inhibitors is important to enhance a patient's response to anticancer drugs. Thus, Nrf2 activity could be targeted for cancer treatment and for chemoprevention [58, 62-80].

In the case of the type 2 diabetes mellitus (DM), which has reached pandemic proportions, there is a pressing need for effective prevention strategies [82]. Its onset is accompanied by cellular distress, Nrf2 is a transcription factor that boosts cytoprotective responses, and many phytochemicals activate Nrf2 signaling [82]. Thus, Nrf2 activation by natural-products could presumably alleviate DM through the amelioration of insulin resistance, β-cell dysfunction, and diabetic complications [82].

The Nrf2 pathway plays an important role in acute and chronic inflammation. Increasing susceptibility to various inflammatory diseases may result from the disruption of this pathway, such as rheumatoid arthritis, asthma, emphysema, gastritis, colitis, and atherosclerosis [83, 84]. Unfortunately, long-term inflammatory signaling can reduce the Nrf2 activity and decrease antioxidant and defence capacity. Indeed, studies have demonstrated that Nrf2 responds to pro-inflammatory stimuli and rescues cells/tissues from inflammatory injury [85, 86]. Conversely, it has been proven that Nrf2-activating agents inhibit inflammation in several experimental models. The Nrf2 is, thus, a critical regulator of the innate immune response [58, 87].

Nrf2 defence is a very important cellular mechanism to control oxidative stress implicated in wound healing. Nrf2 can induce many cytoprotective genes, including nuclear heme oxygenase-1 (HO-1), NAD(P)H quinone oxidoreductase-1 (NQO1), and glucose-6-Phosphate dehydrogenase (G6PD) [88].

The skin, constituted of three main layers: the epidermis, the dermis, and the underlying subcutaneous fat layer (hypodermis) (Figure 1.5A) [89], is the largest organ of the body and plays the function of a protective barrier between outside and inside the body. It is continuously exposed to various exogenous and endogenous stressors (e.g., air pollutants, ionizing and non-ionizing irradiation, toxins, mitochondrial metabolism, enzyme activity, inflammatory process, etc.) producing reactive oxygen species (ROS), and physical damage (e.g., wounds, inflammation) also resulting in reactive oxygen species production [90, 91].

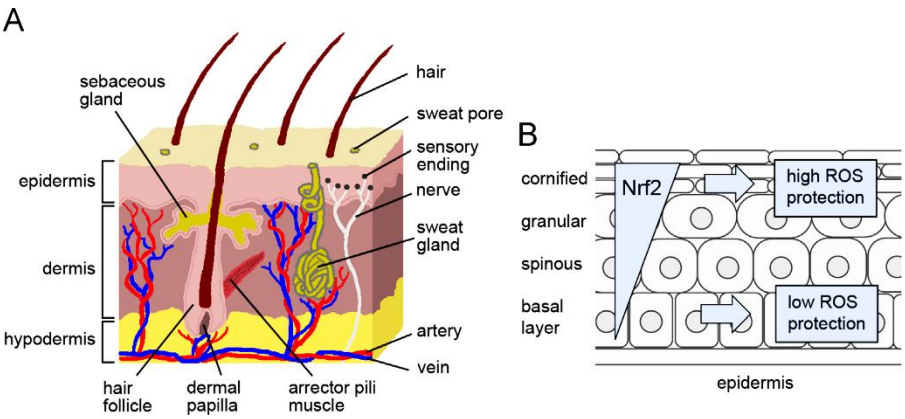

Figure 1.5: *(A) Scheme of the skin and its appendages. (B) Nrf2 expression and activity increase on differentiation of keratinocytes (taken from M Schäfer et al. [89])*

Despite its array of defence mechanisms to protect the body against aggressive reactive oxygen species, increased and continued exposure to reactive oxygen species might result in excessive oxidative stress, breaking then the skin redox balance which is a gentle equilibrium between ROS and their detoxification, leading to many skin disorders including inflammatory diseases, cancer, pigmenting disorders, and some types of cutaneous malignancy [90, 91]. Under homeostatic conditions, the ROS production and detoxification processes are intimately regulated by a scaffold of skin defence mechanisms [92, 93].

However, the regulation capacity of these highly efficient skin defence

mechanisms is limited. A continuous flux and accumulation of ROS is capable of stunning that regulation capacity and causes an imbalance in skin redox [92]. Therefore, an efficient antioxidant defence strategy is of major importance in this tissue. By its capability to regulate a battery of genes involved in the defence against ROS and in compound metabolism, the Nrf2 transcription factor plays a key role in skin homeostasis, repair, and disease [89]. The particular Nrf2 role in keratinocytes has been well described in intensive investigations from various laboratories demonstrating its expression in all skin cell types [94].

More interesting is the detection of a gradient of Nrf2 expression and activity in the murine epidermis, and the fact that differentiated suprabasal cells were found to express significantly higher levels of Nrf2 and its target genes compared to non-differentiated basal cells [92, 94] (Figure 1.5B). This is in accordance with the Nrf2- dependent induction of the NAD(P)H: Quinone Oxidoreductase (NQO1), a flavoenzyme that catalyzes the two-electron reduction of quinones to their hydroquinone forms, on *in vitro* differentiation of normal human epidermal keratinocytes (NHEKs) [89, 95, 96]. In short, the protection of suprabasal keratinocytes is crucial for the maintenance of skin integrity.

Although activated moderately by oxidative stress itself, robust activation of the Nrf2 defence mechanism requires the additional presence of co-factors that facilitate electron exchange [88].

1.1.6. Activation of Nrf2 Signaling by Natural-Products

Several investigations conducted during the past few decades have demonstrated the importance of natural products counteracting oxidative stress throughout modulating the Nrf2/ARE pathway [58]. Natural products have emerged as a potential source of bioactive compounds, which have shown to activate or desactivate Nrf2 signaling pathways [97].

Inducers natural-products are those which increase the expression of cytoprotective genes, their common characteristic is their capability to react with sulfhydryl groups by alkylation, oxidation, or reduction [58]. Numerous natural-products inducers have been reported such as [58]: quercetin found particularly in onions, apples, tea, broccoli, red wine, and grains; dihydroquercetin from *Larix gmelinii*, epicatechin from cocoa and teas; kaempferol present in green tea, broccoli, apple, and berries; genistein from soybean; butein found in fruits, vegetables, nuts, tea, coffee, and red wine; andalusol isolated from *Sideritis* spp.; antroquinonol extracted from *Antrodia camphorate*; curcumine found in *Curcuma longa* and lycopene, a carotenoid pigment mainly found in tomatoes.

As mentioned earlier, activating Nrf2 has therapeutic potential as a cell response to defend cells against oxidative stress [58]. However, some concerns have risen with increasing Nrf2 signaling: continuous activation of the Nrf2/ARE pathway promotes some deleterious effects such as multi-drug resistance and atherosclerosis [58]. Moreover, free-radical production increases with ageing, which is a root cause of neurodegenerative diseases, diabetes, cancer, and cardiovascular diseases; thus, inhibition of the Nrf2/ARE pathway might provide a beneficial approach against multi-drug resistance [58]. Some known natural-products are able to inhibit the Nrf2 pathway, like for example: apigenin from fruits and vegetables; ascorbic acid present in *Citrus* fruits; retinoic acid from dietary *β*-carotene; luteolin found in celery, green pepper, parsley, perilla leaf, and chamomile tea [58].

1.2. Problem Statement and Justification

Human cancer is one of the most deadly diseases in the world, and the existing treatments are not effective enough to provide full protection from this disease. Despite the fact that the enormous complexity of cancer is progressively getting understood with the use of modern technologies, there are few success, stories as far as the treatment of cancer is concerned, and, in spite of occasional successes, the treatment for most cancers is still a challenging reality; pancreatic cancer is even referred to as the “silent” [98]

disease because it does not often show early symptoms and also in the later stages patients with pancreatic cancer show non-specific symptoms. Moreover the symptoms tend to vary and may depend on the location of the cancer.

Based on this, there is a real need for efficient, more affordable drugs with less or no side effects. It has been acknowledged that natural products and their derivatives constitute about 50% of drugs that are used in cancer treatment [99]. Among these natural-products, some naphthylisoquinoline alkaloids isolated from *Ancistrocladus* species had been reported to exhibit good anti-cancer activity [49, 51, 52, 100-103].

Oxidative stress caused by an imbalance in reactive species plays a key role in several diseases including cancers, cardiovascular diseases, Alzheimer's disease, Parkinson's disease, Huntington's disease, amyotrophic lateral sclerosis, atherosclerosis, chronic kidney diseases, and diabetes [58]. As response to environmental stress caused by these reactive species, cells have developed adaptive, dynamic programs to maintain cellular redox homeostasis and reduce oxidative damage through a series of antioxidant molecules and detoxifying enzymes that can provide control over these reactive species either by quickly removing or detoxifying them [58]. The Nuclear Factor (Erythroid 2-Related) Factor 2 pathway plays a crucial role in cellular redox homeostasis and activating this pathway is one of the main defense mechanisms against oxidative or electrophilic stress [58]. Several studies have demonstrated the benefits of natural-products counteracting oxidative stress by modulating the Nrf2/ARE pathway [58]. Dietary sources of natural-products are assumed to be Nrf2/ARE modulators including fruits, vegetables and spices yielding biologically active components such as curcumin, resveratrol, cucurbitacins, isoflavones, saponins, phytosterols, lycopene, and many others [58].

Indigenous edible plants are widely used by Africa communities as foods, beverages, and drugs such as teas, e.g. *Monsonia* tea is a special herbal

tea made from the aerial part of *Monsonia burkeana*, it is used for blood cleansing and anti-inflammation by local communities, other *Monsonia* species are claimed to exhibit wound healing and skin regenerating properties. As mentioned previously, Nrf2 is the major defensive response to the oxidative and electronic stress of the body. There are probably compounds contained in the *Monsonia* plants that may have modulator effects on the Nrf2, and need to be identified to sustain the curative and nutraceutical values of these plants. Studies have been conducted on selected *Monsonia* plants showing their efficacy towards selected diseases but there is no report about the Nfr2 activity of these species. The aim of this part of the work was to expose selected indigenous food of South Africa to this unique assay.

In this project, selected *Ancistrocladus* and *Monsonia* species from the Democratic Republic of the Congo and South Africa respectively were phytochemically and biologically investigated.

1.3. Aims of the Study

The main aims of the study were:

a) To identify and characterize new and known naphthylisoquinoline compounds with antiausterity activities against human PANC-1 cells from a Congolese *Ancistrocladus* species and

b) - To evaluate the potency of selected *Monsonia* species for their Nuclear Factor (Erythroid 2-Related) Factor 2 activation and identify compounds responsible of the activity and

- To isolate and characterize compounds with anti-cancer activity.

1.4. Overall Objectives of the Study

The overall objectives of the study were:

- The identification of the plant species under investigation, their processing and extraction.
- The phytochemical profiling of the investigated plant extracts.

- The isolation, purification and structure elucidation of pure compounds.
- The biological screening of crude extracts, fractions, semi-pure and pure compounds for their anti-cancer activities and Nrf2 regulation.
- The interrogation of geo-chemotaxonomy of the plants under investigation.

1.5. Significance of the Study

Data generated from this study will provide reliable information on the chemical ingredients contained in the plants under investigation, and on their bioactivities and cytotoxicity. Information from that investigation will also constitute a database on which pharmacists can lean on to develop new and more efficient drugs, and formulations. The same database will also be used by scientists for further investigations on the plants investigated in this study.

1.6. Subdivision of the Work

Apart from the General introduction, which is provided in Chapter 1, this work comprises two other chapters, each containing an Introduction, an Experimental Section and Results and Discussion with a Partial Conclusion. A General Conclusion will be presented at the end of the work.

Chapter 2 will deal with the Phytochemical Investigations and Antiausterity Acitivities against Human PANC-1 Pancreatic Cancer Cells of Naphthylisoquinoline Alkaloids from a Congolese *Ancistrocladus* sp.

Chapter 3 will talk about the Phytochemistry of Selected *Monsonia* Species and their Anti-Pancreatic Cancer and Nrf2 Activator Properties.

1.7. References

1. WHO: **Fact sheet N° 134**. In., vol. 137: WHO; 2008.
2. Gurib-Fakim A: **Medicinal Plants: Traditions of Yesterday and Drugs of Tomorrow**. *Molecular Aspects of Medicine* 2006, **27**(1):1-93.
3. Suroowan S, Mahomoodally F: **Complementary and Alternative Medicine Use among Mauritian Women**. *Complementary Therapies in Clinical Practice* 2013, **19**(1):36-43.
4. Chintamunnee V, Mahomoodally F: **Herbal Medicine Commonly Used against non-Communicable Diseases in the Tropical Island of Mauritius**. *Journal of Herbal Medicine* 2012, **2**:113–125.
5. Nunkoo DH, Mahomoodally MF: **Ethnopharmacological Survey of Native Remedies Commonly Used against Infectious Diseases in the Tropical Island of Mauritius**. *Journal of Ethnopharmacology* 2012, **143**(2):548-564.
6. Mahomoodally MF: **Traditional Medicines in Africa: An Appraisal of Ten Potent African Medicinal Plants**. *Evidence-Based Complementary and Alternative Medicine* 2013, **2013**:14.
7. Gurib-Fakim A, Mahomoodally MF: **African Flora as Potential Sources of Medicinal Plants: towards the Chemotherapy of Major Parasitic and Other Infectious Diseases: A Review** *Jordan Journal of Biological Sciences* 2013, **6**: 77–84.
8. Street RA, Prinsloo G: **Commercially Important Medicinal Plants of South Africa: A Review**. *Journal of Chemistry* 2013, **2013**:1-16.
9. Mander ND, Ham C, Mander M, Geldenhuys C, Mitchell D, Crouch N, Wynberg R, Drewes S, McKean S, Feiter U *et al.*: **Commercialising Medicinal Plants: A Southern African Guide**: African Sun Media; 2006.
10. Rybicki PE, Chikwamba R, Koch M, Rhodes IJ, Groenewald J-H: **Plant-Made Therapeutics: An Emerging Platform in South Africa**. *Biotechnology Advances* 2012, **30**(2):449-459.

11. Eisenberg DM, Davis RB, Ettner SL, *et al*.: **Trends in Alternative Medicine Use in the United States, 1990-1997: Results of a Follow-up National Survey**. *Journal of American Medical Association* 1998, **280**(18):1569-1575.

12. Richmond E, Adams D, Dagenais S, Clifford T, Baydala L, King WJ, Vohra S: **Complementary and Alternative Medicine: A Survey of its Use in Children with Chronic Respiratory Illness**. *Canadian Journal of Respiratory Therapy* 2014, **50**(1):27-32.

13. Vickers A, Zollman C: **ABC of Complementary Medicine: Herbal Medicine**. *British Medical Journal* 1999, **319**(7216):1050-1053.

14. Dias DA, Urban S, Roessner U: **A Historical Overview of Natural Products in Drug Discovery**. *Metabolites* 2012, **2**(2):303.

15. Kinghorn AD, Pan L, Fletcher JN, Chai H: **The Relevance of Higher Plants in Lead Compound Discovery Programs**. *Journal of Natural Products* 2011, **74**(6):1539-1555.

16. Hicks S: **Desert Plants and People**, 1st edn. San Antonio, TX, USA: Naylor Co; 1966.

17. Der Marderosian A, Beutler JA: **The Review of Natural Products**, 2nd edn. Seattle, WA, USA: Facts and Comparisons; 2002.

18. Hien TT, Day NPJ, Phu NH, Mai NTH, Chau TTH, Loc PP, Sinh DX, Chuong LV, Vinh H, Waller D *et al.*: **A Controlled Trial of Artemether or Quinine in Vietnamese Adults with Severe *Falciparum* Malaria**. *New England Journal of Medicine* 1996, **335**(2):76-83.

19. Katiyar C, Gupta A, Kanjilal S, Katiyar S: **Drug Discovery from Plant Sources: An Integrated Approach**. *An International Quarterly Journal of Research in Ayurveda* 2012, **33**(1):10-19.

20. Pan S-Y, Zhou S-F, Gao S-H, Yu Z-L, Zhang S-F, Tang M-K, Sun J-N, Ma D-L, Han Y-F, Fong W-F *et al.*: **New Perspectives on How to Discover Drugs from Herbal Medicines: CAM's Outstanding Contribution to Modern Therapeutics**. *Evidence-Based Complementary and Alternative Medicine* 2013, **2013**:627375-627375.

21. Butler MS: **The Role of Natural Product Chemistry in Drug Discovery**. *Journal of Natural Products* 2004, **67**(12):2141-2153.

22. Koehn FE, Carter GT: **The Evolving Role of Natural Products in Drug Discovery**. *Nature Reviews Drug Discovery* 2005, **4**:206.

23. Wang H, Naghavi M, Allen C, Barber RM, Bhutta ZA, Carter A, Casey DC, Charlson FJ, Chen AZ, Coates MM *et al.*: **Global, Regional, and National Life Expectancy, all-Cause Mortality, and Cause-Specific Mortality for 249 Causes of Death, 1980–2015: A Systematic Analysis for the Global Burden of Disease Study 2015**. *The Lancet* 2016, **388**(10053):1459-1544.

24. Balkenhohl F, von dem Bussche-Hünnefeld C, Lansky A, Zechel C: **Combinatorial Synthesis of Small Organic Molecules**. *Angewandte Chemie International Edition in English* 1996, **35**(20):2288-2337.

25. Kraljevic S, Stambrook PJ, Pavelic K: **Accelerating Drug Discovery**. *European Molecular Biology Organization reports* 2004, **5**(9):837-842.

26. Cragg GM, Newman DJ, Snader KM: **Natural Products in Drug Discovery and Development**. *Journal of Natural Products* 1997, **60**(1):52-60.

27. Newman DJ, Cragg GM, Snader KM: **Natural Products as Sources of New Drugs over the Period 1981−2002**. *Journal of Natural Products* 2003, **66**(7):1022-1037.

28. Newman DJ, Cragg GM: **Natural Products as Sources of New Drugs over the 30 years from 1981 to 2010**. *Journal of Natural Products* 2012, **75**(3):311-335.

29. Cordier C, Morton D, Murrison S, Nelson A, O'Leary-Steele C: **Natural Products as an Inspiration in the Diversity-Oriented Synthesis of Bioactive Compound Libraries**. *Natural Product Reports* 2008, **25**(4):719-737.

30. Lee K-H: **Novel Anti-Tumor Agents from Higher Plants**. *Medicinal Research Reviews* 1999, **19**(6):569-596.

31. Newman DJ, Cragg GM: **Natural Products as Sources of New Drugs over the Last 25 Years**. *Journal of Natural Products* 2007, **70**(3):461-477.

32. Newman DJ, Cragg GM: **Natural Products as Sources of New Drugs from 1981 to 2014**. *Journal of Natural Products* 2016, **79**(3):629-661.

33. Atanasov AG, Waltenberger B, Pferschy-Wenzig E-M, Linder T, Wawrosch C, Uhrin P, Temml V, Wang L, Schwaiger S, Heiss EH *et al.*: **Discovery and Resupply of Pharmacologically Active Plant-Derived Natural Products: A Review**. *Biotechnology Advances* 2015, **33**(8):1582-1614.

34. Longnecker D: **Anatomy and Histology of the Pancreas**. *Pancreapedia: Exocrine Pancreas Knowledge Base* 2014:1-26.

35. Kleeff J, Korc M, Apte M, La Vecchia C, Johnson DC, Biankin A, Neale ER, Tempero M, Tuveson AD, Hruban HR *et al.*: **Pancreatic Cancer.** *Nature Reviews Disease Primers* 2016, **2**:16022.

36. Li D, Xie K, Wolff R, Abbruzzese JL: **Pancreatic Cancer**. *The Lancet* 2004, **363**(9414):1049-1057.

37. Arteaga LC, Adamson CP, Engelman AJ, Foti M, Gaynor BR, Hilsenbeck GS, Limburg JP, Lowe WS, Mardis RE, Ramsey S *et al.*: **AACR Cancer Progress Report 2014**. *Clinical Cancer Research* 2014, **20**(19 Supplement):S1-S112.

38. Strong K, Mathers C, Epping-Jordan J, Resnikoff S, Ullrich A: **Preventing Cancer through Tobacco and Infection Control: How Many Lives Can We Save in the Next 10 Years?** *European Journal of Cancer Prevention* 2008, **17**(2):153-161.

39. Surlin V, Bintintan V, Petrariu FD, Dobrin R, Lefter R, Ciobica A, Timofte D: **Prognostic Factors in Resectable Pancreatic Cancer**. *Revista Medico-Chirurgicala a Societatii de Medici si Naturalisti din Iasi* 2014, **118**:924–931.

40. Ilic M, Ilic I: **Epidemiology of Pancreatic Cancer**. *World Journal of Gastroenterol* 2016, **22** 9694–9705.

41. Gordon-Dseagu LV, Devesa SS, Goggins M, Stolzenberg-Solomon R: **Pancreatic Cancer Incidence Trends: Evidence from the Surveillance, Epidemiology and End Results (SEER) Population-Based Data**. *International Journal of Epidemiology* 2018, **47**(2):427-439.

42. Rahib L, Smith DB, Aizenberg R, Rosenzweig BA, Fleshman MJ, Matrisian ML: **Projecting Cancer Incidence and Deaths to 2030: The Unexpected Burden of Thyroid, Liver, and Pancreas Cancers in the United States**. *Cancer Research* 2014, **74**(11):2913-2921.

43. Maitra A, Hruban HR: **Pancreatic Cancer**. *Annual Review of Pathology* 2008, **3**:157-188.

44. Gillet J-P, Gottesman MM: **Mechanisms of Multidrug Resistance in Cancer**. In: *Multi-Drug Resistance in Cancer.* Edited by Zhou J. Totowa, NJ: Humana Press; 2010: 47-76.

45. Izuishi K, Kato K, Ogura T, Kinoshita T, Esumi H: **Remarkable Tolerance of Tumor Cells to Nutrient Deprivation: Possible New Biochemical Target for Cancer Therapy**. *Cancer Research* 2000, **60**(21):6201-6207.

46. Yue Q, Gao G, Zou G, Yu H, Zheng X: **Natural Products as Adjunctive Treatment for Pancreatic Cancer: Recent Trends and Advancements**. *Biomedical Research International* 2017, **2017**:8412508-8412508.

47. Chen L, Cheng C-s, Gao H, Zhan L, Wang F, Qu C, Li Y, Wang P, Chen H, Meng Z *et al.*: **Natural Compound Methyl Protodioscin Suppresses Proliferation and Inhibits Glycolysis in Pancreatic Cancer**. *Evidence-Based Complementary and Alternative Medicine* 2018, **2018**:9.

48. Srivastava RK, Tang S-N, Zhu W, Meeker D, Shankar S: **Sulforaphane Synergizes with Quercetin to Inhibit Self-Renewal Capacity of Pancreatic Cancer Stem Cells**. *Frontiers in Bioscience* 2011, **3**:515-528.

49. Fayez S, Feineis D, Mudogo V, Awale S, Bringmann G: **Ancistrolikokines E–H and Related 5,8′-Coupled**

Naphthylisoquinoline Alkaloids from the Congolese Liana *Ancistrocladus likoko* with Antiausterity Activities against PANC-1 Human Pancreatic Cancer Cells. *RSC Advances* 2017, **7**(85):53740-53751.

50. Awale S, Dibwe DF, Balachandran C, Fayez S, Feineis D, Lombe BK, Bringmann G: **Ancistrolikokine E3, a 5,8′-Coupled Naphthylisoquinoline Alkaloid, Eliminates the Tolerance of Cancer Cells to Nutrition Starvation by Inhibition of the Akt/mTOR/Autophagy Signaling Pathway**. *Journal of Natural Products* 2018, **81**(10):2282-2291.

51. Kavatsurwa SfM, Lombe BK, Feineis D, Dibwe DF, Maharaj V, Awale S, Bringmann G: **Ancistroyafungines A-D, 5,8′- and 5,1′-Coupled Naphthylisoquinoline Alkaloids from a Congolese *Ancistrocladus* Species, with Antiausterity Activities against Human PANC-1 Pancreatic Cancer Cells**. *Fitoterapia* 2018, **130**:6-16.

52. Fayez S, Feineis D, Aké Assi L, Kaiser M, Brun R, Awale S, Bringmann G: **Ancistrobrevines E-J and Related Naphthylisoquinoline Akaloids from the West African Liana *Ancistrocladus abbreviatus* with Inhibitory Activities against *Plasmodium falciparum* and PANC-1 Human Pancreatic Cancer Cells**. *Fitoterapia* 2018, **131**:245-259.

53. Castelao JE, Gago-Dominguez M: **Risk factors for Cardiovascular Disease in Women: Relationship to Lipid Peroxidation and Oxidative Stress**. *Medical Hypotheses* 2008, **71**(1):39-44.

54. Reuter S, Gupta CS, Chaturvedi MM, Aggarwal BB: **Oxidative Stress, Inflammation, and Cancer: How Are They Linked?** *Free Radical Biology and Medicine* 2010, **49**(11):1603-1616.

55. Valko M, Rhodes CJ, Moncol J, Izakovic M, Mazur M: **Free-Radicals, Metals and Antioxidants in Oxidative Stress-Induced Cancer**. *Chemico-Biological Interactions* 2006, **160**(1):1-40.

56. Halliwell B: **Oxidative Stress and Cancer: Have We Moved Forward?** *Biochemical Journal* 2007, **401**(1):1-11.

57. Li H, Horke S, Förstermann U: **Oxidative Stress in Vascular Disease and its Pharmacological Prevention**. *Trends in Pharmacological Sciences* 2013, **34**(6):313-319.

58. Kumar H, Kim I-S, More S, Kim B, Choi D-K: **Natural Product-Derived Pharmacological Modulators of Nrf2/ARE Pathway for Chronic Diseases**. *Natural Product Reports* 2013, **31**:109-139.

59. Nguyen T, Nioi P, Pickett CB: **The Nrf2-Antioxidant Response Element Signaling Pathway and its Activation by Oxidative Stress**. *The Journal of Biological Chemistry* 2009, **284**(20):13291-13295.

60. Senger RD, Li D, Jaminet S-C, Cao S: **Activation of the Nrf2 Cell Defense Pathway by Ancient Foods: Disease Prevention by Important Molecules and Microbes Lost from the Modern Western Diet**. *Public Library of Science One* 2016, **11**(2): 0148042-0148042.

61. Sova M, Saso L: **Design and Development of Nrf2 Modulators for Cancer Chemoprevention and Therapy: A Review**. *Drug Design, Development and Therapy* 2018, **12**:3181-3197.

62. Yang K, Lamprecht S, Liu YH, Shinozaki H, Fan KH, Leung D, Newmark H, Steele V, Kelloff GJ, Lipkin M: **Chemoprevention Studies of the Flavonoids Quercetin and Rutin in Normal and Azoxymethane-Treated Mouse Colon**. *Journal of Carcinogenesis* 2000, **21**:1655-1660.

63. Wang J, Eltoum I-E, Lamartiniere AC: **Genistein Chemoprevention of Prostate Cancer in TRAMP Mice**. *Journal of Carcinogenesis* 2007, **6**:3-3.

64. Wang J, Cotroneo MS, Fritz WA, Lamartiniere CA, Elgavish A, Mentor-Marcel R: **Genistein Chemoprevention: Timing and Mechanisms of Action in Murine Mammary and Prostate**. *The Journal of Nutrition* 2002, **132**(3):552S-558S.

65. Patel R, Maru G: **Polymeric Black Tea Polyphenols Induce Phase II Enzymes *via* Nrf2 in Mouse Liver and Lungs**. *Free Radical Biology and Medicine* 2008, **44**(11):1897-1911.

66. Ikeda H, Nishi S, Sakai M: **Transcription Factor Nrf2/MafK Regulates Rat Placental Glutathione S-Transferase Dene During Hepatocarcinogenesis**. *The Biochemical Journal* 2004, **380**(Pt 2):515-521.

67. Lau A, Villeneuve FN, Sun Z, Wong KP, Zhang DD: **Dual Roles of Nrf2 in Cancer**. *Pharmacological Research* 2008, **58**(5-6):262-270.

68. Wang X-J, Sun Z, Villeneuve FN, Zhang S, Zhao F, Li Y, Chen W, Yi X, Zheng W, Wondrak TG *et al.*: **Nrf2 Enhances Resistance of Cancer Cells to Chemotherapeutic Drugs, the Dark Side of Nrf2**. *Journal of Carcinogenesis* 2008, **29**(6):1235-1243.

69. Selvakumaran M, Pisarcik AD, Bao R, Yeung TA, Hamilton CT: **Enhanced Cisplatin Cytotoxicity by Disturbing the Nucleotide Excision Repair Pathway in Ovarian Cancer Cell Lines**. *Cancer Research* 2003, **63**(6):1311-1316.

70. Fujii R, Mutoh M, Niwa K, Yamada K, Aikou T, Nakagawa M, Kuwano M, Akiyama S: **Active Efflux System for Cisplatin in Cisplatin-Resistant Human KB Cells**. *Japanese Journal of Cancer Research* 1994, **85**(4):426-433.

71. Tew DK: **Glutathione-Associated Enzymes in Anti-Cancer Drug Resistance**. *Cancer Research* 1994, **54**(16):4313-4320.

72. Ren D, Villeneuve FN, Jiang T, Wu T, Lau A, Toppin AH, Zhang DD: **Brusatol Enhances the Efficacy of Chemotherapy by Inhibiting the Nrf2-Mediated Defense Mechanism**. *Proceedings of the National Academy of Sciences of the United States of America* 2011, **108**(4):1433-1438.

73. Wang L, Qu G, Gao Y, Su L, Ye Q, Jiang F, Zhao B, Miao J: **A Small Molecule Targeting Glutathione Activates Nrf2 and Inhibits Cancer Cell Growth through Promoting Keap-1 S-Glutathionylation and Inducing Apoptosis**. *Royal Society of Chemistry Advances* 2018, **8**(2):792-804.

74. Tang X, Wang H, Fan L, Wu X, Xin A, Ren H, Wang XJ: **Luteolin Inhibits Nrf2 Leading to Negative Regulation of the Nrf2/ARE Pathway and Sensitization of Human Lung Carcinoma A549 Cells**

to Therapeutic Drugs. *Free Radical Biology and Medicine* 2011, **50**(11):1599-1609.

75. Bao L-J, Jaramillo CM, Zhang Z-B, Zheng Y-X, Yao M, Zhang DD, Yi X-F: **Nrf2 Induces Cisplatin Resistance Through Activation of Autophagy in Ovarian Carcinoma**. *International Journal of Clinical and Experimental Pathology* 2014, **7**(4):1502-1513.
76. Cho J-M, Manandhar S, Lee H-R, Park H-M, Kwak M-K: **Role of the Nrf2-Antioxidant System in Cytotoxicity Mediated by Anti-Cancer Cisplatin: Implication to Cancer Cell Resistance**. *Cancer Letters* 2008, **260**(1):96-108.
77. Gao L, Mann EG: **Vascular NAD(P)H Oxidase Activation in Diabetes: a Double-Edged Sword in Redox Signaling**. *Cardiovascular Research* 2009, **82**(1):9-20.
78. Hayes DJ, McMahon M: **The Double-Edged Sword of Nrf2: Subversion of Redox Homeostasis During the Evolution of Cancer**. *Molecular Cell* 2006, **21**(6):732-734.
79. Zhang DD: **The Nrf2-Keap1-ARE Signaling Pathway: The Regulation and Dual Function of Nrf2 in Cancer**. *Antioxidants and Redox Signaling* 2010, **13**(11):1623-1626.
80. Sporn BM, Liby TK: **NRF2 and Cancer: the Good, the Bad and the Importance of Context**. *Nature Reviews Cancer* 2012, **12**(8):564-571.
81. Bringmann G, Pokorny F: **The Naphthylisoquinoline Alkaloids**. *in The Alkaloids: Pharmacy and Chemistry, (Editor: G A Cordell), Academic Press, New York,* 1995, **46**:127-271.
82. Matzinger M, Fischhuber K, Heiss HE: **Activation of Nrf2 Signaling by Natural Products: Can It Alleviate Diabetes?** *Biotechnology Advances* 2018, **36**(6):1738-1767.
83. Rojo IA, Innamorato GN, Martín-Moreno MA, De Ceballos LM, Yamamoto M, Cuadrado A: **Nrf2 Regulates Microglial Dynamics and Neuroinflammation in Experimental Parkinson's Disease**. *Glia* 2010, **58**(5):588-598.

84. Kwon S-H, Ma S-X, Hwang J-Y, Ko Y-H, Seo J-Y, Lee B-R, Lee S-Y, Jang C-G: **The Anti-Inflammatory Activity of *Eucommia ulmoides* Oliv. Bark. Involves NF-κB Suppression and Nrf2-Dependent HO-1 Induction in BV-2 Microglial Cells**. *Biomolecules and Therapeutics* 2016, **24**(3):268-282.

85. Biswal S, Thimmulappa KR, Harvey JC: **Experimental Therapeutics of Nrf2 as a Target for Prevention of Bacterial Exacerbations in COPD**. *Proceedings of the American Thoracic Society* 2012, **9**(2):47-51.

86. Dworski R, Han W, Blackwell TS, Hoskins A, Freeman ML: **Vitamin E Prevents NRF2 Suppression by Allergens in Asthmatic Alveolar Macrophages *in vivo***. *Free-Radic Biology and Medicine* 2011, **51**(2):516-521.

87. Lee J-M, Chan K, Kan YW, Johnson AJ: **Targeted Disruption of Nrf2 Causes Regenerative Immune-Mediated Hemolytic Anemia**. *Proceedings of the National Academy of Sciences of the United States of America* 2004, **101**(26):9751-9756.

88. Senger RD, Cao S: **Diabetic Wound Healing and Activation of Nrf2 by Herbal Medicine**. *Journal of Natural Sciences* 2016, **2**(11):e247.

89. Schäfer M, Werner S: **Nrf2-A Regulator of Keratinocyte Redox Signaling**. *Free-Radical Biology and Medicine* 2015, **88**:243-252.

90. Ben-Yehuda Greenwald M, Ben-Sasson S, Bianco-Peled H, Kohen R: **Skin Redox Balance Maintenance: The Need for an Nrf2-Activator Delivery System**. *Cosmetics* 2016, **3**(1):1.

91. Trouba JK, Hamadeh KH, Amin PR, Germolec RD: **Oxidative Stress and Its Role in Skin Disease**. *Antioxidants and Redox Signaling* 2002, **4**(4):665-673.

92. Bickers RD, Athar M: **Oxidative Stress in the Pathogenesis of Skin Disease**. *Journal of Investigative Dermatology* 2006, **126**(12):2565-2575.

93. Wagener ADTGF, Carels EC, Lundvig MSD: **Targeting the Redox Balance in Inflammatory Skin Conditions**. *International Journal of Molecular Sciences* 2013, **14**(5):9126-9167.

94. Wölfle U, Seelinger G, Bauer G, Meinke MC, Lademann J, Schempp CM: **Reactive Molecule Species and Antioxidative Mechanisms in Normal Skin and Skin Aging**. *Skin Pharmacology and Physiology* 2014, **27**(6):316-332.

95. Siegel D, Yan C, Ross D: **NAD(P)H: Quinone Oxidoreductase 1 (NQO1) in the Sensitivity and Resistance to Anti-Tumor Quinones**. *Biochemical Pharmacology* 2012, **83**(8):1033-1040.

96. Vasiliou V, Ross D, Nebert WD: **Update of the NAD(P)H: Quinone Oxidoreductase (NQO) Gene Family**. *Human Genomics* 2006, **2**(5):329-335.

97. Ooi BK, Chan K-G, Goh BH, Yap WH: **The Role of Natural Products in Targeting Cardiovascular Diseases *via* Nrf2 Pathway: Novel Molecular Mechanisms and Therapeutic Approaches**. *Frontiers in Pharmacol* 2018, **9**(1308).

98. Chakraborty S, Rahman T: **The Difficulties in Cancer Treatment**. *eCancer Medical Science* 2012, **6**:16-20.

99. Mangal M, Sagar P, Singh H, Raghava GPS, Agarwal SM: **NPACT: Naturally Occurring Plant-Based Anti-Cancer Compound-Activity-Target Database**. *Nucleic Acids Research* 2013, **41**(Database issue):1124-1129.

100. Ibrahim RMS, Mohamed AG: **Naphthylisoquinoline Alkaloids Potential Drug Leads**. *Fitoterapia* 2015, **106**:194-225.

101. Lombe BK, Feineis D, Mudogo V, Brun R, Awale S, Bringmann G: **Michellamines A6 and A7, and further Mono- and Dimeric Naphthylisoquinoline Alkaloids from a Congolese *Ancistrocladus* Liana and their Antiausterity Activities against Pancreatic Cancer Cells**. *RSC Advances* 2018, **8**(10):5243-5254.

102. Tshitenge DT, Bruhn T, Feineis D, Schmidt D, Mudogo V, Kaiser M, Brun R, Würthner F, Awale S, Bringmann G: **Ealamines A–H, a Series of Naphthylisoquinolines with the Rare 7,8′-Coupling Site, from the Congolese Liana *Ancistrocladus ealaensis*, Targeting Pancreatic Cancer Cells**. *Journal of Natural Products* 2019.

103. Fayez S, Li J, Feineis D, Aké Assi L, Kaiser M, Brun R, Anany AM, Wajant H, Bringmann G: **A Near-Complete Series of Four Atropisomeric Jozimine A_2-Type Naphthylisoquinoline Dimers with Antiplasmodial and Cytotoxic Activities and Related Alkaloids from *Ancistrocladus abbreviatus***. *Journal of Natural Products* 2019.

Chapter 2: Phytochemical Investigations and Antiausterity Activities against Human PANC-1 Pancreatic Cancer Cells of Naphthylisoquinoline Alkaloids from a Congolese *Ancistrocladus* sp.

2.1. Introduction

2.1.1. The Ancistrocladaceae Family

Ancistrocladus WALLICH is the only known genus of the Ancistrocladaceae family. It occurs mainly in the evergreen forests of West and Central Africa, with a few species locally found isolated in Eastern Africa (Kenya and Tanzania); in tropical countries of South East Asia, India, and Sri Lanka, and Africa [1-5]. All species of the genus *Ancistrocladus* are found in dry to wet evergreen forests, often in swamps, riversides, roadsides, or other disturbed areas [3, 5, 6].

They are woody lianas or shrubs, provided with a series of circinate tendril-like modified hoody hooks in the same plane serving as grapnels anchoring the liana to the vegetation [3, 7] (Figure 2.1).

Figure 2.1: *Ancistrocladus sp. 1. Leaves + twigs, 2. Buds + Flowers and 3. Stem. Photos: S. Muyisa*

Their entire, acuminate leaves are often borne in dense, evergreen rosettes, and bear different sorts of glands and epidermal pits having a single wax-

secreting glandular trichome on the abaxial surface [1, 3, 7] (Figure 2.1). The small, bisexual flowers are mostly pentamerous, ranged in sympodial branched panicles, with a basally connate corolla. The fruit is a nut with often wing-like accrescent sepals [3, 6, 8].

According to the taxonomical revision published in 2005 [6], 16 liana species including *A. abbreviatus*, *A. attenuatus*, *A. barteri*, *A. congolensis*, *A. ealaensis*, *A. grandiflorus*, *A. griffithii*, *A. guineensis*, *A. hamatus*, *A. heyneanus*, *A. korupensis*, *A. letestui*, *A. likoko*, *A. robertsoniorum*, *A. tanzaniensis*, and *A. tectorius*, endemic to the tropical evergreen forests across Africa and Southeast Asia (Figure 2.2) jointly form the genus *Ancistrocladus*.

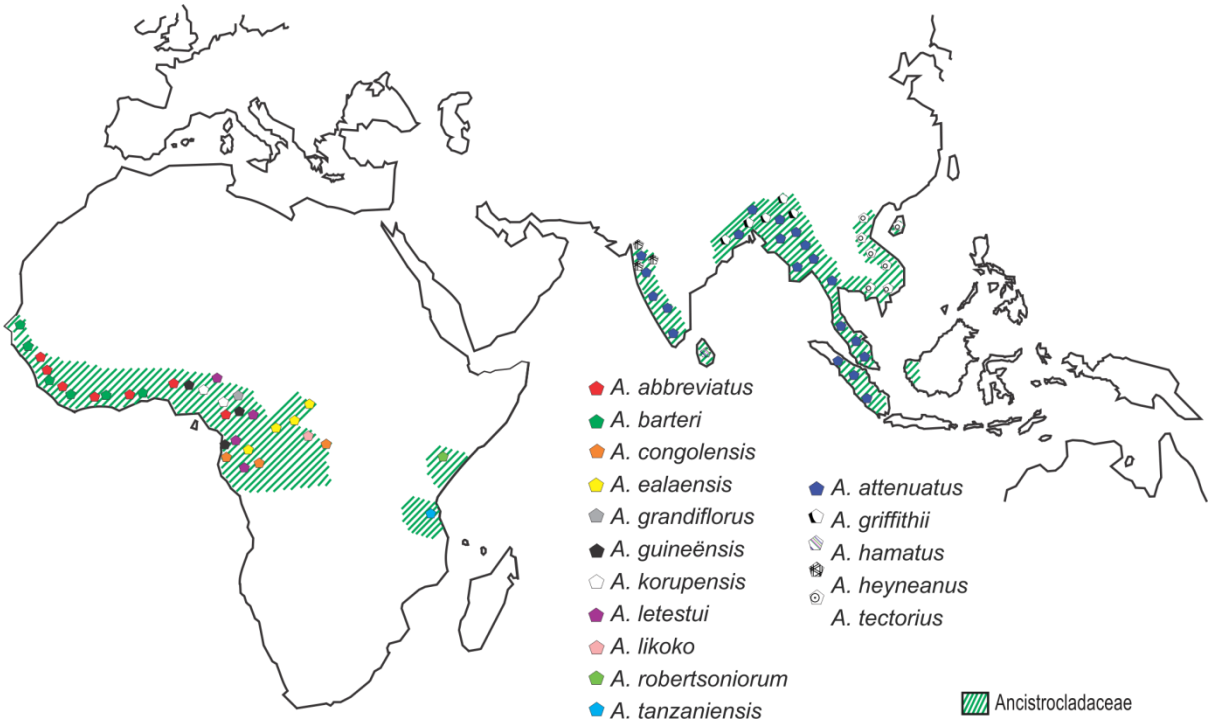

Figure 2.2: *Distribution of revised Ancistrocladus species in the 'Old World' [6]. (Inspired from Prof. G Bringmann's group in Würzburg)*

Further investigations have meanwhile brought out two additional taxa of this type, *A. benomensis* RISCHER and G BRINGMANN [9], occurring in the Southeast of the peninsular Malaysia and *A. ileboensis* HEUBL, MUDOGO & G BRINGMANN [10], found in the South-Central part of the wide and biodiversity-rich Congolese rainforest, where three *Ancistrocladus* taxa were

described earlier: *A. congolensis* J. LÉONARD, *A. ealaensis* J. LÉONARD, and *A. likoko* J. LÉONARD [7] (Figure 2.3).

Recent field expeditions corroborated by both phylogenetic [3] and phytochemical studies [11-16] provided evidence of a strong probability to find further new taxa and/or subspecies in the vast Congolese forest.

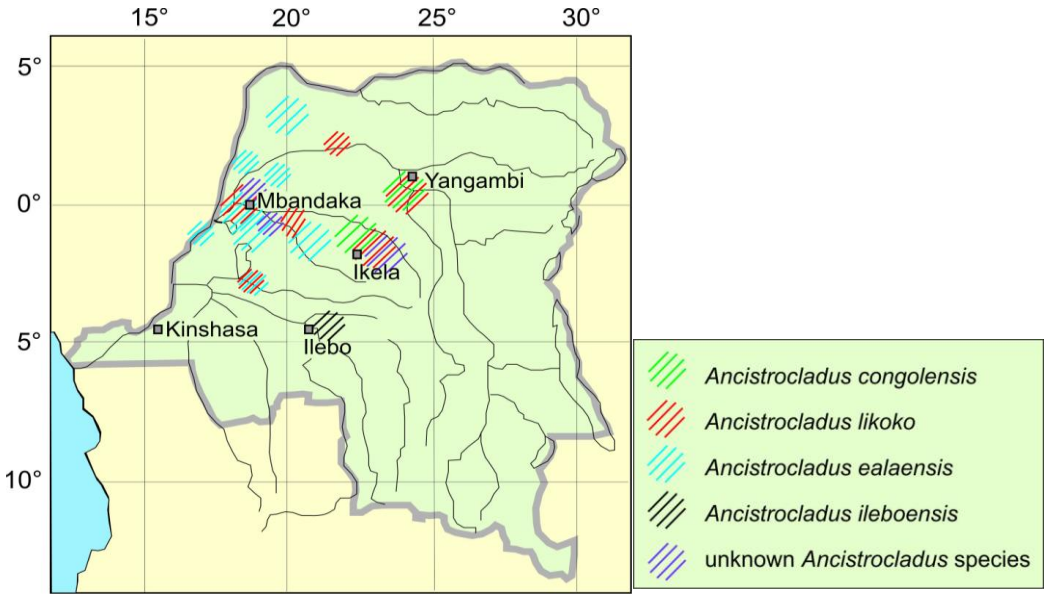

Figure 2.3: *Distribution of reported Ancistrocladus species in the Democratic Republic of the Congo (taken from Prof. G Bringmann's group in Würzburg) [3, 7]*

However, species identification based on morphological, phytochemical, and pharmacological characteristics is often subject to controversy because of the complexity and the strong morphological similarity of the species [6]. *Ancistrocladus* can, at first sight, be confused with several lianas that climb by similar-appearing hooks of various developmental origins, though none of these bear the small pits on their leaves that are characteristic of *Ancistrocladus* [6].

Leaves, stem barks, and stem roots of plants from the Ancistrocladaceae family have been widely used in traditional medicine by local communities to cure dysentery, malaria, fever, elephantiasis, and other diseases [17-19].

The family Ancistrocladaceae and the closely related Dioncophyllaceae are reported as the only source of a group of structurally and biosynthetically intriguing metabolites, the naphthylisoquinoline alkaloids [3]. Consequently, *Ancistrocladus* plants have been the subject to intensive chemical and pharmacological research aimed at investigating the alkaloids in different species and evaluating their bioactivity, with ongoing research effort in this field [3].

2.1.2. Naphthylisoquinoline Alkaloids

2.1.2.1. Definition

Naphthylisoquinoline (NIQ) alkaloids are a specific class of structurally diverse and fascinating secondary metabolites of high interest due to their unprecedented structures, outstanding chemotaxonomical implications, unique biosynthetic origin, and promising biological activities [20].

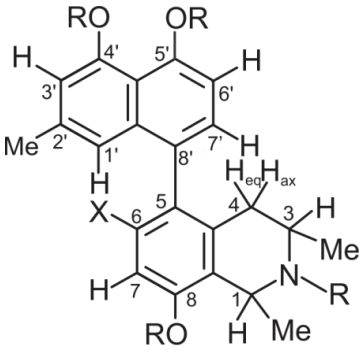

Figure 2.4: *General structure of a 5,8'-coupled naphthylisoquinoline monomer (R = H or Me and X = H, OH, OMe, or N)*

They are constituted of naphthalene and isoquinoline moieties (Figure 2.4) coupled to each other *via* a *C,C*- or an *N,C*- biaryl axis to form monomeric naphthylisoquinolines, which can, in turn, be linked to produce dimeric metabolites [20, 21] (Figure 2.5).

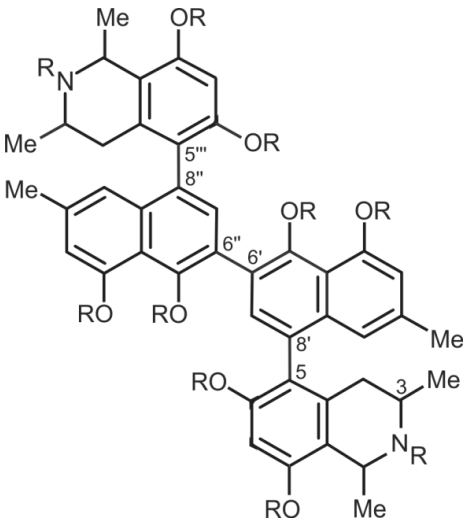

Figure 2.5: *A structure sample of 5,8'-coupled NIQ dimers (R = H or Me)*

Their occurrence is as yet restricted to the small West African plant family Dioncophyllaceae [22], and to the closely related family Ancistrocladaceae [4, 6].

2.1.2.2. Complexity of the Structures of Naphthylisoquinoline Alkaloids

Structurally, the naphthylisoquinolines are chiral compounds displaying atropisomerism, since the biaryl axis is usually hindered rotationally because of the presence of bulky *ortho*-substituents; as compared to 'normal' isoquinoline alkaloids, they are characterized by an unusual substitution pattern, including an unprecedented methyl group at C-3 and the presence of a *meta*-oxygen pattern at positions C-8 and C-6 (only observed for Ancistrocladaceae-type NIQs) [20]. The large structural variation also include the degree of unsaturation in the isoquinoline moiety, the OMe/OH substitution, various coupling possibilities (5,1'-, 5,3'-, 5,8'-, 7,1'-, 7,3'-, 7,6'-, 7,8'-, and *N,C*- coupling), and also the possibility for monomeric NIQs to be linked and form dimeric NIQs; and all these interdependent factors together form a remarkable overall complexity of this rapidly growing class of natural biaryls [20].

Chemotaxonomically, the naphthylisoquinoline alkaloids are divided into three main subclasses: the Dioncophyllaceae-type exhibiting *R*- configuration at C-

3 and deprived of an oxygen at C-6, which is typical of West African Dioncophyllaceae species; the Ancistrocladaceae-type, which are 3*S*-configured and have a C-6 oxygen function, and are found in Asia and East Africa *Ancistrocladus*, and the hybrids of both types characterized by an oxygen function at C-6 but a 3*R*-configuration specific to *Ancistrocladus* plants from the Congo Basin [21, 23, 24].

2.1.2.3. Biosynthetic Origin of Naphthylisoquinoline Alkaloids

In spite of the vast structural variations of all reported naphthylisoquinoline alkaloids, all these natural products share a common key step in their biosynthesis [25-29], which starts with a hexaketide intermediate originated from acetyl CoA and malonyl CoA catalyzed by a polyketide synthase (PKS) through incomplete reduction and dehydration steps (Scheme 2.1).

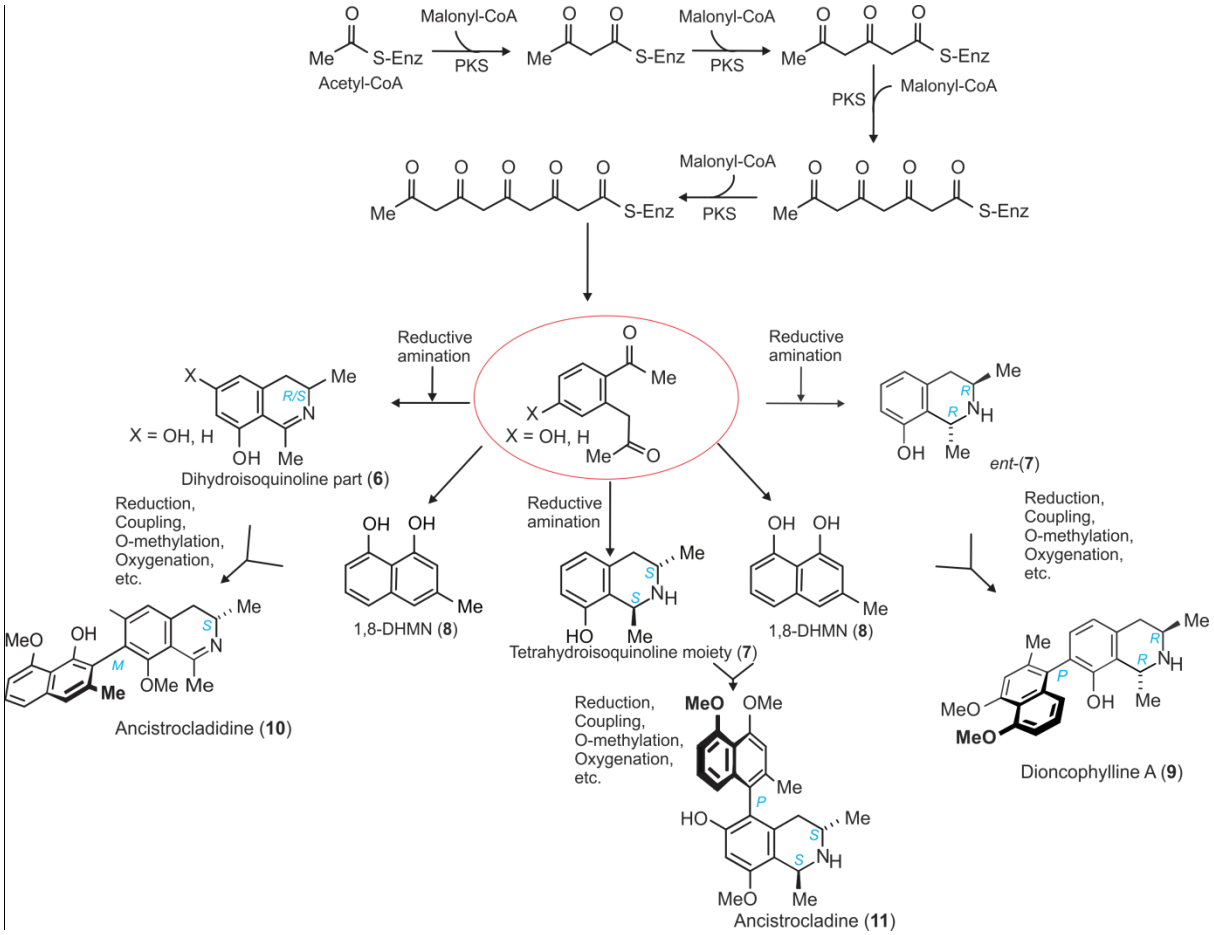

Scheme 2.1: *Biosynthetic pathways to naphthylisoquinoline alkaloids (taken from RMS Ibrahim et al. [21]) and modified by Prof. G Bringmann's group in Würzburg)*

The 1,8-dihydroxy-3-methylnaphthalene (**8**) is then formed [21]. Furthermore, throughout a reductive amination reaction, the tetrahydroisoquinoline half, (3*R*)-configured isomers *ent*-(**7**), and dihydroisoquinoline will be formed; the two molecular moeties, *ent*-(**7**) and **8**, formed from the same precursors, will convergently be linked together according to the principle of phenol-oxidative biaryl coupling, leading eventually, after some follow-up reactions, to the production of complete naphthylisoquinoline alkaloids e.g., to dioncophylline A (**9**) [21]. By reduction, coupling, *O*-methylation, and oxygenation reactions, the tetrahydroisoquinoline moiety (**7**) and 1,8-DHMN (**8**) can be joined together to yield another type of complete NIQ e.g., ancistrocladine (**11**), or ancistrocladidine (**10**) resulting from the coupling of **8** with dihydroisoquinoline (**6**) through the same process [21].

2.1.2.4. Structural Elucidation of Naphthylisoquinoline Alkaloids

A set of modern spectroscopic technics combined with chemical methods is a key to determine the constitution, the relative configuration, and the absolute configuration of naphthylisoquinoline alkaloids. Their constitutions and relative configurations are elucidated by 1D-NMR (^{1}H, ^{13}C, dept) and 2D-NMR (^{1}H-^{1}H-COSY, HSQC, HMBC, NOESY, and ROESY), while their full absolute configurations are established unequivocally by means of the combination of Electronic Circular Dichroism (ECD) spectroscopy [20, 30, 31] and the oxidative degradation reaction [32]. Mass spectrometry is used as an efficient method to identify and quantify naphthylisoquinolines since these compounds have characteristic $[M+H]^{+}$ masses for monomeric alkaloids and doubly protonated ones $[M+2H]^{2+}$ for dimers [33].

The configuration of the stereocenters at C-1 and C-3 is determined by Nuclear Overhauser Enhancement (NOE) and Rotating-Frame Overhauser Enhancement (ROE) investigations [34]. Further valuable information about the structural elucidation are provided by total synthesis [35]. The configuration at the biaryl axis is deduced by comparing the calculated spectra with the experimental Electronic Circular Dichroism (ECD) spectra [31].

A reliable oxidative degradation method for the determination of the absolute configuration of chiral naphthylisoquinolines has been developed by the group in Würzburg (G Bringmann *et al.*) based on a ruthenium-mediated oxidation procedure [32]; this oxidative degradation of the di- or tetrahydropyridine part of the alkaloids provides simple amino acid derivatives, which are analyzed by GC coupled to a Mass Selective Detector (MSD) after Mosher-type derivatization (Scheme 2.2). The method is efficient for the unambiguous determination of the absolute configuration at the stereocenters C-1 and/or mainly C-3 in a single step, even on a sub-mg scale.

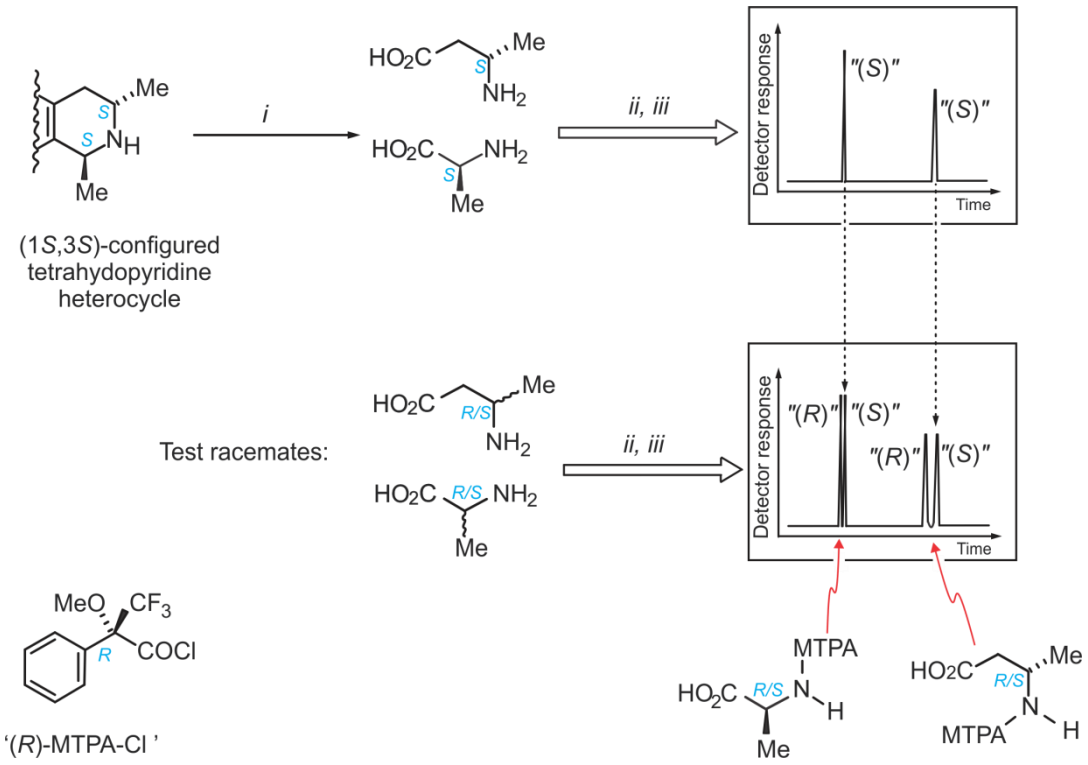

Scheme 2.2: *General scheme for the ruthenium-mediated oxidative degradation of the tetrahydropyridine heterocycle (i) $RuCl_3$, $NaIO_4$; (ii) MeOH, $SOCl_2$; (iii) '(R)-MTPA-Cl' {'(R)-Mosher's chloride' [36]}, NEt_3 (taken from G Bringmann et al. [32])*

Another efficient method for the determination of the absolute configuration at the stereocenters of naphthylisoquinolines is the X-ray analysis of suitable crystals. Unfortunately, in most of cases, this technique cannot be used since naphthylisoquinolines do not crystallize suitably to furnish crystals of suitable

quality [21].

Even more fascinating than the complexity resulting from different substitution and coupling possibilities, and the existence of stereo elements in monomeric naphthylisoquinoline alkaloids, are the dimeric naphthylisoquinoline alkaloids which even possess three biaryl axes. These dimers are a the result of further coupling of monomeric naphthylisoquinolines (Figure 2.5), each of which may be identical (case of homodimers) or different (case of heterodimers) [37].

2.1.2.5. Nomenclature of Naphthylisoquinoline Alkaloids

Due to the complexity of their structure, trivial names are preferred to name naphthylisoquinoline alkaloids instead of applying the IUPAC system [38]. Some are named after the species from which they were isolated for the first time, e.g., ancistrolikokine A [39], isolated from *A. likoko*, ancistrocongoline A [40] discovered in *A. congolensis*, ancistroguineines A and B [41] isolated from *A. guineënsis*. Some others are named after the name of the place where the plant material from which the alkaloid was first isolated is coming from, e.g., mbandakamine A [13], ancistrobonsoline [12], and ancistroyafungines A-D [16] isolated for the first time from *Ancistrocladus* species collected near Mbandaka, Bonsole, and Yafunga villages respectively, found in the Congo Basin.

2.1.2.6. Bioactivity of Naphthylisoquinoline Alkaloids

Naphthylisoquinoline alkaloids have been reported to exhibit remarkable biological activities. In an earlier publication [43] only the spasmolytic and anti-tumor activities for these alkaloids are reported. More recently, biological investigations of the naphthylisoquinolines have demonstrated that they exhibit several interesting activities. Selected naphthylisoquinoline alkaloids reported to exhibit biological activities are given in Figures 2.6 to 2.8.

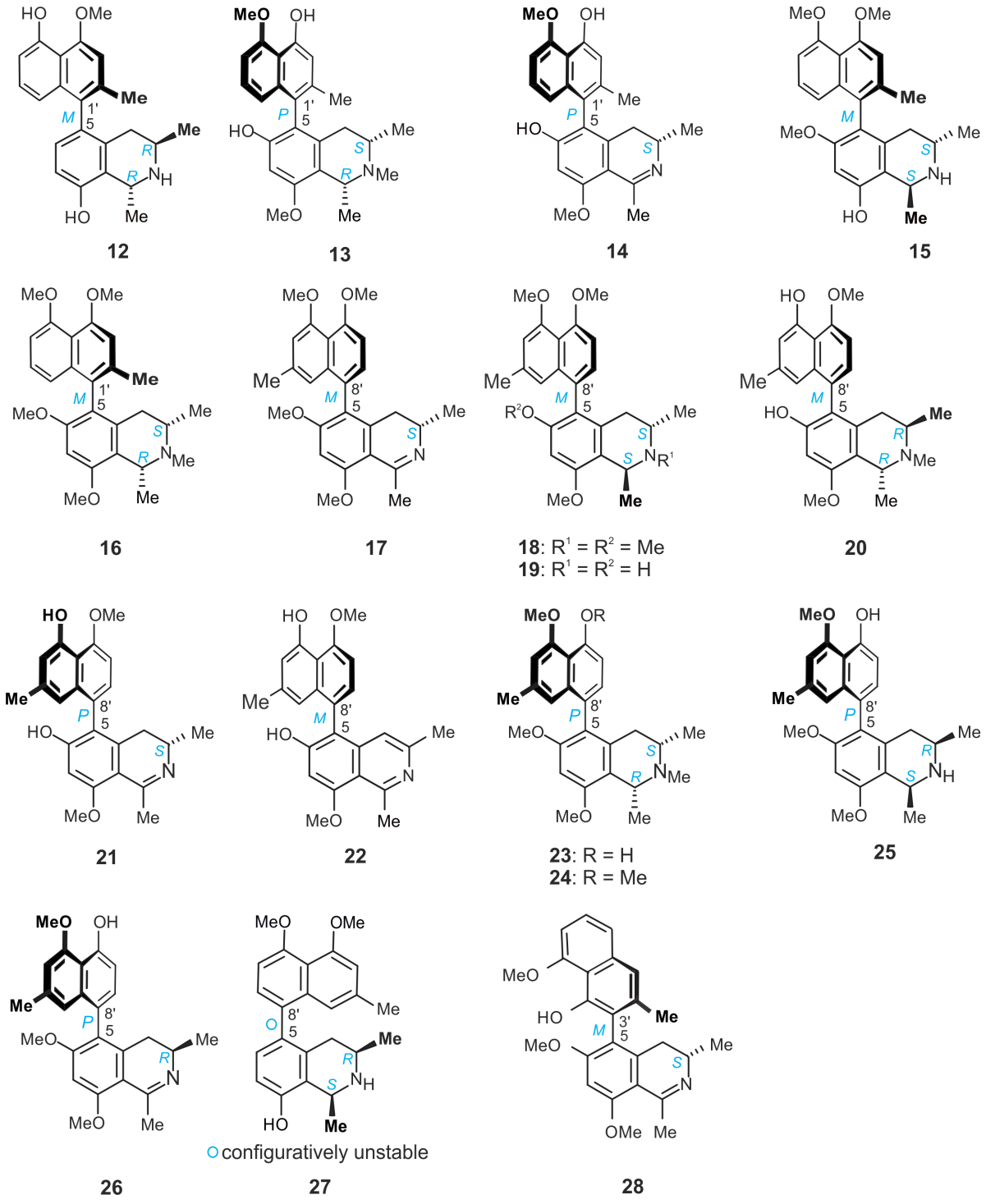

Figure 2.6: *Selected NIQs reported to possess biological activities 1: dioncophyllines C (**12**) and F (**27**), N-methylancistectorine A_1 (**13**), ancistectorine A_3 (**14**), 5-epi-ancistectorine A_2 (**15**), ancistrobertsonines B (**16**) and C (**24**), ancistrotanzanines A (**28**) and B (**17**), 5-epi-6-O-methylancistrobertsonine A (**18**), ancistrobrevine B (**19**), and ancistrolikokines C (**20**), D (**21**), G (**22**), H_2 (**23**), I (**25**), and E_3 (**26**)*

a. Antiprotozoal Activities

Naphthylisoquinoline-containing extracts from several species of Ancistrocladaceae and Dioncophyllaceae are used in folk medicine to treat protozoal diseases [17]. These applications hint at an obvious antiprotozoal potential of constituents of these extracts, and thus warrant further investigations [42, 43]. Dioncophylline C (**12**), *N*-methylancistectorine A_1 (**13**), ancistectorine A_3 (**14**), and 5-*epi*-ancistectorine A_2 (**15**) [44, 45] were reported to exhibit strong and highly specific antiplasmodial activities against the K1 strain of *Plasmodium falciparum* (chloroquine- and pyrimethamine-resistant) with IC_{50} values ≤ 0.08 µM comparable to that of chloroquine (IC_{50} 0.26 µM). They showed high selectivity indexes, and have been therefore considered as antimalarial compounds in accordance with the Tropical Diseases Research/World Health Organisation (TDR/WHO) guidelines [46].

In earlier studies, ancistrobertsonine A (**50**) [47, 48], ancistrobertsonine B (**16**) [48, 49], ancistrobertsonine C (**24**) [48], ancistrobertsonine D (**32**) [48], and ancistrobrevine B (**19**) [48] were reported to show pronounced activities towards the chloroquine-resistant K1 strain, and 2-5 fold less against the chloroquine-susceptible NF54 strain of *P. falciparum*, the antimalarial activity being specific against intra-erythrocytic forms of the parasite [48]. More recently, the monomer dioncophylline F (**27**) [50] and some dimeric naphthylisoquinolines have been reported to display impressive antimalarial activities e.g.: shuangancistrotectorines A and B (**38**) [51], ealapasamine C (**39**) [52], jozimine A_2 [53], mbandakamine B_2 [11], spirombandakamines A_1 and A_2 [11], cyclombandakamine A_1 and A_2 [54], and mbandakamine C (**41**), [55] with IC_{50} values ranging from 0.004 to 0.094 µM against the chloroquine-resistant K1 strain and/or 0.001 to 0.226 µM towards the chloroquine sensitive NF54 strain. Ancistectorine D [56] and 5-*epi*-6-*O*-methylancistrobertsonine A (**18**) [57] were reported to exhibit strong activity towards *Leishmania donovani,* with remarkable IC_{50} values of 1.2 and 1.6 µM, respectively; even better was the activity of 4'-*O*-demethylancistrocladinium A (**37**) [58], with an IC_{50} value of 0.1 µM, whereas ancistrocladinium A (**55**) and

B (**56**) showed good leishmanicidal activities against intracellular amastigote stage of *Leishmania major* [59].

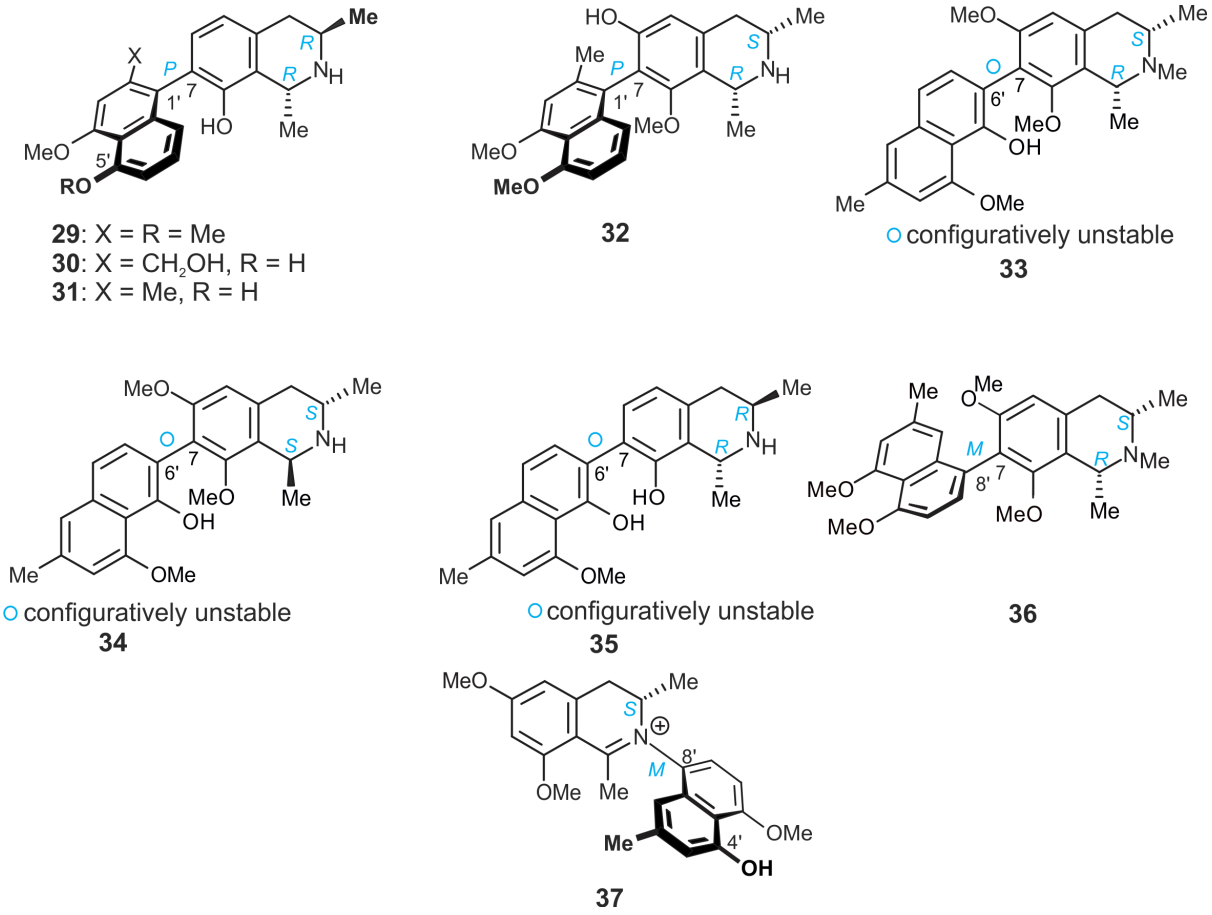

Figure 2.7: *Selected NIQs reported to possess biological activities 2: dioncophyllines A (**29**) and B (**35**), dioncopeltine A (**30**), 5'-O-demethyldioncophylline A (**31**), ancistrobertsonine D (**32**), ancistrotectorines A (**33**), B (**34**), and E (**36**), and 4'-O-demethylancistrocladinium A (**37**)*

The dimeric naphthylisoquinoline mbandakamine B_2 has been reported to strongly inhibit the growth of *Trypanosoma brucei rhodesiense* [11], with an excellent IC_{50} value of 0.005 µM, far better than the previously reported alkaloids shuangancistrotectorine A [51], ancistrocladinium A (**55**) and 4'-*O*-demethylancistrocladinium A (**37**) [58], whose IC_{50} values were 0.318, 0.200, and 0.300 µM, respectively. The naphthylisoquinoline alkaloid 4'-*O*-demethylancistrocladinium A (**37**) [58] was reported to exhibit strong activity

against *Trypanosoma cruzi*, with an IC_{50} value of 0.030 µM, better than those of shuangancistrotectorine A [51] and ancistectorine D [56], whose IC_{50} values against *Trypanosoma cruzi* were 3.8 and 4.439 µM, respectively.

b. Anti-HIV Activity

Some dimeric naphthylisoquinoline alkaloids inhibit HIV-induced cell killing and viral replication in a variety of human cell lines, as well as in cultures of human peripheral blood leucocytes and monocytes [20]. Michellamine B isolated from *A. korupensis* [60, 61] as well as its related michellamines D-F (**42**) [62] showed inhibition of the enzymatic activities of reverse transcriptases (RTs) from both HIV type 1 and 2 as well as two different nonnucleoside drug-resistant RTs with specific amino acid substitutions. FY Hallock *et al.* [63] revealed korundamine A, also isolated from *A. korupensis* to have inhibitory activity towards the cytopathic effects of HIV-1, with an EC_{50} value of 2 µM. The compound showed activities against several resistant strains of HIV such as CEM-SS/OC100, MT2/A17, and MT2/G9106 host cell/virus strain combinations with EC_{50} values of 8, 10, and 6 µM, respectively [63].

c. Anti-Cancer Activities

Both monomeric and dimeric naphthylisoquinoline alkaloids were reported to show promising cytotoxic activities against various cancer cells with IC_{50} values ≤ 10 µM. From investigations done by C Jiang *et al*. [49], ancistrotectorines A (**33**), B (**34**), and E (**36**) and ancistrotanzanines A (**28**) and B (**17**) showed growth inhibition towards human promyelocytic leukemia HL-60, human erythromyeloblastoid leukemia K562, and human macrophage U937 cell lines, with very good IC_{50} values ranging from 1.70 to 8.55 µM. Both the mono- and dimeric naphthylisoquinolines 5'-*O*-methyldioncophylline D [50], shuangancistrotectorines A and B (**38**) [51] exhibited good cytotoxicity activity against rat skeletal myoblast L6 cells with IC_{50} values 4.02, 5.68, and 7.59 µM, respectively, greater than that of mbandakamine D, of which the IC_{50} value was 8.87 µM [55]. Recently [64], ancistrolikokines E_3, G, and I displayed strong growth-retarding activities towards drug-sensitive CCRF-

CEM leukemia cancer cells, with IC_{50} values 4.36, 4.73, and 4.49 μM, respectively.

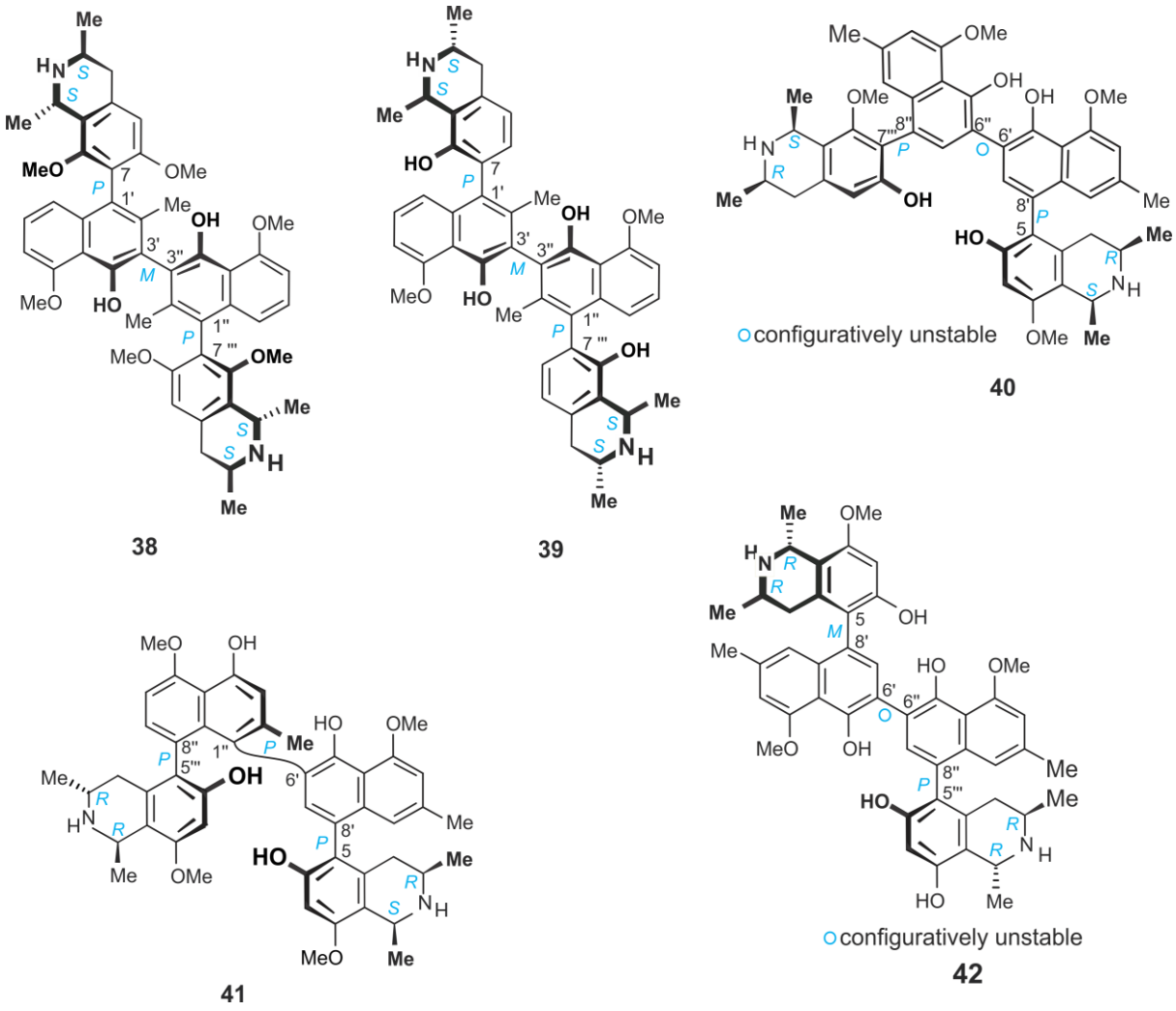

Figure 2.8: *Selected NIQs reported to possess biological activities 3: shuangancistrotectorine B (**38**), jozimine A_2 (**39**), ealapasamine C (**40**), mbandakamine C (**41**), and michellamine F (**42**)*

Ancistrolikokine G (**22**) showed excellent half-maximum inhibitory concentrations in the low micromolar range against multidrug-resistant CEM/ADR5000 leukemia cells (IC_{50} = 7.73 μM).

On the other hand, 6-*O*-methyl-4'-*O*-demethylhamatine [65], ancistroyafungines B (**44**) and D (**46**), 6,4'-*O,O*-didemethylancistroealaine A (**52**) [16], ancistrobonsoline A_1 [12], ancistrolikokines C (**20**), D (**21**), and H_2 (**23**), korupensamine E [66], and the dimeric naphthylisoquinolines

jozilebomines A and B were reported to display very good inhibitory activities against PANC-1 human pancreatic cancer cells line with PC_{50} values less than 10 μM.

Michellamines A_6 and E, along with ancistrobonsoline A_1 were reported to exhibit excellent activity towards HeLa cervical cancer cells with IC_{50} values of respectively 14.8, 8.8, and 14.3 μM, michellamine E being even better than the control, 5-fluorouracil, of which the IC_{50} value was 13.9 μM [12].

Based on the reported remarkable activities of naphthylisoquinoline alkaloids towards various types of tumor, the isolated compounds as part of this study were tested for their anti-pancreatic cancer potential and the results are given in Section 2.3.4.

d. Anti-Microbial Activities

Michellamine B was reported to display anti-microbial activities against *Escherichia coli* MraY and *Bacillus subtilis* MraY with respective IC_{50} values of 456 and 386 μM; however there are limited studies on the anti-microbial activities of the naphthylisoquinoline alkaloids, probably because of their relatively low potency compared to that of the active phloxine B (IC_{50} 32 and 165 μM, towards *E. coli* and *B. subtilis* respectively) [67].

e. Fungicidal, Larvicidal, and Molluscicidal Potencies

Dioncophyllines A (**29**), B (**35**), and C (**9**), and dioncopeltine A (**30**) were reported to possess good activities against the important plant-pathogenic species *Botrytis cinerea* and *Plasmopara viticola* [20].

The younger larval stages of the malarial vector *Anopheles stephensi* were reported to be sensitive to dioncophylline A (**29**) [21]. Dioncophylline A (**29**) and its related analog 5'-*O*-demethyldioncophylline A (**31**) showed activities towards the growth of the neonate larvae of the pest herbivore insect *Spodoptera littoralis* [68]. The fungicidal, larvicidal, and molluscicidal activities of naphthylisoquinoline alkaloids are barely documented.

2.1.3. Aims and Objectives

The main aims of this study were the isolation and identification of both novel and known bioactive naphthylisoquinoline alkaloids with antiausterity activities against human PANC-1 cells from a Congolese *Ancistrocladus* species.

The project had the following specific objectives:

1. Collection and processing of the *Ancistrocladus* plant under investigation.
2. UPLC-QTOF MS profiling of leaves, stem, and root bark extracts of the *Ancistrocladus* plant under study.
3. Extraction, purification, and isolation of naphthylisoquinoline alkaloids from the collected Congolese *Ancistrocladus* species.
4. Structural elucidation and assignment of the absolute configuration of the isolated naphthylisoquinoline alkaloids.
5. Evaluation of the isolated compounds for antiausterity activities against human PANC-1 pancreatic cancer cells.
6. Identification and interrogation of the geo-chemotaxonomy of the investigated *Ancistrocladus* species.

2.2. Experimental Section

2.2.1. Plant Collection

The *Ancistrocladus* species used in this study was collected in December 2014 in the proximity of Yafunga-rive (Figure 2.9), a village (locality) found in Yawembe Sector, downstream the Congo River, on the left bank, in the Province Tshopo, in the Democratic Republic of the Congo. The swampy forest surrounding the village is under the protected biosphere area managed by the National Institution for Agronomic Studies (INERA/Yangambi). The collection was done 3 km from Yafunga-rive village: 00°43'46.6" longitude, 024°20'16.8" latitude, and 387 m altitude. Local communities know the liana under the name *Akombe ndjala* (Lokele dialect), which literally means "claws of sparrow-hawk", obviously because of the presence of hooks on it. The liana has no medicinal use locally but is used to weave seats.

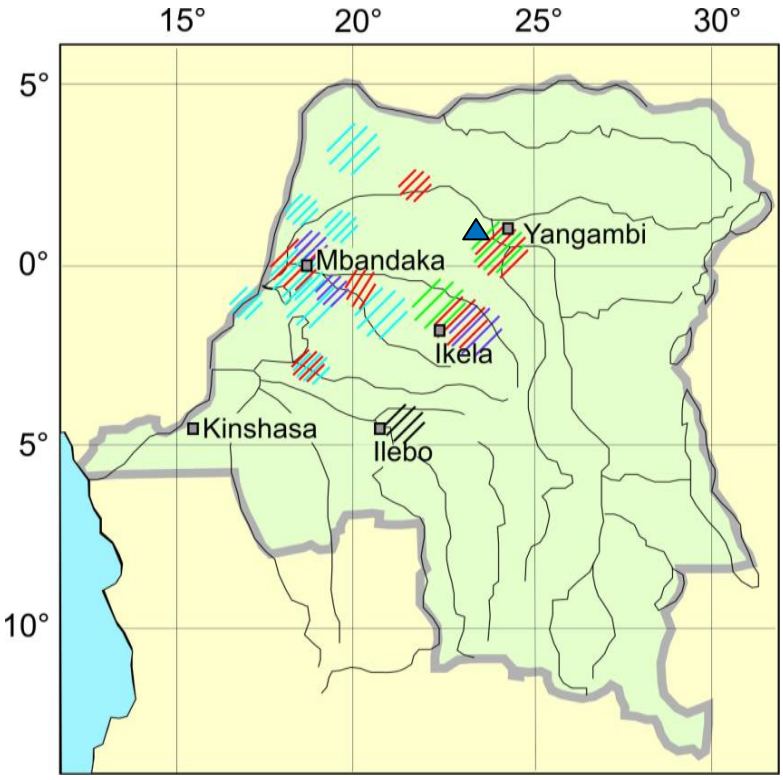

Figure 2.9: *Sampling site (Yafunga-rive in blue triangle). (Adapted from Prof. G Bringmann's group in Würzburg)*

Plant material (leaves, stems, and root barks) were collected by the author of

this thesis and stored separately. For each sample, the precise localization (altitude, latitude, and longitude), the date of collection and collector's name were recorded and stuck on the sample. In each site, the numbers of constituted samples depended on the numbers of liana feet found in the site; hence, a total of 7 samples were collected (1 to 3 kg each of fresh material). It was only after chemical profiling of the plant parts that leaves were combined; the same was done for the rest of plant material. Only stem barks were considered for isolation of compounds, because of the complexity of the root bark extract, and due to the small number of peaks found in the leaves according to the LC-MS profiles of their extracts (comparative LC-MS chromatograms are given in the Supplementary Information).

2.2.2. Analytical Instrumentation

2.2.2.1. Ultraviolet Spectroscopy (UV)

UV spectra were obtained at room temperature on a Shimadzu UV-1800 spectrophotometer, with 1 cm cell length, λ refers to the wavelength. The concentrations ranged from 0.1 to 0.5 mg/ml in methanol (MeOH).

2.2.2.2. Infrared Spectroscopy (IR)

The IR spectra were determined on a Jasco FT-IR-4600 type A spectrometer. The spectra were measured at room temperature, ν refers to the wavelength number.

2.2.2.3. Nuclear Magnetic Resonance Spectroscopy (NMR)

1D and 2D spectra were recorded at room temperature on Bruker Advance III HD 400 (400 MHz, ^{1}H) or 600 (600 MHz, ^{1}H) instruments using deuterated methanol (CD_3OD) as the solvent, the chemical shifts (δ) are reported in parts per million (ppm) with the ^{1}H and ^{13}C signals of the solvent at δ = 3.31 ppm and δ = 49.15 ppm respectively, as the internal reference, with reference to δ_{TMS} = 0 ppm. NMR spectra data were processed by the TopSpin-software from Bruker. Signal multiplicity is given by the following abbreviations: singlet = s, doublet = d, doublet of doublets = dd, triplet = t, doublet of triplets = dt,

quartet = q, and multiplet = m. The coupling constants are given in Hertz (Hz), where the number of bonds is given by n*J*. The homonuclear through-bond correlations were determined through COSY (Correlation Spectroscopy), the through-space correlations were given by NOESY (Nuclear Overhauser Effect Spectroscopy), and proton-detected, heteronuclear through-bond correlations were analyzed using HSQC (Heteronuclear Single Quantum Coherence Spectroscopy) and HMBC (Heteronuclear Multiple Quantum Correlation Spectroscopy).

2.2.2.4. Mass Spectrometry (MS)

Electrospray ionization (ESI) and high-resolution electrospray ionization HRMS (ESI) mass spectra were determined on a Bruker Daltonics microTOF focus, the software modul IsotopePattern of the software Compass 1.1 from Bruker Daltonics was used for calculation of the respective mass values of the isotopic distribution. The concentrations ranged from 0.1 mg/ml for pure compounds to 1 mg/ml for extracts. The solvent used was methanol.

2.2.2.5. Gas Chromatography-Mass Selective Detector (GC-MSD)

Capillary GC-MSD analyses were performed on a GC-MS-QP 2010SE Shimadzu instrument.

2.2.2.6. Optical Rotation

Optical rotation values were recorded on a Jasco P-1020-polarimeter equipped with a sodium light source (λ = 589 nm).

2.2.2.7. Electronic Circular Dichroism (ECD)

ECD spectra were measured at room temperature with a Jasco J-715 spectropolarimeter, using spectrophotometric-grade MeOH and a standard quartz crystal cell (0.02 cm). The ECD spectra were measured 3 times from 200 nm to 400 nm wavelength using the software Jasco-Borwin Version 1.50, and processed with the SpecDis_win7 software [30]. They are reported in $\Delta\varepsilon$ values [cm^2/mol]. A blank sample of the eluent was measured to correct the baseline.

2.2.3. Other Apparatuses and Materials

Garmin GPS MAP 64s: was used to record the latitude, the longitude, and the altitude of the sampling site.

Grinding of Plant Material: A Retsch-SM1 impact mill with a wire netting of 1 mm whole size was used to grind air-dried plant material.

2.2.4. Chromatographic Methods

Thin Layer Chromatography (TLC): The monitoring of extracts and fractions were done by TLC using Merck aluminium foil silica gel 60 F_{254} precoated plates. The optimum elution was obtained using the mixture dichloromethane,methanol, and acetic acid (CH_2Cl_2/MeOH/HOAc) in the proportion 18:1:1 as the solvent system. Spots were visualized under fluorescent light at both 254 nm and 365 nm.

High Pressure Liquid Chromatography (HPLC): Analytical HPLC was carried out using a Jasco equipment; pump PU-1580, degassing unit DG-1580, auto sampler AS-2055 Plus, mixer LG-1580, column oven CO-1560, diode array detector MD-2010 Plus. Measurement processing was done using the Borwin software from Jasco. The column used was a Symmetry-C_{18} Waters; 4.6 x 250 mm, 5 µm) with mobile phases consisting of water (H2O) + 0.05% trifluoroacetic acid (TFA) (A), MeOH + 0.05% TFA (B); flow: 0.8 ml/min, binary gradient: 0 min 20 % B, 5 min 30 % B, 22 min 100 % B, 24 min 100% B, 25 min 20% B, 30 min 20% B. The injection volume was 5 µl.

Preparative HPLC was carried out using a Jasco HPLC system (PU-2087, UV-2077, LC-NetII/ADC), using a SymmetryPrep C18 column (Waters, 19 x 300 mm, 7 µm) with the UV absorption wave length set at 232, 254, and 315 nm. The flow rate was 8-10 ml/min, the injection volume ranged from 50 to 100 µl. Both gradient and isocratic systems were used as described in Section 2.2.6.

2.2.5. Chemicals

Solvents: All used solvents (methanol, acetone, dichloromethane, chloroform, ethyl acetate (EtOAc), and *n*-hexane were of analytical grade. Water for HPLC was degassed prior to use. Methanol and acetonitrile (MeCN) for the HPLC, UV, ECD, and specific rotation value measurements, as well as TFA were purchased from Merck without other purification procedures performed.

2.2.6. Extraction and Isolation of NIQs

The powdered air-dried stem bark material (150 g) was exhaustively extracted with a mixture of CH_2Cl_2/MeOH (1:1) using mechanical shaking (160 RPM) at room temperature, resulting in a yield of 14 g of a solid crude residue after filtering on a Whatman filter paper, and concentrating the resulting extract *in vacuo*. The solid residue was then suspended in *n*-hexane to remove most lipophilic compounds. After filtration and drying, the remaining, defatted residue was suspended in H_2O and sonicated (2 x 15 min). After decantation followed by filtration, the resulting aqueous filtrate was exhaustively extracted with CH_2Cl_2. The organic phase was evaporated and dried to produce 2 g of a naphthylisoquinoline concentrated crude extract, of which 1 g was dissolved in a mixture H_2O/MeOH (4:1) and filtered over a 0.2 µm PTFE membrane (PHENEX), followed by extraction with EtOAc (Figure 2.10).

The organic phase was concentrated under reduced pressure to produce 367 mg a fraction enriched in NIQs, from which 200 mg were dissolved in 4 ml of MeOH, and purified by preparative HPLC using the following gradient system A/B: 0 min 20% B, 22 min 30% B, 35 min 60% B, and 37 min 100% B, with A = H_2O/MeCN (9:1) + 0.05 TFA and B = H_2O/MeCN (1:9) + 0.05 TFA, and 10 ml/min flow rate, injection volume varied from 250 to 500 µl.

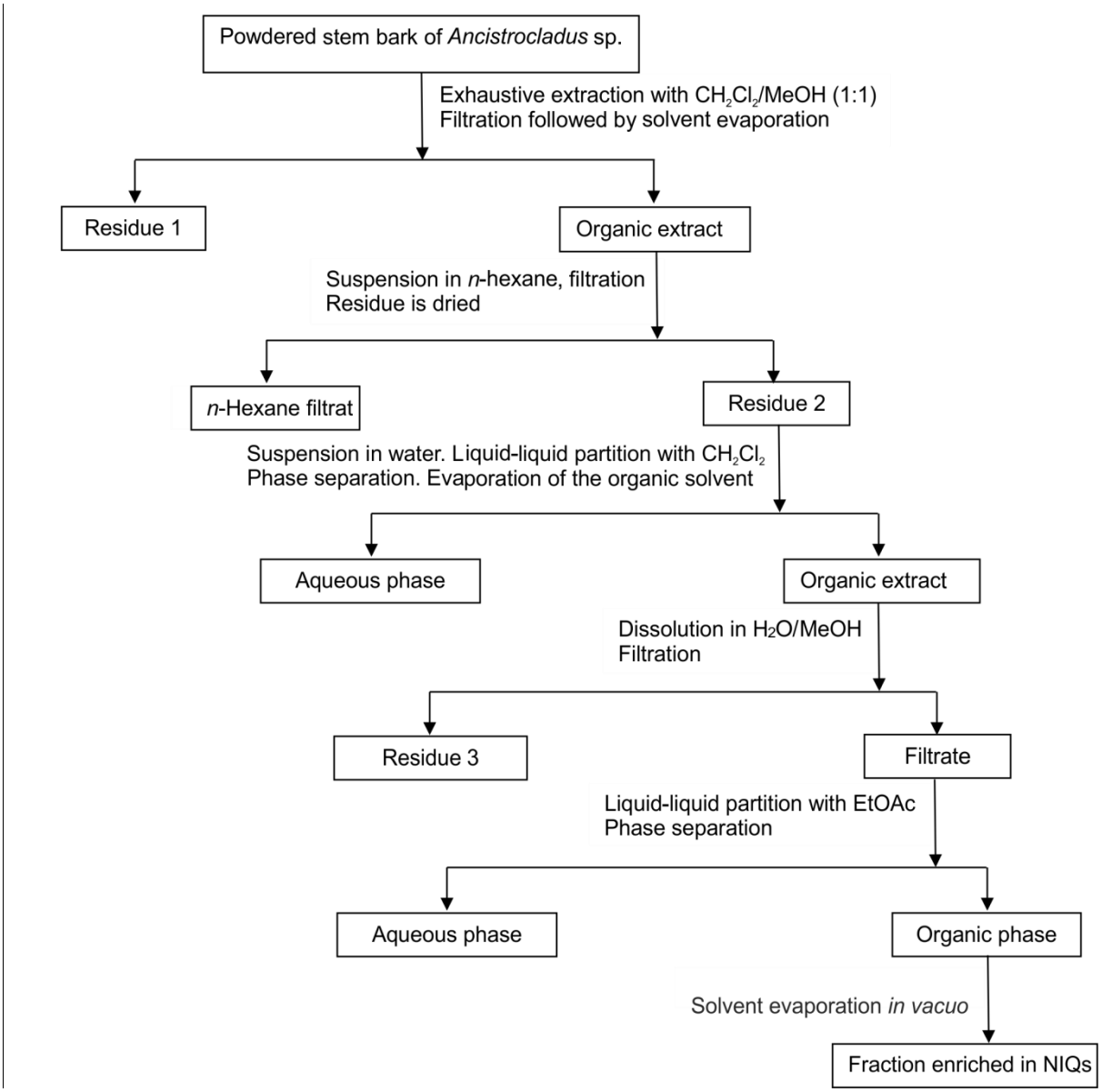

Figure 2.10: *General extraction process for NIQs from the Ancistrocladus species investigated*

The purification of naphthylisoquinoline alkaloids was done in collaboration with Dr. BK Lombe in Prof. G Bringmann's laboratory.

The collections were UV based, and they produced 16 fractions including 2.8 mg of 4'-*O*-demethylancistrocladine (**48**, t_R: 19.4 min), 3.5 mg of 7-*epi*-ancistrobrevine D (**54**, t_R: 21.9 min), 2.1 mg of 6,5'-*O,O*-didemethylancistroealaine A (**52**, t_R: 24.0 min), 7 mg of ancistrocladinium A (**55**, t_R: 35.9 min), 13 mg of ancistrocladinium B (**56**, t_R: 39.6 min), and eleven further fractions labelled as F1 to F11.

The resolution of Fraction 1 (collected at 15-18 min) by preparative HPLC using an isocratic system consisting of 20% of MeCN (flow: 12 ml/min) produced 2.3 mg of ancistrobrevine B (**19**, t_R: 17.1 min), 1.9 mg of ancistroyafungine A (**43**, t_R: 21.9 min), and 4 mg of ancistrobertsonine A (**50**, t_R: 22.6 min).

Further, Fraction 4 (collected at 20-21.5 min; 8 ml/min) was purified by preparative HPLC, using an isocratic system of MeOH/H_2O as the eluent (54:46), to provide 1.9 mg of ancistroguineine A (**49**, t_R: 9.3 min), 2.1 mg of ancistroyafungine B (**44**, t_R: 10.8 min), and 3.5 mg of 6-*O*-demethylancistroealaine A (**54**, t_R: 12.4 min).

Using the same chromatographic conditions, Fraction 7 (25.1-26.5 min) was also purified (flow: 10 ml/min), and produced 6 mg of 6-*O*-mathylhamatine (**47**, t_R: 15.3 min) and 7 mg of ancistrotectoriline A (**51**, t_R: 16.2 min).

The elution of Fraction 8 (26.5-28.1 min) with isocratic 56% aqueous MeOH yielded 5.1 mg of ancistroyafungine C (**45**, t_R: 14.5 min). Lastly, ancistroyafungine D (**46**, 2.5 mg) was obtained from Fraction 9 by isocratic 58% aqueous MeOH on HPLC at t_R: 12.1 min.

2.2.7. Characterization of Isolated Compounds

The characterization of the isolated naphthylisoquinoline alkaloids was done in collaboration with Dr. BK Lombe in Prof. G Bringmann's laboratory, in Würzburg.

a. Ancistroyafungine A (**43**)

Isolated as a beige amorphous solid: $[\alpha]_D^{25}$ +16.1 (*c* 0.10, MeOH). UV/Vis (MeOH): λ_{max} (logε): 204 (1.43), 231 (1.51), 306 (0.32), 321 (0.25), 335 (0.18) nm. ECD (MeOH): λ_{max} ($\Delta\varepsilon$): 196 (+17.4), 211 (-17.4), 217 (-14.9), 224 (-17.3), 239 (+18.2), 286 (-0.87), 307 (-0.84) nm. IR (ATM): ν_{max}: 3430, 1669, 1582, 1448, 1273, 1173, 1132, 830, 798, 719 cm^{-1}. ^1H and ^{13}C NMR data are

given in Table 2.1 and Section 2.3.2.1. HRESIMS: *m/z* 422.2333 $[M + H]^+$ (calculated for $C_{26}H_{32}NO_4$, 422.2326).

b. Ancistroyafungine B (**44**)

Isolated as a yellow amorphous solid: $[\alpha]_D^{25}$ +8.1 (*c* 0.40, MeOH). UV/Vis (MeOH): λ_{max} (logε): 206 (1.63), 231 (1.61), 306 (0.34), 321 (0.28), 336 (0.21) nm. ECD (MeOH): λ_{max} ($\Delta\varepsilon$): 192 (+8.8), 209 (-9.2), 216 (-6.9), 223 (-7.6), 238 (+10.8), 286 (-0.6) nm. IR (ATM): ν_{max}: 3372, 1671, 1583, 1448, 1364, 1173, 1273, 1196, 1134, 1093, 832, 799, 720 cm^{-1}. ^1H and ^{13}C NMR data are given in Table 2.1 and Section 2.3.2.2. HRESIMS: *m/z* 408.2173 $[M + H]^+$ (calculated for $C_{25}H_{30}NO_4$, 408.2169).

c. Ancistroyafungine C (**45**)

Beige amorphous solid: $[\alpha]_D^{25}$ -5.1 (*c* 0.43, MeOH). UV/Vis (MeOH): λ_{max} (logε): 206 (1.56), 231 (1.54), 306 (0.32), 321 (0.26), 336 (0.19) nm. ECD (MeOH): λ_{max} ($\Delta\varepsilon$): 201 (-10.4), 228 (+22.9), 243 (-8.3), 281 (+0.5) nm. IR (ATM): ν_{max}: 3388, 1671, 1583, 1451, 1316, 1274, 1273, 1199, 1133, 1093, 1061, 966, 832, 800, 720 cm^{-1}. ^1H and ^{13}C NMR data are given in Table 2.2 and Section 2.3.2.3. HRESIMS: *m/z* 436.2486 $[M + H]^+$ (calculated for $C_{27}H_{34}NO_4$, 436.2482).

d. Ancistroyafungine D (**46**)

Yellow amorphous solid: $[\alpha]_D^{25}$ +5.9 (*c* 0.41, MeOH). UV/Vis (MeOH): λ_{max} (logε): 204 (0.3), 230 (0.22), 288 (0.05), 305 (0.04), 322 (0.03), 336 (0.03) nm. ECD (MeOH): λ_{max} ($\Delta\varepsilon$): 200 (-7.2), 227 (+18.8), 241 (-8.6), 284 (+0.3) nm. IR (ATM): ν_{max}: 3431, 1673, 1584, 1450, 1364, 1316, 1273, 1200, 1134, 834, 800, 720 cm^{-1}. ^1H and ^{13}C NMR data are given in Table 2.2 and Section 2.3.2.4. HRESIMS: *m/z* 408.2168 $[M + H]^+$ (calculated for $C_{25}H_{30}NO_4$, 408.2169).

e. Known Naphthylisoquinoline Alkaloids Isolated

Along with the above new alkaloids, eleven known naphthylisoquinoline alkaloids were isolated in collaboration with Dr. BK Lombe in Prof. G

Bringmann's laboratory, in Würzburg, and identified, *viz*., 6-*O*-methylhamatine (**47**) [14, 57, 69, 70], 4′-*O*-demethylancistrocladine (**48**) [58, 69, 71], ancistroguineine A (**47**) [41], ancistrobertsonine A (**50**) [47], ancistrobrevine B (**19**) [48, 72], ancistrotectoriline A (**51**) [55, 56, 73, 74], 6,5′-*O*,*O*-didemethylancistroealaine A (**52**) [57], 6-*O*-demethylancistroealaine A (**53**) [57], 7-*epi*-ancistrobrevine D (**54**) [49, 75], and ancistrocladinium A (**55**) [15, 61] and B (**56**) [15, 57, 58, 76], by means of spectroscopic, physical, and/or chromatographic technics and comparison with the previously reported data.

2.2.8. Oxidative Degradation

This procedure was carried out by Mrs M Michel and Mrs S Fayez in Prof. G Bringmann's laboratory in Würzburg, as described by G Bringmann *et al*. [32]. Briefly, ca. 0.5 mg of the respective alkaloid was subjected to a ruthenium (III)-catalyzed periodate oxidation, followed by derivatization of the resulting aminoacids with MeOH/HCl and (*R*)-*α*-methoxy-*α*-trifluoromethylphenylacetyl chloride [(*R*)-MTPA-Cl, which was prepared from (*S*)-MTPA]. The resulting derivatized amino acids (*R/S*)-*N*-methyl-3-aminobutyric acid and (*R/S*)-3-aminobutyric acid were analyzed by GC-MSD along with standards isolated previously.

2.2.9. Antiausterity Assay

The evaluation of antiausterity properties of isolated naphthylisoquinolines was conducted by Prof. S Awale's group at the University of Toyama in Japan, through a collaboration project of the University of Pretoria, the University of Würzburg (Germany), and the Division of Natural Drug Discovery, Institute of Natural Medicine at University of Toyoma in Japan. The procedure [16] is described below.

The human pancreatic cancer cell line PANC-1 (RBRC-RCB2095, Tsukuba, Japan) was purchased from the Riken BRC cell bank, and maintained in the standard Dulbecco's modified Eagle's medium (DMEM) with 10% fetal bovine serum (FBS) supplement under a humidified atmosphere of 5% CO_2 in an incubator at 37 °C. For the antiausterity evaluation, exponentially growing

cells were seeded in 96-well plates (1.5 x 10^4 well) in DMEM, and incubated for 24 h for the cell attachment. After this incubation time, the cells were washed twice with PBS, the medium was changed to serially diluted test samples in both, DMEM and NDM (nutrient-deprived medium), with a control and a blank in each test plate. Arctigenin, isolated from the seeds of *Arctium lappa* [77], was used as the positive control. The composition of the NDM was as follow: 0.1 mg/l $Fe(NO_3)_3$ (9 H_2O), 265 mg/l $CaCl_2$ (2 H_2O), 400 mg/l KCl, 200 mg/l $MgSO_4$ (7 H_2O), 6400 mg/l NaCl, 700 mg/l $NaHCO_3$, 125 mg/l NaH_2PO_4, 15 mg/l phenol red, 25 mM/l HEPES buffer (pH 7.4), and MEM vitamin solution (Life Technologies, Inc., Rockville, MD, USA); the final pH was adjusted to 7.4 with 10% aqueous $NaHCO_3$. After 24 h of incubation with the respective test compound in DMEM and NDM, the cells were washed twice with PBS, and replaced by 100 µl of DMEM containing 10% WST-8 cell counting kit solution. After 3 h of incubation, the absorbance at 450 nm was measured on an EnSpire Multimode plate reader (Perkin Elmer, Inc., Waltham, MA, USA). Cell viabilities were calculated from the mean values from three wells using the following equation:

$$Cell\ viability = \left[(Abs_{test\ sample} - Abs_{blank})/(Abs_{control} - Abs_{blank})\right] \times 100$$

2.3. Results and Discussion

2.3.1. Description of the Collected Plant

The liana studied in this thesis grows in a secondary forest, seasonally invaded by the river Congo waters. The underwood soil is always humid even when the waters recede back to the river. The underwood is not cluttered, but the summit is so bushy that sunlight does not reach the soil well. The collection site is threatened by agricultural activities, mainly rice cultivation.

The collected liana was 10 to 15 m long and 6 to 8 cm of diameter. The sub-sessile leaves were up to 38 cm long and 12 cm wide (Figure 2.11), those of the floriferous branches were elliptic, elliptic ob-oval or closely elliptic ob-oval, shrunk to the basis then large, obtuse, and sharp or finished sometimes by a short 0.5-cm long acumen with 8 to 14 secondary rib pairs (Figure 2.11). Flowers were of 8 to 10 mm of diameter spread (Figure 2.11); pedicel were of 3 to 4 mm of total length, articulate to the third superior, little or non accrescent; sepals of 3-5 mm long and 2 to 3 mm wide, green; petals of 2.0 to 2.5 mm long and of large, sallow; ten stamens. A voucher specimen (No. 106) was deposited at the Herbarium Bringmann, University of Würzburg.

Figure 2.11: *A floriferous twig and leaves of Ancistrocladus collected at Yafunga Rive. Photo: S. Muyisa*

2.3.2. Structural Elucidation of Isolated Naphthylisoquinolines

Four new naphthylisoquinoline alkaloids, the 5,8'-coupled ancistroyafungines A-C (**43**-**45**), and the 5,1'-linked ancistroyafungine D (**46**), were isolated and structurally elucidated, in collaboration with Dr. BK Lombe in Prof. G Bringmann's laboratory, from the stem bark of an as yet unidentified *Ancistrocladus* (Ancistrocladaceae) liana recently discovered by the author of this thesis near the village Yafunga, in the North-Central region of the Democratic Republic of the Congo. Along with the four new compounds, eleven previously identified compounds **19** and **47-56** from related African and Asian *Ancistrocladus* species were also isolated and structurally elucidated also in collaboration with Dr. BK Lombe in Prof. G Bringmann's laboratory (Figure 2.12).

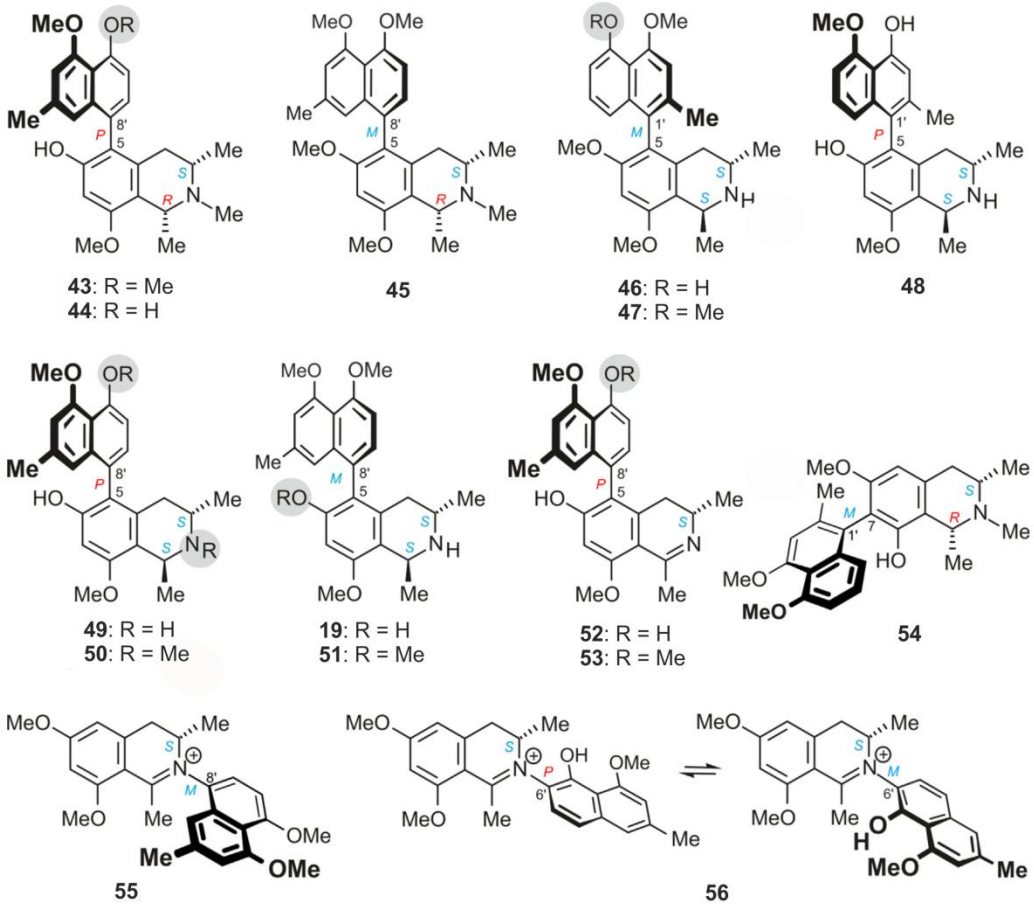

Figure 2.12: *Structures of the naphthylisoquinoline alkaloids **19** and **43-56** isolated from the Congolese Ancistrocladus species investigated*

2.3.2.1. Structural Elucidation of Ancistroyafungine A (**43**)

a. Spectroscopic Characteristics

The molecular formula of the first new metabolite was $C_{26}H_{31}NO_4$, as determined from its monoprotonated ion at *m/z* 422.2333 by HRESIMS as well as from the number of signals in the in the ^{13}C NMR spectra, which, combined with the UV spectrum, suggested it to be a naphthyltetrahydroisoquinoline alkaloid. This was further corroborated by its ^1H NMR spectrum (Table 2.1). Its aliphatic region exhibited a quartet for H-1 (δ_H 4.65), a multiplet for H-3, (δ_H 4.65), two diastereotopic protons H-4_{ax} [δ_H 2.58 (J = 17.2, 11.5Hz)] and H-4_{eq} [δ_H 2.21, (J =17.2, 3.1 Hz)], and three *O*-methyl groups (δ_H 3.92, 3.93, and 3.96). Likewise, two three-proton doublets (δ_H 1.26 and 1.72) were observed in that aliphatic part of the spectra, characteristic of Me-3 and Me-1, and two three-proton singlets: one at 2.31 ppm, suggesting an aryl-methyl group (Me-2′), and the other one at 3.02 ppm, indicating the presence of an *N*-methyl group. In the aromatic region of the spectrum, the presence of two *meta*-coupled protons (δ_H 6.69 and 6.79, J = 0.9 Hz), together with one singlet (δ_H 6.60), and an AB spin system (δ_H 6.94 and 7.16, J = 7.9 Hz), demonstrated the coupling axis of the naphthalene moiety to be located at either C-8′ or C-6′.

The C-6′ coupling possibility was excluded based on the fact that one of the AB spin system protons (the doublet signal at 6.79 ppm) was proven to be at C-6′ by HMBC correlations from both, H-6′ and OMe-5′ to the carbon atom C-5′, so that the biaryl axis in this molecular portion had to be located at C-8′ (Figure 2.10).

The coupling position in the isoquinoline part was deduced to be C-5, from the joint HMBC correlations of the diastereotopic protons (H-4_{ax} and H-4_{eq}), and H-7′ with C-5. These interactions were confirmed by another long-range HMBC coupling between the same carbon atom (C-5) and the aromatic singlet proton H-7.

Table 2.1: ^{1}H (400 MHz) and ^{13}C (100 MHz) NMR data of ancistroyafungine A (**43**) and B (**44**)

Position	**43**		**44**	
	δ_H (*J* in Hz)	δ_C	δ_H (*J* in Hz)	δ_C
1	4.65, q (6.6)	62.4	4.65, q (6.4)	62.3
3	3.16, m	60.9	3.16, m	60.5
4_{ax}	2.58, dd (17.2, 11.5)	34.3	2.57, dd (17.3, 11.4)	34.3
4_{eq}	2.21, dd (17.3, 3.1)	34.3	2.22, dd (17.3, 3.1)	
5		120.3		119.9
6		158.0		158.1
7	6.60, s	99.2	6.59, s	99.1
8		157.6		157.7
9		114.3		114.5
10		134.7		134.9
1′	6.69, s	118.5	6.69, t (1.1)	119.2
2′		137.6		137.8
3′	6.79, s	110.5	6.81, s	107.8
4′		158.9		157.4
5′		158.6		156.1
6′	6.94, d (7.9)	106.9	6.80, d (7.9)	110.5
7′	7.16, d (7.9)	131.5	7.10, d (7.9)	132.1
8′		126.3		124.3
9′		137.7		137.0
10′		117.6		115.0
1-Me	1.72, d (6.5)	20.0	1.72, d (6.6)	20.0
3-Me	1.26, d (6.5)	18.0	1.27, d (6.6)	18.1
2′-Me	2.31, s	22.5	2.32, d (0.7)	22.3
8-OMe	3.92, s	56.2	3.91, s	56.2
4′-OMe	3.93, s	57.1	4.09, s	56.9
5′-OMe	3.96, s	56.9		
N-Me	3.02, s	41.9	3.03, s	41.5

The aforementioned proton NMR aliphatic feature indicated the presence of an *N*-methyl group, which was further confirmed by the deshielded chemical shift of the carbon signal corresponding to the methyl group (δ_C 41.9), as well as by the HMBC cross-peaks between the *N*-methyl protons and both, C-1 and C-3 (Figure 2.13).

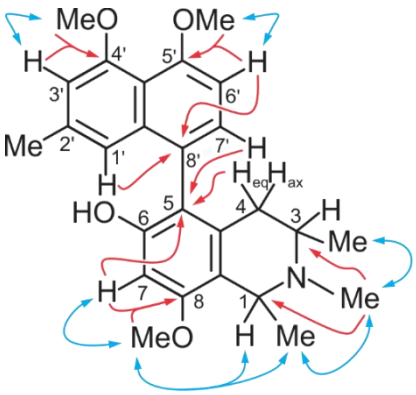

Figure 2.13: *Selected HMBC (red single arrows) and NOESY (blue double arrows) indicative of the constitution of ancistroyafungine A (**43**)*

Further HMBC signals involving a methoxy group at 3.92 ppm, the protons H-7, and H-1, all of them interacting with a deshielded quaternary carbon at 157.6 ppm, confirmed the latter nuclei to be C-8, to which that *O*-methyl substituent was attached. The remaining, third *O*-methyl group (δ_H 3.93 ppm) was assigned to be located at C-4′, based on its ROESY interactions with H-3′ and the joint HMBC correlations of the 4′-*O*-methyl protons and H-3′ with C-4′ (Figure 2.13).

b. The Absolute Configuration

The relative configuration at the stereocenters C-1 and C-3 was deducted to be *cis* from NOESY interactions between H-1 and H-3 (Figure 2.11A). Ruthenium-mediated oxidative degradation [32] of the compound yielded *N*-methyl-3-aminobutyric acid (**57**) exclusively as its *S*-enantiomer (Scheme 2.3), as assessed by GC-MSD analysis of its Mosher derivatives. This unambiguously indicated that the stereocenter C-3 of the alkaloid was *S*-configured, and given the above-assigned *cis*-array of the two methyl groups at the chiral centers, C-1 was deduced to be *R*-configured.

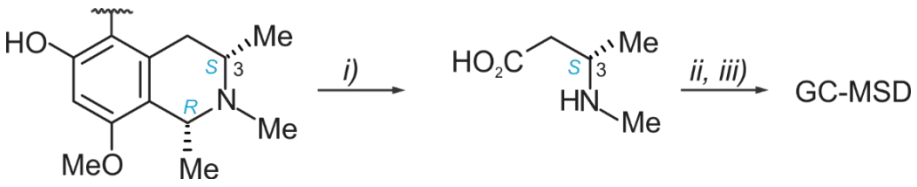

57

Scheme 2.3: *Oxidative degradation of **43** and **44**, and analysis of the resulting amino acids for the determination of the absolute configuration of naphthylisoquinoline alkaloids after esterification and derivatization: i) $RuCl_3$, $NaIO_4$; ii) MeOH, $SOCl_2$, iii) '(R)-MTPA-Cl' {'(R)-Mosher's chloride'* [32]*}, NEt_3. (MTPA: α-methoxy-α-trifluoromethylphenylacetic acid)*

In NOESY experiments, correlations between the equatorial proton at C-4 and the aromatic proton at C-1′ were observed (Figure 2.14A). This through-space correlations showed the involved spin systems (H-4_{eq} and H-1′) to be on the same side of the isoquinoline plane, which when combined with the already established *S*-configuration at C-3, should be the upper face, as illustrated in Figure 2.14A, so that the configuration at the biaryl axis should be *P*.

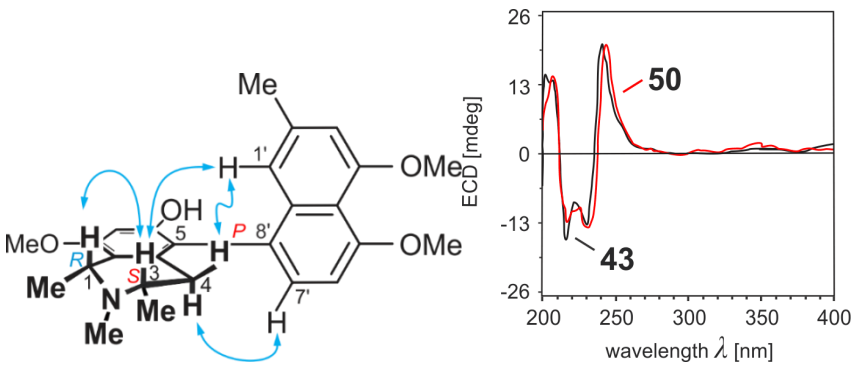

A B

Figure 2.14: *Configuration at the biaryl axis of ancistroyafungine A (**43**) relative to the stereogenic center through NOE interactions (A), and ECD spectra of **43** and ancistrobertsonine A (**50**) (B), both recorded in MeOH*

This stereochemical assignment was further corroborated by the complementary dipolar coupling of H-4_{ax} with H-7′, both underneath, *i.e.*, on

the bottom side of the isoquinoline plane (Figure 2.14A). This was further confirmed by the ECD curve of this compound, which was very similar to that of the likewise *P*-configured co-isolated alkaloid ancistrobertsonine A (**50**) (Figure 2.14B). Therefore, the isolated metabolite had the absolute stereostructure **43** (Figure 2.12), and was given the name ancistroyafungine A, after the Congolese village Yafunga, where the plant material was collected. The metabolite **43** may also be referred to as the 6-*O*-demethylated analogue of ancistrobertsonine C [48] or as the 1-epimer of ancistrobertsonine A (**50**) [47].

2.3.2.2. Structural Elucidation of Ancistroyafungine B (**44**)

a. Spectroscopic Features

The second new metabolite had the molecular formula $C_{25}H_{29}NO_4$, as deducted from HRESIMS measurement (*m/z* 408.2167 $[M + H]^+$). Its ^{1}H NMR spectrum (Table 2.1) was very similar to that of ancistroyafungine A (**43**), except for the fact that it had two methoxy groups (δ_H 4.09 and 3.91), *i.e.*, one *O*-methyl signal less than **43**, which indicated that it was an *O*-demethylated analog of **43**. The missing *O*-methyl group, as compared to **43**, was presumed to be the one at *O*-5′, based on the fact that, while superposing the proton NMR spectrum of **9** and that of the new alkaloid, the signal of H-6 of both appeared to be the most affected one among all aromatic protons ($\Delta\delta_{H\text{-}6}$ = 0.13 and $\Delta\delta$ of other protons ≤ 0.06 unit; Figure 2.15 and Table 2.1).

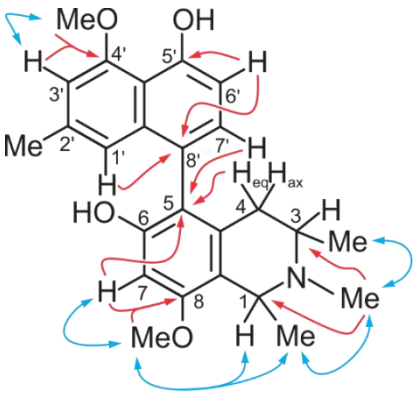

Figure 2.15: *Selected HMBC (red single arrows) and NOESY (blue double arrows) indicative of the constitution of ancistroyafungine B (**44**)*

Further analysis of the 1D and 2D NMR spectra of the second new metabolite corroborated the above deduced constitution, being similar to that of **43** (Figure 2.15), but with a free phenolic hydroxy function at C-5′, instead of a methoxy group.

b. The Absolute Configuration

In the NOESY experiment, the interactions of the protons at C-1 and C-3, and of those across the biaryl axis, were all similar to that of ancistroyafungine A (**43**): H-1 interacted with H-3, H-4_{ax} with H-1′, and H-4_{eq} with H-7′, so that the full absolute configuration of the isolated alkaloid would be either 1*R*, 3*S*, 5*P*, similar as for compound **43**, or 1*S*, 3*R*, 5*M*, *i.e.*, fully opposite to it.

The oxidative degradation, which produced (*S*)-*N*-methyl-3-amino-butyric acid similar to compound **43**, showed C-3 to be *S*-configured, and the overall absolute configuration consequently had to be 1*R*, 3*S*, 5*P*, *i.e*. the same as that of **43**. This configuration was further confirmed by the almost perfect similarity of the ECD curves of the isolated alkaloid with that of ancistroyafungine A (**43**) (Figure 2.16B).

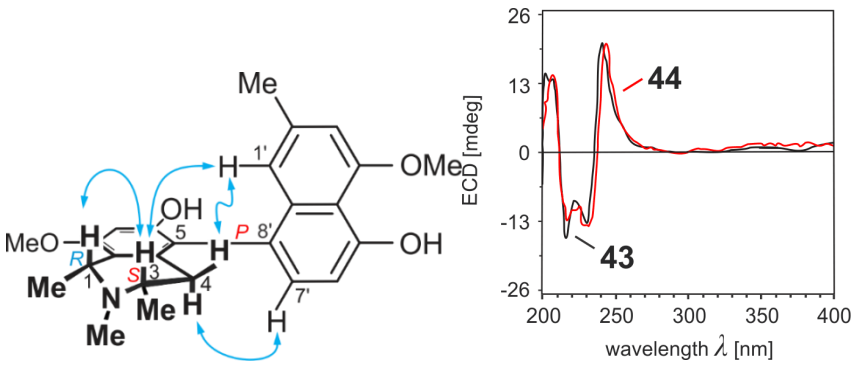

A B

Figure 2.16: *Configuration at the biaryl axis of ancistroyafungine B (**44**) relative to the stereogenic center through NOE interactions (A), and ECD spectra of compound **44** and ancistroyafungine A (**43**) (B), both recorded in MeOH*

Hence, the second new alkaloid had the absolute stereostructure of compound **44** as given in Figure 2.12. It was, then, the 5′-*O*-demethyl analogue of **43**, and was given the name of ancistroyafungine B. It could likewise be named as 8-*O*-methylkorupensamine D [78].

2.3.2.3. Structural Elucidation of Ancistroyafungine C (45)

a. Spectroscopic Pattern

Compound **45**, the third unreported metabolite, had 14 mass units more than ancistroyafungine A (**43**), having the molecular formula $C_{27}H_{33}NO_4$ (HRESIMS *m/z* 436.2486 $[M + H]^+$), which suggested the presence of a fully *O*- and *N*-methylated naphthyltetrahydroisoquinoline alkaloid. Its ^{1}H NMR spectrum pattern (Table 2.2) showed the presence of an AB spin system {H-6′ (δ_H 6.91, J = 8.5 Hz) and H-7′ (δ_H 7.10, J = 8.0 Hz)}, and an aryl methyl singlet at 2.30 ppm, evidencing this alkaloid also to be 5,8′-coupled (Figure 2.17), as already determined for ancistroyafungines A (**43**) and B (**44**).

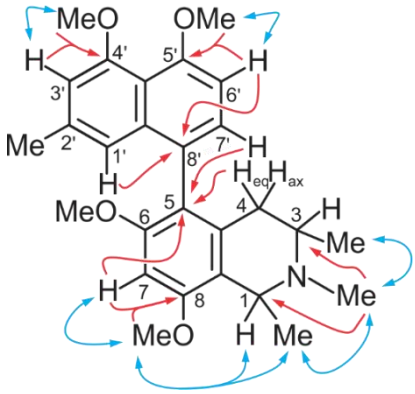

Figure 2.17: *Selected HMBC (red single arrows) and NOESY (blue double arrows) indicative of the constitution of ancistroyafungine C (**45**)*

This was confirmed by joint HMBC correlations from H-4_{eq} {δ_H 2.49 (*J* = 17.8, 3.5 Hz)}, H-7 (δ_H 6.79), and H-7′ to C-5 (δC 122.0) (Figure 2.14).

b. The Absolute Configuration

As in the case of ancistroyafungines A (**43**) and B (**44**), from NOESY interactions between H-1 and H-3, the relative configuration at the stereocenters C-1 *versus* C-3 of that naphthylisoquinoline alkaloid was determined to be *cis* (Figure 2.18A). Likewise similar to **43** and **44** was the result of the oxidative degradation, which produced (*S*)-*N*-methyl-3-aminobutyric acid too, showing that C-3 was *S*-configured, and C-1 *R*-configured, as a consequence of the above mentioned *cis*-configuration. However, the interactions across the biaryl axis were opposite to those observed in **43** and **44,** as H-4_{eq} interacted with H-7′, and H-4_{ax} with H-1′, indicating that the axial configuration of the compound to be also opposite, *i.e. M*, as shown in Figure 2.18A.

This was strongly supported by its negative ECD couplet, as expected for an *M*-array, which was very similar to that of the co-occurring, likewise *M*-configured ancistrotectoriline A (**51**) (Figure 2.18B).

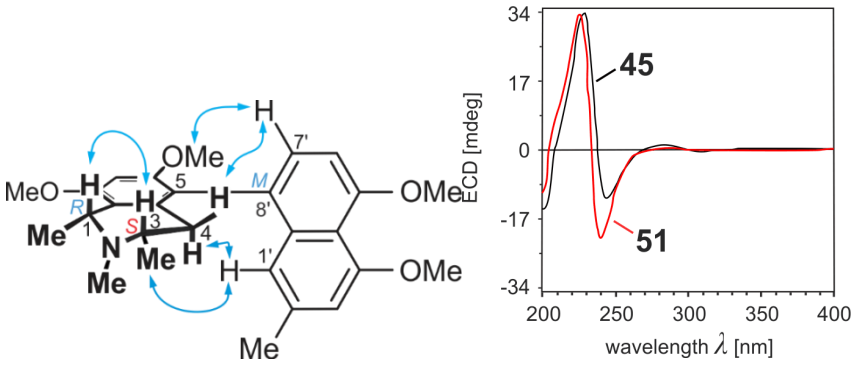

A B

Figure 2.18: *Configuration at the biaryl axis of ancistroyafungine C (**45**) relative to the stereogenic center through NOE interactions (A), and ECD spectra of **45** (B) and ancistrotectoriline A (**51**), both recorded in MeOH*

This metabolite was hence assigned the new absolute stereostructure of **45**, as presented in Figure 2.12, and was named ancistroyafungine C, in continuation of the series of new alkaloids isolated from this as yet unknown Congolese *Ancistrocladus* liana. It was, therefore, the atropo-diastereomer of the known ancistrobertsonine C (**24**) isolated from the Kenyan plant *A. robertsoniorum* J. LÉONARD [48].

Table 2.2: ^{1}H (400 MHz) and ^{13}C (100 MHz) NMR data of ancistroyafungine C (**45**) and D (**46**)

Position	**45**		**46**	
	δ_H (*J* in Hz)	δ_C, type	δ_H (*J* in Hz)	δ_C, type
1	4.67, q (6.4)	61.9	4.80, q (6.8)	48.9
3	3.23, m	60.2	3.70, m	45.1
4ax	2.35, dd (17.3, 11.0)	33.1	2.10, dd (18.0, 11.3)	32.9
4eq	2.49, dd (17.3, 3.3)		2.42, dd (17.3, 4.8)	
5		122.0		120.5
6		160.0		159.7
7	6.79, s	96.2	6.78, s	95.6
8		157.9		158.1
9		114.9		115.2
10		134.8		132.9
1′	6.65, t (0.9)	118.4		126.6
2′		138.0		136.1
3′	6.78, d (1.2)	109.9	6.92, s	108.1
4′		158.9		157.1
5′		158.3		156.3
6′	6.91, d (8.1)	106.7	6.70, dd (7.7, 1.0)	110.5
7′	7.10, d (8.1)	130.2	7.11, dd (8.4, 7.7)	128.9
8′		126.5	6.53, dd (8.4, 1.0)	116.9
9′		138.0		137.3
10′		117.6		115.2
1-Me	1.77, d (6.5)	20.1	1.64, d (6.9)	18.7
3-Me	1.29, d (6.7)	18.1	1.20, d (6.4)	19.3
2′-Me	2.30, d (0.7)	22.2	2.09, s	20.7
6-OMe	3.69, s	56.5	3.68, s	56.4
8-OMe	4.00, s	56.4	4.01, s	56.4
4′-OMe	3.93, s	57.1	4.12, s	56.9
5′-OMe	3.95, s	56.9		
N-Me	3.02, s	41.6		

2.3.2.4. Structural Elucidation of Ancistroyafungine D (**46**)

a. Spectroscopic Pattern

The fourth new compound discovered as part of the study was found to be isomeric to ancistroyafungine B (**44**) as revealed by from HRESIMS measurement ($C_{25}H_{29}NO_4$, m/z 408.2168 $[M + H]^+$). Its ^{1}H NMR spectrum (Table 2.2) exhibited an aromatic proton system of two singlets (δ_H 6.92 and 6.78), and an AMX spin system {δ_H 7.11 (*J* = 7.7, 8.4 Hz), 6.70 (*J* = 1.0, 7.7

Hz), 6.54 (*J* = 1.1, 8.4 Hz), which suggested four coupling possibilities: 7,1′-, 7,3′-, 5,1′-, or 5,3′-coupled naphthylisoquinoline alkaloid. In the aliphatic part, the Me-3 doublet signal appeared upfield (1.20 ppm), similar to compounds **43**-**45**, suggesting the location of the biaryl axis in the isoquinoline portion to be at C-5, and not at C-7 as in the co-isolated compound **54** (Figure 2.12), in which the ring current of the naphthalene substituent would have affected Me-3 only marginally. In accordance with the above-mentioned information, one aromatic singlet was assigned to be at H-7, based on the joint HBMC correlations of both H-7 and H-1 with an *O*-substituted aromatic carbon atom, C-8 (Figure 2.19).

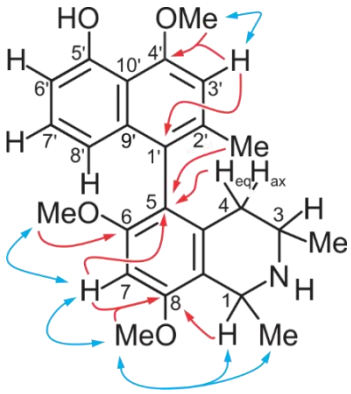

Figure 2.19: *Selected HMBC (red single arrows) and NOESY (blue double arrows) indicative of the constitution of ancistroyafungine D (**46**)*

Through its NOESY interactions with one of the three *O*-methyl groups displayed by this compound, the other aromatic singlet was deduced to be located at H-3′, and was complemented by joint HMBC interactions from these nuclei (OMe-4′ and H-3′) to C-4′. Therefore, this new compound, different from the three afore described new alkaloids, belonged to the subclass of 5,1′-coupled naphthylisoquinolines (Figure 2.19). The two remaining methoxy groups were assigned at C-6 and C-8, based on the joint HMBC cross peaks from OMe-6 and H-7 to C-6, and from H-7, H-1, and OMe-8 to C-8. This was confirmed by the NOESY interactions of OMe-6 with H-7, and that of OMe-8 and Me-1.

b. The Absolute Configuration

The NOE interaction between H-3 and Me-1 allowed the deduction of the relative configuration at the stereocenters C-1 *versus* C-3 to be *trans* (Figure 2.20A). The oxidative degradation of the compound produced the *S*-enantiomer of 3-aminobutyric acid, which revealed that C-3 was *S*-configured. Given the above-mentioned *trans*-arrangement of the methyl groups at the chiral centers, C-1 had to be *S*-configured, too (Figure 2.20A).

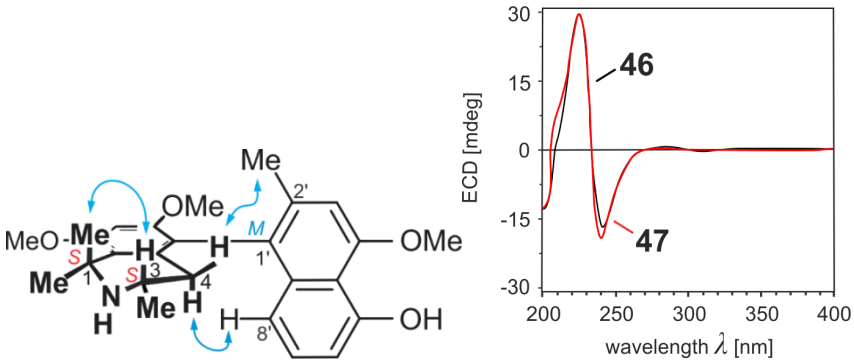

A B

Figure 2.20: *Configuration at the biaryl axis of ancistroyafungine D (**46**) relative to the stereogenic center through NOE interactions (A), and ECD spectra of **46** and 6-O-methylhamatine (**47**), both recorded in MeOH (B)*

From NOESY interactions between H-8′ and H_{ax}-4, the naphthalene-isoquinoline biaryl axis was shown to be *M*-configured (Figure 2.17A). The excellent matching of the ECD curve of this naphthylisoquinoline alkaloid with that of the known [57] and co-isolated, 1*S*,3*S*,5*M*-configured 6-*O*-methylhamatine (**47**) (Figure 2.20B) confirmed the stereochemical assignment at the biaryl axis (Figure 2.20A). The compound had the absolute stereostructure of **46**, as presented in Figure 2.12. Hence, it was the new 5′-*O*-demethyl-6-*O*-methyl analogue of the well-known alkaloid hamatine isolated earlier from various African and Asian Ancistrocladus species [49, 53, 69]. The new compound was named ancistroyafungine D.

2.3.2.5. Structural Elucidation of Known Naphthylisoquinoline Alkaloids

Along with the four new naphthylisoquinoline alkaloids, **43**, **44**, **45,** and **46**, eleven well-known monomeric naphthylisoquinoline alkaloids were isolated from the collected *Ancistrocladus* species, and identified as 6-*O*-methylhamatine (**47**) [14, 57, 69, 70], 4′-*O*-demethylancistrocladine (**48**) [58, 69, 71], ancistroguineine A (**49**) [41], ancistrobertsonine A (**50**) [47], ancistrobrevine B (**19**) [48, 72], ancistrotectoriline A (**51**) [55, 56, 73, 74], 6,5′-*O*,*O*-didemethylancistroealaine A (**52**) [57], 6-*O*-demethylancistroealaine A (**53**) [57], 7-*epi*-ancistrobrevine D (**54**) [49, 75], and ancistrocladinium A (**55**) [15, 61] and B (**56**) [15, 57, 58, 76], the confirmation of their structures was achieved by means of HPLC-MS, HPLC co-elution, and by comparison of NMR, and optical rotation data with those of authentic samples, previously obtained by isolation or synthesis. Their structures are shown in Figure 2.12. The tables of comparison of their ^{1}H and ^{13}C NMR data with those reported for the known compounds are provided in the Supplementary Information Section.

2.3.3. Geo-Chemotaxonomic Considerations

The information collected from the stereostructures of the naphthylisoquinoline alkaloids isolated from this as yet unreported Congolese *Ancistrocladus* liana reveals many pertinent aspects. The phytochemical results presented here sustain the already evoked preliminary hints at the absence of dimeric compounds, and strongly support the initial detection of alkaloids with an exclusive *S*-configuration at C-3 in the alkaloid-enriched plant extract. The findings now clearly show a chemotaxonomical demarcation of this liana from its morphologically related species, *A. congolensis,* despite the fact that both contained the characteristic alkaloid ancistrocladinium B (Figure 2.21), and from all the other botanically recognized Congolese *Ancistrocladus* taxa, since they produce 3*R*- and 3*S*-configured alkaloids, and a number of dimers [52, 55, 66, 69, 79]. This delineation is further highlighted by the variety of isolated compounds, showing five different coupling types, *viz*. 5,8′; 5,1′; 7,1′; *N*,6′, and *N*,8′, a

structural diversity that none of the known Congolese species had shown so far.

Moreover, all of the 15 isolated metabolites possessed an oxygen function at C-6, which, together with the 3*S*-configuration, placed them into the subclass of “Ancistrocladaceae-type” alkaloids [20], typical of *Ancistrocladus* lianas from Asia and East Africa [20, 21]. Thus, from a chemotaxonomic point of view, the investigated liana appeared to occupy a special phylogenetic position, it ranged between the naphthylisoquinoline-producing species from Asia and East Africa and the *Ancistrocladus* lianas from the Congo Basin; with the latter plants it shared morphological similarities.

Apart from the plant investigated here, only one other liana, likewise yet undescribed and morphologically related to *A. congolensis* [57], had so far been found to occupy a similar position as a geo- and chemotaxonomic link between the central African species and the east African taxa, with distinct similarities in particular to *A. robertsoniorum* from Kenya. From the latter, and from those two as yet unidentified Congolese species, a series of 5,1′-linked naphthylisoquinoline alkaloids related to ancistrocladine (**11**) and hamatine had been isolated, along with a large number of 5,8′-coupled alkaloids [57]. Some of the metabolites discovered in the two unknown Congolese lianas are analogues of the two main constituents of *A. robertsoniorum*, *viz*., ancistrobertsonines A (**43**) and C (**45**).

But there are also clear differences in the metabolic profiles of those two as yet unidentified plants, as obvious from comparative HPLC-UV-MS investigations (the chromatograms are given in Figure 2.21) and, in particular, from the discovery of the new ancistroyafungines A-D (**43**-**46**) in the liana, as presented in this work.

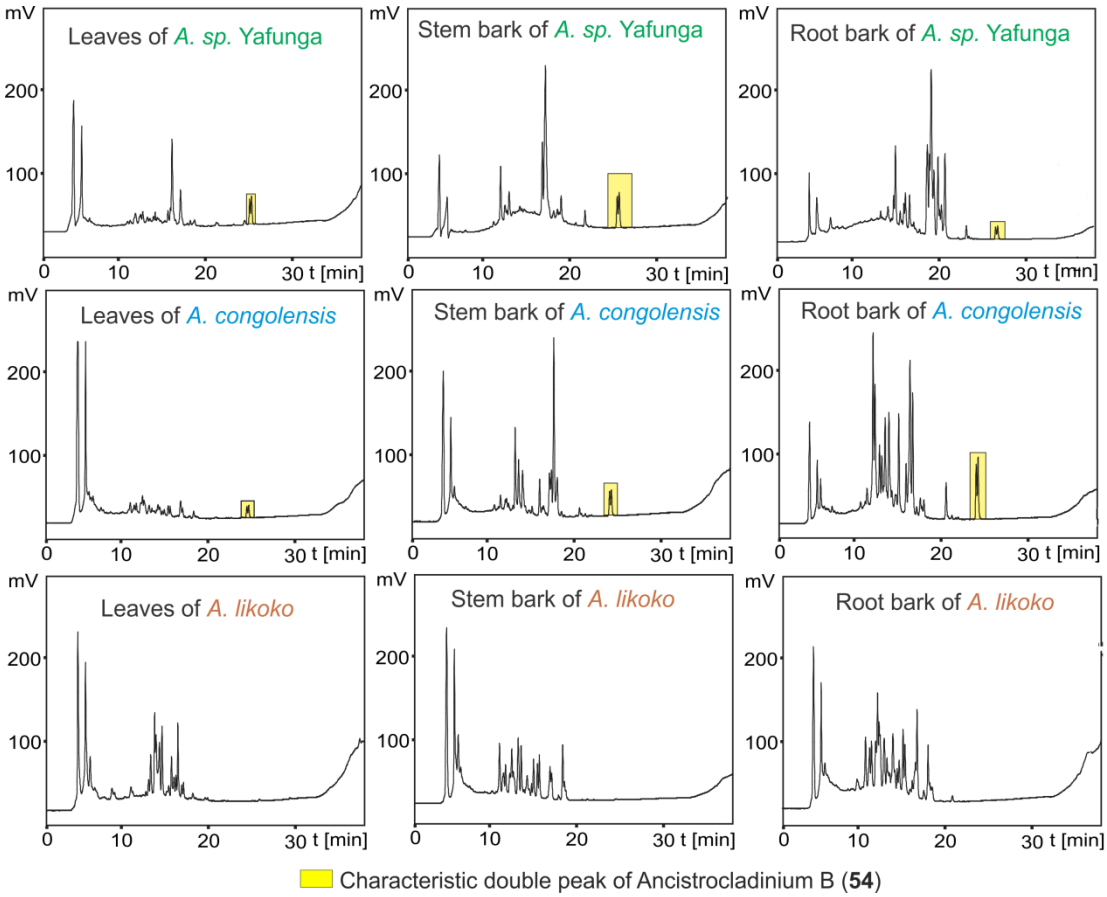

Figure 2.21: *HPLC profiles of the collected Ancistrocladus species (A. sp. Yafunga) compared to Ancistrocladus species collected in the same region*

This metabolic variance and the fact that the two unidentified plants occur in two different regions (one was found in the Central part of the Congo rainforest near the city of Ikela, and the other, the liana studied here, was discovered far away, in the North-Central Congolese village Yafunga) suggests that these lianas may represent different, but closely related new species or subspecies. Further botanical investigations need to be initiated to fully identify the species/subspecies.

2.3.4. Antiausterity Activity of the Isolated Metabolites against Human PANC-1 Pancreatic Cancer Cells

Antiausterity is an emerging approach in the field of anti-cancer drug development pursued by the group of Prof. S Awale in Japan in collaboration with the group of Prof. G Bringmann in Germany, aiming at the discovery of

new agents that inhibit the growth of cancer cells preferentially in nutrient-deprived medium (NDM) [77, 80-83]. This preferential cytotoxicity, also referred to as antiausterity activity, is given by PC_{50} values, *i.e.*, the concentration at which 50% of the pancreatic cancer cells are killed in NDM without displaying toxicity in normal, nutrient-rich Dulbecco's modified Eagle's medium (DMEM). Using this approach, some naphthylisoquinoline alkaloids have been identified as potent cytotoxic agents against human PANC-1 pancreatic cancer cells [12, 66, 79]. Given these promising results, and in order to gain more understanding on the anti-cancer potential of this class of natural products, the alkaloids **19** and **43-54** isolated during the phytochemical investigations reported in this work were evaluated for their antiausterity activities against human PANC-1 pancreatic cancer cells. The results for the anti-cancer activity are shown in Table 2.3.

Table 2.3: Preferential cytotoxicity of the naphthylisoquinoline alkaloids **19** and **43-54** against human pancreatic cancer PANC-1 cells in NDM

Compound	PC_{50}[a] (μM)	Compound	PC_{50}[a] (μM)
43	22.7	**50**	11.8
44	7.6	**19**	20.2
45	15.0	**51**	67.8
46	9.7	**52**	9.8
47	31.9	**53**	14.0
48	11.2	**54**	29.9
49	15.8	Arctigenin[b]	0.8

[a] Concentration at which 50% of the cells were killed preferentially in NDM.
[b] Used as a reference compound.

All the tested compounds displayed moderate to strong antiausterity activities against PANC-1 cancer cells, in a concentration-dependent manner (Figure 2.55). Their PC_{50} values were at a micromolar level, ranging from 7.6 to 67.8 μM. The new compounds ancistroyafungines B (**44**) and D (**46**) were the most potent representatives among this series of alkaloids, and their PC_{50} values (7.6 and 9.7 μM, respectively) were even similar to those of the most active reported monomeric alkaloids identified in previous investigations [12, 66].

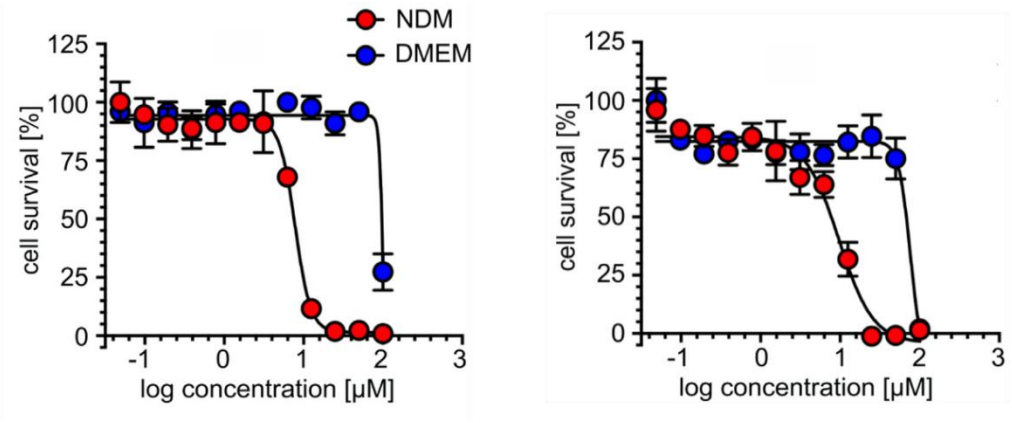

Figure 2.22: *Cytotoxic activities of (A) ancistroyafungine B (**44**) and (B) ancistroyafungine D (**46**) against the PANC-1 human pancreatic cancer cell line in nutrient-deprived medium (NDM) and in Dulbecco's modified Eagle's medium (DMEM)*

The biological assay results indicated that the degree of *O*-methylation in the naphthalene portion played an important role for the cytotoxic activities of the naphthylisoquinolines. Ancistroyafungine A (**43**) (PC_{50}, 22.7 µM), with two methoxy functions at C-5′ and C-4′, was found to be almost three times less active than its 5′-*O*-demethyl analogue ancistroyafungine B (**44**) (PC_{50}, 7.6 µM), which showed that an OMe/OH pattern seems favorable for the antiausterity activities. This tendency was also sustained by the activity of 6-*O*-methylhamatine (**47**) (PC_{50} = 31.9 µM), which was far less potent than that of its 5′-*O*-demethyl analogue ancistroyafungine D (**46**) (PC_{50} = 9.7 µM).

In a similar way, the substitution pattern of the isoquinoline portion seemed to play a crucial role for the cytotoxic activity of the alkaloids. This could be seen from the activity of ancistrobrevine B (**19**) (PC_{50}, 20.2 µM), possessing a mixed 6-OH/8-OMe substituted tetrahydroisoquinoline subunit, as compared to that of ancistrotectoriline A (**51**) (PC_{50}, 67.8 µM), possessing two methoxy groups at C-8 and C-6. This finding complemented previous results obtained for the two related alkaloids ancistrolikokines E and E_2 [66], yet both with *P*-configuration at the axis and *R*-configuration at C-3. The impact of stereochemical features on the preferential cytotoxicity thus proven was also

emphasised by the different PC_{50} values of the 1-epimers ancistroyafungine A (**43**) (PC_{50}, 22.7 μM) and ancistrobertsonine A (**50**) (PC_{50}, 11.8 μM).

The location of the biaryl axis was also another structural feature likewise showing a strong influence on the bioactivity: the cytotoxic effect of 6-*O*-methylhamatine (**47**) (PC_{50}, 31.9 μM), a 5,1′-coupled alkaloid, was more than two times stronger as compared to that of its 5,8′-coupled analogue ancistrotectoriline A (**51**) (PC_{50}, 67.8 μM). On the other hand, 6-*O*-methylhamatine (**47**) and ancistrotectoriline (**51**) could also be considered as regioisomers with respect to the methyl group at C-2′ (once being in the axis-bearing naphthalene ring of **47**, or once in the distant ring in the case of **51**).

The most active compound, ancistroyafungine B (**44**), was further investigated for its effects against PANC-1 cell morphology under nutrient-deprived conditions using the ethidium bromide (EB) acridine orange (AO) double-staining fluorescence assay. PANC-1 cells were treated with 20 μM of **44**, and incubated in NDM, along with an untreated control. After 24 h, both treated and untreated cells were stained with the EB/AO reagents as described previously [12]. AO emits bright green fluorescence in living cells, while EB is permeable only in dead or dying cells through ruptured cell membrane, and emits red fluorescence. As shown in Figure 2.23, control PANC-1 emitted bright green fluorescence with intact cell morphology.

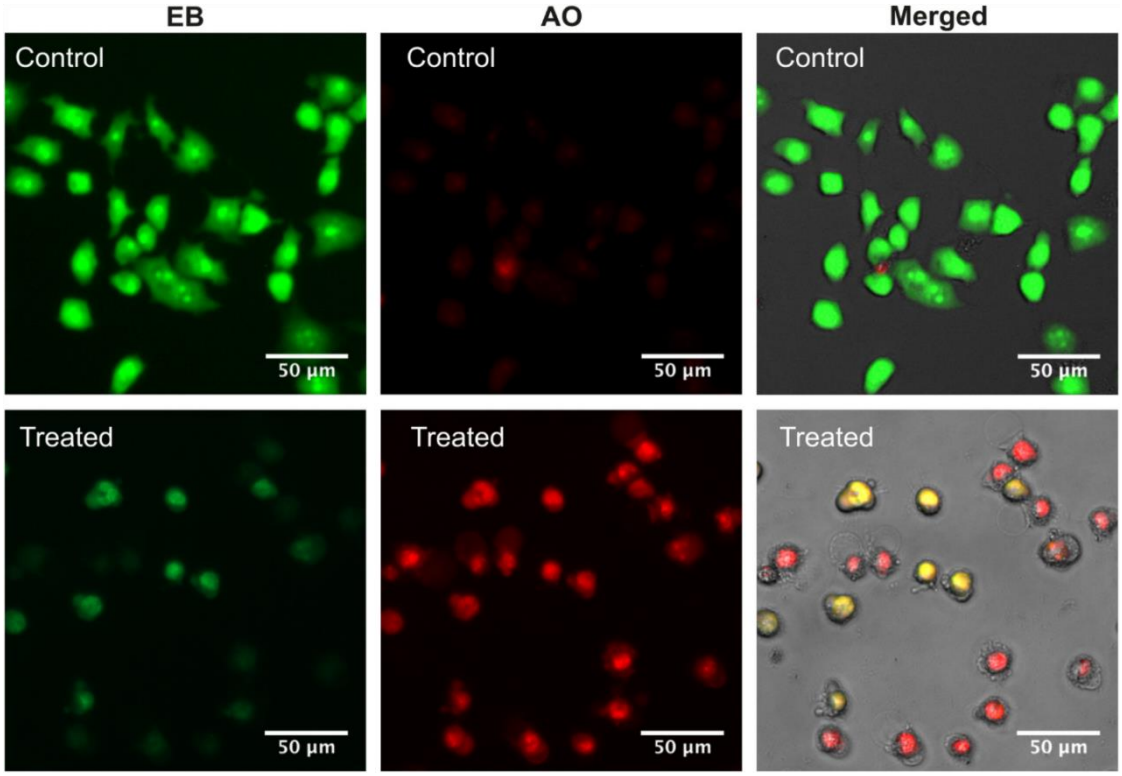

Figure 2.23: *Morphological changes of PANC-1 cells induced by 20 µM of ancistroyafungine B (**44**) in comparison with the untreated control*

However, those treated with 20 µM of ancistroyafungine B (**44**) emitted red fluorescence exclusively (Figure 2.23), with a dramatic change in PANC-1 cell morphology. Ancistroyafungine B (**44**) was further studied for its effects against PANC-1 cells in NDM in real time using a live-cell imaging system. PANC-1 cells were treated with 20 µM of the compound in NDM and incubated in a stage-top humidified incubator at 37 °C and 5% CO_2; images were captured every 10 min on an EVOS FL digital cell imaging system for 19 h. The dynamic responses of the PANC-1 cells against the treatment with the alkaloid 44 are given in the captures shown in Figure 2.24. PANC-1 cells at the start of the test (T_0) had an intact morphology. Within 4 h, the cells lost the membrane integrity, and showed membrane blebbing and rounding, followed by rupture of cell membrane, leading to total cell death within 10 h.

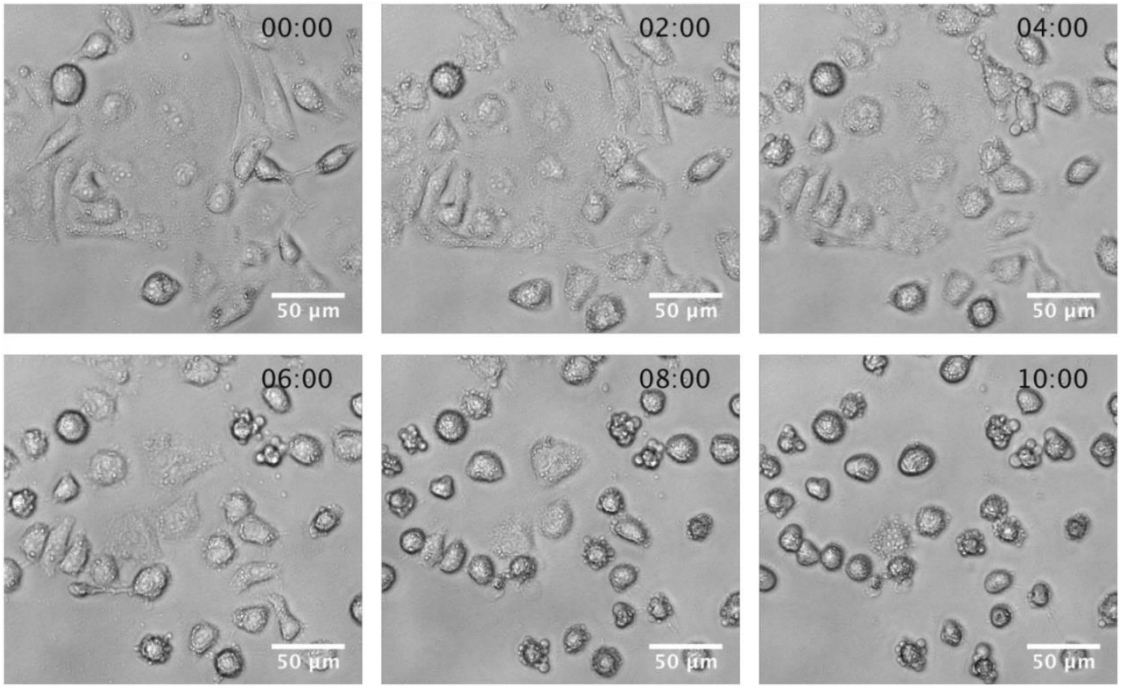

Figure 2.24: *Captures of the live imaging of the effect of 20 µM of ancistroyafungine B (**44**) on PANC-1 cells at different intervals of time (hour:minute)*

Based on the promising results obtained from this research done in Japan, and from previous studies, the preferential cytotoxicities of naphthylisoquinoline alkaloids against pancreatic cancer cells was demonstrated [12, 66, 79], thus suggesting that these natural products are promising lead structures for anti-cancer drug development. The metabolites of this as yet botanically unknown Congolese *Ancistrocladus* species, as presented here provide valuable information for the ongoing SAR (structure-activity relationship) investigations. Further, more-in-depth studies regarding the anti-cancer potential of naphthylisoquinolines are presently in progress.

2.4. Concluding Remarks

Four new naphthylisoquinoline alkaloids, the 5,8'-coupled ancistroyafungines A-C (**43-45**), and the 5,1'-linked ancistroyafungine D (**46**), were isolated, in collaboration with Prof. G Bringmann's group in Würzburg, from the stem bark of an as yet unidentified *Ancistrocladus* (Ancistrocladaceae) liana recently discovered near the village Yafunga, in the North-Central region of the Democratic Republic of the Congo. In addition, eleven previously identified compounds from related African and Asian *Ancistrocladus* species were isolated, exhibiting five different coupling types, *viz*., 5,8', 5,1', 7,1', *N*,6', and *N*,8'. All the isolated alkaloids were *S*-configured at C-3, and possessed an oxygen function at C-6 in the isoquinoline portion, thus belonging to the subclass of "Ancistrocladaceae-type" alkaloids.

This finding was geo- and chemotaxonomically remarkable, since apart from one other *Ancistrocladus* species from the Central Congo Basin, only South-East Asian and East African Ancistrocladaceae are known to exclusively produce naphthylisoquinolines with these structural features. Moreover, the alkaloid pattern of this Congolese liana clearly demarcated this plant from all other *Ancistrocladus* taxa that had so far been botanically described, which suggested that it might represent a new species or subspecies. As assessed by the group of Prof. S Awale in Japan, the new ancistroyafungines displayed strong to moderate preferential cytotoxic activities towards human PANC-1 pancreatic cancer cells in nutrient-deprived medium, without showing toxicity in normal, nutrient-rich conditions.

2.5. References

1. Lien L, Mai NC, Linh T, Giang VH, Trung L, Van NT, Ban N, Anh LDN, Kiem P, Minh CV: **Phylogenetic Analysis of *Ancistrocladus* Species (Ancistrocladaceae) from Vietnam**. *International Journal of Agriculture and Biology* 2017, **19**:1125-1130.
2. Cheek M: **A Synoptic Revision of *Ancistrocladus* (Ancistrocladaceae) in Africa, with a New Species from Western Cameroon**. *Kew Bulletin* 2000, **55**(4):871-882.
3. Turini GF, Steinert C, Heubl G, Bringmann G, Lombe BK, Mudogo V, Meimberg H: **Microsatellites Facilitate Species Delimitation in Congolese *Ancistrocladus* (Ancistrocladaceae), a Genus with Pharmacologically Potent Naphthylisoquinoline Alkaloids**. *Taxon* 2014, **63** (2):329-341.
4. Gereau ER: **Typification of Names in *Ancistrocladus* Wallich (Ancistrocladaceae)**. *Novon* 1997, **7**(3):242-245.
5. Thwaites GHK: **Note on the Genus *Ancistrocladus* of Wallich**. *Transactions of the Linnean Society of London* 1854, **21**(3):225-226.
6. Taylor CM, Gereau RE, Walters GM: **Revision of *Ancistrocladus* Wall. (Ancistrocladaceae)**. *Annals of the Missouri Botanical Garden* 2005, **92**:360-399.
7. Léonard J: **Flore d'Afrique Centrale (Zaïre-Rwanda-Burundi). Spermatophytes: Ancistrocladaceae**. *Bulletin de la Société Royale de Botanique de Belgique* 1949, **82**:27-40.
8. Porembski S: **Ancistrocladaceae. in: Kubitzki, K. (Editor), The Families and Genera of Vascular Plants, Flowering Plants: Dicotyledons; Malvales, Capparales and Non-Betalain Caryophyllales.** *Springer* 2002, **4**:25-27.
9. Rischer H, Heubl G, Meimberg H, Dreyer M, Hadi HA, Bringmann G: ***Ancistrocladus benomensis* (Ancistrocladaceae): A New Species from Peninsular Malaysia**. *Blumea* 2005, **50**:357-365.

10. Heubl G, Turini F, Mudogo V, Kajahn I, Bringmann G: ***Ancistrocladus ileboensis* (D.R.Congo), a New Liana with Unique Alkaloids**. *Plant Ecology and Evolution* 2010, **143**(1): 63-69.

11. Lombe BK, Bruhn T, Feineis D, Mudogo V, Brun R, Bringmann G: **Antiprotozoal Spirombandakamines A_1 and A_2, Fused Naphthylisoquinoline Dimers from a Congolese *Ancistrocladus* Plant**. *Organic Letters* 2017b, **19**(24):6740-6743.

12. Lombe BK, Feineis D, Mudogo V, Brun R, Awale S, Bringmann G: **Michellamines A_6 and A_7, and further Mono- and Dimeric Naphthylisoquinoline Alkaloids from a Congolese *Ancistrocladus* Liana and their Antiausterity Activities against Pancreatic Cancer Cells**. *The Royal Society of Chemistry Advances* 2018, **8**(10):5243-5254.

13. Bringmann G, Lombe BK, Steinert C, Ndjoko K Ioset, Brun R, Turini F, Heubl G, Mudogo V: **Mbandakamines A and B, Unsymmetrically Coupled Dimeric Naphthylisoquinoline Alkaloids, from a Congolese *Ancistrocladus* Species**. *Organic Letters* 2013, **15**(11):2590-2593.

14. Unger M, Dreyer M, Specker S, Laug S, Pelzing M, Neusüß C, Holzgrabe U, Bringmann G: **Analytical Characterisation of Crude Extracts from an African *Ancistrocladus* Species Using High-Performance Liquid Chromatography and Capillary Electrophoresis Coupled to Ion Trap Mass Spectrometry**. *Phytochemical Analysis* 2004, **15**:21-26.

15. Bringmann G, Kajahn I, Reichert M, Pedersen SEH, Faber JH, Gulder T, Brun R, Christensen SB, Ponte-Sucre A, Moll H, Heubl G, Mudogo V: **Ancistrocladinium A and B, the First *N,C*-Coupled Naphthyldihydroisoquinoline Alkaloids, from a Congolese *Ancistrocladus* Species**. *Journal of Organic Chemistry* 2006, **71**:9348-9356.

16. Kavatsurwa SfM, Lombe BK, Feineis D, Dibwe DF, Maharaj V, Awale S, Bringmann G: **Ancistroyafungines A-D, 5,8′- and 5,1′-Coupled Naphthylisoquinoline Alkaloids from a Congolese *Ancistrocladus***

Species, with Antiausterity Activities against Human PANC-1 Pancreatic Cancer Cells. *Fitoterapia* 2018, **130**:6-16.

17. Ruangrungsi N, Wongpanich V, Tantivatana P, Cowe HJ, Cox PJ, Funayama S, Cordell GA: **Traditional Medicinal Plants of Thailand, V: Ancistrotectorine, a New Naphthalene-Isoquinoline Alkaloid from *Ancistrocladus tectorius***. *Journal of Natural Products* 1985, **48**(4):529-535.
18. Meimberg H, Rischer H, Turini F, Chamchumroon V, Dreyer M, Sommaro M, Bringmann G, Heubl G: **Evidence for Species Differentiation within the *Ancistrocladus tectorius* Complex (Ancistrocladaceae) in Southeast Asia: a Molecular Approach**. *Plant Systematics and Evolution* 2010, **284**(1-2):77-98.
19. Wiart C: **Medicinal Plants of the Asia-Pacific: Drugs for the Future?** New Jersey, London: World Scientific Publishing Private Limited Company; 2006.
20. Bringmann G, Pokorny F: **The Naphthylisoquinoline Alkaloids**. *in The Alkaloids, (Editor: Cordell GA), Academic Press, New York,* 1995, **46**:127-271.
21. Ibrahim RMS, Mohamed AG: **Naphthylisoquinoline Alkaloids Potential Drug Leads**. *Fitoterapia* 2015, **106**:194-225.
22. Shaw HKA: **On the Dioncophyllaceae, a Remarkable New Family of Flowering Plants**. *Kew Bulletin* 1951, **6**(3):327-347.
23. Bringmann G, Pokorny F, Stäblein M, Schäffer M, Aké Assi L: **Ancistrobrevine C from *Ancistrocladus abbreviatus*: The First Mixed 'Ancistrocladaceae/Dioncophyllaceae-Type' Naphthylisoquinoline Alkaloid**. *Phytochemistry* 1993, **33**(6):1511-1515.
24. Kubitzki K: **The Families and Genera of Vascular Plants**, Vol. 6. Berlin Heidelberg, New York: Springer-Verlag; 2003.
25. Bringmann G, Feineis D: **Stress-Related Polyketide Metabolism of Dioncophyllaceae and Ancistrocladaceae**. *Journal of Experimental Botany* 2001, **52**(363):2015-2022.

26. Fujii I, Mori Y, Watanabe A, Kubo Y, Tsuji G, Ebizuka Y: **Heterologous Expression and Product Identification of *Colletotrichum lagenarium* Polyketide Synthase Encoded by the PKS1 Gene Involved in Melanin Biosynthesis**. *Bioscience, Biotechnology, and Biochemistry* 1999, **63**(8):1445-1452.

27. Watanabe A: ***Aspergillus fumigatus* alb1 Encodes Naphthopyrone Synthase when Expressed in *Aspergillus oryzae.*** *Federation of European Microbiology Society, Microbiology Letters* 2000, **192**:39-44.

28. Elsebai FM, Saleem M, Tejesvi VM, Kajula M, Mattila S, Mehiri M, Turpeinen A, Pirttilä AM: **Fungal Phenalenones: Chemistry, Biology, Biosynthesis and Phylogeny**. *Natural Product Reports* 2014, **31**(5):628-645.

29. Ibrahim RMS, Mohamed AG: **Naturally Occurring Naphthalenes: Chemistry, Biosynthesis, Structural Elucidation, and Biological Activities**. *Phytochemistry Reviews* 2016, **15**(2):279-295.

30. Bringmann G, Bruhn T, Maksimenka K, Hemberger Y: **The Assignment of Absolute Stereostructures through Quantum Chemical Circular Dichroism Calculations**. *European Journal of Organic Chemistry* 2009, **2009**(17):2717-2727.

31. Bringmann G, Gulden K-P, Busse H, Fleischhauer J, Kramer B, Zobel E: **Circular Dichroism of Naphthyltetrahydroisoquinoline Alkaloids: Calculation of CD Spectra by Semiempirical Methods**. *Tetrahedron* 1993, **49**(16):3305-3312.

32. Bringmann G, God R, Schäffer M: **An Improved Degradation Procedure for Determination of the Absolute Configuration in Chiral Isoquinoline and β-Carboline Derivatives**. *Phytochemistry* 1996, **43**(6):1393-1403.

33. Bringmann G, Rückert M, Schlauer J, Herderich M: **Separation and Identification of Dimeric Naphthylisoquinoline Alkaloids by Liquid Chromatography Coupled to Electrospray Ionization Mass Spectrometry**. *Journal of Chromatography* 1998, **810**(1-2):231-236.

34. Bringmann G, Koppler D, Scheutzow D, Porzel A: **Determination of Configuration at the Biaryl Axes of Naphthylisoquinoline Alkaloids**

by Long-Range NOE Effects. *Magnetic Resonance in Chemistry 1997*, **35**:297-301.

35. Bringmann G, Gulder T, Hertlein B, Hemberger Y, Meyer F: **Total Synthesis of the *N,C*-Coupled Naphthylisoquinoline Alkaloids Ancistrocladinium A and B and Related Analogues**. *Journal of the American Chemical Society* 2010, **132**(3):1151-1158.

36. Dale AJ, Mosher SH: **Nuclear Magnetic Resonance Enantiomer Regents. Configurational Correlations *via* Nuclear Magnetic Resonance Chemical Shifts of Diastereomeric Mandelate, O-Methylmandelate, and Alpha-Methoxy-Alpha-Trifluoromethylphenylacetate (MTPA) Esters**. *Journal of the American Chemical Society* 1973, **95**(2):512-519.

37. Bringmann G, Harmsen S, Holenz J, Geuder T, Götz R, Keller AP, Walter R, Hallock FY, Cardellina II JH, Boyd RM: **'Biomimetic' Oxidative Dimerization of Korupensamine A: Completion of the First Total Synthesis of Michellamines A, B, and C**. *Tetrahedron* 1994, **50**(32):9643-9648.

38. Bringmann G, Saeb W, Koppler D, François G: **Jozimine A ('Dimeric' Dioncophylline A), a Non-Natural Michellamine Analog with High Antimalarial Activity**. *Tetrahedron* 1996, **52**(42): 13409-13418.

39. Bringmann G, Günther C, Saeb W, Mies J, Wickramasinghe A, Mudogo V, Brun R: **Ancistrolikokines A−C: New 5,8'-Coupled Naphthylisoquinoline Alkaloids from *Ancistrocladus likoko***. *Journal of Natural Products* 2000, **63**(10):1333-1337.

40. Bringmann G, Messer K, Brun R, Mudogo V: **Ancistrocongolines A-D, New Naphthylisoquinoline Alkaloids from *Ancistrocladus congolensis***. *Journal of Natural Products* 2002, **65**:1096-1101.

41. Bringmann G, Günther C, Busemann S, Schäffer M, Olowokudejo DJ, Alo BI: **Ancistroguineines A and B as well as Ancistrotectorine Naphthylisoquinoline Alkaloids from *Ancistrocladus guineënsis***. *Phytochemistry* 1998, **47**(1):37-43.

42. François G, Bringmann G, Dochez C, Schneider C, Timperman G, Aké Assi L: **Activities of Extracts and Naphthylisoquinoline Alkaloids**

from *Triphyophyllum peltatum*, *Ancistrocladus abbreviatus* and *Ancistrocladus barteri* against *Plasmodium berghei* (Anka Strain) *in vitro*. *Journal of Ethnopharmacology* 1995, **46**(2):115-120.

43. François G, Bringmann G, Phillipson JD, Aké Assi L, Dochez C, Rübenacker M, Schneider C, Wéry M, Warhurst CD, Kirby CG: **Activity of Extracts and Naphthylisoquinoline Alkaloids from *Triphyophyllum peltatum*, *Ancistrocladus abbreviatus* and *Ancistrocladus barteri* against *Plasmodium falciparum in vitro***. *Phytochemistry* 1994, **35**(6):1461-1464.

44. François G, Timperman G, Holenz J, Aké Assi L, Geuder T, Maes L, Dubois J, Hanocq M, Bringmann G: **Naphthylisoquinoline Alkaloids Exhibit Strong Growth-Inhibiting Activities against *Plasmodium falciparum* and *Plasmodium berghei in vitro* Structure-Activity Relationships of Dioncophylline C**. *Annals of Tropical Medicine and Parasitology* 1996, **90**(2):115-123.

45. Bringmann G, Zhang G, Ölschläger T, Stich A, Wu J, Chatterjee M, Brun R: **Highly Selective Antiplasmodial Naphthylisoquinoline Alkaloids from *Ancistrocladus tectorius***. *Phytochemistry* 2013, **91**(0):220-228.

46. Nwaka S, Ramirez B, Brun R, Maes L, Douglas F, Ridley R: **Advancing Drug Innovation for Neglected Diseases: Criteria for Lead Progression**. *Public Library of Science. Neglected Tropical Diseases* 2009, **3**(8):440-453.

47. Bringmann G, Teltschik F, Schäffer M, Haller R, Bär S, Robertson SA, Isahakia AM: **Ancistrobertsonine A and Related Naphthylisoquinoline Alkaloids from *Ancistrocladus robertsoniorum***. *Phytochemistry* 1998, **47**(1):31-35.

48. Bringmann G, Teltschik F, Michel M, Busemann S, Rückert M, Haller R, Bär S, Robertson SA, Kaminsky R: **Ancistrobertsonines B, C, and D as well as 1,2-Didehydroancistrobertsonine D from *Ancistrocladus robertsoniorum***. *Phytochemistry* 1999, **52**(2):321-332.

49. Jiang C, Li Z-L, Gong P, Kang S-L, Liu M-S, Pei Y-H, Jing Y-K, Hua H-M: **Five Novel Naphthylisoquinoline Alkaloids with Growth**

Inhibitory Activities against Human Leukemia Cells HL-60, K562 and U937 from Stems and Leaves of *Ancistrocladus tectorius*. *Fitoterapia* 2013, **91**:305-312.

50. Li J, Seupel R, Feineis D, Mudogo V, Kaiser M, Brun R, Brünnert D, Chatterjee M, Seo E-J, Efferth T, Bringmann G: **Dioncophyllines C_2, D_2, and F and Related Naphthylisoquinoline Alkaloids from the Congolese Liana *Ancistrocladus ileboensis* with Potent Activities against *Plasmodium falciparum* and against Multiple Myeloma and Leukemia Cell Lines**. *Journal of Natural Products* 2017, **80**(2):443-458.

51. Xu M, Bruhn T, Hertlein B, Brun R, Stich A, Wu J, Bringmann G: **Shuangancistrotectorines A-E, Dimeric Naphthylisoquinoline Alkaloids with Three Chiral Biaryl Axes from the Chinese Plant *Ancistrocladus tectorius***. *Chemistry - A European Journal* 2010, **16**(14):4206-4216.

52. Tshitenge DT, Feineis D, Mudogo V, Kaiser M, Brun R, Bringmann G: **Antiplasmodial Ealapasamines A-C,'Mixed' Naphthylisoquinoline Dimers from the Central African Liana *Ancistrocladus ealaensis***. *Scientific Reports* 2017, **7**(1):57-67.

53. Bringmann G, Zhang G, Büttner T, Bauckmann G, Kupfer T, Braunschweig H, Brun R, Mudogo V: **Jozimine A_2: The First Dimeric Dioncophyllaceae-Type Naphthylisoquinoline Alkaloid, with Three Chiral Axes and High Antiplasmodial Activity**. 2013, **19**:916-923.

54. Lombe BK, Bruhn T, Feineis D, Mudogo V, Brun R, Bringmann G: **Cyclombandakamines A_1 and A_2, Oxygen-Bridged Naphthylisoquinoline Dimers from a Congolese *Ancistrocladus* Liana**. *Organic Letters* 2017a, **19**(6):1342-1345.

55. Tshitenge DT, Feineis D, Mudogo V, Kaiser M, Brun R, Seo E-J, Efferth T, Bringmann G: **Mbandakamine-Type Naphthylisoquinoline Dimers and Related Alkaloids from the Central African Liana *Ancistrocladus ealaensis* with Antiparasitic and Antileukemic Activities**. *Journal of Natural Products* 2018, **81**(4):918-933.

56. Bringmann G, Seupel R, Feineis D, Zhang G, Xu M, Wu J, Kaiser M, Brun R, Seo E-J, Efferth T: **Ancistectorine D, a Naphthylisoquinoline Alkaloid with Antiprotozoal and Antileukemic Activities, and Further 5,8'- and 7,1'-Linked Metabolites from the Chinese Liana *Ancistrocladus tectorius***. *Fitoterapia* 2016, **115**:1-8.

57. Bringmann G, Spuziak J, Faber JH, Gulder T, Kajahn I, Dreyer M, Heubl G, Brun R, Mudogo V: **Six Naphthylisoquinoline Alkaloids and a Related Benzopyranone from a Congolese *Ancistrocladus* Species Related to *Ancistrocladus congolensis***. *Phytochemistry* 2008, **69**(4):1065-1075.

58. Bringmann G, Hertlein-Amslinger B, Kajahn I, Dreyer M, Brun R, Moll H, Stich A, Ndjoko K Ioset, Schmitz W, Ngoc LH: **Phenolic Analogs of the *N,C*-Coupled Naphthylisoquinoline Alkaloid Ancistrocladinium A, from *Ancistrocladus cochinchinensis* (Ancistrocladaceae), with Improved Antiprotozoal Activities**. *Phytochemistry* 2011, **72**(1):89-93.

59. Ponte-Sucre A, Faber JH, Gulder T, Kajahn I, Pedersen SEH, Schultheis M, Bringmann G, Moll H: **Activities of Naphthylisoquinoline Alkaloids and Synthetic Analogs against *Leishmania major***. *Antimicrobial Agents and Chemotherapy* 2007, **51**:188-194.

60. McMahon JB, Currens MJ, Gulakowski RJ, Buckheit RW, Jr., Lackman-Smith C, Hallock YF, Boyd MR: **Michellamine B, a Novel Plant Alkaloid, Inhibits Human Immunodeficiency Virus-Induced Cell Killing by at Least two Distinct Mechanisms**. *Antimicrobial Agents and Chemotherapy* 1995, **39**(2):484-488.

61. Boyd MR, Hallock YF, Cardellina II JH, Manfredi KP, Blunt JW, McMahon JB, Buckheit RWJ, Bringmann G, Schäffer M, Cragg GM, Thomas WD, Jato JG: **Anti-HIV Michellamines from *Ancistrocladus korupensis***. *Journal of Medicinal Chemistry* 1994, **37**:1740-1745.

62. Hallock YF, Cardellina II JH, Schäffer M, Stahl M, Bringmann G, François G, Boyd RM: **Yaoundamines A and B, New Antimalarial**

Naphthylisoquinoline Alkaloids from *Ancistrocladus korupensis*. *Tetrahedron* 1997, **53**(24):8121-8128.

63. Hallock YF, Cardellina II JH, Schäffer M, Bringmann G, François G, Boyd MR: **Korundamine A, a Novel HIV-Inhibitory and Antimalarial "Hybrid" Naphthylisoquinoline Alkaloid Heterodimer from *Ancistrocladus korupensis***. *Bioorganic and Medicinal Chemistry Letters* 1998, **8**(13):1729-1734.

64. Fayez S, Feineis D, Mudogo V, Seo E-J, Efferth T, Bringmann G: **Ancistrolikokine I and Further 5,8′-Coupled Naphthylisoquinoline Alkaloids from the Congolese Liana *Ancistrocladus likoko* and their Cytotoxic Activities against Drug-Sensitive and Multidrug Resistant Human Leukemia Cells**. *Fitoterapia* 2018a, **129**:114-125.

65. Fayez S, Feineis D, Aké Assi L, Kaiser M, Brun R, Awale S, Bringmann G: **Ancistrobrevines E-J and Related Naphthylisoquinoline Akaloids from the West African Liana *Ancistrocladus abbreviatus* with Inhibitory Activities against *Plasmodium falciparum* and PANC-1 Human Pancreatic Cancer Cells**. *Fitoterapia* 2018, **131**:245-259.

66. Fayez S, Feineis D, Mudogo V, Awale S, Bringmann G: **Ancistrolikokines E-H and Related 5,8′-Coupled Naphthylisoquinoline Alkaloids from the Congolese Liana *Ancistrocladus likoko* with Antiausterity Activities against PANC-1 Human Pancreatic Cancer Cells**. *The Royal Society of Chemistry Advances* 2017, **7**(85):53740-53751.

67. Mihalyi A, Jamshidi S, Slikas J, Bugg DHT: **Identification of Novel Inhibitors of Phospho-MurNAc-Pentapeptide Translocase MraY from Library Screening: Isoquinoline Alkaloid Michellamine B and Xanthene Dye Phloxine B**. *Bioorganic and Medicinal Chemistry* 2014, **22**(17):4566-4571.

68. Bringmann G, Holenz J, Wiesen B, Nugroho BW, Proksch P: **Dioncophylline A as a Growth-Retarding Agent against the Herbivorous Insect *Spodoptera littoralis*: Structure-Activity Relationships**. *Journal of Natural Products* 1997, **60**(4):342-347.

69. Bringmann G, Steinert C, Feineis D, Mudogo V, Betzin J, Scheller C: **HIV-Inhibitory Michellamine-Type Dimeric Naphthylisoquinoline Alkaloids from the Central African Liana *Ancistrocladus congolensis***. *Phytochemistry* 2016, **128**:71-81.

70. Bringmann G, Seupel R, Feineis D, Xu M, Zhang G, Kaiser M, Brun R, Seo E-J, Efferth T: **Antileukemic Ancistrobenomine B and Related 5,1′-Coupled Naphthylisoquinoline Alkaloids from the Chinese Liana *Ancistrocladus tectorius***. *Fitoterapia* 2017, **121**:76-85.

71. Montagnac A, Hadi AAH, Remy F, Païs M: **Isoquinoline Alkaloids from *Ancistrocladus tectorius***. *Phytochemistry* 1995, **39**(3):701-704.

72. Bringmann G, Zagst R, Reuscher H, Aké Assi L: **Ancistrobrevine B, the First Naphthylisoquinoline Alkaloid with A 5,8'-Coupling Site, and Related Compounds from *Ancistrocladus abbreviatus***. *Phytochemistry* 1992, **31**(11):4011-4014.

73. Bringmann G, Dreyer M, Faber JH, Dalsgaard PW, Jaroszewski JW, Ndangalasi H, Mbago F, Brun R, Reichert M, Maksimenka K, Christensen SB: **Ancistrotanzanine A, the First 5,3'-Coupled Naphthylisoquinoline Alkaloid, and Two Further, 5,8'-Linked Related Compounds from the Newly Described Species *Ancistrocladus tanzaniensis***. *Journal of Natural Products* 2003, **66**(9):1159-1165.

74. Tang C-P, Yang Y-P, Zhong Y, Zhong Q-X, Wu H-M, Ye Y: **Four New Naphthylisoquinoline Alkaloids from *Ancistrocladus tectorius***. *Journal of Natural Products* 2000, **63**(10):1384-1387.

75. Nguyen HA, Porzel A, Ripperger H, Bringmann G, Schäffer M, God R, Van Sung T, Adam G: **Naphthylisoquinoline Alkaloids from *Ancistrocladus cochinchinensis***. *Phytochemistry* 1997, **45**(6):1287-1291.

76. Seupel R, Hemberger Y, Feineis D, Xu M, Seo E-J, Efferth T, Bringmann G: **Ancistrocyclinones A and B, Unprecedented Pentacyclic *N,C*-Coupled Naphthylisoquinoline Alkaloids, from the Chinese Liana *Ancistrocladus tectorius***. *Organic and Biomolecular Chemistry* 2018, **16**(9):1581-1590.

77. Awale S, Lu J, K Kalauni S, Kurashima Y, Tezuka Y, Kadota S, Esumi H: **Identification of Arctigenin as an Anti-tumor Agent Having the Ability to Eliminate the Tolerance of Cancer Cells to Nutrient Starvation**. *Cancer Research* 2006, **66**:1751-1757.

78. Hallock YF, Manfredi PK, Blunt WJ, Cardellina II JH, Schaeffer M, Gulden K-P, Bringmann G, Lee YA, Clardy J: **Korupensamines A-D, Novel Antimalarial Alkaloids from *Ancistrocladus korupensis***. *The Journal of Organic Chemistry* 1994, **59**(21):6349-6355.

79. Li J, Seupel R, Bruhn T, Feineis D, Kaiser M, Brun R, Mudogo V, Awale S, Bringmann G: **Jozilebomines A and B, Naphthylisoquinoline Dimers from the Congolese Liana *Ancistrocladus ileboensis*, with Antiausterity Activities against the PANC-1 Human Pancreatic Cancer Cell Line**. *Journal of Natural Products* 2017, **80**(10):2807-2817.

80. Izuishi K, Kato K, Ogura T, Kinoshita T, Esumi H: **Remarkable Tolerance of Tumor Cells to Nutrient Deprivation: Possible New Biochemical Target for Cancer Therapy**. *Cancer Research* 2000, **60**(21):6201-6207.

81. Magolan J, Coster JM: **Targeting the Resistance of Pancreatic Cancer Cells to Nutrient Deprivation: Antiausterity Compounds**. *Current Drug Delivery* 2010, **7**(5):355-369.

82. Awale S, Nakashima MNE, Kalauni KS, Tezuka Y, Kurashima Y, Lu J, Esumi H, Kadota S: **Angelmarin, a Novel Anti-Cancer Agent Able to Eliminate the Tolerance of Cancer Cells to Nutrient Starvation**. *Bioorganic and Medicinal Chemistry Letters* 2006, **16**(3):581-583.

83. Esumi H, Izuishi K, Kato K, Hashimoto K, Kurashima Y, Kishimoto A, Ogura T, Ozawa T: **Hypoxia and Nitric Oxide Treatment Confer Tolerance to Glucose Starvation in a 5′-AMP-Activated Protein Kinase-Dependent Manner**. *Journal of Biological Chemistry* 2002, **277**(36):32791-32798.

Chapter 3: Evaluation of Selected South African *Monsonia* Species as a Source of Anti-cancer and *Nrf2* Activator Compounds

3.1. Introduction

3.1.1. Overview of South African Medicinal Plants

South Africa is a country with a long history of the traditional use of medicinal plants, hosting more than 30,000 flowering plant species [1] accounting for almost 10% of the World's higher plant species [2]. Currently more than a 1000 species of South African plants are used for medicinal purposes; this includes many introduced plants that over generations have been incorporated into South African traditional medicine, such as Dutch, Indian, and Chinese medicinal plants [3-5]. Among the introduced species one can find *Glycyrrhiza glabra* (liquorice), *Ruta graveolens* [6], *Zingiber officinalis* (ginger), and *Acorus calamus* (calamus) [4]. Medicinal plants have been used for centuries, and numerous local communities still rely on indigenous medicinal plants for their primary health care needs, and to cover these needs, about 80% of the South African population use traditional medicines [2, 7].

Medicinal plants are now universally recognized as a basis for a number of critical human health, social, and economic support systems and benefits [2, 8]. There has been a noticeable increase of both international and local initiatives actively focused on the exploration of botanical resources of Southern Africa with the intention to screen indigenous plants for their pharmacologically active compounds [2, 9]. The use and trade of medicinal plants in Southern Africa has been recognized as providing important primary health care benefits, livelihood opportunities, and as being culturally significant [8].

In South Africa, there is a rising interest in natural plant-based remedies but only a few South African medicinal plants used for primary health care have been exploited to their full potential with regard to their commercialization [2].

It is estimated that 3000 medicinal plant species are used in traditional medicine in South Africa, but only about 38 indigenous species have been commercialized to some extent in various forms such as teas, tinctures, tablets, capsules, or ointments [10].

Agathosma betulina, commonly known as “Buchu”, a plant endemic to the Western Cape region demonstrated anti-microbial, antioxidant, and anti-inflammatory activities [2]. *Aloe ferox*, generally known as Cape aloe or bitter aloe, is sold for its scientifically proven laxative, antioxidant, anti-inflammatory, anti-microbial, anthelmintic, and anti-cancer properties [2, 11]. The well-known herbal Rooibos tea from *Aspalathus linearis*, also endemic to the South African Fynbos species, has a growing reputation of having significant health benefits, including antispasmodic, antioxidant, antiaging, and anti-eczema activities [2]. A recent hypothesis claims that *Harpagophytum procumbens* inhibits induction of pro-inflammatory gene expression, perchance by blocking the AP-1 pathway. The hydrolyzed products of the compounds from the plant, harpagide and harpagoside, have significant anti-inflammatory activity [12].

Some South African plant species that are widely spread in Africa are commercialized in other parts of Africa and/or in other parts of the World. As an example, *Adansonia digitate* is used to cure fever, diarrhoea, hemoptysis, hiccup, urinary disorders [4]. *Centella asiatica* is a general tonic, used also to treat leprosy, wounds, and cancer. And the powdered fruit of *Kigelia africana* is applied to treat sores, wounds, and rheumatism; the bark is employed against dysentery and stomach ailments, and it is used for skin care and cosmetic [4]. *Prunus africana* is used against chest pain and benign prostate hyperplasia, and *Trichilia emetic* is utilized in the treatment of stomach ailments, dysentery, kidney ailments, indigestion, fever, and parasites; its poultices are applied in the case of bruises and eczema, and the seed oil for the treatment of rheumatism [4]. *Pelargonium sidoides,* a small, perennial herb with tuberous roots, also called black pelargonium, is a well-known medicinal plant in South Africa [4, 13], claimed to safely and

effectively treat acute upper respiratory tract infections such as bronchitis, tonsillopharyngitis, sinusitis, and the common cold. *P. sidoides* can also be used for the treatment of infections such as cough, fever, sore throat, as well as fatigue and weakness [4, 13]. The plant is used by Zulu people to treat gonorrhea, diarrhea, and dysentery [13].

A rapid increase in the number of publications and patent citations for several indigenous species that were scientifically nearly unknown and not investigated before 1995, has more recently been observed [2, 4]. The data for some well-established commercial species (e.g. *Aspalathus linearis* and *Xysmalobium undulatum*, as first commercialized more than 100 years ago) are made available, and this reflects recent research and development activity in the sector of traditional medicine [4].

The commercialization of Southern African medicinal plants is a process that has been rapidly gaining interest during the last 25 years [4]. The development of medicinal plants species into new products is a complex process which needs a multidisciplinary collaboration, involving biosystematics, ethnobotany, organic chemistry, pharmacology, and horticulture [4, 14]. To fully benefit from plant potency as marketable drugs, taxonomic and systematic studies of the plants and of their environment are needed to better understand the full genetic and metabolic diversity of the population. This should be followed by an ethnobotanical survey to record and explore the socio-cultural context of the medicinal plants, the chemical studies will come after to identify the active ingredients/chemical compounds or marker compounds. It should also include the possibility of synthesizing the active compounds or producing derivatives with better activity and less toxicity, pharmacological studies to determine the mode of action, horticultural or autecological studies to find out if the plants can be produced in large-scale, and sustainable harvesting. Finally, reproductive biology of the plants must be studied to develop propagation protocols, and to give orientations in crop development [4]. The first step for new innovations in the future will be fundamental biological knowledge about the species, including

their phylogeny, taxonomy, genetics, chemical variation, and reproductive biology [15].

As mentioned before, traditional medicine has been used for treating diseases over centuries, and scientific studies have revealed that many medicinal plants used are potentially toxic [4, 16], this toxicity can also result from the coexistence in the same medicinal plant two or more compounds leading to drug-drug interactions [16]. Another risky practice observed from herbal healers is the mixing of herbs and pharmaceutical drugs to enhance the activity, this may magnify or oppose the effect of drugs, and should therefore be used only when the chemical composition of the plants extract is known, and also if the interactions between the compounds from the plant and the pharmaceutical drug are well understood [16, 17].

Intellectual property rights is another challenge which can both positively and negatively impact the interests of primary producers and final producers of plant based drugs [16]. In South Africa, bioprospecting and regulation thereof has been profoundly debated during the past years to minimize exploitation of South African resources without benefit and recognition for knowledge holders, and in the scientific community, this regulation continues to be observed as another barrier to bioactives promotion and development [16].

Studies to determine the chemical profile and composition of medicinal plants are receiving more and more attention to reveal the complexity and variety of compounds assumed to be responsible for bioactivity. Significant research and development opportunities need to be provided to discover novel and useful biological activities for South African medicinal plants.

3.1.1.1. Background to *Monsonia* Species

The genus *Monsonia* belongs to the family Geraniaceae, and is part of the Geraniales order, which also contains the families Francoaceae, Greyiaceae, Ledocarpaceae, Melianthaceae, and Vivianiaceae [18-20]. A

number of molecular and morphological studies have included the monogeneric sub-family Hypseocharitaceae within the family Geraniaceae [20]. Phylogenetic relationships were examined in four genera: *Geranium* [20-22], *Pelargonium* [20, 23-26], *Erodium* [27], and *Monsonia* [28]. Geraniaceae have a worldwide distribution but are best represented in Southern Africa [20]. Most identified species of *Monsonia* inhabit Africa and Southwestern Asia [20, 29].

The *Monsonia* genus preferably grows in grasslands, savannas, and deserts in Africa and Southwest Asia. The highest diversity of the genus can be found in Southern Africa, with 21 of the 25 species, of which nine are endemic to South Africa and seven to Namibia [20, 29]. The different species vary in life form, root type, leaf and stipule shape, inflorescence types, sepal, and gynoecium indumentum, petal size, nectary types, anther size, stamen number, exine ornamentation, stigma size and shape, fruit features, and cotyledon arrangement (Figure 3.1) [20, 29].

Previous phytochemical studies on *Monsonia* species showed them to contain polyphenols, anti-oxidants, and tannins [30], however no detailed information was available on the structures of these classes of compounds, warranting further phytochemical research.

Monsonia burkeana is the most documented of all the *Monsonia* species due to its use as a “special tea”, and as a herbal medicine used for blood cleansing, in the treatment of erectile dysfunction, and to improve libido [31]. *Monsonia brevirostrate*, is commonly used by Sotho people to cure skin disorders, especially syphilitic sores [32].

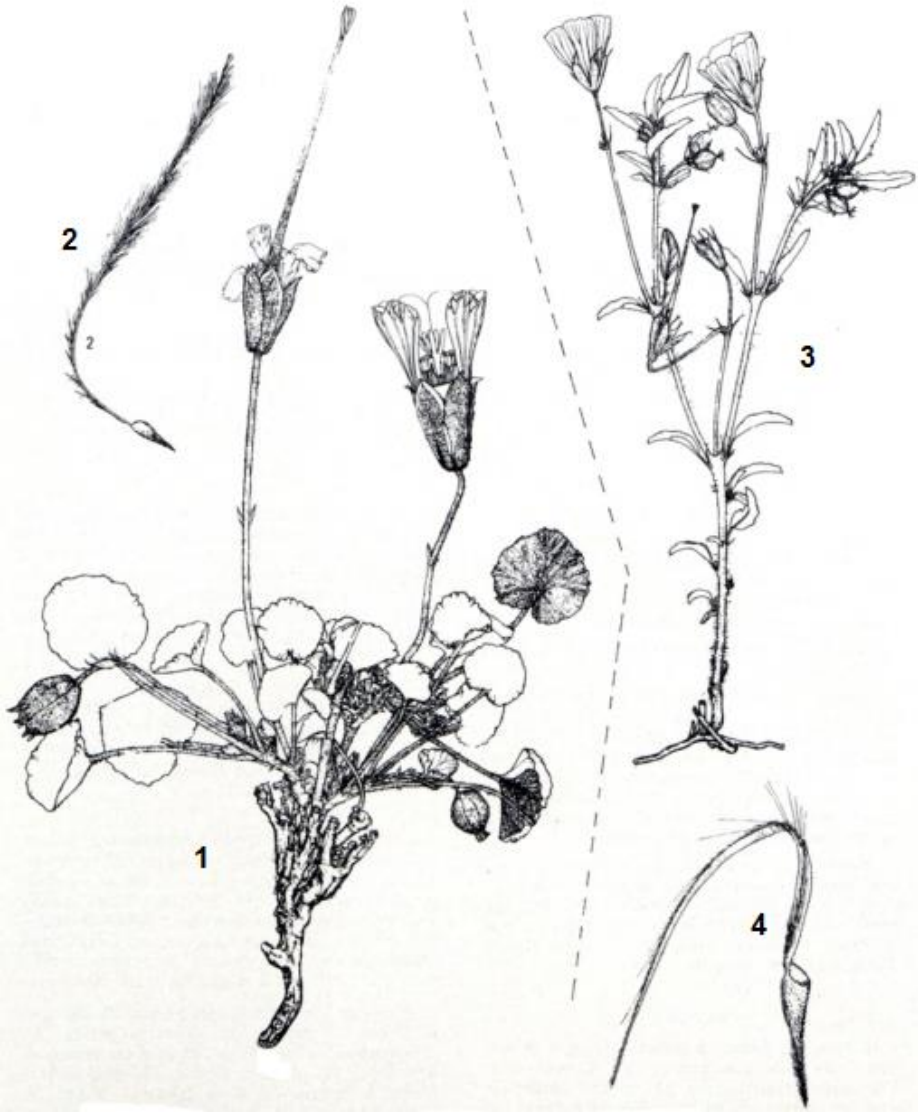

Figure 3.1: *1. Monsonia drudeana 2. Monsonia drudeana mericarp plumose tail 3. Monsonia burkeana 4. Monsonia burkeana mericarp crested tail (taken from Venter HJ* [29])

Based on the use of the *Monsonia* species, *Monsonia angustifolia*, and *Monsonia glauca* were investigated for their phytochemical properties and their biological activities.

3.1.1.2. Ethnobotany, Phytochemistry, and Biological Activities of *Monsonia angustifolia* Sond

The genus *Monsonia* was named after Lady Anne Monson (1714-1766), great-granddaughter of King Charles II of England, botanical collector, who collected plants in India (Bengal) and South Africa (Cape of Good Hope) with CP Thunberg and F Masson. The specific epithet, *angustifolia*, is Latin meaning narrow-leafed [33].

This species is an annual herb with wavy leaves found in open grasslands, and often along roadsides throughout South Africa and Tropical Africa, it grows up to 0.5 m, although usually shorter; the stems are slightly woody at the base, pubescent, and covered with very short gland-tipped hairs among the longer stems; the leaves are narrowly oblong or elliptic, with margins irregularly toothed provided with cuneate bases [33]. *Monsonia angustifolia* possesses mauve to blue, or rarely white or yellowish, flowers, and the fruits are held erect, 50-90 mm long; the plant is widely distributed in the Southern African region (in South Africa, Lesotho, Swaziland, Namibia, and Mozambique), where it usually occurs on granite, often on rocky areas and along the side of roads [33]. The seeds are dispersed by wind and water during rain, the flower colors attract insects and bees for pollination. It is not commonly cultivated as a horticultural plant, as it grows easily from seed [33].

In traditional medicine, the aerial part of *M. angustifolia* is used as a blood cleanser, to treat erectile dysfunction, and to enhance the libido [34], which was also confirmed by the evaluation of the *in vivo* aphrodisiac activities of the *M. angustifolia* crude extracts [35]. Local communities and traditional practitioners indicate that it is used as a sexual stimulant, blood cleanser, and against heartburn, anthrax, and diarrhoea [14, 33].

Studies conducted on the effect of the ethanol extract of dried aerial parts of *M. angustifolia* on the production of neurotoxic *β*-amyloid (A*β*) peptides, and

spatial learning ability as protection against Alzheimer's disease (AD) demonstrated its potency to significantly ameliorate behavioral deficits of the AD transgenic mice, and reduced the level of insoluble A*β*42 in the cerebral cortex and hippocampus [36]; the same extract was effective for memory function recovery after shorter treatment (4 months). In addition, justicidin A isolated from the plant potently decreased the formation of A*β* in APPsw-transfected cells [36]. Investigations on the acute and subacute toxicity of aerial part extract of the plants showed it to be safe, and virtually nontoxic within certain doses interval and a limited period [37].

From *M. angustifolia,* five lignans including justicidin A (**58**), 6-methoxyjusticidin A (**59**), chinensinaphthol (**60**), retrochinensinaphthol methyl ether (**61**), and succhilactone (**62**) were isolated and identified by YS Chun *et al.* and E. Khorombi [36, 38].

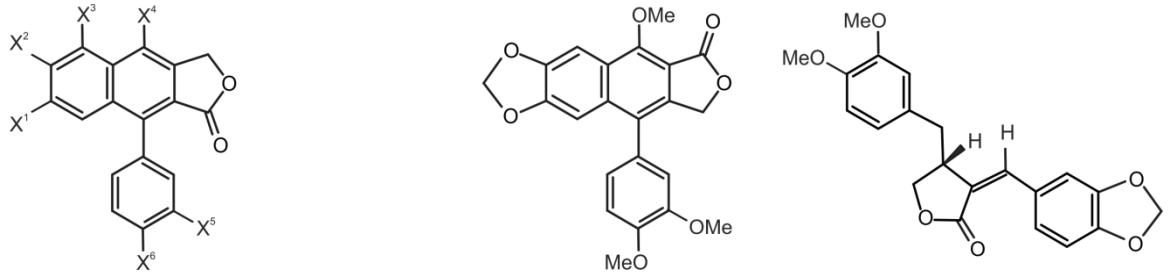

58: $X^1 = X^2 = X^4 = OMe$, $X^3 = H$, $X^5 = X^6 = O\text{-}CH_2\text{-}O$
59: $X^1 = X^2 = X^3 = X^4 = OMe$, $X^5 = X^6 = O\text{-}CH_2\text{-}O$
60: $X^1 = X^2 = O\text{-}CH_2\text{-}O$, $X^3 = H$, $X^4 = OH$, $X^5 = X^6 = OMe$

61 **62**

Figure 3.2: *Selected known lignans isolated from Monsonia angustifolia: justicidin A (**58**), 6-methoxyjusticidin A (**59**), chinensinaphthol (**60**), retrochinensinaphthol methyl ether (**61**), and succhilactone (**62**)* [36, 38]

An exciting investigation demonstrated that justicidin A (**58**), 6-methoxy justicidin A (**59**), and chinensinaphthol (**60**) had an excellent inhibition of the formation of *β*-amyloid, thus playing a role of prevention and/or treatment for dementia [39].

Apart from the knowledge about lignans, the chemical constituents of *M. angustifolia* needed further investigation since there were limited phytochemical studies and information on further biological activities. Even the known isolated compounds needed to be screened in other bioassays since lignans were known to exhibit a wide range of bioactivities such as anti-cancer, anti-inflammation, and antioxidant activities [40]. In addition, the traditional use of a tea should be further explored through biological assaying against relevant assays to show any health benefits.

3.1.1.3. Background Information on *Monsonia glauca* Knouth

M. glauca is an erect, decumbent or prostrate, perennial herb reaching a size of up to 4 m, with a woody base growing in scrubby grassland. Its stems are densely covered with gland-tipped hairs. Leaves are opposite, ovate, basal mostly folded along midrib, cordate at base, with toothed margins. Flowers are white or creamy with dark greenish veins, with petals shallowly lobed at the apex. Fruits are held erect, 6.5-10.0 cm long [34].

According to the South African Biodiversity Institute (SANBI), *Monsonia glauca* is Red-Listed as LC (Least Concern) [41]. *M. glauca* is mostly found in the four Northern provinces of South Africa, Limpopo, North West, Gauteng, and Mpumalanga, and also in the North Eastern Cape. The preferred habitat is grassland and thornbush field in the summer rainfall interior of South Africa [34]. *M. glauca* grows amongst grasses at an altitude of 600-1700 m, in scrubby grasslands, in Mopane woodlands, or on stony soils. The distribution of *M. glauca* extends beyond Namibia, Botswana, and Zimbabwe, well into tropical Africa, including Kenya [34]. The species name *glauca* is Latin for glaucous or bluish-green.

In a personal communication between Khoisan and CSIR (Council for Scientific and Industrial Research) researchers as part of the CSIR's Bioprospecting project, the plant was claimed to be used traditionally for wound healing purposes. Based on this use, studies were initiated at the

CSIR on the mouse skin, the findings demonstrated significant activity in wound closure from both aqueous and organic extracts of the dried aerial part (see the report in the Supplementary Information).

Before this work, the bioactivities and the phytochemical properties of *M. glauca* had not been previously reported. The species itself is barely documented, and research on its chemical constituents and bioactivity supporting its traditional use seemed necessary.

3.1.2. Aims and Objectives of the Study

The aim of the study was the evaluation of the Nrf2 activation of extracts prepared through sequential extraction of *M. angustifolia* and *M. glauca*, followed by fractionation, purification, and structure elucidation of compounds from the most active extract. In addition, the purification and isolation of lignans from both *M. angustifolia* and *M. glauca* was carried out, and the isolated lignans were screened for their anti-cancer activities.

The study had the following specific objectives:

1. Plant identification and processing.
2. Sequential extraction of the dried aerial parts of *M. angustifolia* and *M. glauca* plants.
3. Bio-assaying of sequential extracts for Nrf2 activation.
4. Bioassay-guided fractionation of the most active extract using Nrf2 activation as the target assay.
5. Purification and structure elucidation of compounds from the active fractions.
6. Comparison of the chemical profiles of *M. angustifolia* and *M. glauca* based on the UPLC-MS fingerprints of their sequential extracts.
7. Isolation and identification of lignans from *M. angustifolia* and *M. glauca*, and evaluation of their anti-cancer activity.

3.2. Experimental Section

3.2.1. Processing and Sequential Extraction of the Plant Material

3.2.1.1. Plant Collection

The aerial parts of *Monsonia angustifolia* and *Monsonia glauca* species were obtained from CSIR (The Council for Scientific and Industrial Research). *M. angustifolia* sample was collected near Polokwane area in Limpopo Province. A plant specimen of it was sent to the South African National Biodiversity Institute (SANBI) for identification, and was identified as *Monsonia angustifolia* E. Mey. Ex A. Rich., voucher specimen number 582251.0. The collection of *M. glauca* was made all over South Africa based on the availability of the plant material, and the identification of the plant was also done at SANBI in Pretoria, voucher specimen number XA 01056.

3.2.1.2. Analytical Instrumentation

Ultraviolet spectroscopy (*UV*): The UV spectra were obtained at room temperature on a Waters 600 Controller Millipore spectrophotometer equipped with a Waters 996 PDA detector. The system was driven by Millennium32 software for data acquisition, λ refers to wavelength.

Nuclear magnetic resonance spectroscopy: 1D and 2D NMR spectra were recorded at room temperature on Bruker Ultrashield Plus 400 (400 MHz) or Bruker Ascend 500 (500 MHz) instruments using CD_3OD, $CDCl_3$, or $(CD_3)_2CO$ as the solvents, the chemical shift (δ) are reported in parts per million (ppm) with the ^{1}H and ^{13}C signals of the solvents at δ = 3.31 ppm and δ = 49.15 ppm for CD_3OD, 7.24 ppm and 77.23 ppm for $CDCl_3$, and 2.05 ppm and 29.92, 206.68 ppm for $(CD_3)_2CO$ with reference to δ_{TMS} = 0 ppm. NMR spectra data were processed by using the TopSpin-software from Bruker. Signal multiplicity is given by the following abbreviations: singlet = s, doublet = d, doublet of doublets = dd, triplet = t, doublet of triplets = dt, quartet = q, and multiplet = m. The coupling constants are given in Hertz

(Hz), where ^{n}J gives the number of bonds. Proton-detected, heteronuclear correlations were analyzed using HSQC and HMBC.

Mass spectrometry (*MS*): Both negative and positive ion data were acquired on a Waters Synapt G2 high definition QTOF mass spectrometer equipped with an ESI source, and MassLynx V 4.1 software (Waters Inc., Milford, Massachusetts, USA) was used for data acquisition. MS calibration was performed by direct infusion of 5 mM aqueous sodium formate solution at a flow rate of 10 µl/min, and using Intellistart functionality over the mass range of 50-1200 Da. For both the positive and negative mode, the MS source parameters were set as follows: Source temperature 110 °C, sampling cone 25 V, extraction cone 4.0 V, desolvation temperature 300 °C, cone gas flow 10 l/h, desolvation gas flow (500 l/h). The capillary was 2.8 kV in the positive and 2.6 kV in the negative modes.

3.2.1.3. Other Apparatuses

A Polymix PX-MFC 90D with a wire netting of 2 mm whole size was used to grind air-dried plant material.

Büchi Rotavapor RII served to evaporate organic solvents.

Genvac EZ-2 Plus was utilized to remove solvents under vacuum.

3.2.1.4. Chemicals

All used solvents (methanol, acetone, dichloromethane, chloroform, and *n*-hexane) were of analytical grade. Water for the HPLC was filtered and degassed prior to use. Methanol and acetonitrile for HPLC and for UV measurements as well as trifluoroacetic acid (TFA) were purchased from RADCHEM South Africa without other purification procedures performed. Deuterated solvents were used for NMR analysis. The standards of hyperoside and isoquercetin were purchased from SIGMA South Africa.

3.2.1.5. Extraction of Plant Material

The powdered air-dried aerial part (250 g) of *M. angustifolia* was defatted with 750 ml of *n*-hexane at room temperature using a stirrer plate (200 RPM)

and a magnetic stirrer bar, followed by filtration through Whatman filter paper (110 mm diameter). The process was repeated two times, the filtrates were combined, and the solvent was evaporated using a rotatory evaporator to produce the *n*-hexane extract (Figure 3.3).

The solid residue resulting from the *n*-hexane extraction was extracted with 750 ml of CH_2Cl_2 through agitation with a stirrer bar. After filtration through Whatman filter paper, the extraction was repeated three more times with CH_2Cl_2, the filtrates were combined and evaporated to dryness to give the dry CH_2Cl_2 extract (Figure 3.3).

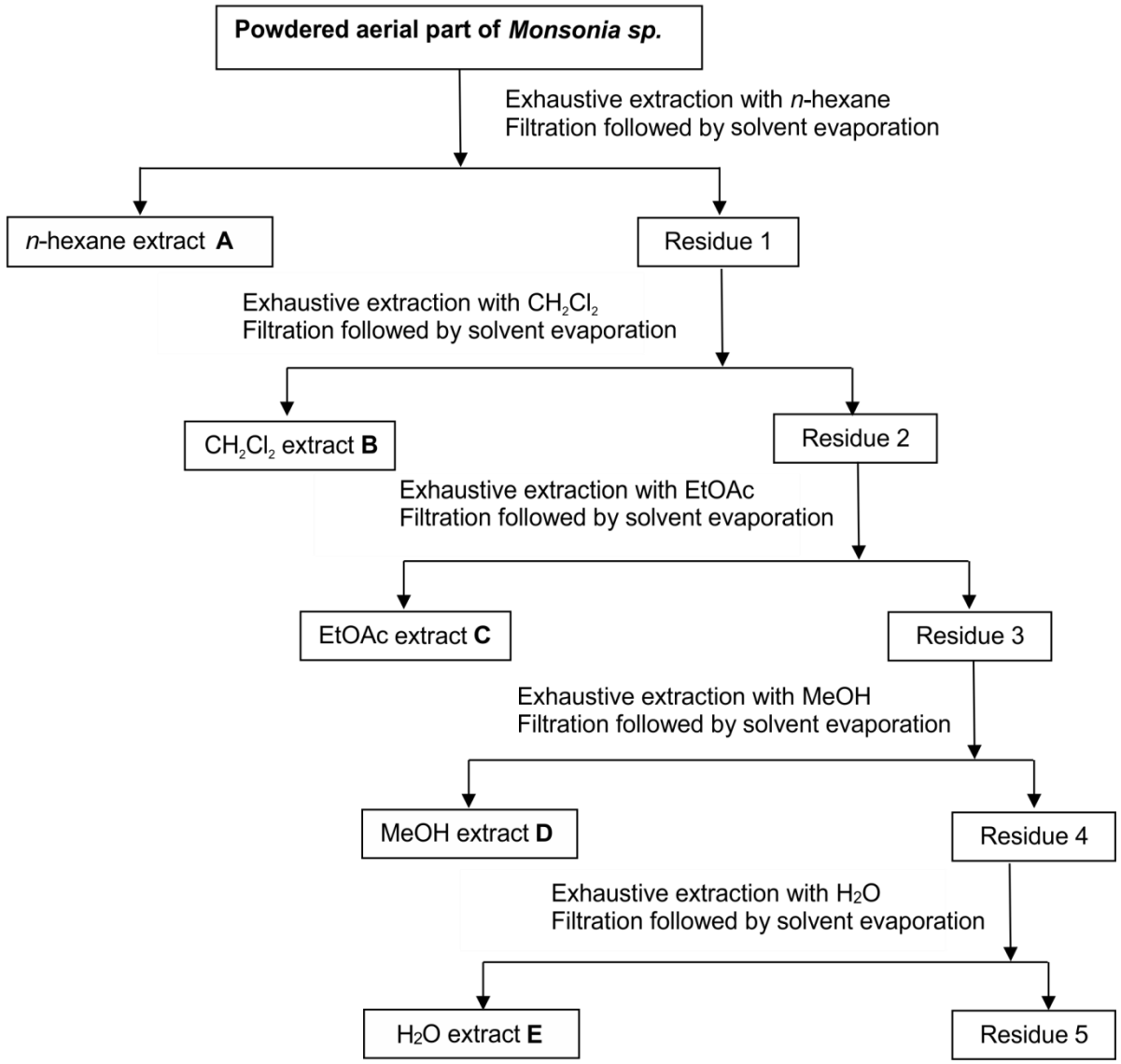

Figure 3.3: *General flow diagram for the sequential extraction of the Monsonia species*

The remaining residue from CH_2Cl_2 extraction was subjected to EtOAc extraction two more times with 750 ml of the solvent, followed by filtration on Whatman filter paper, the filtrates were combined, and after solvent evaporation to dryness under *vacuo*, the EtOAc extract was obtained (Figure 3.3).

The residue from EtOAc extraction was then extracted with 750 ml of MeOH, followed by filtration, and the process was repeated three times more, then the filtrates were combined, the solvent was evaporated to provide the MeOH extract (Figure 3.3).

Finally, the residue from MeOH extraction was extracted with 750 ml of H_2O, after filtration, the extraction was repeated three more times, the filtrates were combined, the solvent was evaporated to produce the aqueous extract (Figure 3.3).

The same procedure (Figure 3.3) was followed for sequential extraction of 250 g of *Monsonia glauca*, providing five separate extracts.

All the crude extracts from both plants were screened for Nrf2 activation prior to further fractionation.

3.2.2. Bioassay-Guided Chromatographic Fractionation of Extracts

Bioassay-guided fractionation may be defined as a process by which an extract is chromatographically partitioned and repartitioned guided by bioassaying until a pure biologically active compound is isolated. Each fraction produced during the fractionation process is assessed in a bioassay system, and only active fractions are further fractionated [41]. Bioassay-guided fractionation method is regularly used in drug discovery investigation because of its effectiveness to directly link the analyzed extract or fraction, and targeted compounds using a step-by-step fractionation procedure, which will be followed by biological activity tests. Chromatography is performed using various techniques such as thin layer chromatography

(TLC) for the monitoring of extracts and fractions, column chromatography (CC) for fractionation, Ultra-Performance Liquid Chromatography Mass Spectrometry (UPLC-MS) for monitoring of fractions and sub-fractions, and High-Performance Liquid Chromatography (HPLC) for purification of active compounds. The detailed procedure followed in the bioassay-guided fractionation of the two *Monsonia* species is described in the following Sections.

3.2.2.1. Thin Layer Chromatography

Thin-layer chromatography (TLC) was carried out using pre-coated aluminum base sheets ALUGRAM Xtra SIL G/UV_{254} covered with silica gel 60 (0.20 mm, 20 x 20 cm). Standard chromatograms of plant extracts and fractions were prepared by applying a concentrated sample to a silica gel TLC plate, and developing it with suitable solvent systems. Chromatograms were detected using ultraviolet (UV) light (both 254 and 366 nm). The vanillin-H_2SO_4 reagent (15 g vanillin dissolved in 247.5 ml absolute ethanol and 2.5 ml of concentrated H_2SO_4) was used as general staining reagent, and the sprayed TLC plate was heated under a hair drier for a few minutes. This technique was used to monitor extracts before changing the solvent, and fractions before combining them according to similarity of spots on the TLC plates.

3.2.2.2. Silica Gel Column Chromatography

The adsorbent used for column chromatography was silica gel 60 normal grade (0.063-0.200 mm Fluca 70-230 mesh). Chromatography was performed with analytical grade solvents. After screening the extracts of both *M. angustifolia* and *M. glauca* for Nfr2 activation, the methanol extract of *M. angustifolia* showed the best activity, and was, thus, chosen for further fractionation (Figure 3.4).

The dried MeOH extract (2 g) was fractionated by column chromatography with CH_2Cl_2/EtOAc as the starting solvent and EtOAc/MeOH at the end of the chromatography. The increasing polarity of the solvent was as follows:

CH_2Cl_2/EtOAc 1:1, 2:3, 3:7, 1:4, 1:9, 100% EtOAc, EtOAc/MeOH 9:1, and 4:1 at the end to flush the column. Before each modification of the polarity or any combination of the fractions, TLC was used to monitor the chemical profiles of the fractions. The collection was done manually in test tubes, with TLC monitoring being done for each test tube prior to any combination based on the similarity of spots on the TLC plates to generate fractions.

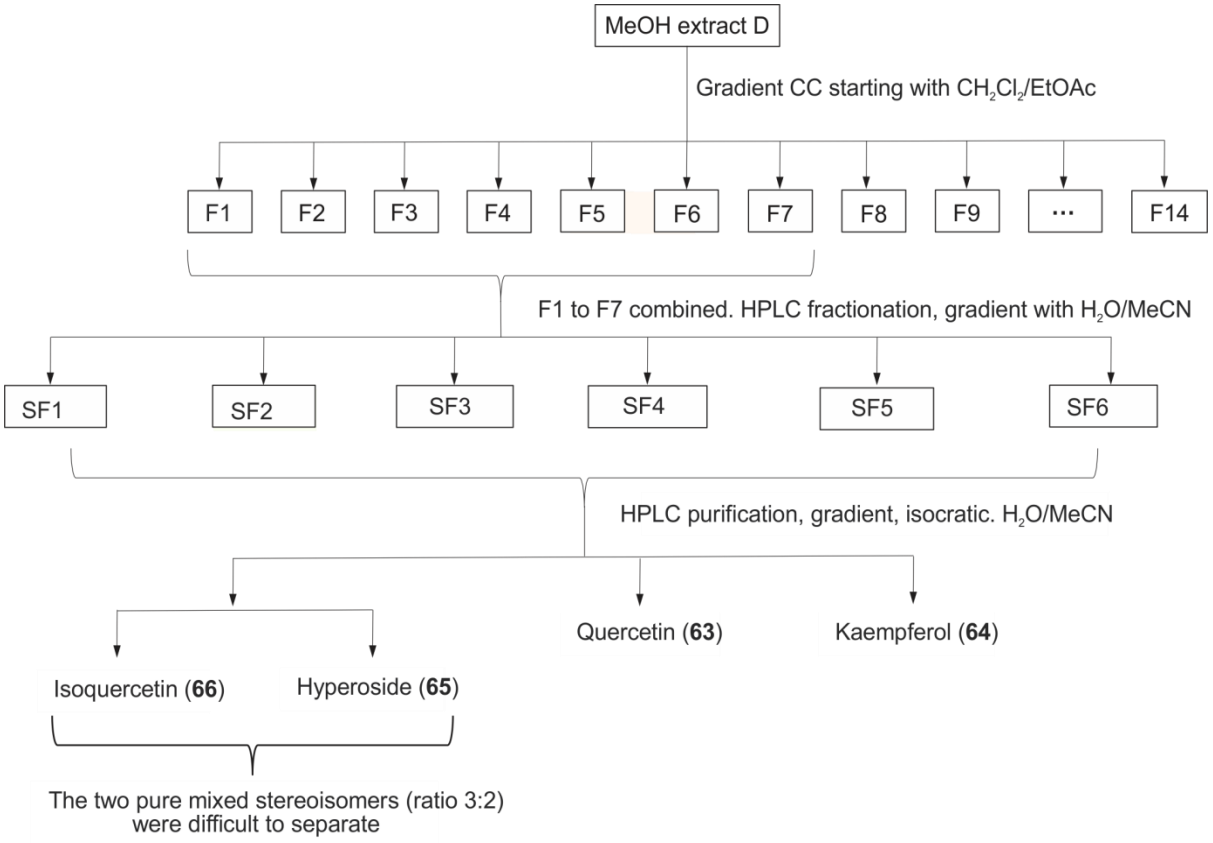

Figure 3.4*: General flow diagram of fractionation of the methanol extract. F: fraction, SF: sub-fraction. Only sub-fractions were not screened for Nfr2 activity*

The collected fractions from the column were screened for Nrf2 activation, and fractions with good activity were subsequently prioritized for further purification using HPLC.

The ultra-performance liquid chromatography coupled to a mass spectrometer (UPLC-MS) was used to analyze the extracts and fractions to determine the purity and phytochemical profiles of the samples.

3.2.2.3. UPLC-QTOF-MS Profiling

Samples for analysis were prepared at a concentration of 1 mg/ml for extracts, fractions, and sub-fractions, 0.1 mg/ml for pure compounds. A binary solvent system (water and acetonitrile 1:1 v/v) was used to analyze the samples with an injection volume of 5 µl per analysis. Samples were analyzed on an Acquity UPLC™ BEH C_{18} column (1.7 µm particle size, 100 mm x 2.1 mm, Waters, Ireland) using 0.1% (v/v) formic acid in water (eluent A) (Fluka Analytical, Sigma-Aldrich, Switzerland), and 0.1% (v/v) formic acid in acetonitrile (eluent B) (Ultra gradient, ROMIL LTD, Cambridge, Britain). Solvent gradient varied over time as follows (eluent A%:eluent B% – time): 97:3 – 0.1 min, 80:20 – 6 min, 70:30 – 9 min, 70:30 – 9.2 min, 0:100 – 20 min, 0:100 – 23.5 min, 97:3 – 24 min, 97:3 – 25 min. The flow rate was set at 0.4 ml/min at a pressure of 0 – 15000 psi. Electrospray ionization both in positive and negative modes (ESI +ve and -ve mode) was used for mass spectral data. Data acquisition and processing was done by MassLynx (Version 4.6) software.

After the UPLC-MS profiling of the 14 fractions (F1 to F14) as well as their bioassay for Nrf2 activity, the seven first fractions (F1 to F7) were combined for further purification (see Figure 3.4).

For comparative purposes, extracts from both *Monsonia* species were analyzed by UPLC-QTOF-MS, which showed the presence of lignans in the CH_2Cl_2 extracts of both *M. angustifolia* and *M. glauca.* Since lignans are reported to have good anti-tumor activity [40], these extracts were also subjected to the isolation of the compounds.

3.2.2.4. HPLC Fractionation and Isolation of Active Compounds as NRF2 Activators

Development of a purification method was carried out on a Waters HPLC 660 Controller, Millipore, equipped with a Waters 996 Photodiode Array

detector. Measurement processing was done using the Millennium[32] software from Waters. The column used was a Phenomenex, Luna, 5 µm C_{18} [(2)], (4.6 x 250 mm 5 µm) with a mobile phase consisting of H_2O + 0.05% TFA (A), MeCN + 0.05% TFA (B); flow: 1 ml/min, binary gradient for flavonoids: 0 min 7.5% B, 3 min 7.5% B, 10 min 40% B, 12 min 40% B, 15 min 55% B, 20 min 55% B, 22 min 100% B, 30 min 100% B, 33 min 7.5% B, and 35 min 7.5% B.

Semi-preparative HPLC was carried out using the same HPLC instrument, and the same column as described above, only the concentration was increased from 1 to 20 mg/ml, and the injection volume from 5 to 20 µl and above with the UV absorption wave length set at 210-400 nm. Several injections were done to get the needed quantity for spectroscopic studies and biological screening; the flow rate was kept the same as for analytical HPLC.

The most active fractions (F1-F7) were combined after analysis by UPLC-MS, and 100 mg of the combined fraction were dissolved in 5 ml of a mixture of H_2O and MeOH (2:3) and resolved by HPLC using the above mentioned gradient system. The collection was done manually and UV based. Six sub-fractions, SF1-SF6, were generated, and analyzed by UPLC-MS.

Sub-Fractions SF2 and SF4 appeared to contain all major compounds resulting from the combination of Fractions F1-F7 based on their UPLC-MS chromatographic profiles, while the remaining sub-fractions were set aside due to their limited number of peaks as well as their limited quantities.

The resolution of Sub-Fraction SF4, showing two major compounds from its UPLC-MS profile was achieved by semi-preparative HPLC using isocratic system 15% of ACN + 0.05% TFA (B), (flow: 0.8 ml/min, injection volume 20 to 50 µl).

Sub-Fraction SF2 showed two major peaks with closely related retention

times, and could not be fully separated neither using a gradient nor an isocratic system. Further NMR analysis identified these as stereoisomers (Section 3.3.4.3).

3.2.3. HPLC Purification of Lignans from the CH_2Cl_2 Extracts of *Monsonia angustifolia* and *Monsonia glauca*

The UPLC-MS fingerprint of the sequentially extracted CH_2Cl_2 extracts of both *M. glauca* and *M. angustifolia* showed them to contain molecular ions corresponding to known lignans. Since lignans are reported to possess excellent biological properties [40], these extracts were fractionated for the isolation compounds in a pure form.

The purification of the CH_2Cl_2 extract of *M. glauca* was carried out on a Waters HPLC 660 Controller, Millipore, equipped with a Waters 996 Photodiode Array detector. Measurement processing was done using the Waters Millennium[32] software. The column used was a Phenomenex, Luna, 5 µm C_{18} $^{(2)}$, (4.6 x 250 mm 5 µm) with the mobile phase consisting of H_2O + 0.05% TFA (A) and ACN + 0.05% TFA (B). A binary isocratic system of 60% B was used, with a 1 ml/min flow, and a run time of 25 min. For analytical HPLC, a 1 mg/ml solution of the CH_2Cl_2 extract in methanol was used, and 5 µl as the injection volume.

The isolation of compounds from 50 mg of the CH_2Cl_2 extract of *M. glauca* was carried out using the same HPLC instrument and the already described column, with the concentration being increased to 20 mg/ml in MeOH, and the injection volume to 50 µl with the UV absorption wave length set at 210-400 nm. Numerous injections were done to get sufficient quantity of the compounds for spectroscopic studies and biological screening.

The resolution of the CH_2Cl_2 extract of *M. angustifolia* (50 mg) was done using the same conditions as for *M*. *glauca*.

3.2.4. Structure Elucidation of the Isolated Compounds

The structure elucidation of the isolated compounds were done by means of a combination of a set of spectroscopic techniques including 1D and 2D NMR spectroscopy, UPLC-MS spectrometry, UV spectra, and UPLC-MS co-elution with known standards.

3.2.5. Evaluation of Nrf2 Activation through NQO1 Enzyme Activity

The Nrf2 screening was done by Prof. RT Kumar's group in India, as part of collaboration between the University of Pretoria and the Department of Biochemistry, JSS Medical College, JSS Academy of Higher Education and Research, in Mysore, India.

The Nfr2 activation was used to guide the fractionation with all sequential extracts first being evaluated; extracts showing good activity were further fractionated followed by bioassaying of the fractions. Pure compounds were isolated from most active fractions, and tested for Nrf2 activation. The estimation of Nrf2 activation was done through the NAD(P)H quinone oxidoreductase-1 (NQO1) enzyme activity.

The NQO1 enzyme activity was measured using the method reported by Prochaska and Santamaria [43]. Human normal bronchial epithelial cells (Beas-2B) were grown in DMEM (Dulbecco's Modified Eagle Medium) medium supplemented with 10% FBS (fetal bovine serum), and 1% Penn-Strep antibiotic. The cells were seeded in 96-well microtiter plate at a density of 10,000/well, maintained at 37 ^{o}C in the presence of 5% CO_2 for 24 h, and subsequently treated with increasing concentrations of test extract or compound for 24 h. After incubation, cells were washed with phosphate buffered saline (PBS), then lysed with 50 µl of lysis buffer (2 mM EDTA/ 0.85% NP40) for 20 min with constant shaking. After centrifugation, 10 µl of cell lysates were used for protein measurement by using the bicinchoninic

acid (BCA) method (Thermo Scientific), and the remaining cell lysate was used for measuring NQO1 enzyme activity.

Briefly, 20 µl of cell lysates were added to the reaction mixture (200 µl final volume) containing Tris (25 mM, pH 7.5), Tween-20 (0.01%), BCA (0.066%), menadione (833 nM), FAD (5 µM), NADH (3 µM), glucose-6-phosphate (1 mM), glucose-6-phosphate-dehydrogenase enzyme (2 U/ml), and MTT (0.003%). The reaction was carried with or without specific NQO1 enzyme inhibitor, dicoumarol (40 nM). The rate of reduction of MTT [3-(4,5-dimethylthiazol-2-yl)-2,5-diphenyltetrazolium bromide] by menadione was monitored by increase in absorbance at 590 nm for 30 min. The specific activity of NQO1 was calculated as the difference between the rates of the MTT reduction in the presence and the absence of dicoumarol, and was estimated by using the molar extinction coefficient of 13,000/M.cm for reduced MTT.

Cytotoxicity: Cytotoxicity was measured by the MTT assay [43]. For this assay, after treatment of the cells with test extract(s) or compound(s), the cells were washed with PBS, and incubated with MTT (0.5 mg/ml) for another 4 h at 37 ^{o}C in 5% CO_2 incubator. After incubation, the cells were washed with phosphate-buffered saline (PBS), and 200 µl of DMSO (formazan solubilizing agent) were added to each well, and mixed well. The color developed was measured at 570 nm using micro-plate reader.

3.2.6. Antiausterity Assay

The tests of antiausterity properties of isolated lignans were carried out by Prof. S Awale's group in Japan, through a cooperation of the University of Pretoria with the University of Würzburg (Germany), and the Division of Natural Drug Discovery, Institute of Natural Medicine at University of Toyama in Japan.

As some lignans are reported to have good anti-tumor activities [40], the compounds justicidin A (**58**), 6-methoxyjusticidin A (**59**), chinensinaphthol

(**60**), retrochinensinaphthol methyl ether (**61**), and justicidin B (**67**) isolated from the extracts of the two plants were tested for their antiausterity activities against human PANC-1 pancreatic cancer cells. The procedure for antiausterity assay was the same as described earlier in Chapter 2 (Section 2.2.9).

3.2.7. Cytotoxicity Assay against Cervical HeLa Cells

The assessment of the cytotoxicity activities was also conducted by Prof. S Awale's group in Japan, under a collaborative project of the University of Pretoria with the University of Würzburg (Germany), and the Division of Natural Drug Discovery, Institute of Natural Medicine at University of Toyama in Japan.

The isolated lignans **58**, **59**, **60**, **61**, and **67** (structures are given in section 3.3.4) were also evaluated for *in vitro* activities against cervical HeLa cancer cells following the protocol of Setiawati A. [44]. In brief, cell viability in the presence or absence of tested compounds was determined using the Cell Counting Kit-8 (Dojindo Molecular Technologies, Inc., Rockville, MD, USA). The HeLa cell line was obtained from the Riken BRC cell bank (Tsukuba, Japan), and maintained in standard DMEM with 10% fetal bovine serum (FBS) supplement, 0.1% $NaHCO_3$, and 1% antibiotic antimycotic solution. For cytotoxicity evaluation, exponentially growing cells were harvested, and plated in 96-well plates (2 × 103/well) in DMEM at 37 °C under an atmosphere of humidified 5% CO_2 and 95% air for 24 h. After washing the cells with PBS, the medium was changed to serially diluted test samples in DMEM, with the control and blank in each plate. Paclitaxel was used as the positive control in this study. After 72 h of incubation, the cells were washed twice with PBS, and 100 *μ*l of DMEM containing 10% WST-8 cell counting kit solution was added to each well. After incubation for 3 h, the absorbance at 450 nm was measured on an EnSpire multimode plate reader (PerkinElmer, Inc., Waltham, MA, USA). The following equation was used to determine the cell viability from the mean values from three wells:

Cell viability (%) = $[Abs_{(test\ sample)} - Abs_{(blank)}/Abs_{(control)} - Abs_{(blank)}] \times 100$

3.3. Results and Discussion

3.3.1. Extraction and Bioassaying for Nrf2 Activation of Extracts

The sequential extraction of the powdered dried plant material of *M. angustifolia* (250 g) using *n*-hexane, dichloromethane, ethyl acetate, methanol, and water was undertaken to separate polar from non-polar compounds. The extraction provided five extracts with a yield of 2.6 g for *n*-hexane extract, 6.4 g of CH_2Cl_2 extract, 2.0 g EtOAc extract, 15.6 g of MeOH extract, and 44.2 g of the water extract.

For *Monsonia glauca*, the sequential extraction produced 1.8 g of the *n*-hexane crude extract, 7.9 g of the CH_2Cl_2 crude extract, 1.7 g of the EtOAc crude extract, 14.4 g of the MeOH crude extract, and 40.1 g of the aqueous crude extract after filtration and solvent evaporation under vacuum.

In the sequential extraction, the less polar solvents *n*-hexane, CH_2Cl_2, and ethyl acetate had lower extraction yields (less than 5% for both *Monsonia angustifolia* and *Monsonia glauca*) as compared to the polar solvents methanol and water extracts accounting for more than 21% yield, suggesting a higher abundance of polar compounds in the aerial part of both *Monsonia* species. The comparison between the two species showed that *M. angustifolia* contained more slightly polar compounds 24% than *M. glauca* with 22% while the contents in non-polar compounds were similar (4.4 and 4.6% respectively).

All ten crude extracts from the sequential extraction were screened for their Nrf2 activation prior to further fractionation. The results of the most active fractions are shown in Table 3.1.

Table 3.1: Nrf2 activities and cell viability of sequential extracts of *M. angustifolia* and *M. glauca*

Sample name	Concentration (µg/ml)	MTT assay (% cell viability)	NQO1 assay (% increase over the control)
DMSO[a]	10[c] and 25[d]	100	100
Sulforaphane[b]	0.9	98.4	170.0
MAH	10	NA	169.0
MAM	1	92.3	236.1
MAW	1	104.3	130.1
MGM	10	95.4	207.2

[a] Vehicle. [b] Positive control. [c] Concentration of the vehicle for MTT assay. [d] Concentration of the vehicle for NQO1 assay. NA: not available. MAH: *M. angustifolia n*-hexane extract. MAM: *M. angustifolia* methanol extract. MAW: *M. angustifolia* water extract. MGM: *M. glauca* methanol extract.

The evaluation of extracts, fractions or compounds for Nfr2 activity is based on two main factors, the toxicity expressed in terms of percentage of cell viability (100% viability means no toxicity), and the activity itself expressed as percentage of increase over a given control (sulforaphane for this study considered as 170% active) [45, 46]. Any extract, fraction, or compound with an increase of greater than 100% compared to the control is considered as an Nrf2 modulator [46].

The analysis was done in triplicate, the values given in the tables are average values. All samples were analyzed at 100, 10, and 1 µg/ml. Concentrations greater than 100 µg/ml were toxic to cells in most cases, as a result the Nrf2 activation is reported only for concentrations at which there was no toxicity to normal cells, except for the *n*-hexane extract of *M. angustifolia*, where the toxicity data was not available.

The most potent extracts as observed by their good Nrf2 activation were: for *M. angustifolia* extracts, *n*-hexane extract with 169.0% increase at 10 µg/ml, the water extract with 130.1% increase at 1 µg/ml, and methanol extract with 236.1% increase at 1 µg/ml concentrations over the sulforaphane used as a positive control (170.0% increase at 0.9 µg/ml); for *M. glauca*, only the methanol extract showed good activity with 207.2% increase at 10 µg/ml concentration (Table 3.1).

3.3.2. Bioassay-Guided Fractionation and UPLC-MS Chemical Profiling

Bioassay-guided fractionation of plant extracts linked to different chromatographic separation techniques results in the isolation of biologically active compounds. In this approach, only biologically active fractions of interest [42, 47] are purified further until single chemical entities are identified, purified, and chemically characterized.

As a result of its strong activity (236% increase over the control at the concentration of 1 µg/ml), which also compared favorably to the positive control (170.0%), together with its low cytotoxicity (92.3% cell viability), the dried methanol extract of *M. angustifolia* (2 g) was subjected to gravitational column chromatography (Experimental Section 3.2.2.2). A total of 107 test tubes containing 15 ml each were collected, analyzed by TLC, and according to the similarity of the patterns, fractions were combined to generate 14 fractions labelled as F1-F14 (F1 = 33.00 mg, F2 = 19.70 mg, F3 = 50.00 mg, F4 = 59.20 mg, F5 = 255.00 mg, F6 = 24.00 mg, F7 = 108.01 mg, F8 = 112.55 mg, F9 = 87.28 mg, F10 = 62.07 mg, F11 = 50.29 mg, F12 = 221.01 mg, F13 = 181.04 mg, F14 = 116.45 mg).

The recovery from the column was approximately 69%, including the flushing of the column to obtain the Fractions F12-F14. All fractions were evaluated for their NRF2 activation, and the results are shown in Table 3.2.

All fractions were analyzed in triplicate each at 100, 10, and 1 µg/ml, and the values given in the Table are the average of three analyzes. The higher concentrations showed low cell viability in most cases. The Nrf2 activation values are provided only for concentrations of 10 or 1 µg/ml as these showed lower toxicity.

Table 3.2: Nrf2 activities and cell viability of fractions from the column chromatography

Sample name	Concentration (µg/ml)	MTT assay (% cell viability)	NQO1 assay (% increase over the control)
DMSO[a]	10[c] and 25[d]	100	100
Sulforaphane[b]	0.9	98.4	170.0
F1	10	93.0	131.0
F2	10	94.0	199.0
F3	1	86.0	153.0
F4	1	123.0	121.0
F5	1	115.0	133.0
F6	1	122.0	184.1
F7	10	128.1	106.0
F8	1	79.0	67.0
F9	1	79.0	26.0
F10	1	90.0	72.0
F11	1	69.0	118.0
F12	1	81.0	87.0
F13	1	91.0	60.0
F14	1	78.0	76.0

[a] Vehicle. [b] Positive control. [c] Concentration of the vehicle for MTT assay. [d] Concentration of the vehicle for NQO1 assay. F1-F14 are the fractions collected from the chromatographic column.

The best Nfr2 activation was found for Fractions F1-F7 with an increase ranging from 106.0 to 199.0%, and cell viability above 86.0% compared favorably to the positive control (170.0% increase and 98.4% cell viability). All the remaining Fractions F8-F14 were generally toxic to cells and had almost no Nrf2 activity (< 100% increase), except for Fraction F11, which displayed 118% increase but was toxic (69.0% cell viability). The active compounds were assumed to be contained in the first seven fractions.

To identify the compounds responsible for the activity, and to establish which compounds are common in the active fractions, the seven active fractions (F1-F7) were analyzed by UPLC-QTOF-MS. The illustrative chromatograms of F1, F4, and F7 are given in Figure 3.5.

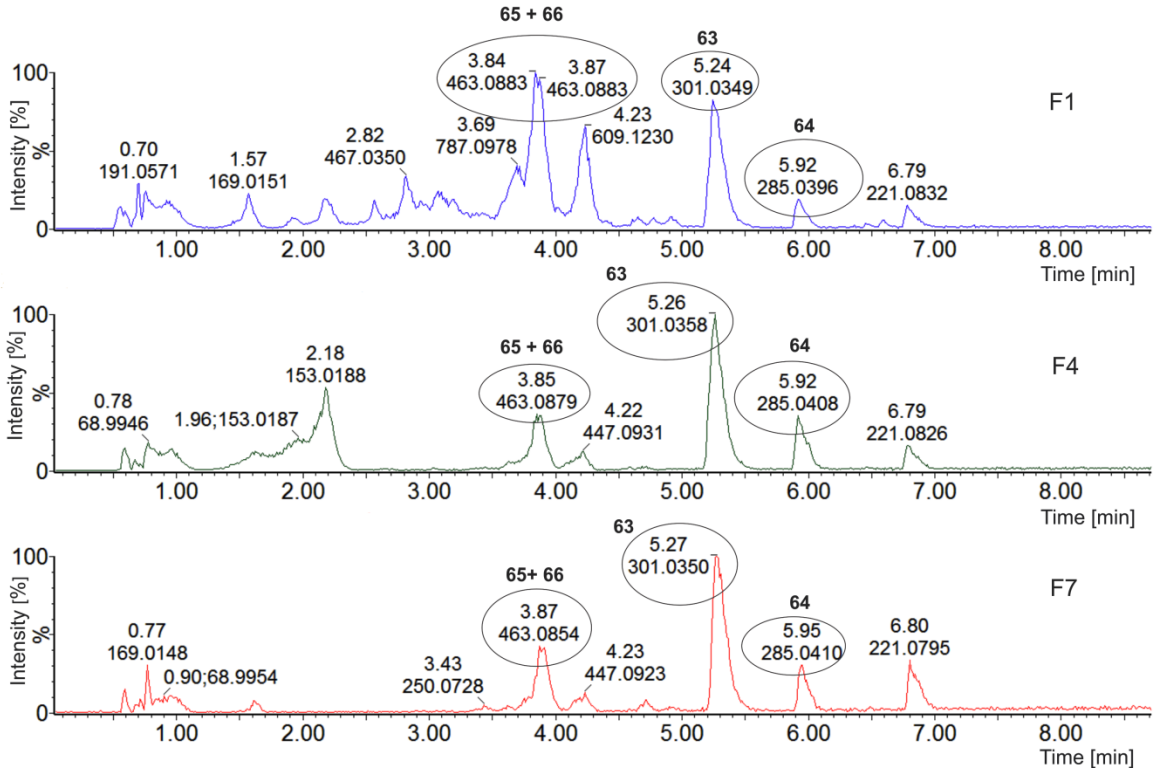

Figure 3.5*: UPLC-MS profiles of the selected Fractions F1, F4, and F7 showing the similar major compounds quercetin (**63**), kaempferol (**64**), hyperoside (**65**), and isoquercetin (**66**)*

The UPLC-MS profiles of the seven active fractions were similar, they displayed comparable chemical chromatographic patterns showing major common $[M-H]^-$ ions at *m/z* 463.0861, 463.0854, 301.0350, and 285.0410 at t_R 3.87min, 3.87 min, 5.27 min, and 5.95 min, respectively. Further spectroscopic studies revealed these masses to correspond to hyperoside (**65**)**,** isoquercetin (**66**), quercetin (**63**), and kaempferol (**64**) (details are given in Section 3.3.4). The seven fractions were then combined for further purification.

The resolution of the seven combined active fractions by HPLC using the already mentioned (Experimental Section 3.2.2.4) gradient system provided the six Sub-Fractions SF1-SF6 (Figure 3.4).

These six sub-fractions were analyzed by UPLC-MS, and Sub-Fractions SF1, SF3, SF5, and SF6 were set aside, due to limited number of peaks in

their chromatograms (Figure 3.6), and their poor yield. The UPLC-MS of Sub-Fractions SF2 and SF4 displayed the major peaks found in the combined Fractions F1-F7. The chromatogram of SF2 showed two major peaks with same $[M-H]^-$ ions at *m/z* 463.0861 and 463.0854 at t_R 6.10 min and 6.22 min (Figure 3.6), and that of Sub-Fraction SF4 displayed two major peaks with $[M-H]^-$ ions at *m/z* 301.0367 (t_R 5.44 min) and 285.0426 (t_R 6.08 min) (Figure 3.7).

The purification on HPLC provided 7.8 mg of a mixture (SF2) of two compounds **65** and **66** (3:2) (t_R: 9.4 min), 18.4 mg of a Sub-Fraction SF4 containing **63** and **64** as major compounds (t_R: 16.9 and 17.6 min), and four minor fractions with a small number of peaks (SF1, SF3, SF5, and SF6), which were set aside (Figure 3.6.).

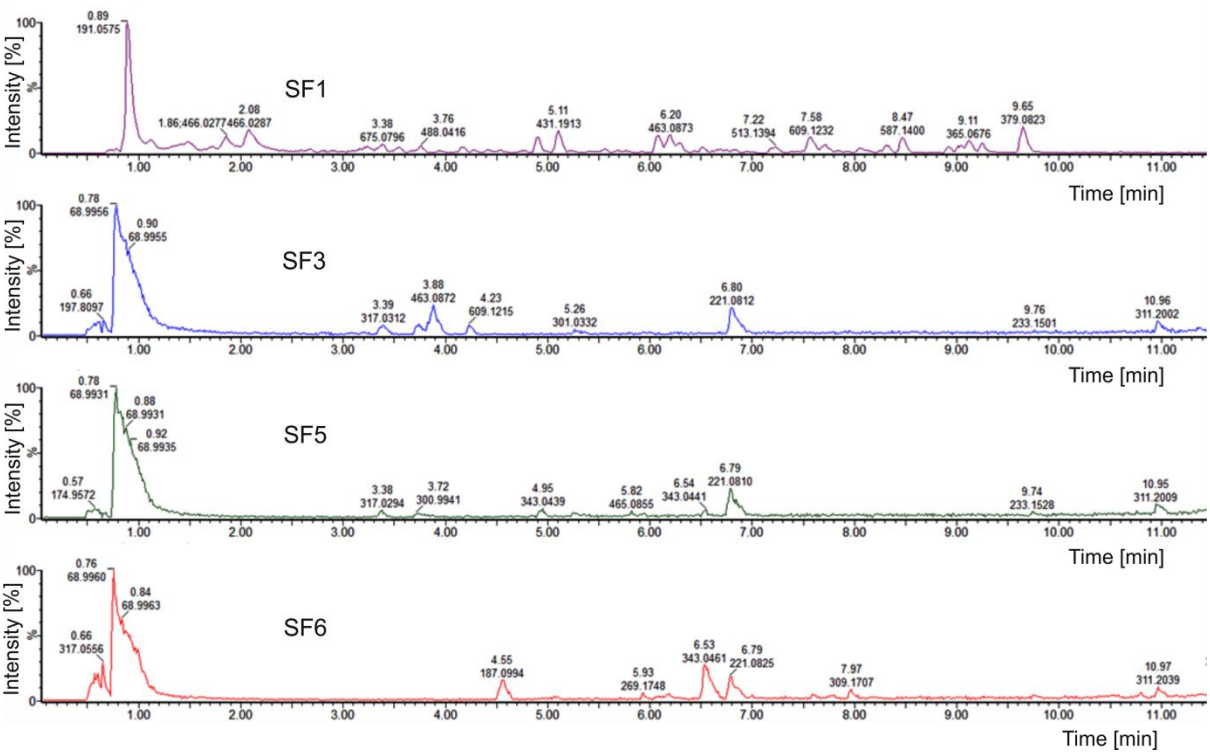

Figure 3.6*: UPLC-MS profiles of Sub-Fractions SF1, SF3, SF5, and SF6*

Sub-Fraction SF2, which contained a mixture of the compounds **65** and **66**, was not resolved on a normal C18 HPLC column.

The resolution of Sub-Fraction SF4 (18.4 mg/ml in a mixture of

MeOH/Water (3:2) by semi-preparative HPLC using an isocratic system 15% of MeCN + 0.05% TFA (B), (flow: 0.8 ml/min) produced 8.2 mg of compound **63** and 2.6 mg of compound **64**.

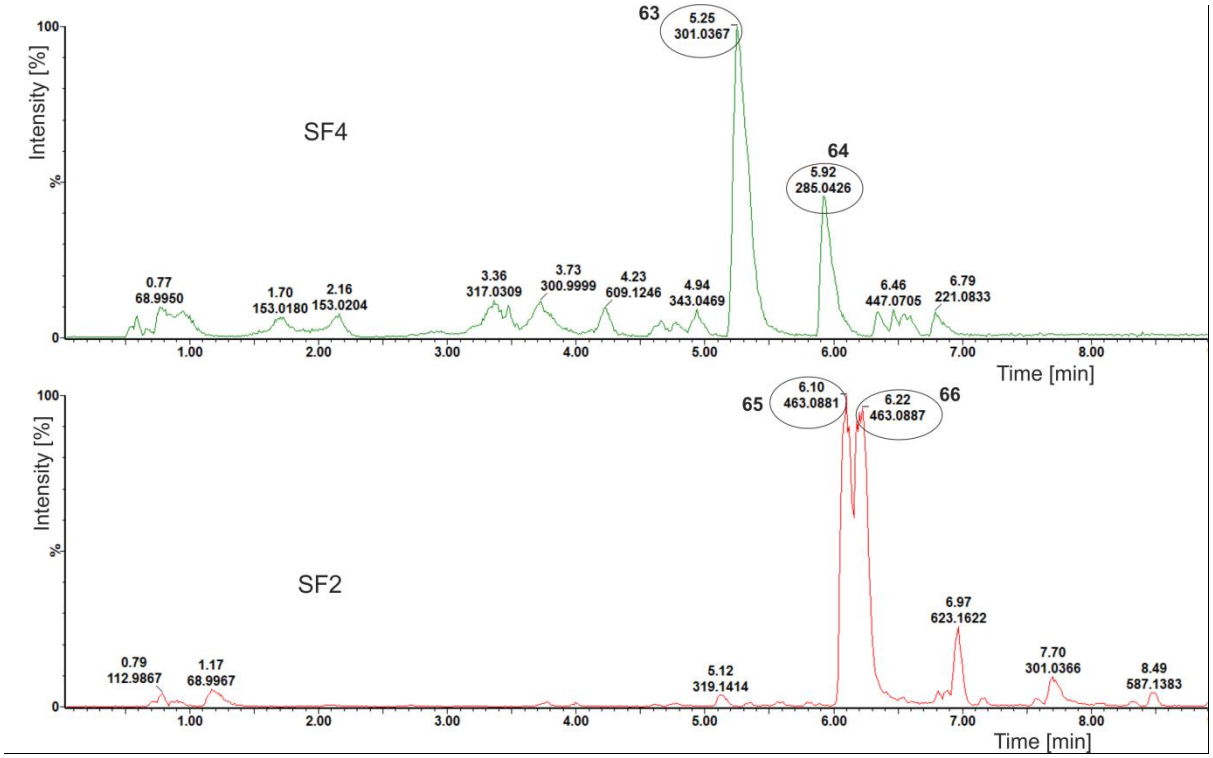

Figure 3.7*: UPLC-MS profiles of selected Sub-Fractions SF2 and SF4: quercetin (**63**), kaempferol (**64**), hyperoside (**65**), and isoquercetin (**66**)*

The four isolated compounds were also tested in the Nrf2 activation assay to verify that they were responsible of the activity in the most active extract. The results are given in Section 3.3.6.

3.3.3. Isolation of Lignans from the CH_2Cl_2 Extracts of *M. angustifolia* and *M. glauca*

The resolution of 50 mg of the CH_2Cl_2 extract of *M. glauca* by semi-preparative HPLC produced 4.7 mg of chinensinaphthol (**60**) (t_R: 3.0 min), 6.6 mg of justicidin B (**67**) (t_R: 4.3 min), and 5.2 mg of retrochinensinaphthol

methyl ether (**61**) (t_R: 12.2 min) (structures are given in Section 3.3.4).

The CH_2Cl_2 extract of *M. angustifolia* (50 mg in MeOH) also resolved by semi-preparative HPLC, provided 6.9 mg of chinensinaphthol (**60**) (t_R: 4.3 min), 4.9 mg of retrochinensinaphthol methyl ether (**61**) (t_R: 7.4 min), 4.0 mg of justicidin A (**58**) (t_R: 12.2 min), and 9.2 mg of 6-methoxyjusticidin A (**59**) (t_R: 16.8 min).

The structure elucidation (Section 3.3.4) of the above isolated compounds revealed them to be lignans, and lignans are known to exhibit anti-tumor activities [40], thus the isolated lignans were screened for cytotoxicity activity against selected human tumor cells. Results are given in Section 3.3.5.

3.3.4. Structure Elucidation of the Isolated Compounds

The confirmation of the structures of the four known flavonoids, quercetin (**63**) [48-52], kaempferol (**64**) [53-56], hyperoside (**65**) [57], and isoquercetin (**66**) [52], along with five lignans justicidin A (**58**) [38, 58-62], justicidin B (**67**) [63-73], 6-methoxyjusticidin A (**59**) [38], chinensinaphthol (**60**) [38], and retrochinensinaphthol methyl ether (**61**) [38] were done by NMR. They were found to be identical in their spectroscopic, physical, and/or chromatographic properties with the data previously reported. To the best of our knowledge, this was the first report showing the presence of quercetin, kaempferol, hyperoside, and isoquercetin in *M. angustifolia*. It was also the first study on the phytochemical composition of *M. glauca*, a species which had not been investigated for its biological activities and phytochemical properties before.

3.3.4.1. Quercetin

Compound **63**, identified as quercetin, isolated as a yellow amorphous solid, with λ_{max} 256 and 371 nm. The molecular formula of $C_{15}H_{10}O_7$ was deduced from its monodeprotonated ion at *m/z* 301.0349 (calculated for $C_{15}H_9O_7$, 301.0348), together with its fragmentation pattern with characteristic daughter ions at *m/z* 271 $[C_{14}H_7O_6]^{-1}$, 179 $[C_8H_4O_5]^{-1}$, 151 $[C_7H_3O_4]^{-1}$, 121

$[C_7H_5O_2]^{-1}$, and 93 $[C_6H_5O]^{-1}$ suggested it to be a flavonoid [74-76]. The ^{13}C NMR spectroscopic data showed it to have a flavonol skeleton confirming the presence of 15 carbon atoms, of which five were aromatic CH groups; ten quaternary carbon atoms (one carbonyl, five O-bearing, and four aliphatic) as deduced from its Dept135 signals, hinting at a 3,5,7,3′,4′-pentahydroxyflavone, commonly known under the name quercetin [77]. ^1H NMR spectrum (400 MHz, MeOH-d_4, δ, ppm, J/Hz) showed the presence of five aromatic protons (Table 3.4): two peaks at δ 6.17 (1H, d, J = 1.8 Hz) and 6.37 ppm (1H, d, J = 1.8 Hz) consistent with the *meta*-coupled protons H-6 and H-8 on the A-ring, and an ABX system at 7.73 (1H, d, J = 2.0 Hz, H-2′), 7.62 (1H, dd, J =2.0 Hz, 8.5 Hz, H-6′), and 6.87 (1H, d, J = 8.5 Hz, H-5′) corresponding to the catechol protons on the B-ring. This was corroborated by the COSY correlation between H-5′ and H-6′, HMBC interactions of both H-2′ and H-6′ with C-2, and also the HMBC correlation of H-6 with C-10 (Figure 3.8). The HSQC provided correlations between the carbon and its attached proton(s).

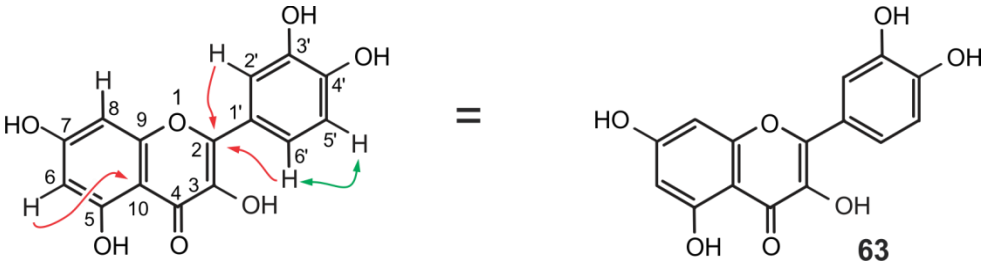

Figure 3.8: *Key HMBC (red arrows) and COSY (green double arrows) interactions, and the structure of the known compound quercetin (**63**)*

The NMR data compared favorably with those reported in the literature for quercetin [48-52, 78], and a comparison of the ^1H (CD_3OD, 400 MHz) and ^{13}C (CD_3OD, 100 MHz) data is shown in Table 3.3. Further confirmation was done by comparing the UPLC-MS retention times and the MS data of the purified quercetin with those of a purchased standard. The retention times of the two compounds in the UPLC-MS chromatograms were both at 5.25 min and both had the same molecular ion of 301.0349 ($[M-H]^-$).

Table 3.3: ^{1}H (400 MHz) and ^{13}C (100 MHz) NMR data of isolated quercetin (**63**) in CD_3OD and the published data

Position	Isolated quercetin (**63**)		Data published for quercetin in DMSO (^{1}H, 500 MHz ^{13}C, 125 MHz) [79]	
	*δ*C (ppm)	*δ*H (ppm), *J* in Hz	*δ*C (ppm)	*δ*H (ppm), *J* in Hz
1	-	-	-	-
2	148.1	-	147.7	-
3	137.4	-	136.4	-
4	177.6	-	176.5	-
5	162.7	-	161.4	-
6	99.6	6.17 (1H, d, 1.8)	98.8	6.19 (1H, d, 2.0)
7	165.9	-	164.5	-
8	94.7	6.37 (1H, d, 1.8)	94.0	6.40 (1H, d, 2.0)
9	158.5	-	156.8	-
10	104.8	-	103.7	-
1'	124.5	-	122.6	-
2'	116.1	7.73 (1H, d, 2.0)	115.7	7.68 (1H, d, 2.2)
3'	146.4	-	145.7	-
4'	149.1	-	148.3	-
5'	116.2	6.87 (1H, d, 8.5)	116.2	6.88 (1H, d, 8.4)
6'	121.9	7.62 (1H, dd, 8.5, 2.0)	120.6	7.54 (1H, dd, 8.4, 2.2)

3.3.4.2. Kaempferol

Compound **64,** identified as kaempferol, and obtained as a yellow amorphous solid, absorbing at λ_{max} 204, 265, and 365 nm had a molecular formula of $C_{15}H_{10}O_6$ as deduced from its monodeprotonated molecule at *m/z* 285.0410 (calculated for $C_{15}H_9O_6$, 285.0399) by ESI-MS, 16 units less than quercetin (**63**), indicative of one fewer hydroxy group. Its fragmentation with daughter ions at *m/z* 227 $[C_{13}H_7O_4]^{-1}$, 211 $[C_{13}H_7O_3]^{-1}$, 184 $[C_8H_7O_5]^{-1}$, 151 $[C_7H_3O_4]^{-1}$, 107 $[C_6H_3O_2]^{-1}$, and 93 $[C_6H_5O]^{-1}$ confirmed the compound to be a flavonoid [80, 81].

Its ^{1}H and ^{13}C NMR spectroscopic data showed it to have a flavonol skeleton with 15 carbons like compound **63**. Its Dept135 showed nine

quaternary carbons (one carbonyl, four O-bearing, and four aliphatic), indicative of a 3,5,7,4′-tetrahydroxyflavone, the ^{1}H NMR spectrum exhibited six aromatic protons (Table 3.4): ^{1}H NMR (400 MHz, MeOH-d_4, δ, ppm, *J*/Hz) 8.08 (2H, d, *J* = 9.0 Hz, H-2',6'), 6.90 (2H, d, *J* = 9.0 Hz, H-3', 5'), 6.39 (1H, d, *J* = 2.1 Hz, H-8), 6.18 (1H, d, *J* = 2.1 Hz, H-6). This compound resembled the previously described quercetin (**63**), but differed from it by the absence of a hydroxy group at C-3' as shown by the COSY interaction H-2' ↔ H-3'. The correlations between a carbon and its attached proton(s) were determined through HSQC signals.

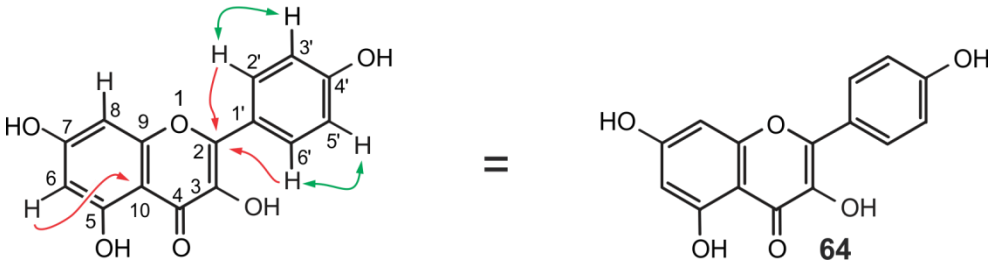

Figure 3.9: *Key HMBC (red arrows) and COSY (green double arrows) interactions, and the structure of kaempferol (**64**)*

The ^{1}H and ^{13}C chemical shift values (δ) obtained showed a good agreement with the previously published flavonoid kaempferol (Table 3.4) [53-56]. This was confirmed by the COSY and the HMBC correlations (Figure 3.9), and also by comparing the UPLC-MS retention times and MS data of the isolated kaempferol with those of a purchased standard. The retention times of the two were both at 5.90 min, and both had the same molecular ion of 285.0410 ($[M-H]^-$).

Table 3.4: ^{1}H (400 MHz) and ^{13}C (100 MHz) NMR data of isolated kaempferol (**64**) in CD_3OD and the published data

Position	Kaempferol (**64**)		Data published for kaempferol in CD_3OD (^{1}H, 500 MHz ^{13}C, 125 MHz) [79]	
	*δ*C (ppm)	*δ*H (ppm), *J* in Hz	*δ*C (ppm)	*δ*H (ppm), *J* in Hz
1	-	-	-	-
2	148.2	-	148.2	-
3	137.4	-	137.8	-
4	177.8	-	177.8	-
5	163.0	-	162.3	-
6	99.7	6.18 (1H, d, 2.1)	99.4	6.20 (1H, br, s)
7	165.7	-	165.7	-
8	95.2	6.39 (1H, d, 2.1)	95.2	6.41 (1H, br, s)
9	158.2	-	158.2	-
10	104.6	-	104.6	-
1'	123.7	-	123.7	-
2'	130.4	8.08 (1H, d, 9.0)	130.4	8.12 (1H, d, 8.6)
3'	116.3	6.90 (1H, d, 9.0)	116.3	6.92 (1H, d, 8.6)
4'	160.5	-	160.5	-
5'	116.3	6.90 (1H, d, 9.0)	116.3	6.92 (1H, d, 8.6)
6'	130.4	8.08 (1H, d, 9.0)	130.4	8.12 (1H, d, 8.6)

3.3.4.3. Hyperoside and Isoquercetin

As described earlier (Sections 3.2.2.4 and 3.3.2), Fraction SF2, containing hyperoside (**65**) and isoquercetin (**66**) (in ratio 4:3 according to the ^{1}H NMR peaks), could not be resolved by HPLC (Figure 3.10) as they were stereoisomers of each other (Figure 3.12). They were isolated as an amorphous yellow solid after purification by HPLC.

The confirmation of the presence of two stereoisomers, hyperoside (**65**) and isoquercetin (**66**) (t_R 6.10 and 6.22 min respectively), was done using UPLC-MS, and comparing the retention times (t_R 6.29 and 6.53 min) of the two isolated compounds with a mixed solution (ratio 2 to 1) of the purchased standards of hyperoside and isoquercetin (Figure 3.10).

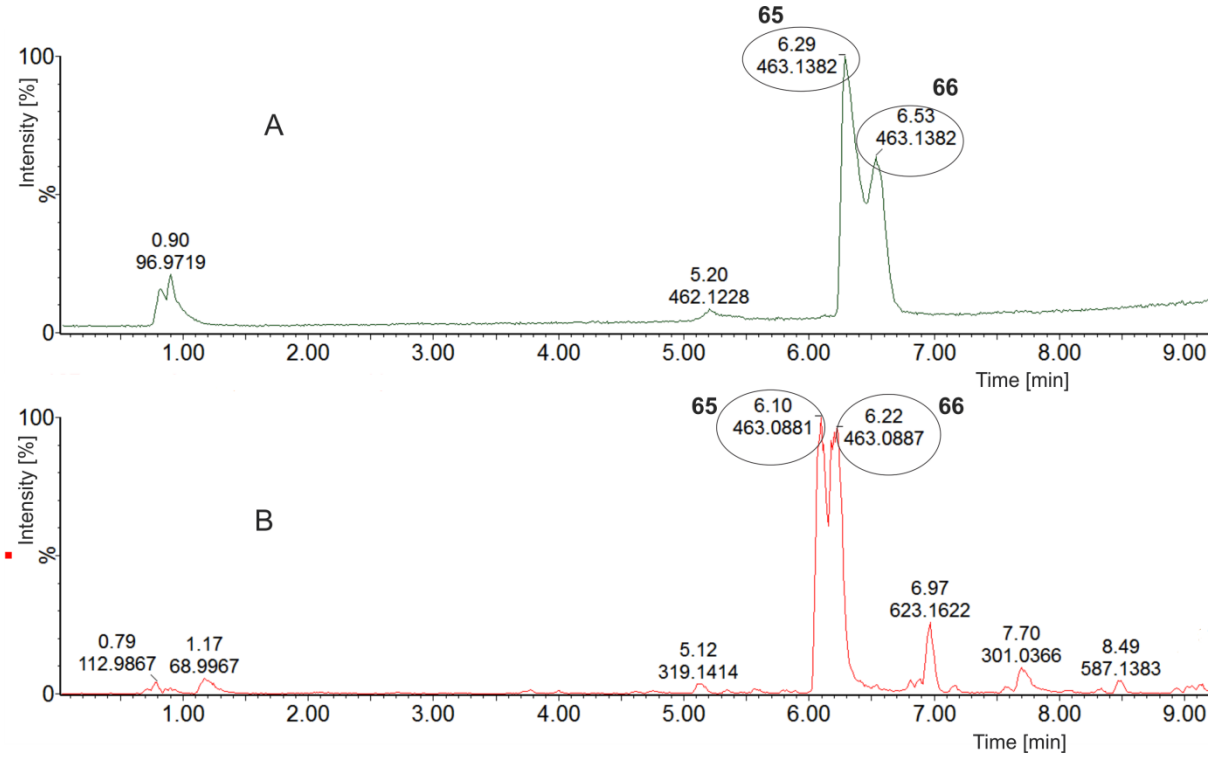

Figure 3.10: *UPLC-MS profiles of a mixture (ratio 2:1) of purchased standards of hyperoside (**65**) and isoquercetin (**66**) (A) and that of the isolated compounds hyperoside (**65**) and isoquercetin (**66**) (B)*

From ESI-MS, both compounds had the molecular formula $C_{21}H_{20}O_{12}$, showing $[M-H]^-$ ions at *m/z*: 463.0881 and 463.0887 (calculated for $C_{21}H_{19}O_{12}$, 463.0877). Product ions in the second-order mass spectrum (Figure 3.11) showed the base peak ion at *m/z* 300.0269 [M-H-163] evidencing the loss of a glucosyl entity and a galactosyl unit.

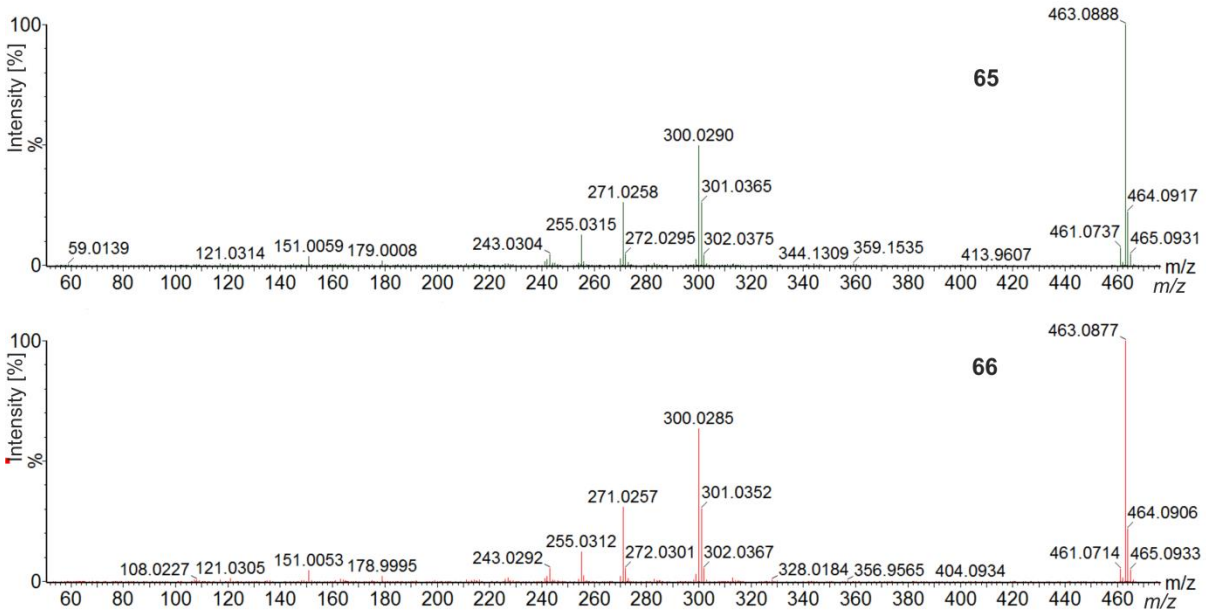

Figure 3.11: *Fragmentation pattern of hyperoside (**65**) and isoquercetin (**66**)*

The fragment ion observed at *m/z* 300/301 is characteristic of flavonoids containing the quercetin aglycon [75, 82-84]. The recorded NMR data of the isolated mixture of **65** and **66** were compared to the NMR data reported in the literature for hyperoside [85] and isoquercetin [88] to assign the ^{1}H and ^{13}C chemical shifts (Table 3.5 and 3.6).

Table 3.5: ^{1}H (400 MHz) and ^{13}C (100 MHz) NMR data of isolated hyperoside (**65**) in CD_3OD and the published data

Position	Hyperoside (**65**)		Data published for hyperoside in DMSO-d_6 (^{1}H, 500 MHz ^{13}C, 100 MHz) [85]	
	*δ*C (ppm)	*δ*H (ppm), *J* in Hz	*δ*C (ppm)	*δ*H (ppm), *J* in Hz
1	-	-	-	-
2	158.3	-	156.3	-
3	135.9	-	133.5	-
4	179.8	-	177.5	-
5	163.3	-	161.3	-
6	100.2	6.21 (1H, d, 2.1)	98.7	6.19 (1H, d, 1.9)
7	166.4	-	164.1	-
8	94.9	6.41 (1H, d, 2.1)	93.5	6.39 (1H, d, 1.9)
9	158.6	-	156.2	-
10	105.4	-	103.9	-
1'	123.4	-	121.1	-
2'	116.4	7.84 (1H, d, 2.2)	115.2	7.51 (1H, d, 2.1)
3'	146.1	-	144.8	-
4'	150.2	-	148.5	-
5'	117.7	6.87 (1H, d, 8.5)	115.9	6.80 (1H, d, 8.5)
6'	123.5	7.59 (1H, dd, 8.5, 2.2)	122.0	7.65 (1H, dd, 8.5, 2.1)
1''	106.2	5.17 (1H, d, 8.0)	108.1	5.35 (1H, d, 7.7)
2''-6''	61.9-78.9	3.20-3.85 (6H, m)	60.1-75.9	3.15-3.63 (6H, m)

The positions of the glucosyl and galactosyl groups were determined to be at C-3 based on the HMBS correlation between the anomeric proton 1H″ and C-3 (Figure 3.12), and also on the similarity with the characteristic fragmentation pattern of quercetin-3-glucuronides (absence of fragments at *m/z* 459, 415, 371, and 343 specific to the glucuronide unit located on the B ring) as suggested by M Dueñas *et al.* [75], the fragments at *m/z* 271.0256 and *m/z* 255.0305 obviously resulted from the loss of CO and CO_2, respectively, from quercetin [75].

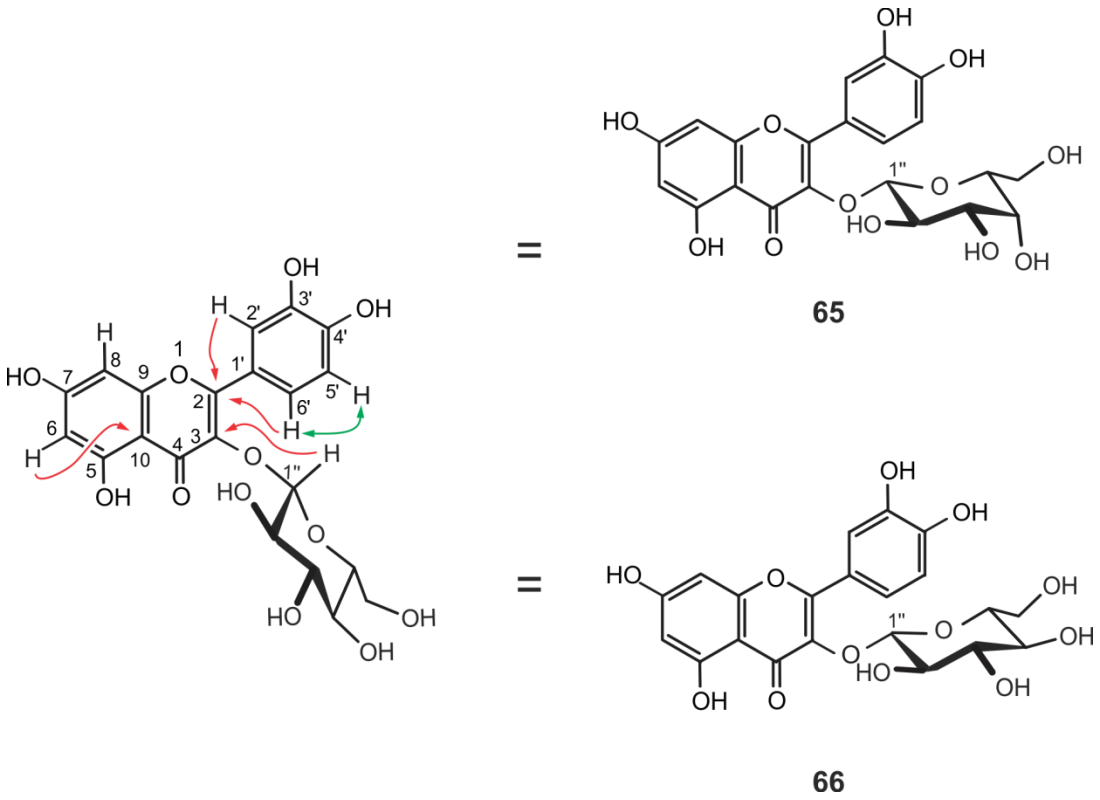

Figure 3.12: *Key HMBC (red arrows) and COSY (green double arrows) interactions, and the structures of hyperoside (**65**) and isoquercetin (**66**)*

Previously, Sukito and Tachibana [86], and also Güvenalp and Demirezer [87] isolated hyperoside and isoquercetin from *Camellia sasanqua*. Their ^{1}H NMR data (Table 3.5 and 3.6) were in accordance with those recorded for compounds **65** and **66**.

Table 3.6: ^{1}H (400 MHz) and ^{13}C (100 MHz) NMR data of isolated isoquercetin (**66**) in CD_3OD and the published data

Position	Isoquercetin (**66**)		Published data for isoquercetin in CD_3OD (^{1}H, 500 MHz ^{13}C, 125 MHz) [88]	
	δC (ppm)	δH (ppm), *J* in Hz	δC (ppm)	δH (ppm), *J* in Hz
1	-	-	-	-
2	159.2	-	156.1	-
3	135.9	-	133.3	-
4	179.8	-	177.4	-
5	163.3	-	161.2	-
6	100.2	6.21 (1H, d, 2.1)	98.8	6.21 (1H, d, 2.0)
7	166.4	-	164.4	-
8	94.9	6.40 (1H, d, 2.1)	93.6	6.41 (1H, d, 2.0)
9	158.6	-	156.4	-
10	104.5	-	103.8	-
1'	123.4	-	121.1	-
2'	116.4	7.71 (1H, d, 2.2)	115.2	7.61 (1H, d, 2.2)
3'	146.1	-	144.8	-
4'	150.2	-	148.5	-
5'	117.9	6.87 (1H, d, 8.5)	116.2	6.86 (1H, d, 9.0)
6'	123.5	7.59 (1H, dd, 8.5, 2.2)	126.6	7.58 (1H, dd, 9.0, 2.2)
1''	106.2	5.26 (1H, d, 8.0)	100.9	5.47 (1H, d, 7.4)
2''-6''	61.9-78.9	3.35-3.85 (6H, m)	61.0-77.6	3.10-3.60 (6H, m)

3.3.4.4. Justicidin B

Justicidin B (**67**) was obtained as a colorless solid, possessing a molecular formula $C_{21}H_{16}O_6$ as revealed from its ESI-MS (*m/z* 365.1082 $[M+H]^+$) (calculated for $C_{21}H_{17}O_6$, 365.1025). Its UV spectra (PDA detector of HPLC) showed λ_{max} at 254, 288, and 300 nm. The ^{1}H NMR ($CDCl_3$, 400 MHz) (Table 3.7) exhibited two singlets at δ_H 3.80, and 4.04 corresponding to two methoxy groups located at C-4 and C-5 as confirmed by the NOESY and the HMBC correlations (Figure 3.13). A singlet of two protons resonating at δ_H 5.38 indicated the presence of a methylene group located in a five-membered lactone ring as confirmed by the HMBC interactions, which was characteristic of lignans. Two peaks at δ_H 6.04 (1H, d, *J* = 1.0 Hz) and δ_H

6.09 (1H, d, *J* = 1.1 Hz) revealed the presence of a methylenedioxy group located at C-3′ and C-4′ as shown by HMBC correlations of the two protons with both C-3′ and C-4′. In the aromatic region of the spectrum, a characteristic pattern of a 1,3,4-trisubstituted phenyl group was observed: a doublet of doublet at δ_H 6.82 (1H, dd, *J* = 8.0 and 1.6 Hz, H-6′), two doublets at δ_H 6.85 (1H, d, *J* = 1.6 Hz, H-2′) and δ_H 6.96 (1H, d, *J* = 8.0 Hz, H-5′), with an *ortho*-coupling between H-5′ and H-6′ confirmed by the COSY (Figure 3.13). Three singlets resonating at δ_H 7.09, 7.17 and 7.69 were assigned to be at H-3, H-6 and H-7 respectively, based on the NOESY interactions H-3 ↔ 4-OMe and 5-OMe ↔ H-6, leaving the only possibility to locate the remaining proton at C-7. This was further corroborated by HMBC correlations between H-7 and C-9.

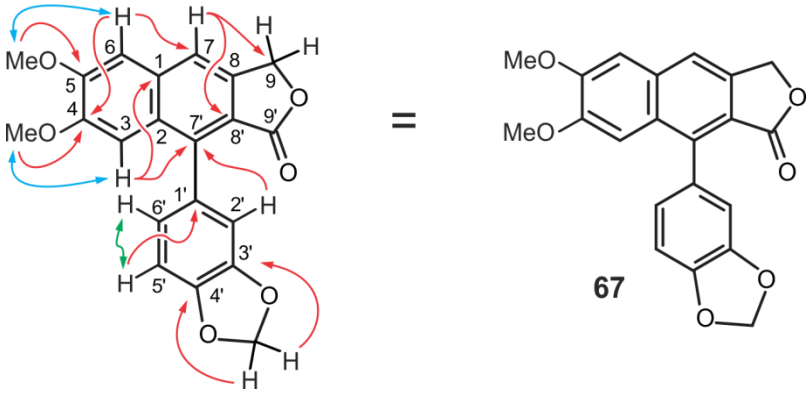

Figure 3.13: *Key HMBC (red arrows), NOESY (blue double arrows), and COSY (green double arrows) interactions, and the structure of justicidin B (**67**)*

The compound was found to conform in its spectroscopic and physical properties to those of justicidin B isolated from *Polygala chinensis* [89] and from other sources [63-73, 90].

Table 3.7: ^{1}H (400 MHz) and ^{13}C (100 MHz) NMR data of isolated justicidin B (**67**) in $CDCl_3$ and published data

Position	Justicidin B (**67**)		Data published for justicidin B in $CDCl_3$ (^{1}H, 400 MHz ^{13}C, 100 MHz) [90]	
	*δ*C (ppm)	*δ*H (ppm), *J* in Hz	*δ*C (ppm)	*δ*H (ppm), *J* in Hz
1	130.0	-	133.4	-
2	129.8	-	128.9	-
3	109.0	7.09 (1H, s)	108.0	7.11 (1H, s)
4	153.3	-	152.2	-
5	151.5	-	151.1	-
6	106.5	7.17 (1H, s)	106.0	7.23 (1H, s)
7	119.7	7.69 (1H, s)	118.3	7.71 (1H, s)
8	139.1	-	138.5	-
9	68.6	5.38 (2H, s)	68.0	5.32 (1H, s)
1'	129.5	-	128.4	-
2'	111.7	6.85 (1H, d, 1.6)	110.5	6.82 (1H, d, 1.7)
3'	148.5	-	147.6	-
4'	148.2	-	147.5	-
5'	107.4	6.96 (1H, d, 8.0)	106.2	6.95 (1H, d, 7.9)
6'	124.5	6.82 (1H, dd, 8.0, 1.6)	123.5	6.81 (1H, dd, 7.9, 1.7)
7'	141.1	-	139.6	-
8'	119.7	-	118.5	-
9'	170.2	-	169.9	-
4-OMe	55.9	3.80 (3H, s)	55.8	3.87 (3H, s)
5-OMe	56.5	4.04 (3H, s)	56.1	4.17 (3H, s)
3'-OCH_2O-4'	102.4	6.04 (1H, d, 1.0) 6.09 (1H, d, 1.1)	101.3	6.04 (1H, d, 1.2) 6.11 (1H, d, 1.2)

To the best of our knowledge, it is the first time that justicidin B was isolated from *Monsonia* species; it is frequently found in plant species of the genera *Polygala* and *Justicia*.

3.3.4.5. Justicidin A

Justicidin A (**58**) was isolated as a white amorphous solid. Its molecular formula was deduced to be $C_{22}H_{18}O_7$ (ESI-MS *m/z* 395.1190 $[M+H]^+$) (calculated for $C_{22}H_{19}O_7$, 395.1131). Its UV spectra (PDA detector of HPLC) showed λ_{max} at 264, 295, 309, and 350 nm. Its ^{1}H NMR spectrum ($CDCl_3$, 400 MHz) was similar to that of justicidin B (**67**) (Table 3.8). The main difference was that the spectrum of justicidin A (**58**) had three methoxy groups (δ_H 3.78, 4.05, 4.12), located at C-7 as deduced from the HMBC correlations of both H-6 and H-9 with C-7, as well as the HMBC interaction of 7-OMe with C-7 (Figure 3.14).

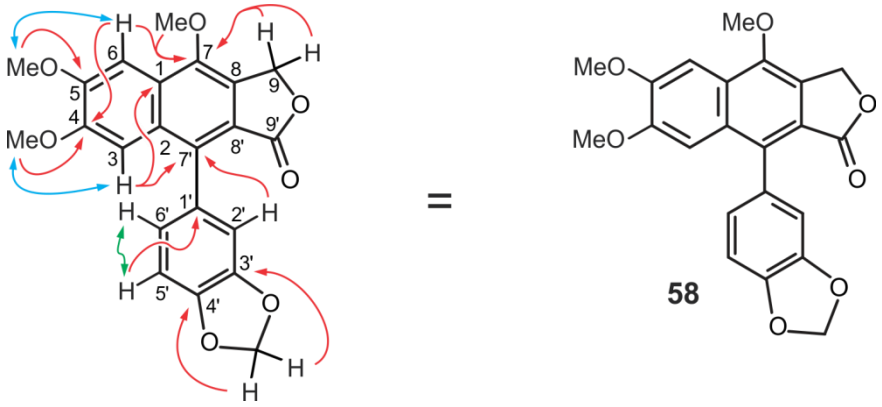

Figure 3.14: *Key HMBC (red arrows), NOESY (blue double arrows), and COSY (green double arrows) interactions, and the structure of justicidin A (**58**)*

The three methoxy groups were thus located at C-7, C-4, and C-5. The methylene signal at δ_H 5.53 of the furanone ring, a pair of proton doublets characteristic for the methylenedioxy substituent at δ_H 6.04 (J = 1.5 Hz) and 6.08 (J = 1.5 Hz), and the three aromatic protons at δ_H 6.78 (1H, dd, J = 7.8 and 1.8 Hz, H-6′), δ_H 6.80 (1H, d, J = 1.8 Hz, H-2′), and δ_H 6.94 (1H, d, J = 7.8 Hz, H-5′) forming the 1,3,4-trisubstituted phenyl group found in justicidin B (**64**) were also present in the NMR spectrum for justicidin A. Two aromatic singlets found at δ_H 7.04 and δ_H 7.52 were assigned to be at C-3 and C-6, respectively. From the HMBC correlations of H-3 with 4-OMe and H-6 with 5-OMe, this was corroborated by the HSQC interactions attributing the two protons to C-3 and C-6. This compound was found to be identical in its

spectroscopic and physical properties with the data reported before for justicidin A [38, 58-61, 90, 91].

Table 3.8: ^{1}H (400 MHz) and ^{13}C (100 MHz) NMR data of isolated justicidin A (**58**) in $CDCl_3$ and published data

Position	Justicidin A (**58**)		Data published for justicidin A in $CDCl_3$-d_1 (^{1}H, 400 MHz ^{13}C, 100 MHz) [90]	
	δC (ppm)	δH (ppm), *J* in Hz	δC (ppm)	δH (ppm), *J* in Hz
1	123.8	-	123.6	-
2	134.8	-	134.4	-
3	106.6	7.04 (1H, s)	106.2	7.03 (1H, s)
4	150.2	-	150.1	-
5	151.4	-	150.9	-
6	100.4	7.52 (1H, s)	100.6	7.52 (1H, s)
7	147.7	-	147.7	-
8	130.2	-	130.4	-
9	66.4	5.53 (2H, s)	66.6	5.65 (1H, s)
1'	125.3	-	126.5	-
2'	110.7	6.80 (1H, d, 1.8)	110.7	6.93 (1H, d, 1.3)
3'	147.3	-	147.4	-
4'	147.8	-	147.8	-
5'	107.8	6.94 (1H, d, 7.8)	108.2	6.97 (1H, d, 7.9)
6'	123.6	6.78 (1H, dd, 7.8, 1.8)	123.6	6.77 (1H, dd, 7.8, 1.3)
7'	128.5	-	128.5	-
8'	119.2	-	119.2	-
9'	170.1	-	169.6	-
4-OMe	56.0	3.78 (3H, s)	55.8	3.81 (3H, s)
5-OMe	56.0	4.05 (3H, s)	56.1	4.16 (3H, s)
7-OMe	59.3	4.12 (3H, s)	56.6	4.15 (3H, s)
3'-OCH_2O-4'	101.2	6.04 (1H, d, 1.5)	101.2	6.07 (1H, d, 1.3)
		6.08 (1H, d, 1.5)		6.10 (1H, d, 1.3)

3.3.4.6. 6-Methoxyjusticidin A[1]

6-Methoxyjusticidin A (**59**), also obtained as a white amorphous solid, had a molecular ion peak at *m/z* 425.1329 ($[M+H]^+$) (calculated for $C_{23}H_{21}O_8$, 425.1236) in the positive ESI-MS, indicating the molecular formula to be $C_{23}H_{20}O_8$. The observed UV absorptions were at λ_{max} 237, 263, and 365 nm. Its ^{1}H NMR spectrum (CD_3Cl, 400 MHz) (Table 3.9) exhibited four singlets of three protons each at δ_H 3.75, 4.02, 3.95, and 3.97 assigned to be the methoxy groups located at C-4, C-5, C-6, and C-7 respectively, as deduced from the NOESY and the HMBC correlations (Figure 3.15). A methylene singlet characteristic of the methylene group located in a five-membered lactone ring of lignans was observed at δ_H 5.42.

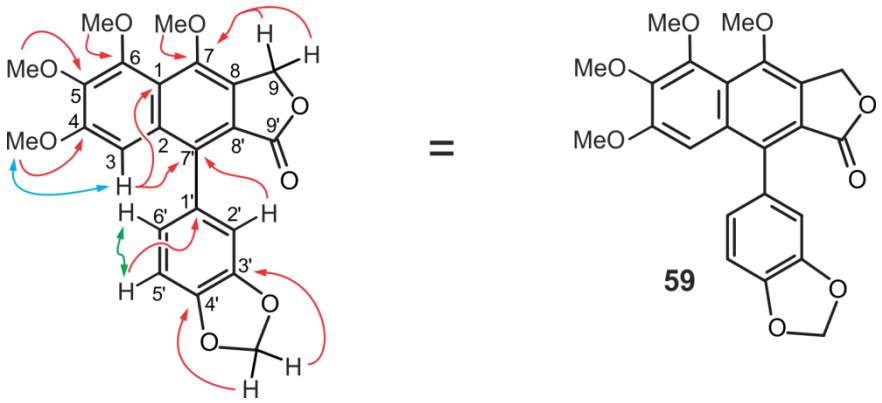

Figure 3.15: *Key HMBC (red arrows), NOESY (blue double arrows), and COSY (green double arrows) interactions, and the structure of 6-methoxyjusticidin A (**59**)*

A pair of proton doublets with a weak coupling constant at δ_H 6.03 (1H, d, *J* = 1.5 Hz) and δ_H 6.08 (1H, d, *J* = 1.5 Hz) was observed for the methylenedioxy substituent. As for justicidin A (**58**), the aromatic region of the spectrum showed a doublet of doublets at δ_H 6.76 (1H, dd, *J* = 7.8 and 1.7 Hz, H-6′), two doublets at δ_H 6.78 (1H, d, *J* = 1.7 Hz, H-2′) and δ_H 6.94 (1H, d, *J* = 7.8 Hz, H-5′), which is characteristic of a 1,3,4-trisubstituted phenyl group. A singlet at δ_H 6.94 was assigned to correspond to a proton at C-3 from its NOESY interaction H-3 ↔ 4-OMe, and the two HMBC correlations H-3 to C-7′ and H-3 to C-1(Figure 3.15). The isolated 6-

[1] «5-Methoxyjusticidin A» is referred to as «6-Methoxyjusticidin A» in this thesis for reasons of consistence with the numbering system based on the biosynthetic pathway [40].

methoxyjusticidin A (**59**) was found to match in its spectroscopic and physical properties with the data previously reported for “5-methoxyjusticidin A” [38, 92].

Table 3.9: ^{1}H (400 MHz) and ^{13}C (100 MHz) NMR data of isolated 6-methoxyjusticidin A (**59**) in $CDCl_3$ and the published data

Position	6-Methoxyjusticidin A (**59**)		Data published for 5-methoxyjusticidin A in $CDCl_3$-d_1 (^{1}H, 500 MHz ^{13}C, 100 MHz) [38]	
	*δ*C (ppm)	*δ*H (ppm), *J* in Hz	*δ*C (ppm)	*δ*H (ppm), *J* in Hz
1	122.6	-	122.2	-
2	135.5	-	133.5	-
3	103.7	6.94 (1H, s)	103.7	6.94 (1H, s)
4	153.4	-	153.1	-
5	144.9	-	144.9	-
6	148.2	-	148.1	-
7	149.2	-	149.1	-
8	121.7	-	120.7	-
9	66.8	5.42 (2H, s)	66.5	5.41 (1H, s)
1'	128.4	-	128.5	-
2'	110.7	6.78 (1H, d, 1.7)	110.6	6.78 (1H, d, 1.3)
3'	148.8	-	147.6	-
4'	148.3	-	147.5	-
5'	108.3	6.94 (1H, d, 7.8)	108.3	6.94 (1H, d, 7.9)
6'	124.0	6.76 (1H, dd, 7.8, 1.7)	123.6	6.75 (1H, dd, 7.9, 1.3)
7'	136.4	-	135.6	-
8'	130.0	-	129.9	-
9'	169.5	-	169.5	-
4-OMe	55.8	3.75 (3H, s)	55.8	3.74 (3H, s)
5-OMe	61.5	4.02 (3H, s)	61.4	4.01 (3H, s)
6-OMe	62.5	3.95 (3H, s)	62.4	3.95 (3H, s)
7-OMe	62.2	3.97 (3H, s)	62.0	3.97 (3H, s)
3'-OCH_2O-4'	101.2	6.03 (1H, d, 1.5)	101.2	6.02 (1H, d, 1.0)
	-	6.08 (1H, d, 1.5)	-	6.07 (1H, d, 1.0)

3.3.4.7. Chinensinaphthol

Chinensinaphthol (**60**), was obtained as a white amorphous substance. It was found to possess a molecular formula of $C_{21}H_{16}O_7$ as deduced by the ESI-MS, and from the number of signals in the ^{13}C NMR spectrum. A mass-to-charge ratio (*m/z*) of 381.1026 $[M+H]^+$ (calculated for $C_{21}H_{17}O_7$, 381.0974) observed in ESI-MS in positive mode was assigned to the molecular ion peak 14 units less than justicidin A (**58**), which was indicative of one fewer CH_3 group. Its UV maximum plot from the HPLC-PDA spectrum showed maximum absorptions at 322.0, 266.4, and 228.8 nm, which was consistent of aryl naphthalene molecules. The ^1H NMR data ($CDCl_3$, 400MHz) (Table 3.10) showed two singlets at δ_H 3.86 (3H, s) and δ_H 4.20 (3H, s) indicating the presence of two methoxy groups on the phenyl group at positions C-3′ and C-4′ respectively, based on the long-range NOESY interactions between H-2′ ↔ 3′-OCH_3 and H-5′ ↔ 4′-OCH_3, as well as HMBC correlations between 3′-OCH_3 and C-3′, and 4′-OCH_3 and C-4′ (Figure 3.16).

A singlet found at δ_H 5.36 (2H, s) was assigned to the lactone methylene group like in the afore described lignans **58**, **59**, and **67**. Another singlet of two protons at δ_H 6.03 (2H, s) characteristic of methylenedioxy group was assigned to be attached to the naphthalene moiety based on the HSQC and the HMBC interactions of these protons with both C-4 and C-5 (Figure 3.16).

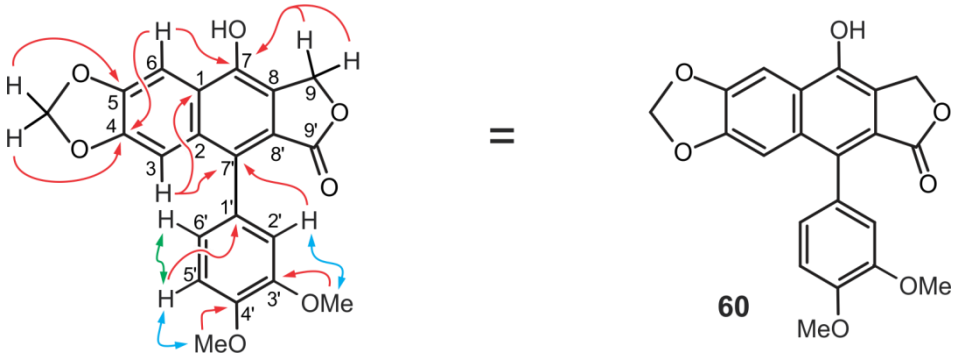

Figure 3.16: *Key HMBC (red arrows), NOESY (blue double arrows), and COSY (green double arrows) interactions, and the structure of chinensinaphthol (**60**)*

The multiplicity pattern of the aromatic protons in the aromatic C ring formed an ABX system characteristic of a trisubstituted phenyl ring as observed for the previous lignans. These protons resonated at δ_H 6.81(1H, dd, J = 8.8 and 2.0 Hz, H-6′), δ_H 6.81(1H, d, J = 2.0 Hz, H-2′), and δ_H 7.03 (1H, d, J = 8.8 Hz, H-5′). This was also supported by the COSY interaction between the protons H-5′ and H-6′ in the C ring. Moreover, two singlets resonating at δ_H 6.87 and δ_H 8.12 were assigned to positions C-3 and C-6 based on their HMBC correlations (H-3 to C-1 and C-7′, and also H-6 to C-4 and C-7). Based on the HMBC correlations of C-7 with both H-6 and the lactone methylene group, the hydroxy group was situated at C-7 (Figure 3.16).

Table 3.10: ^{1}H (400 MHz) and ^{13}C (100 MHz) NMR data of isolated chinensinaphthol (**60**) in $CDCl_3$-d_1 and the published data

Position	Chinensinaphthol (**60**)		Data published for chinensinaphthol in $CDCl_3$ (^{1}H, 500 MHz ^{13}C, 100 MHz) [38]	
	δC (ppm)	δH (ppm), J in Hz	δC (ppm)	δH (ppm), J in Hz
1	125.3	-	124.6	-
2	131.3	-	131.0	-
3	102.2	6.87 (1H, s)	102.5	6.85 (1H, s)
4	148.1	-	148.0	-
5	148.8	-	148.6	-
6	98.6	8.12 (1H, s)	97.9	7.61 (1H, s)
7	145.6	-	145.1	-
8	118.8	-	119.0	-
9	66.7	5.36 (2H, s)	66.4	5.35 (1H, s)
1'	127.5	-	127.5	-
2'	114.2	6.81 (1H, d, 2.0)	114.2	6.83 (1H, d, 2.1)
3'	148.2	-	148.2	-
4'	148.3	-	148.3	-
5'	111.2	7.03 (1H, d, 8.8)	111.2	7.05 (1H, d, 8.2)
6'	122.5	6.81 (1H, dd, 8.8, 2.0)	122.5	6.77 (1H, dd, 8.0, 2.1)
7'	130.3	-	130.3	-
8'	122.3	-	122.3	-
9'	164.4	-	164.4	-

4-OCH_2O-5	101.8	6.03 (1H, s)	101.9	6.15 (1H, s)
3'-OMe	55.7	3.86 (3H, s)	55.5	3.77 (3H, s)
4'-OMe	55.5	4.20 (3H, s)	55.4	3.90 (3H, s)

Based on the similarity of the spectral data with the ones previously published, and the supporting correlations observed in the 2D NMR experiments, the compound was unambiguously identified as chinensinaphthol [38, 92, 93].

3.3.4.8. Retrochinensinaphthol Methyl Ether

The isolated retrochinensinaphthol methyl ether (**61**), a white amorphous substance, was an isomer of justicidin A (**58**) based on the ESI-MS measurements $C_{22}H_{18}O_7$ (ESI-MS *m/z* 395.1191 $[M+H]^+$) (calculated for $C_{22}H_{19}O_7$, 395.1131). This was also corroborated by the number of signals in the ^{13}C NMR spectrum. Its UV maximum plot showed the characteristic of aryl naphthalene molecules with absorptions at 230.0, 265.9, and 321.8 nm.

The ^1H NMR data showed three singlets of three protons each at δ_H 4.20, 3.84, and 3.95 deduced to be situated at C-7, C-3′, and C-4′, respectively, from HMBC interactions of both H-6 and 7-OMe with C-7, 3′-OMe with C-3′, and 4′-OMe with C-4′. This was confirmed by the NOESY interactions of H-2′ with 3′-OMe, and that of H-5′ with 4′-OMe. A singlet of two protons at δ_H 5.37 was observed, which was typical of the lactone methylene, another singlet of two protons resonating at δ_H 6.03 was attributed to methylenedioxy substituent from the HSQC. As in the case of chinensinaphthol (**60**), this methylenedioxy group was attached to the naphthalene part as confirmed by the HMBC correlations of the two protons with C-4 and C-5 (Figure 3.17). Three aromatic protons formed an ABX system characteristic of a trisubstituted phenyl ring as observed in the previous isolated lignans. These protons resonated at δ_H 6.83 (1H, d, *J* = 1.9 Hz, H-2′), 6.99 (1H, d, *J* = 8.2 Hz, H-5′), and 6.88 (1H, dd, *J* = 8.2, 1.9 Hz, H-6′), and also their coupling was supported by a COSY correlation H-5′ with H-6′ (Figure 3.17). The two remaining protons found at δ_H 6.85 (1H, s) and 8.13 (1H, s) were assigned

to be at C-3 and C-6, respectively, based on the HMBC correlations of H-3 with both, C-1 and C-7′, and that of H-6 with both, C-4 and C-7. This was also confirmed by the HSQC correlations. The compound was structurally similar to chinensinaphthol (**60**) but differed from it by the replacement of the hydroxy group at C-7 by a methoxy group as supported by the HMBC (Figure 3.17), and also by the fact that the methylene and the carbonyl groups of the lactone ring were inverted based on the joint HMBC cross signal from H-3 and the two protons of the methylene to C-7′ (Figure 3.17).

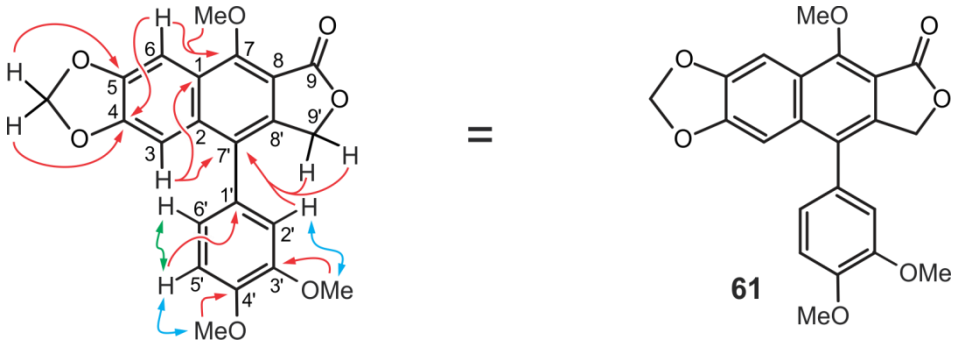

Figure 3.17: *Key HMBC (red arrows), NOESY (blue double arrows), and COSY (green double arrows) interactions, and the structure of retrochinensinaphthol methyl ether (**61**)*

All the spectroscopic data (Table 3.11) and physical properties of this compound were in accordance with those of retrochinensinaphthol methyl ether reported earlier [38, 94].

Table 3.11: ^{1}H (400 MHz) and ^{13}C (100 MHz) NMR data of isolated retrochinensinaphthol methyl ether (**61**) in $CDCl_3$ and the published data

Position	Retrochinensinaphthol ethyl ether (**61**)		Published data for retrochinensinaphthol methyl ether in $CDCl_3$ (^{1}H, 500 MHz ^{13}C, 100 MHz) [38]	
	*δ*C (ppm)	*δ*H (ppm), *J* in Hz	*δ*C (ppm)	*δ*H (ppm), *J* in Hz
1	125.8	-	125.3	-
2	135.7	-	135.3	-
3	102.2	6.85 (1H, s)	102.2	6.98 (1H, s)
4	147.9	-	148.2	-
5	150.8	-	150.8	-
6	100.1	8.13 (1H, s)	100.2	7.71 (1H, s)
7	155.7	-	155.7	-
8	110.1	-	110.1	-
9	68.0	5.37 (2H, s)	68.8	5.11 (1H, s)
1'	128.8	-	128.5	-
2'	112.5	6.83 (1H, d, 1.9)	112.6	6.83 (1H, d, 2.0)
3'	149.4	-	149.4	-
4'	149.0	-	149.0	-
5'	111.8	6.99 (1H, d, 8.2)	111.8	6.99 (1H, d, 8.0)
6'	121.9	6.88 (1H, dd, 8.2, 1.9)	121.9	6.86 (1H, dd, 8.0, 2.0)
7'	127.5	-	127.5	-
8'	140.0	-	139.4	-
9'	169.2	-	169.1	-
4-OCH_2O-5	101.8	6.03 (1H, s)	101.8	6.06 (1H, s)
7-OMe	61.1	4.20 (3H, s)	63.5	4.31 (3H, s)
3'-OMe	55.4	3.84 (3H, s)	56.1	3.86 (3H, s)
4'-OMe	55.6	3.95 (3H, s)	56.0	3.96 (3H, s)

3.3.5. Comparison of the Chemical Composition of *M. glauca* and *M. angustifolia*

The information collected from the UPLC-MS profiles of the various extracts were of interest in many respects. The UPLC-MS chromatograms given in Figure 3.18 and also the compounds isolated from the two plants (Table 3.12) clearly showed a difference between the two *Monsonia* species.

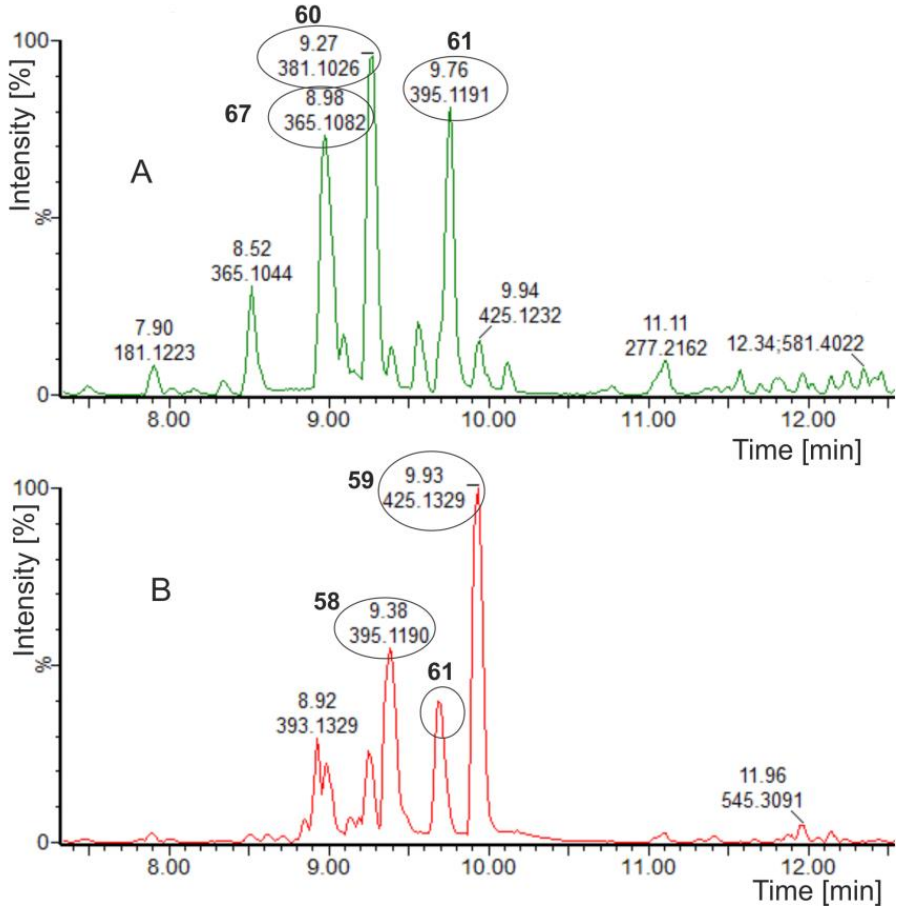

Figure 3.18: *UPLC-MS profiles of the CH_2Cl_2 extracts of M. glauca (A) and M. angustifolia (B): justicidin A (**58**), 6-methoxyjusticidin A (**59**), chinensinaphthol (**60**), retrochinensinaphthol methyl ether (**61**), and justicidin B (**67**)*

From the CH_2Cl_2 extracts, *M. glauca* contained justicidin B (**67**) but not justicidin A (**58**) found preferably in *M. angustifolia*.

Table 3.12: Comparison of the chemical compositions of *M. glauca* and *M. angustifolia*

	Compounds	Species	
		M. glauca	*M. angustifolia*
CH_2Cl_2 extract	Justicidin B (**67**)	Present	Not detected
	Justicidin A (**58**)	Not detected	Present
	6-Methoxyjusticidin A (**59**)	Not detected	Present
	Chinensinaphthol (**60**)	Present	Present
	Retrochinensinaphthol methyl ether (**61**)	Present	Present
MeOH extract	Quercetin (**63**)	Present	Present
	Kaempferol (**64**)	Present	Present
	Hyperoside (**65**)	Present	Present
	Isoquercetin (**66**)	Present	Present

Justicidin B (**67**), chinensinaphthol (**60**), and retrochinensinaphthol methyl ether (**61**) appeared to be the major compounds in the CH_2Cl_2 extract of *M. glauca* while justicidin A (**58**) and 5-methoxyjustidin A (**59**) were major compounds of *M. angustifolia*, supporting the preference for *M. glauca* to locate the methylenedioxy group in the C ring, and the methoxy groups in the A ring.

The UPLC-MS profiles of the methanol extracts of both *Monsonia* species looked qualitatively similar, the four identified flavonoids were present in both plants (Table 3.12), quercetin (**63**) was found to be the main compound in *M. glauca*, and the two stereoisomers isoquercetin (**66**) and hyperoside (**65**) were major in *M. angustifolia* (Figure 3.19).

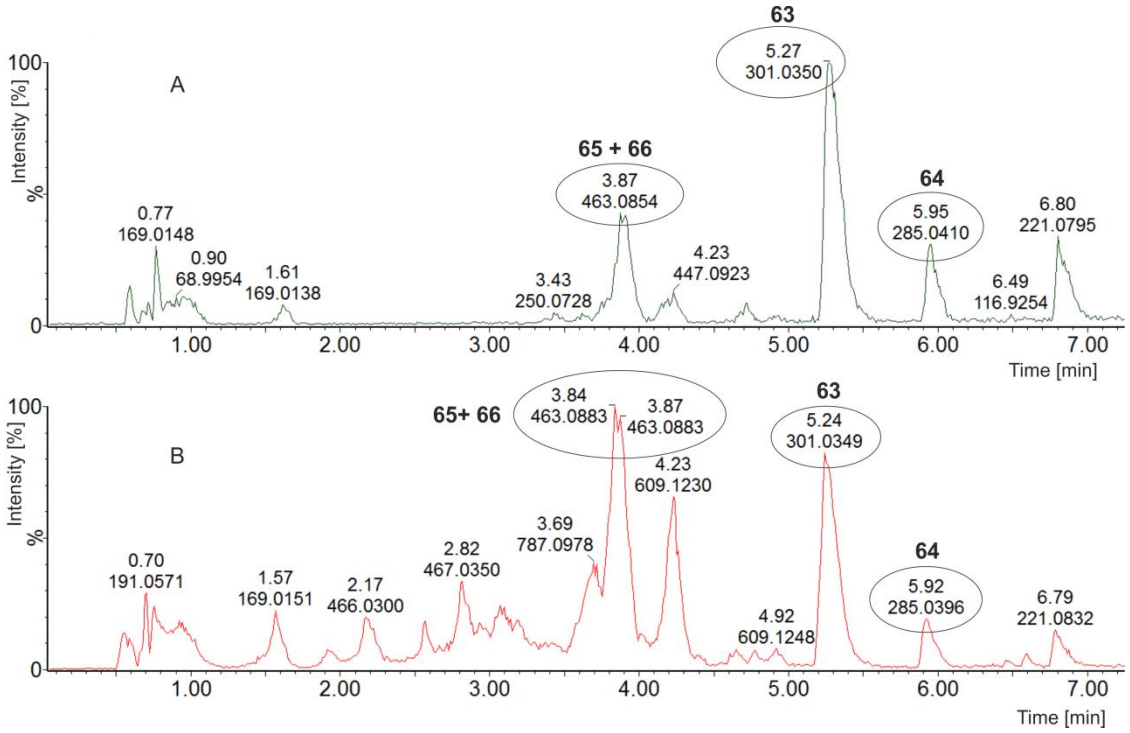

Figure 3.19: *UPLC-MS profiles of the MeOH extracts of M. glauca (A) and M. angustifolia (B): hyperoside (**65**) + isoquercetin (**66**), quercetin (**63**), and kaempferol (**64**)*

3.3.6. Nrf2 Activation of the Isolated Flavonoids

The isolated flavonoids quercetin (**63**), kaempferol (**64**), hyperoside (**65**), and isoquercetin (**66**) were tested for their cytotoxicity and Nrf2 activation.

Most of those compounds showed none to moderate cytotoxicity against human normal bronchial epithelial cells ranging from 70 to 100% survival as shown in Table 3.13. Kaempferol (**64**) exhibited no toxicity at all test concentrations (1 µg/ml, 10 µg/ml, and 50 µg/ml) for normal cells with 100% survival (Table 3.13).

Table 3.13: Cell viability (MTT) and Nrf2 activities (NQO1) of flavonoids identified in *M. angustifolia*

Sample	Concentration (µg/ml)	MTT (% cell viability)	NQO1 assay (% increase over the control)				
			Experiment number				
			1	2	3	4	5
DMEM[a]		100.0	100.0	100.0	100.0	100.0	100.0
DMSO[b]	10	100.0	48.6	116.7	100.0	62.5	100.0
Sulforaphane[c]	0.9	98.4	69.4	109.0	40.9	275.0	220.0
63	1	100.0	68.8	100.0	-09.1	1250.0	-
	10	80.0	62.5	90.3	22.7	312.5	98.0
	50	70.0	62.5	48.6	27.7	1250.0	62.9
64	1	100.0	76.4	94.4	102.3	800.0	-
	10	100.0	79.9	95.8	106.8	1225.0	70.2
	50	95.0	113.2	58.3	86.4	975.0	54.3
65	1	90.0	62.5	72.2	163.6	250.0	-
	10	80.0	61.1	75.0	140.9	125.0	90.2
	50	78.0	65.3	79.2	86.4	187.5	82.4
66	1	90.0	69.4	98.6	54.5	250.0	-
	10	70.0	68.1	61.1	43.6	187.5	80.0
	50	80.0	98.6	6.9	-136.4	175.0	14.1
65 + **66**	1	90.0	69.4	97.2	104.5	500.0	-
	10	70.0	66.7	61.1	113.6	500.0	45.0
	50	73.0	102.8	5.5	40.9	225.0	43.8
MAM	10	-	-	-	-	-	95.0
	50	-	-	-	-	-	107.8

[a] Media control. [b] Vehicle control. [c] Positive control. MAM: *M. angustifolia* methanol extract

The Nrf2 assays were repeated separately five times as initially the positive control, sulforphane, did not show any significant activation of Nrf2 relative to the DMEM media control. Classically the sulforphane is expected to provide an increase greater than 150% [45], and this was only seen in experiments 4 and 5 (Table 3.13). Due to this the Nrf2 activation of the isolated flavonoids was inconclusive in the five repeats.

Apart from hyperoside (**65**), the first test showed the isolated flavonoids to have a better Nrf2 activity increase as compared to the positive control

(69.4%). The increase ranged from 70% to 113% over the media control (Table 3.13). Unfortunately the test was inconclusive since sulforaphane used as the positive control showed an increase below 100% while it was expected to be above 150% over the media control. The experiment had to be repeated one more time.

In the second experiment, the positive control showed 111% as compared to the media control (Table 3.13), however all the isolated flavonoids did not show any Nrf2 activation potential (< 100%) equivalent to the positive control. Based on the fact that the vehicle control showed a better Nrf2 activation (117%) than the positive control, no conclusion could be drawn from this either, and a third attempt was made.

The results from the third experiment showed that the positive control was not effective, as its activity was 40.9% compared to the media control, while most of isolated compounds exhibited better Nrf2 activation than the positive control (Table 3.13).

The fourth experiment displayed a good Nrf2 activation for the freshly prepared positive control with 275% Nfr2 activity increase over the media control; however the isolated flavonoids exhibited excessively high Nrf2 activation reaching up to 1 250% increase over the media control (Table 3.13). This attempt was inconclusive, too, due to the exaggerated percentage increase of the compounds (Table 3.13). However, from the above results it appears that the presence of the glucoside in the flavonoids hyperoside (**65**) and isoquercetin (**66**) reduced the Nrf2 activation potential of the flavonoids with 250% and less percentage increase of the media control (Table 3.13).

An additional fifth attempt was undertaken using the positive control prepared in the fourth experiment, unfortunately the isolated flavonoids seemed to have lost all activity (Table 3.13), which may have been due to decomposition as these compounds were stored in a freezer in a stock

solution over an extended period of time, and the repeated thawing-freezing process would have also contributed to the decomposition.

This was confirmed by the fact that the parent methanol extract of *M. angustifolia* had a 236% increase over the control at 1 µg/ml at the initial stages of screening (Section 3.3.1 on the Nrf2 activities of *Monsonia* extracts) also lost also this activity (> 110%) in the final experiment (Table 3.13).

Nevertheless, the biological activities of the isolated flavonoids as pharmacological modulators of Nrf2 throughout various pathways are well documented [95-98]. Based on the well documented activity, it can be assumed that the good activity of the methanol extract as an Nrf2 activator is in all likelihood due to the presence of the isolated flavonoids quercetin (**63**), kaempferol (**64**), hyperoside (**65**), and isoquercetin (**66**). However the studies should be repeated using freshly prepared samples/compounds.

3.3.7. Cytotoxicity Assay Results of Isolated Lignans against Human Tumor Cells

The compounds justicidin A (**58**), 6-methoxyjusticidin A (**59**), chinensinaphthol (**60**), retrochinensinaphthol methyl ether (**61**), and justicidin B (**67**) were tested by Prof. S Awale's group in Japan, for their preferential cytotoxicity against the pancreatic human cancer cell line (PANC-1) and HeLa human cervical cancer cells.

Despite the fact that arctigenin used as positive control (PC_{50} = 0.83 μM) in that test is also a lignan, all five isolated lignans had almost no activity against the pancreatic cancer cell lines (PC_{50} > 100 μM) (Table 3.14).

The inactivity of these compounds against PANC cell lines can be attributed to the the presence of the arylnaphthalene and the methylenedioxy group in the isolated lignans, which is absent in the positive control (a dibenzoylbutyrolactone).

The compounds however exhibited strong to moderate activities against the HeLa human cervical cancer cell lines (Figure 3.20 and Table 3.14).

Table 3.14: Growth-inhibitory activities of the isolated lignans against human cancer cells

Compound	HeLa (IC_{50} μM)	PANC-1 (PC_{50} in μM)[a]
Paclitaxel[b]	0.001	> 100
Arctigenin[c]		0.83
58	58.4	> 100
59	68.5	> 100
60	100.1	> 100
61	18.3	> 100
67	1.2	> 100

[a] Concentration at which 50% of the cells were killed preferentially in NDM. [b,c] Used as a reference compounds.

Interestingly, justicidin B (**67**) displayed strong cytotoxic activity with an IC_{50} value of 1.2 μM, comparable to the reported activities of the lignans boehmenan H (IC_{50} 1.7 μM) and threo-carolignan K (IC_{50} 0.6 μM) [99]. Retrochinensinaphthol methyl ether (**61**) exhibited a moderate cytotoxic activity with an IC_{50} value of 18.3 μM, while justicidin A (**58**) and 6-methoxyjusticidin A (**59**) displayed week cytotoxicities with IC_{50} values of 58.4 and 68.5 μM respectively. Chinensinaphthol (**60**) was inactive against HeLa human cervical cancer cell lines. Of particular interest is the structure-activity relationship of compounds **58**, **59**, and **67**. These three compounds showed that the OMe/H substitution pattern on the naphthalene part of the lignan played a key role for the bioactivities: a methoxylation appeared to be unfavorable for the cytotoxic activity.

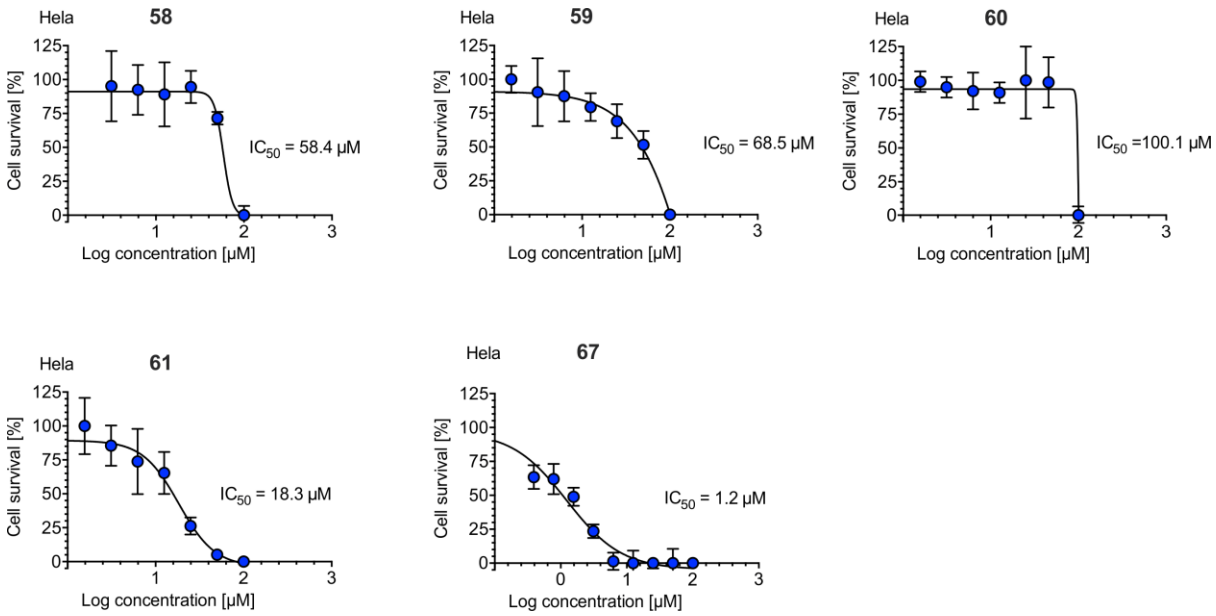

Figure 3.20: *Cytotoxicity activities of **58**, **59**, **60**, **61**, and **67** against the HeLa Human Cervical Cancer Cell Lines*

The fact that the isolated lignans were almost inactive against the PANC-1 human cancer cell line but exhibited strong to moderate activities against the HeLa human cervical cancer cell lines provided evidence of their selective activities against cancer cells.

3.4. Concluding Remarks

The extracts, fractions, and compounds of *M. angustifolia and M. glauca* plants were tested for the first time to assess Nrf2 and anti-cancer activities. The *n*-hexane, methanol, and aqueous extracts of *M. angustifolia*, and the methanol extract of *M. glauca* exhibited strong to good pharmacological activities with regard to Nrf2 activation, the methanol extract of *M. angustifolia* being more active than sulforaphane used as the positive control. This extract was fractionated using column chromatography.

The first seven fractions collected were shown to be good Nrf2 activators, while their UPLC-MS profiles were similar to each other, having four characteristic peaks in various proportions. The fours peaks were resolved using HPLC, and were identified as quercetin (**63**), kaempferol (**64**), hyperoside (**65**), and isoquercetin (**66**), four flavonoids previously reported to be Nrf2 moderators. The structure elucidation of the isolated flavonoids was achieved by interpretation of the combination of UV, MS, and 1D-2D NMR spectroscopic data. The confirmation of the structures was done by UPLC co-elution with the pure standards.

The isolated flavonoids were tested for Nrf2 activity repeatedly, but the assays were inconclusive since the bioassay was not reproducible while at the same time the compounds appeared to have decomposed in the stock solution during the long storage process. The isolated flavonoids are however well documented as Nrf2 activators in the literature, and were probably responsible of the good activity observed in the methanol extract of *M. angustifolia.* Further investigations to confirm their Nrf2 activity and to elucidate the pathways of their Nrf2 activation are ongoing.

This study is the first report on the presence of these flavonoids in *M. angustifolia* and on the potency of *M. glauca* and *M. angustifolia* extracts as Nrf2 activators.

Lignans are reported to have good anti-cancer cell activities. *Monsonia* species are also known to be a source of lignans. From this work, five known lignans including justicidin A (**58**), justicidin B (**67**), 6-methoxyjusticidin A (**59**), chinensinaphthol (**60**), and retrochinensinaphthol methyl ether (**61**) were identified, isolated, and their structures elucidated. This is the first report showing the presence of justicidin B in *Monsonia glauca*.

The isolated lignans from both *M. angustifolia* and *M. glauca* were almost inactive towards the human pancreatic cancer cell lines. However these compounds showed strong to moderate activities against HeLa human cervical cancer cells, with justicidin B (**67**) exhibiting the highest activity. The structure-activity relationship indicated a reduction of the activity due to methoxylation of the naphthalene part of the lignan.

The chemical profiles of the extracts of the two *Monsonia* species showed noticeable differences, mostly for the CH_2Cl_2 extracts as only *M. glauca* contained justicidin B (**67**), while justicidin A (**58**) and 6-methoxyjusticidin A (**59**) were only detected in *M. angustifolia*. The natural products of *M. glauca* and their Nfr2 and anti-cancer activities were investigated for the first time.

3.5. References

1. Louw CAM, Regnier TJC, Korsten L: **Medicinal Bulbous Plants of South Africa and their Traditional Relevance in the Control of Infectious Diseases**. *Journal of Ethnopharmacology* 2002, **82**(2):147-154.
2. Street RA, Prinsloo G: **Commercially Important Medicinal Plants of South Africa: A Review**. *Journal of Chemistry* 2013, **2013**:1-16.
3. Cocks M, Dold A: **The Role of 'African Chemists' in the Health Care System of the Eastern Cape Province of South Africa**. *Social Science and Medicine* 2000, **51**(10):1505-1515.
4. van Wyk BE, Gericke N: **People's Plants: A Guide to Useful Plants of Southern Africa**. *Briza Publications* 2000:1-416.
5. Makunga N: **Medicinal Plants of South Africa**. *South African Journal of Science* 2010, **105** (3):188
6. Wang H, Naghavi M, Allen C, Barber RM, Bhutta ZA, Carter A, Casey DC, Charlson FJ, Chen AZ, Coates MM *et al.*: **Global, Regional, and National Life Expectancy, all-Cause Mortality, and Cause-Specific Mortality for 249 Causes of Death, 1980–2015: A Systematic Analysis for the Global Burden of Disease Study 2015**. *The Lancet* 2016, **388**(10053):1459-1544.
7. Cock IE, Selesho MI, Van Vuuren SF: **A Review of the Traditional Use of Southern African Medicinal Plants for the Treatment of Selected Parasite Infections Affecting Humans**. *Journal of Ethnopharmacology* 2018, **220**:250-264.
8. Mander ND, Ham C, Mander M, Geldenhuys C, Mitchell D, Crouch N, Wynberg R, Drewes S, McKean S, Feiter U, Spring W, Symmonds R: **Commercialising Medicinal Plants: A Southern African Guide**: African Sun Media; 2006:1-7.
9. Rybicki PE, Chikwamba R, Koch M, Rhodes IJ, Groenewald J-H: **Plant-Made Therapeutics: An Emerging Platform in South Africa**. *Biotechnology Advances* 2012, **30**(2):449-459.

10. Abbasi AM, Khan MA, Ahmad M, Zafar M, Jahan S, Sultana S: **Ethnopharmacological Application of Medicinal Plants to Cure Skin Diseases and in Folk Cosmetics among the Tribal Communities of North-West Frontier Province, Pakistan**. *Journal of Ethnopharmacology* 2010, **128**(2):322-335.

11. Hęś M, Dziedzic K, Górecka D, Jędrusek-Golińska A, Gujska E: ***Aloe vera* (L.) Webb.: Natural Sources of Antioxidants: A Review**. *Plant Foods for Human Nutrition* 2019, **74**(3):255-265.

12. Fiebich BL, Muñoz E, Rose T, Weiss G, McGregor GP: **Molecular Targets of the Antiinflammatory *Harpagophytum procumbens* (Devil's claw): Inhibition of TNFα and COX-2 Gene Expression by Preventing Activation of AP-1**. *Phytotherapy Research* 2012, **26**(6):806-811.

13. Careddu D, Pettenazzo A: ***Pelargonium sidoides* Extract EPs 7630: A Review of its Clinical Efficacy and Safety for Treating Acute Respiratory Tract Infections in Children**. *International Journal of General Medicine* 2018, **11**:91-98.

14. van Wyk BE: **The Potential of South African Plants in the Development of New Medicinal Products**. *South African Journal of Botany* 2011, **77**(4):812-829.

15. van Wyk BE: **A Broad Review of Commercially Important Southern African Medicinal Plants**. *Journal of Ethnopharmacology* 2008, **119**(3):342-355.

16. Ekor M: **The Growing Use of Herbal Medicines: Issues Relating to Adverse Reactions and Challenges in Monitoring Safety**. *Front Pharmacology* 2014, **4**:177-186.

17. McFadden R, Peterson N: **Interactions Between Drugs and Four Common Medicinal Herbs**. *Nursing standard (Royal College of Nursing)* 2011, **25**:65-68.

18. The Angiosperm Phylogeny Group: **An Update of the Angiosperm Phylogeny Group Classification for the Orders and Families of Flowering Plants: APG II**. *Botanical Journal of the Linnean Society* 2003, **141**(4):399-436.

19. Albach DC, Soltis DE, Mort ME, Zanis M, Soltis PS, Chase MW, Fay MF, Savolainen V, Hahn WH, Hoot SB, Axtel M, Swensen SM, Prince LM, Kress JW, Nixon KC, Farris JS: **Angiosperm Phylogeny Inferred from 18S rDNA, rbcL, and atpB Sequences**. *Botanical Journal of the Linnean Society* 2008, **133**(4):381-461.

20. Fiz O, Vargas P, Alarcón M, Aedo C, García JL, Aldasoro JJ: **Phylogeny and Historical Biogeography of Geraniaceae in Relation to Climate Changes and Pollination Ecology**. *Systematic Botany* 2008, **33**(2):326-342.

21. Price RA, Palmer JD: **Phylogenetic Relationships of the Geraniaceae and Geraniales from rbcL Sequence Comparisons**. *Annals of the Missouri Botanical Garden* 1993, **80**(3):661-671.

22. Pax DL, Price RA, Michaels HJ: **Phylogenetic Position of the Hawaiian *Geraniums* Based on rbcL Sequences**. *American Journal of Botany* 1997, **84**(1):72-78.

23. Bakker TF, Hellbrügge D, Culham A, Gibby M: **Phylogenetic Relationships within *Pelargonium* sect. *Peristera* (Geraniaceae) Inferred from nrDNA and cpDNA Sequence Comparisons**. *Plant Systematics and Evolution* 1998, **211**(3):273-287.

24. Bakker TF, Culham A, Daugherty CL, Gibby M: **A trnL-F Based Phylogeny for Species of *Pelargonium* (Geraniaceae) with Small Chromosomes**. *Plant Systematics and Evolution* 1999, **216**(3):309-324.

25. Bakker TF, Culham A, Pankhurst EC, Gibby M: **Mitochondrial and Chloroplast DNA-Based Phylogeny of *Pelargonium* (Geraniaceae)**. *American Journal of Botany* 2000, **87**(5):727-734.

26. Bakker TF, Culham A, Priyani H, Tasoula T, Gibby M: **Phylogeny of *Pelargonium* (Geraniaceae) Based on DNA Sequences from Three Genomes**. *Taxon* 2004, **53**(1):17-28.

27. Fiz O, Vargas P, Alarcón ML, Aldasoro JJ: **Phylogenetic Relationships and Evolution in *Erodium* (Geraniaceae) Based on trnL-trnF Sequences**. *International System for Agriculture Science and Technology* 2006, **31**(4):739-763.

28. Touloumenidou T, Bakker FT, Albers F: **The Phylogeny of *Monsonia* L. (Geraniaceae)**. *Plant Systematics and Evolution* 2007, **264**(1):1-14.

29. Venter HJ: **Phytogeography and Interspecies Relationships in *Monsonia* (Geraniaceae)**. *African Biodiversity and Conservation Journal* 1983, **14**(3-4):865-869.

30. Tshivhandekano I, Ntushelo K, Ngezimana W, Tshikalange TE, Mudau FN: **Chemical Compositions and Antimicrobial Activities of *Athrixia phylicoides* DC. (bush tea), *Monsonia burkeana* (Special Tea) and Synergistic Effects of both Combined Herbal Teas**. *Asian Pacific Journal of Tropical Medicine* 2014, **7**:S448-S453.

31. Nnzeru L, Ntushelo K, Mudau F: **Physical Appraisal and Attributes of *Monsonia burkeana* (Special Tea) : the Perspective of Tea Users**. *Indilinga African Journal of Indigenous Knowledge Systems* 2016, **15**:111-122.

32. Moteetee A, Kose LS: **A Review of Medicinal Plants Used by the Basotho for Treatment of Skin Disorders: their Phytochemical, Antimicrobial, and Anti-Inflammatory Potential**. *African Journal of Traditional, Complementary and Alternative Medicines* 2017, **14**:121-137.

33. ***Monsonia angustifolia*** [http://pza.sanbi.org/monsonia-angustifolia]

34. ***Monsonia glauca* Knuth** [http://pza.sanbi.org/monsonia-glauca]

35. Fouche G, Afolayan JA, Wintola AO, Khorombi ET, Senabe J: **Effect of the Aqueous Extract of the Aerial Parts of *Monsonia angustifolia* E. Mey. Ex A. Rich., on the Sexual Behaviour of Male Wistar Rats**. *Biomedical Center Complementary and Alternative Medicine* 2015, **15**(1):343-352.

36. Chun YS, Kim J, Chung S, Khorombi E, Naidoo D, Nthambeleni R, Harding N, Maharaj VJ, Fouche G, Yang HO: **Protective Roles of *Monsonia angustifolia* and Its Active Compounds in Experimental Models of Alzheimer's Disease**. *Journal of Agricultural and Food Chemistry* 2017, **65**(15):3133-3140.

37. Afolayan AJ, Wintola OA, Fouche G: **Acute and Subacute Toxicological Evaluation of the Aerial Extract of *Monsonia***

***angustifolia* E. Mey. ex. A. Rich in Wistar Rats**. *Evidence-Based Complementary and Alternative Medicine* 2016, **4**:8-17.

38. Khorombi T: **A Chemical and Pharmacological Investigation of Three South African Plants**. MSc. Thesis, University of KwaZulu Natal South Africa; 2006.
39. Yang HO, Chung SK, Kwon HC, Cha JW, Kim Y, Fouche G, Nthambeleni R, Naidoo D, Senabe J, Maharaj VJ, Khorombi E, Ham J, Kim JK: **Composition containing arylnaphthalene lignan derivative for preventing and/or treating dementia**. In.: Google Patents; 2014.
40. Cunha W, Silva LA-eM, Veneziani R, Ambrósio RS, Bastos J: **Lignans: Chemical and Biological Properties**: IntechOpen; 2012:213-234.
41. Raimondo D, Von Staden L, Foden W, Victor JE, Helme NA, Turner RC, Kamundi DA, Manyama PA: **Red List of South African Plants**. *South African Journal of Science* 2009, **107**(3-4):01-02.
42. Malviya N, Malviya S: **Bioassay Guided Fractionation: An Emerging Technique Influence the Isolation, Identification and Characterization of Lead Phytomolecules**. *International Journal of Hospital Pharmacy* 2017, **0p901**:318-324.
43. Prochaska JH, Santamaria BA: **Direct Measurement of NAD(P)H: Quinone Reductase from Cells Cultured in Microtiter Wells: A Screening Assay for Anticarcinogenic Enzyme Inducers**. *Analytical Biochemistry* 1988, **169**(2):328-336.
44. Setiawati A, Immanuel H, Utami MT: **The Inhibition of *Typhonium flagelliforme* Lodd. Blume Leaf Extract on COX-2 Expression of WiDr Colon Cancer Cells**. *Asian Pacific Journal of Tropical Biomedicine* 2016, **6**(3):251-255.
45. Houghton AC, Fassett GR, Coombes SJ: **Sulforaphane and other Nutrigenomic Nrf2 Activators: Can the Clinician's Expectation Be Matched by the Reality?** *Oxidative Medicine and Cell Longevity* 2016, **2016**:7857186-7857203.

46. Atilano-Roque A, Wen X, Aleksunes ML, Joy SM: **Nrf2 Activators as Potential Modulators of Injury in Human Kidney Cells**. *Toxicology Reports* 2016, **3**:153-159.

47. Phillipson JD: **Phytochemistry and Medicinal Plants**. *Phytochemistry* 2001, **56**(3):237-243.

48. Chunpeng W, Zheng X, Chen H, Zou X, Song Z, Zhou S, Yan Q: **Flavonoid Constituents from Herbs of *Sarcopyramis bodinieri* var. *delicata***. *China Journal of Chinese Materia Medica* 2009, **34**:172-174.

49. Huang W, Wan C, Zhou S: **Quercetin - A Flavonoid Compound from *Sarcopyramis bodinieri* var. *delicate* with Potential Apoptotic Activity in HepG2 Liver Cancer Cells**. *Tropical Journal of Pharmaceutical Research* 2013, **12**(4):13-18.

50. Mabry JT, Kagan J, Rösler H: **Nuclear Magnetic Resonance Analysis of Flavonoids**, Vol. 17. Austin, Texas: University of Texas; 1964.

51. Yoon H, Eom S-L, Hyun J-Y, Jo G-H, Hwang D-S, Lee S-H, Yong Y-J, Park J-C, Lee Y-H, Lim Y-H: **^{1}H and ^{13}C NMR Data on Hydroxy/Methoxy Flavonoids and the Effects of Substituents on Chemical Shifts**. *Bulletin of the Korean Chemical Society* 2011, **32**:2101-2104.

52. Liu H, Mou Y, Zhao J, Wang J, Zhou L, Wang M, Wang D, Han J, Yu Z, Yang F: **Flavonoids from *Halostachys caspica* and Their Antimicrobial and Antioxidant Activities**. *Molecules* 2010, **15**(11):7933-7945.

53. Napolitano GJ, Lankin CD, Chen S-N, Pauli FG: **Complete ^{1}H NMR Spectral Analysis of Ten Chemical Markers of *Ginkgo biloba***. *Magnetic Resonance in Chemistry* 2012, **50**(8):569-575.

54. Yi X, Zuo J, Tan C, Xian S, Luo C, Chen S, Yu L, Luo Y: **Kaempferol, a Flavonoid Compound from *Gynura medica* Induced Apoptosis and Growth Inhibition in MCF-7 Breast Cancer Cell**. *African Journal of Traditional, Complementary, and Alternative Medicines* 2016, **13**(4):210-215.

55. Telange D, Patil A, Pethe A, Tatode A, Sridhar A, Dave V: **Kaempferol-Phospholipid Complex: Formulation, and Evaluation of Improved Solubility, *in vivo* Bioavailability, and Antioxidant Potential of Kaempferol**. *Journal of Excipients and Food Chemicals* 2016, **7**:89-116a.

56. Aly F, Inas M, Yehia S: **Flavonoids of *Neotorularia aculeolata* Plant**. *Journal of Pharmacy and Nutrition Sciences* 2011, **1**:134-139.

57. Barberá O, Sanz FJ, Sánchez-Parareda J, Marco JA: **Further Flavonol Glycosides from *Anthyllis onobrychioides***. *Phytochemistry* 1986, **25**(10):2361-2365.

58. Horii Z, Tsujiuchi M, Momose T: **On the Structure of Taiwanin E**. *Tetrahedron Letters* 1969, **10**(14):1079-1082.

59. Okigawa M, Maeda T, Kawano N: **The Isolation and Structure of Three New Lignans from *Justicia procumbens* Linn. var. *leucantha* honda**. *Tetrahedron* 1970, **26**(18):4301-4305.

60. Fukamiya N, Lee K-H: **Justicidin-A and Diphyllin, Two Cytotoxic Principles from *Justicia procumbens***. *Journal of Natural Products* 1986, **49**(2):348-350.

61. Kim T, Jeong KH, Kang KS, Nakata M, Ham J: **An Optimized and General Synthetic Strategy to Prepare Arylnaphthalene Lactone Natural Products from Cyanophthalides**. *European Journal of Organic Chemistry* 2017, **2017**(13):1704-1712.

62. Liu B, Yang Y, Liu H, Xie Z, Li Q, Deng M, Li F, Peng J, Wu H: **Screening for Cytotoxic Chemical Constituents from *Justicia procumbens* by HPLC-DAD-ESI-MS and NMR**. *Chemistry Central Journal* 2018, **12**(1):6-21.

63. González AG, Pérez JP, Trujillo JM: **Synthesis of Two Arylnaphthalene Lignans**. *Tetrahedron* 1978, **34**(7):1011-1013.

64. Abdullaev ND, Yagudaev MR, Batirov ÉK, Malikov VM: **^{13}C NMR Spectra of Arylnaphthalene Lignans**. *Chemistry of Natural Compounds* 1987, **23**(1):63-74.

65. Batsuren D, Batirov ÉK, Malikov VM, Zemlyanskii VN, Yagudaev MR: **Arylnaphthalene Lignans of *Haplophyllum dauricum*. The**

Structure of Daurinol. *Chemistry of Natural Compounds* 1981, **17**(3):223-225.

66. Flanagan RS, Harrowven CD, Bradley M: **A New Benzannulation Reaction and Its Application in the Multiple Parallel Synthesis of Arylnaphthalene Lignans**. *Tetrahedron* 2002, **58**(30):5989-6001.
67. Hemmati S, Seradj H: **Justicidin B: A Promising Bioactive Lignan**. *Molecules* 2016, **21**(7):820-839.
68. Munakata K, Marumo S, Ohta K, Chen Y-L: **Justicidin A and B, the Fish-Killing Components of *Justicia hayatai* var. *decumbens***. *Tetrahedron Letters* 1965, **6**(47):4167-4170.
69. Munakata K, Marumo S, Ohta K, Chen Y-L: **The Synthesis of Justicidin B and Related Compounds**. *Tetrahedron Letters* 1967, **8**(39):3821-3825.
70. Ogiku T, Yoshida S-i, Ohmizu H, Iwasaki T: **Efficient Syntheses of 1-Arylnaphthalene Lignan Lactones and Related Compounds from Cyanohydrins**. *The Journal of Organic Chemistry* 1995, **60**(14):4585-4590.
71. Patel RM, Argade NP: **Palladium-Promoted [2 + 2 + 2] Cocyclization of Arynes and Unsymmetrical Conjugated Dienes: Synthesis of Justicidin B and Retrojusticidin B**. *Organic Letters* 2013, **15**(1):14-17.
72. Stevenson R, Weber JV: **Improved Methods of Synthesis of Lignan Arylnaphthalene Lactones *via* Arylpropargyl Arylpropiolate Esters**. *Journal of Natural Products* 1989, **52**(2):367-375.
73. Vasilev N, Elfahmi, Bos R, Kayser O, Momekov G, Konstantinov S, Ionkova I: **Production of Justicidin B, a Cytotoxic Arylnaphthalene Lignan from Genetically Transformed Root Cultures of *Linum leonii***. *Journal of Natural Products* 2006, **69**(7):1014-1017.
74. Scigelova M, Hornshaw M, Giannakopulos A, Makarov A: **Fourier Transform Mass Spectrometry**. *Molecular and Cellular Proteomics* 2011, **10**:1–19.
75. Dueñas M, Hugo M-C, José JP-A, Romina DP, Ana MG-p, Celestino S-B: **Preparation of Quercetin Glucuronides and Characterization**

by HPLC–DAD–ESI/MS. *European Food Research and Technology* 2008, **227**:1069-1076.

76. Tsimogiannis D, Samiotaki M, Panayotou G, Oreopoulou V: **Characterization of Flavonoid Subgroups and Hydroxy Substitution by HPLC-MS/MS**. *Molecules* 2007, **12**(3):593-606.

77. Zhang Y, Wang D, Yang L, Zhou D, Zhang J: **Purification and Characterization of Flavonoids from the Leaves of *Zanthoxylum bungeanum* and Correlation between their Structure and Antioxidant Activity**. *Public Journal of Science One* 2014, **9**:105725.

78. Wei X-H, Yang S-J, Liang N, Hu D-Y, Jin L-H, Xue W, Yang S: **Chemical Constituents of *Caesalpinia decapetala* (Roth) Alston**. *Molecules* 2013, **18**(1):1325-1336.

79. Zhang X-Y, Shen J, Zhou Y, Wei Z-P, Gao J-M: **Insecticidal Constituents from *Buddlej aalbiflora* Hemsl**. *Natural Product Research* 2017, **31**(12):1446-1449.

80. March ER, Miao X-S: **A Fragmentation Study of Kaempferol Using Electrospray Quadrupole Time-of-Flight Mass Spectrometry at High Mass Resolution**. *International Journal of Mass Spectrometry* 2004, **231**(2):157-167.

81. Chen Y, Yu H, Wu H, Pan Y, Wang K, Jin Y, Zhang C: **Characterization and Quantification by LC-MS/MS of the Chemical Components of the Heating Products of the Flavonoids Extract in Pollen Typhae for Transformation Rule Exploration**. *Molecules* 2015, **20**(10):18352-18366.

82. He W, Liu X, Xu H, Gong Y, Yuan F, Gao Y: **On-Line HPLC-ABTS Screening and HPLC-DAD-MS/MS Identification of Free-Radical Scavengers in *Gardenia* (*Gardenia jasminoides* Ellis) Fruit Extracts**. *Food Chemistry* 2010, **123**(2):521-528.

83. Madala NE, Piater L, Dubery I, Steenkamp P: **Distribution Patterns of Flavonoids from Three *Momordica* Species by Ultra-High Performance Liquid Chromatography Quadrupole Time-of-Flight Mass Spectrometry: A Metabolomic Profiling Approach**. *Revista Brasileira de Farmacognosia* 2016, **26**(4):507-513.

84. Shoko T, Maharaj VJ, Naidoo D, Tselanyane M, Nthambeleni R, Khorombi E, Apostolides Z: **Anti-Aging Potential of Extracts from *Sclerocarya birrea* (A. Rich.) Hochst and Its Chemical Profiling by UPLC-Q-TOF-MS**. *Biomedical Central Complementary and Alternative Medicine* 2018, **18**(1):54-54.

85. Li H-Z, Song H-J, Li H-M, Pan Y-Y, Li R-T: **Characterization of Phenolic Compounds from *Rhododendron alutaceum***. *Archives of Pharmacal Research* 2012, **35**(11):1887-1893.

86. Sukito A, Tachibana S: **Isolation of Hyperoside and Isoquercitrin from *Camellia sasanqua* as Antioxidant Agents**. *Pakistan Journal of Biological Sciences* 2014, **17**(8):999:1006.

87. Güvenalp Z, Demirezer LÖ: **Flavonol Glycosides from *Asperula arvensis* L.** *Turkish Journal of Chemistry* 2005, **29**:163-169.

88. Jung M, Choi J, Chae H-S, Cho JY, Kim Y-D, Htwe KM, Lee W-S, Chin Y-W, Kim J, Yoon KD: **Flavonoids from *Symplocos racemosa***. *Molecules* 2015, **20**(1):358-365.

89. Ghosal S, Chauhan PSR, Srivastava SR: **Structure of Chinensin: A New Lignan Lactone from *Polygala chinensis***. *Phytochemistry* 1974, **13**(10):2281-2284.

90. Jiang J, Dong H, Wang T, Zhao R, Mu Y, Geng Y, Zheng Z, Wang X: **A Strategy for Preparative Separation of 10 Lignans from *Justicia procumbens* L. by High-Speed Counter-Current Chromatography**. *Molecules* 2017, **22**(12):2024-2033.

91. Zhu Y, Liu Y, Zhan Y, Liu L, Xu Y, Xu T, Liu T: **Preparative Isolation and Purification of Five Flavonoid Glycosides and One Benzophenone Galloyl Glycoside from *Psidium guajava* by High-Speed Counter-Current Chromatography (HSCCC)**. *Molecules* 2013, **18**(12):15648-15661.

92. Yang M, Wu J, Cheng F, Zhou Y: **Complete Assignments of ^{1}H and ^{13}C NMR Data for Seven Arylnaphthalide Lignans from *Justicia procumbens***. *Magnetic Resonance in Chemistry* 2006, **44**(7):727-730.

93. Chen C-C, Hsin W-C, Ko F-N, Huang Y-L, Ou J-C, Teng C-M: **Antiplatelet Arylnaphthalide Lignans from *Justicia procumbens***. *Journal of Natural Products* 1996, **59**(12):1149-1150.

94. Horii Z, Ohkawa K, Kim S, Momose T: **Structure and Synthesis of Diphyllin**. *Chemical and Pharmaceutical Bulletin* 1971, **19**(3):535-537.

95. Zhao CR, Gao ZH, Qu XJ: **Nrf2–ARE Signaling Pathway and Natural Products for Cancer Chemoprevention**. *Cancer Epidemiology* 2010, **34**(5):523-533.

96. Kumar H, Kim I-S, More S, Kim B, Choi D-K: **Natural Product-Derived Pharmacological Modulators of Nrf2/ARE Pathway for Chronic Diseases**. *Natural Product Reports* 2013, **31**:109-139.

97. Eggler LA, Gay AK, Mesecar DA: **Molecular Mechanisms of Natural Products in Chemoprevention: Induction of Cytoprotective Enzymes by Nrf2**. *Molecular Nutrition and Food Research* 2008, **52**(1):84-94.

98. Chen M, Dai L-H, Fei A, Pan S-M, Wang H-R: **Isoquercetin Activates the ERK1/2-Nrf2 Pathway and Protects against Cerebral Ischemia-Reperfusion Injury *in vivo* and *in vitro***. *Experimental and Therapeutic Medicine* 2017, **13**(4):1353-1359.

99. Moujir L, Seca MLA, Silva MSA, López RM, Padilla N, Cavaleiro ASJ, Neto PC: **Cytotoxic Activity of Lignans from *Hibiscus cannabinus***. *Fitoterapia* 2007, **78**(5):385-387.

Chapter 4: General Conclusion

A total of twenty four compounds were isolated and identified as part of this study. Fifteen of these were naphthylisoquinoline (NIQ) alkaloids including four new compounds, the 5,8'-coupled ancistroyafungines A-C (**43**-**45**) and the 5,1'-linked ancistroyafungine D (**46**) isolated from the stem bark of an as yet unidentified *Ancistrocladus* (Ancistrocladaceae) liana recently discovered near the village Yafunga, in the North-Central region of the Democratic Republic of the Congo. The other eleven known NIQs obtained included 6-*O*-methylhamatine (**47**), 4′-*O*-demethylancistrocladine (**48**), ancistroguineine A (**49**), ancistrobertsonine A (**50**), ancistrobrevine B (**19**), ancistrotectoriline A (**51**), 6,5′-*O*,*O*-didemethylancistroealaine A (**52**), 6-*O*-demethylancistroealaine A (**53**), 7-*epi*-ancistrobrevine D (**54**), and ancistrocladinium A (**55**) and B (**56**) were analogues previously identified in related African and Asian *Ancistrocladus* species, showing five different coupling types, *viz*., 5,8', 5,1', 7,1', *N*,6', and *N*,8'.

Most of the isolated alkaloids were *S*-configured at C-3, and possessed an oxygen function at C-6 in the isoquinoline portion, which is characteristic to the subclass of “Ancistrocladaceae-type” alkaloids. This finding is geo- and chemotaxonomically interesting since, with the exception of only one other *Ancistrocladus* species found in the Central Congo Basin, only Southeast Asian and East African Ancistrocladaceae are known to exclusively produce naphthylisoquinolines with these structural features. Moreover, the alkaloid pattern of this Congolese liana clearly differentiates this plant from all other *Ancistrocladus* taxa that have so far been botanically described, which suggests that it might represent a new species or subspecies. The new ancistroyafungines displayed strong preferential cytotoxic activities (with PC_{50} 7.6 to 22.7 µM) towards human PANC-1 pancreatic cancer cells in nutrient-deprived medium, without showing toxicity in normal, nutrient-rich conditions.

Along with the above described naphthylisoquinoline alkaloids, nine other analytes including four flavonoids: quercetin (**63**), kaempferol (**64**), hyperoside (**65**), and isoquercetin (**66**), and five lignans: justicidin A (**58**)**,**

justicidin B (**67**), 6-methoxyjusticidin A (**59**) chinensinaphthol (**60**), and retrochinensinaphthol methyl ether (**61**) were identified and isolated from *Monsonia angustifolia* and *Monsonia glauca* plants collected in South Africa.

The structure elucidation of isolated compounds was successfully done by means of a set of modern spectroscopic technics including UV spectroscopy, MS, IR spectroscopy, NMR spectroscopy and ECD. These technics were combined to chemical methods (oxidative degradation) for the determination of the absolute configuration of chiral naphthylisoquinolines. The chemical profiling of extracts, fractions and sub-fraction was effectively done using the UPLC MS QTOF.

The extracts, the fractions, and compounds of *M. angustifolia and M. glauca* plants were screened for the first time for Nrf2 activity. *M. angustifolia* sequential extracts exhibited superior Nrf2 activation with three active extracts (n-hexane, methanol, and aqueous extracts showing 169.0, 236.1, and 130.0% increase over the control) as compared to *M. glauca* with only the methanol extract that showed good Nrf2 activation (207.2% increase over the control). Methanol extract of *M. angustifolia* showed the strongest percentage increase, better than that of sulforaphane (170.0% increase) used as positive control.

Seven fractions out of fourteen collected from the column chromatography of the methanol extract of *M. angustifolia* exhibited a good Nrf2 activation with percentage increase ranging from 106.0 to 199.0% over the control. The four flavonoids (**63**, **64**, **65**, and **66**) were screened for Nrf2 activity but the tests were inconclusive as the compounds probably decomposed in DMSO during the process; nevertheless, these compounds were previously reported to be Nrf2 modulators, and were probably responsible of the good activity observed in the methanol extracts of both *M. angustifolia* and *M. glauca.*

This study is the first report on the presence of these flavonoids in *M. angustifolia* and on the potency of *M. glauca* and *M. angustifolia* extracts as Nrf2 activators.

Lignans are reported to have good anti-cancer cell activities. *Monsonia* species are also known to be a source of lignans. From this work, five known lignans including justicidin A (**58**), justicidin B (**67**), 6-methoxyjusticidin A (**59**), chinensinaphthol (**60**), and retrochinensinaphthol methyl ether (**61**) were identified, isolated, and their structures elucidated. This is the first report showing the presence of justicidin B in *Monsonia glauca*.

The isolated lignans were inactive against the human PANC-1 pancreatic cancer cell but they displayed strong to moderate activities against the HeLa cervical cancer cell. Justicidin B (**67**) was the most potent compound of the isolated lignans with the IC_{50} value of 1.2 μM. The fact that the isolated lignans exhibited good activity against one type of cancer cells, and were inactive against another type of cancer cells is of significance as it shows the specificity and selectivity of the compounds for their further development as anti-cancer agents.

The UPLC MS finger prints of the two species showed them to be different, as justicidin B was mainly found in *M. glauca* while justicidin A and 6-methoxyjusticidin A were predominant in *M. angustifolia.* To the best of our knowledge, this is the first report on the phytochemical properties and biological activities of *Monsonia glauca*.

Supplementary Information

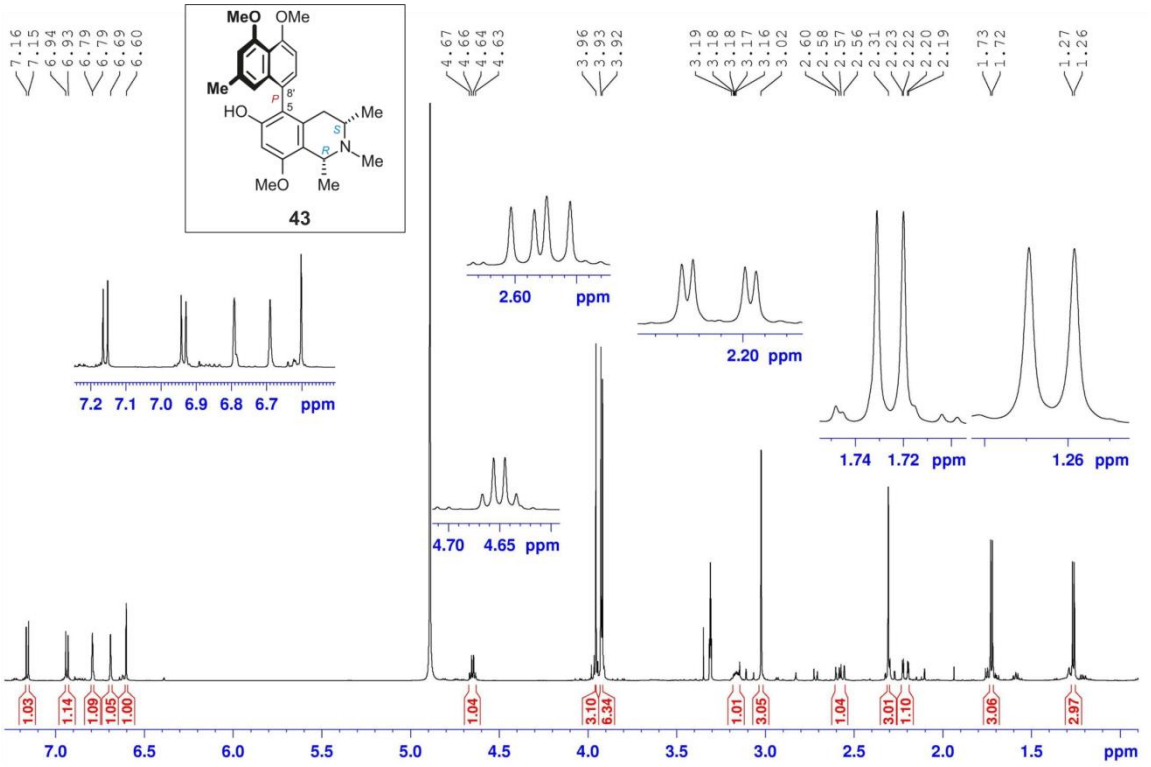

SI 1: *^{1}H NMR spectrum of ancistroyafungine A (**43**) in CD_3OD*

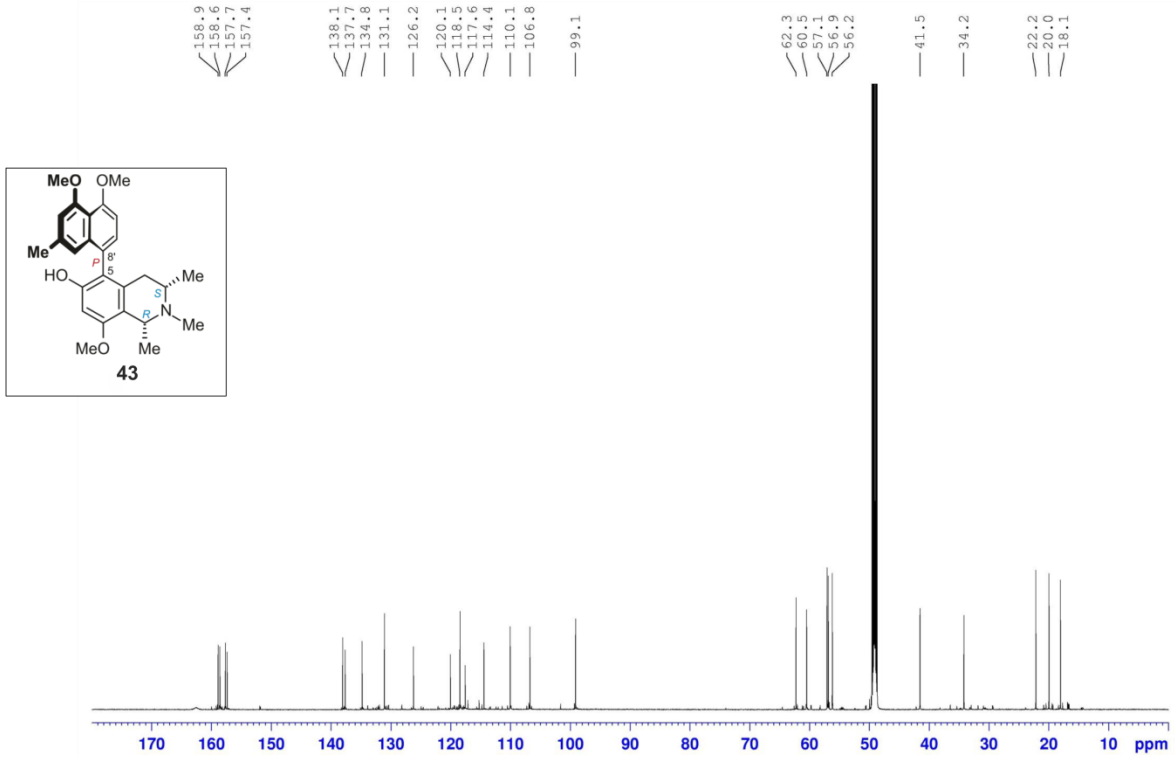

SI 2: *^{13}C NMR spectrum of Ancistroyafungine a (**43**) in CD_3OD*

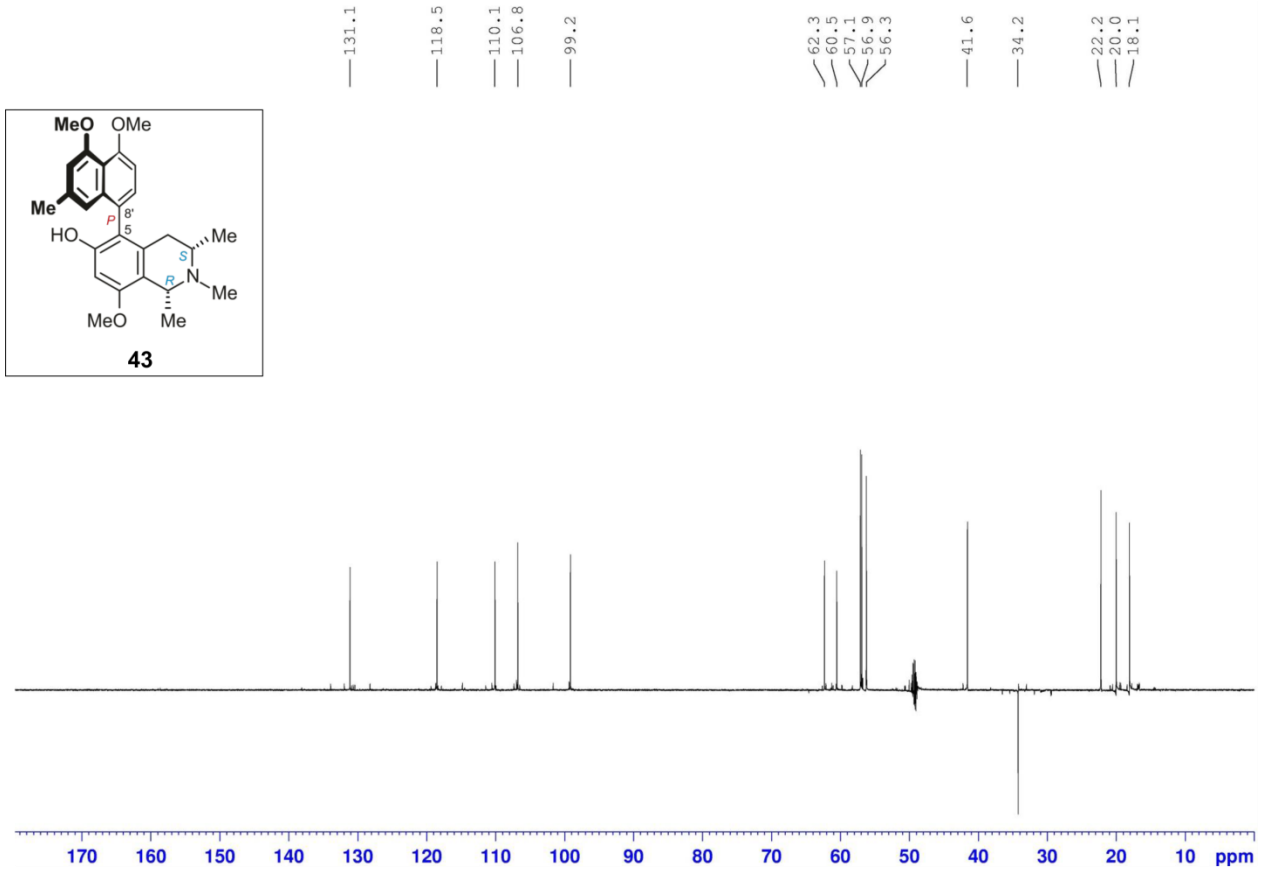

SI 3: *^{13}C DEPT-135 NMR spectrum of ancistroyafungine A (**43**) in CD_3OD*

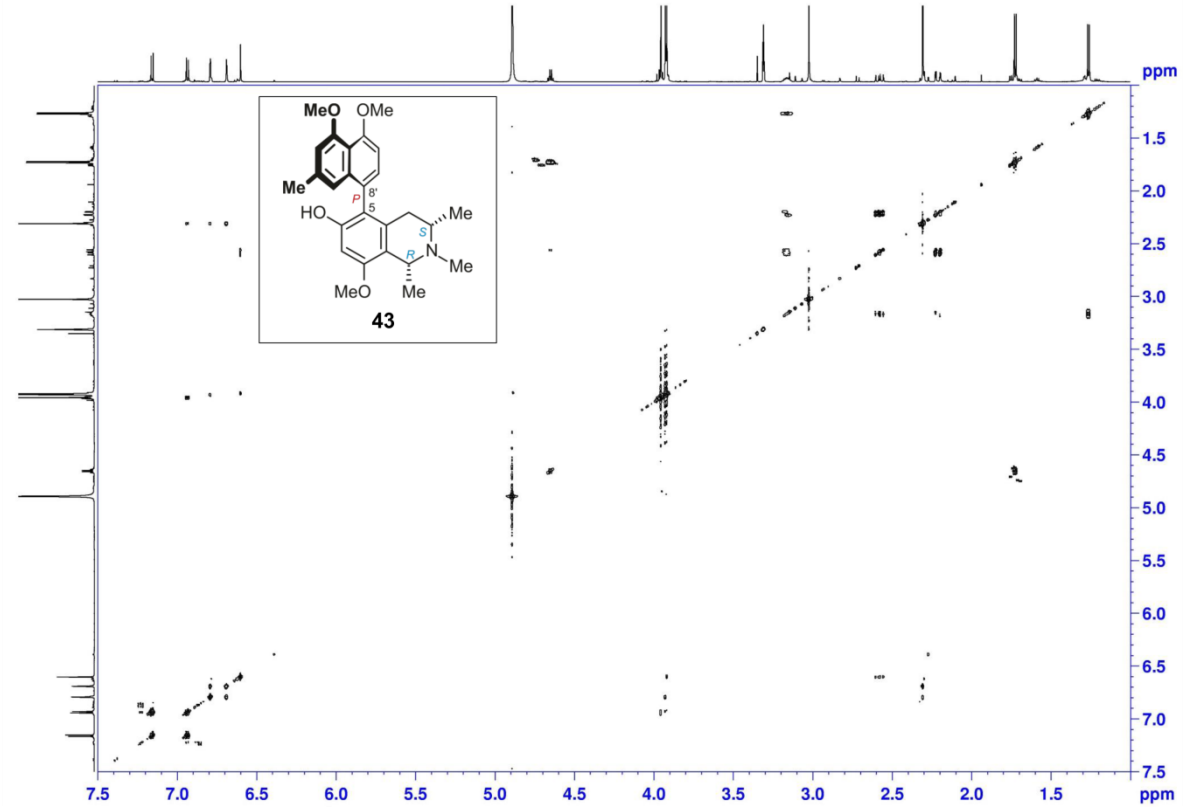

SI 4: *^{1}H-^{1}H COSY NMR spectrum of ancistroyafungine A (**43**) in CD_3OD*

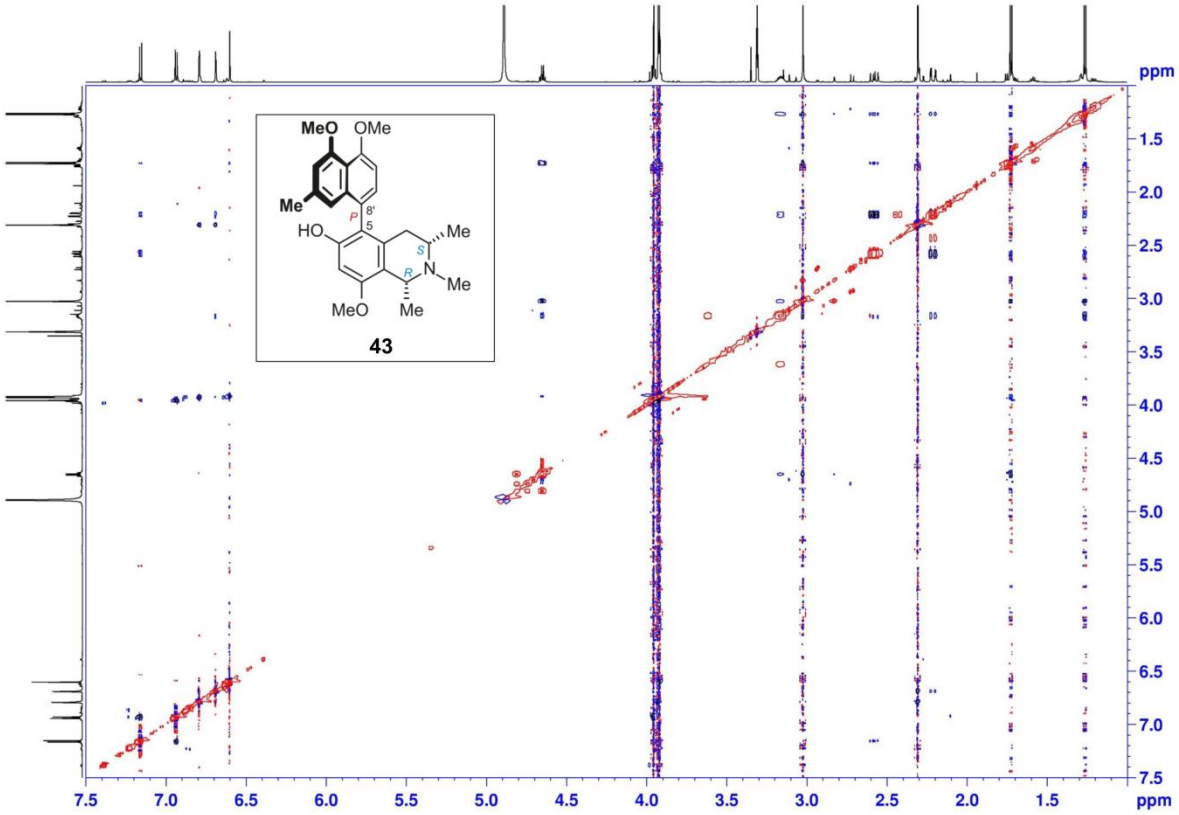

SI 5: *^{1}H-^{1}H NOESY NMR spectrum of ancistroyafungine A (**43**) in CD_3OD*

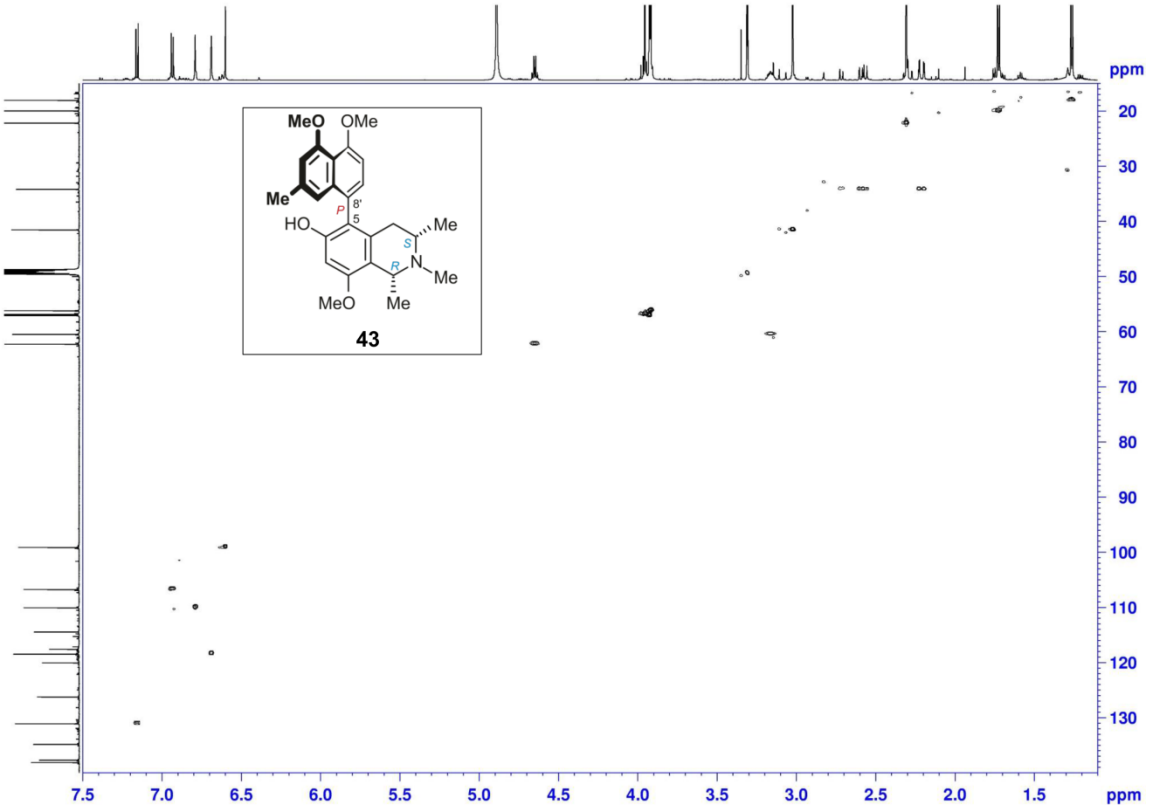

SI 6: *^{1}H-^{13}C HSQC NMR spectrum of ancistroyafungine A (**43**) in CD_3OD*

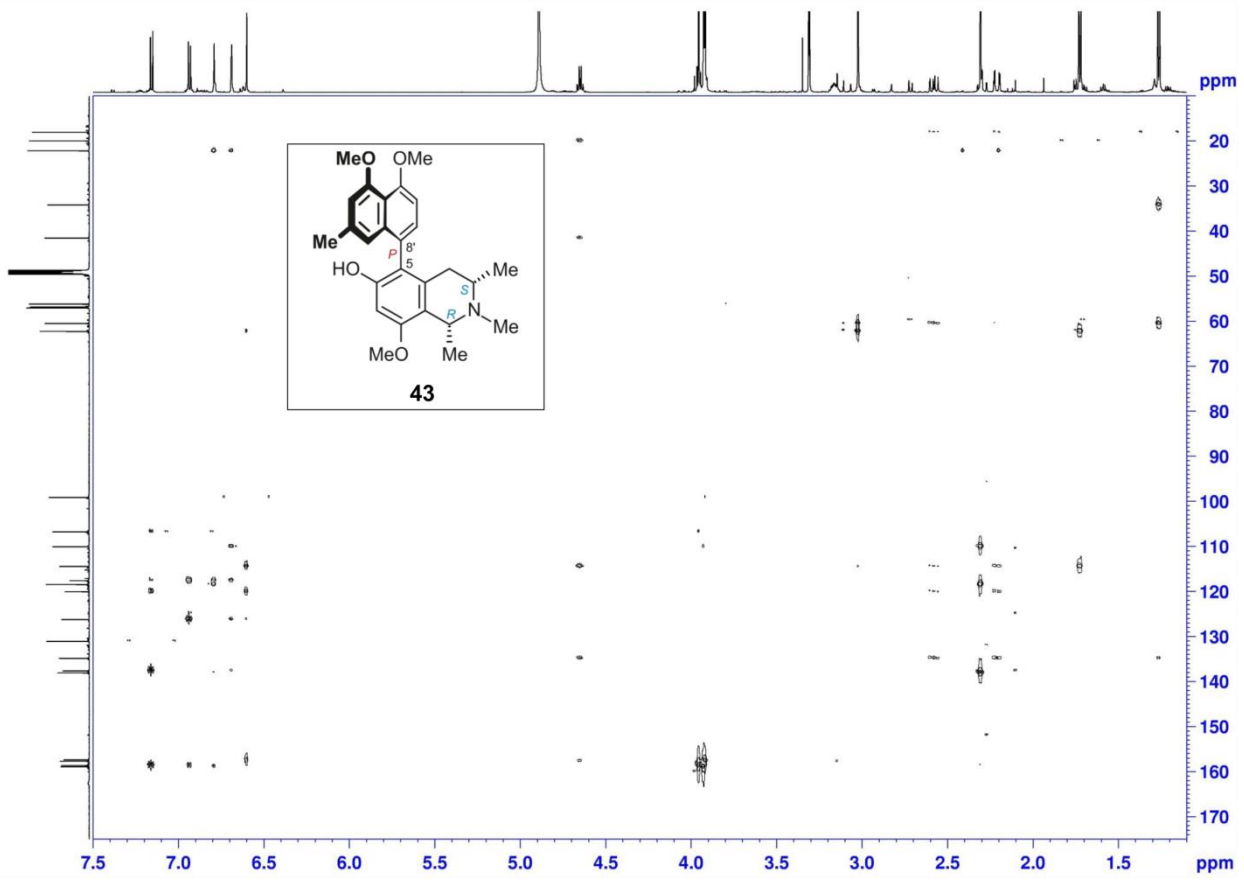

SI 7: *^{1}H-^{13}C HMBC NMR spectrum of ancistroyafungine A (**43**) in CD_3OD*

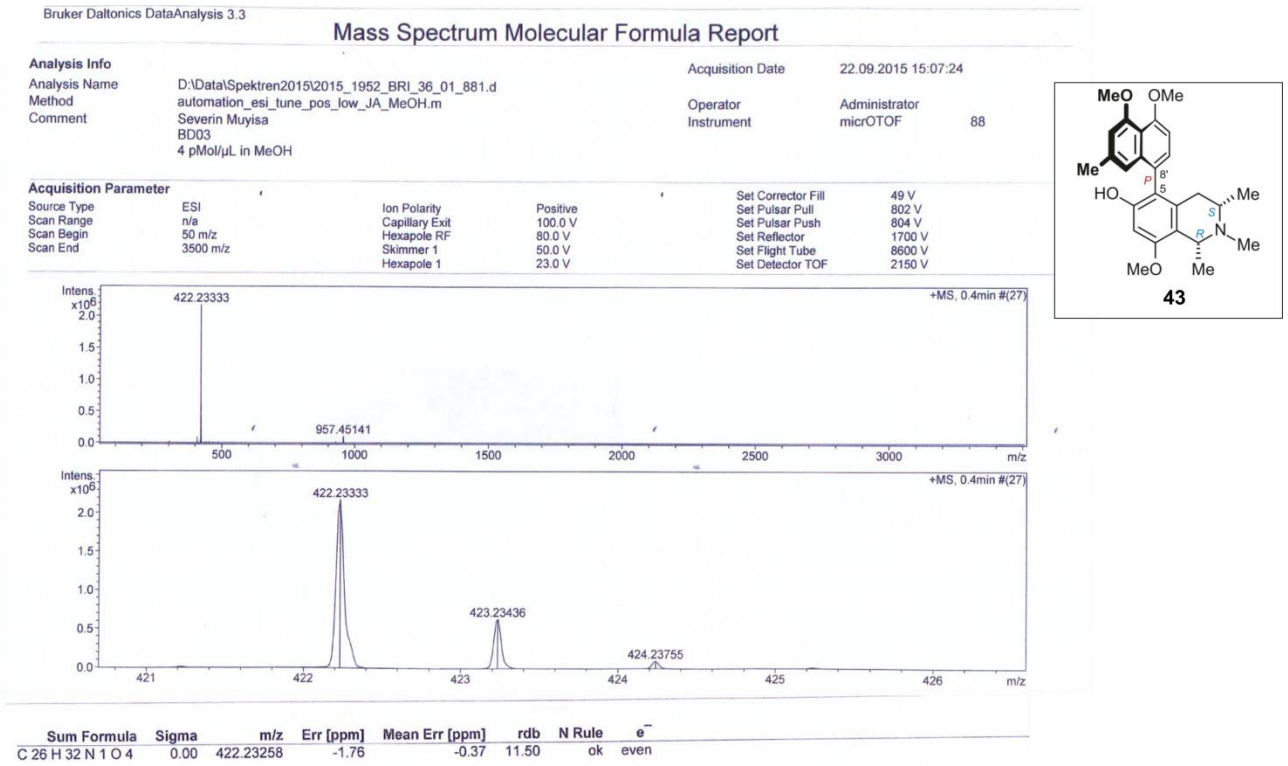

SI 8: *HRESIMS spectrum of ancistroyafungine A (**43**)*

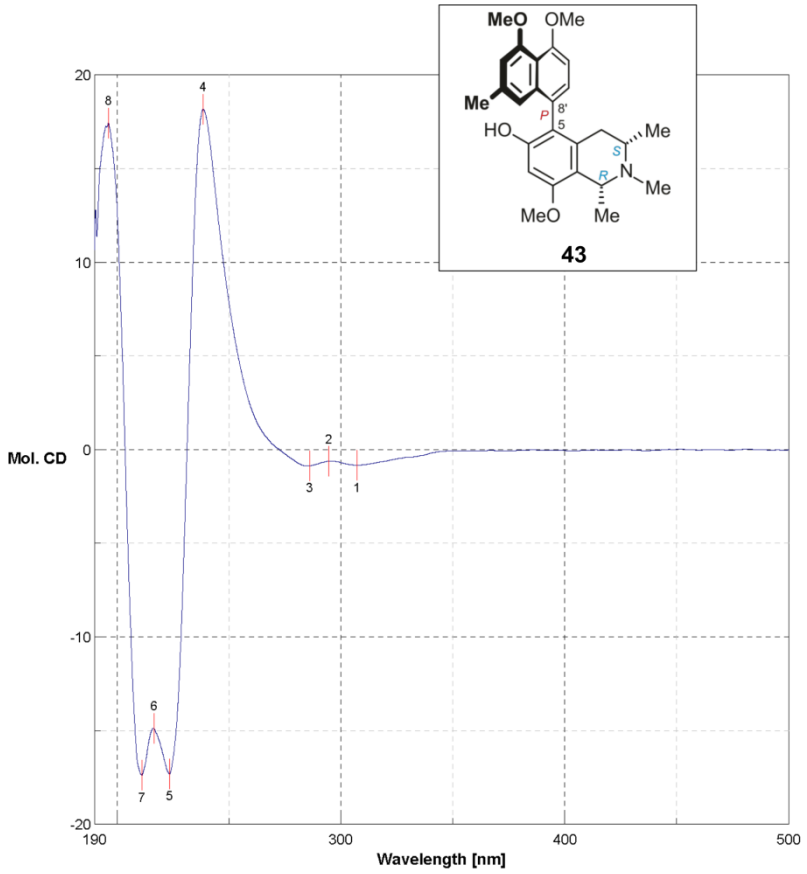

Date/Time	07.03.2018 15:19
Operator	Kimbadi
File Name	SMK-BKL-1-4-ok.jws
Sample Name	SMK-BKL-1-4
Comment	offline

No.	nm	Mol. CD	No.	nm	Mol. CD	No.	nm	Mol. CD
1	307.2	-0.84215	2	294.6	-0.62119	3	286	-0.868903
4	238.6	18.1742	5	223.5	-17.3175	6	216.5	-14.8805
7	211.2	-17.3888	8	196.2	17.4391			

SI 9: *ECD spectrum of ancistroyafungine A (**43**) in methanol*

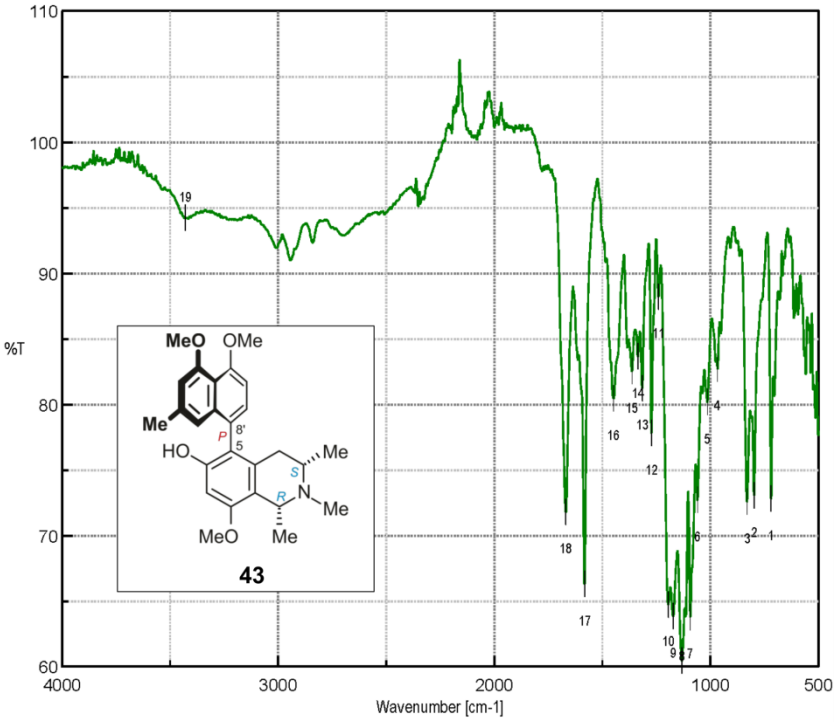

Results of Peak Find

No.	Position	Intensity	No.	Position	Intensity
1	719.318	72.7832	2	798.385	73.0545
3	830.205	72.5894	4	967.126	82.7167
5	1013.41	80.1583	6	1059.69	72.6902
7	1093.44	63.7867	8	1132.01	60.4306
9	1172.51	63.8412	10	1194.69	64.714
11	1240	88.1984	12	1272.79	77.7846
13	1315.21	81.229	14	1335.46	83.6341
15	1363.43	82.5002	16	1448.28	80.446
17	1582.31	66.2852	18	1669.09	71.7957
19	3429.78	94.2054			

[Comments]

Sample name	1-4
Comment	backgd
User	Kimbadi
Division	AK Bringmann
Company	Uni Würzburg

[Measurement Information]

Model Name	FT/IR-4600typeA
Serial Number	D063461786
Accessory	ATR PRO ONE
Accessory S/N	A070661809
Incident angle	45 deg
Measurement Date	13.06.2018 13:28
Light Source	Standard
Detector	TGS
Accumulation	16
Resolution	4 cm-1
Zero Filling	On
Apodization	Cosine
Gain	Auto (4)
Aperture	Auto (7.1 mm)
Scanning Speed	Auto (2 mm/sec)
Filter	Auto (30000 Hz)

SI 10: *IR spectrum of ancistroyafungine A (**43**)*

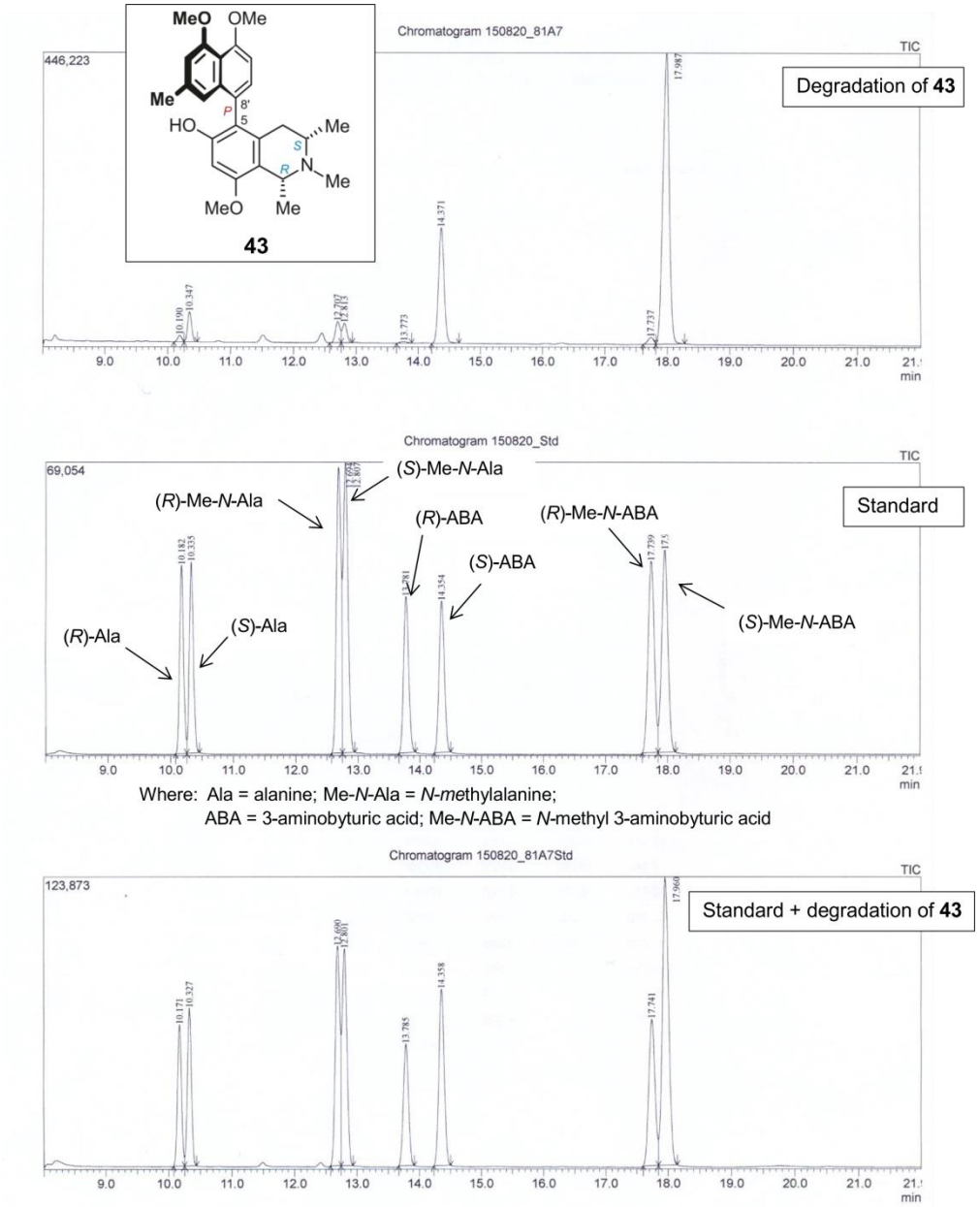

SI 11: *Oxidative degradation of ancistroyafungine A (**43**)*

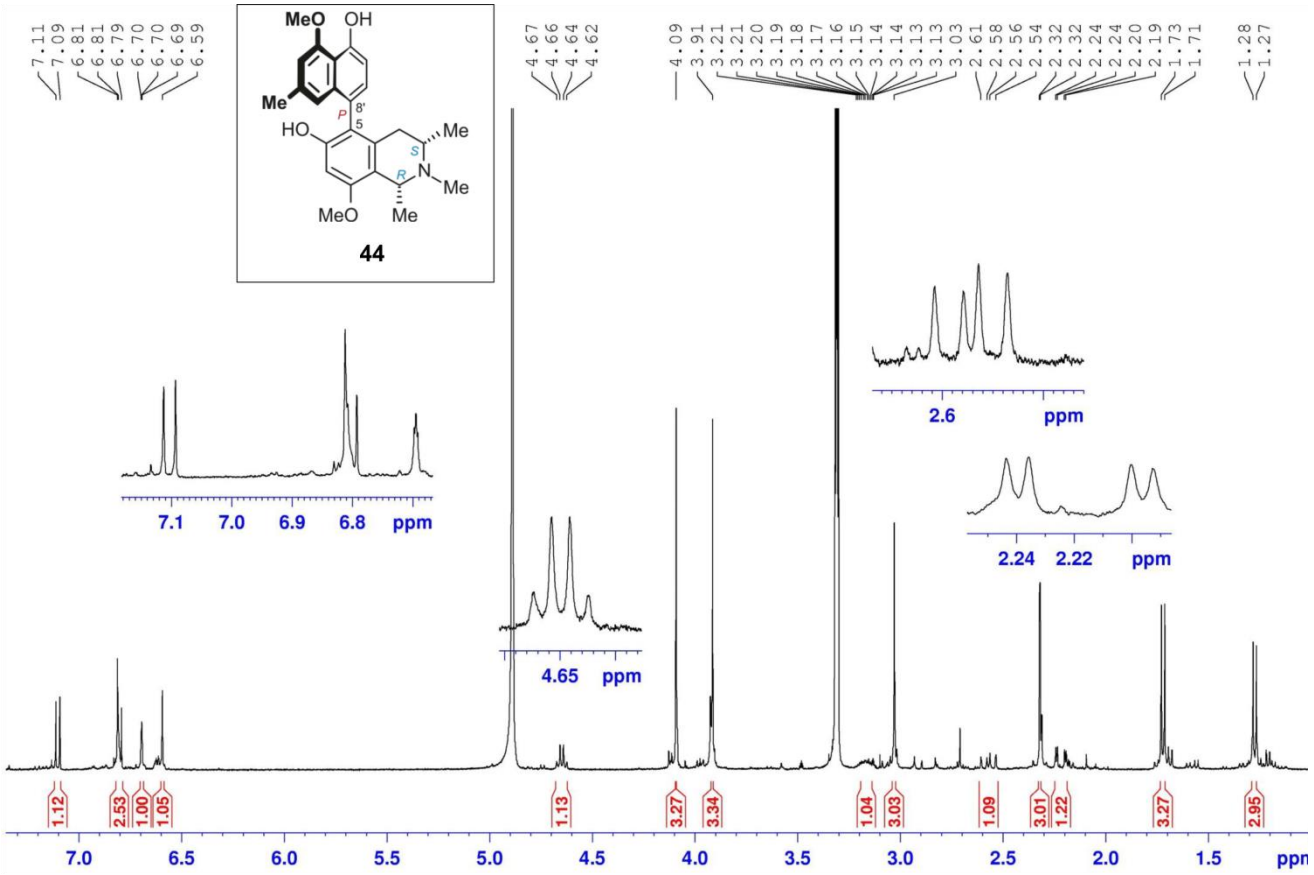

SI 12: *[1]H NMR spectrum of ancistroyafungine B (**44**) in CD_3OD*

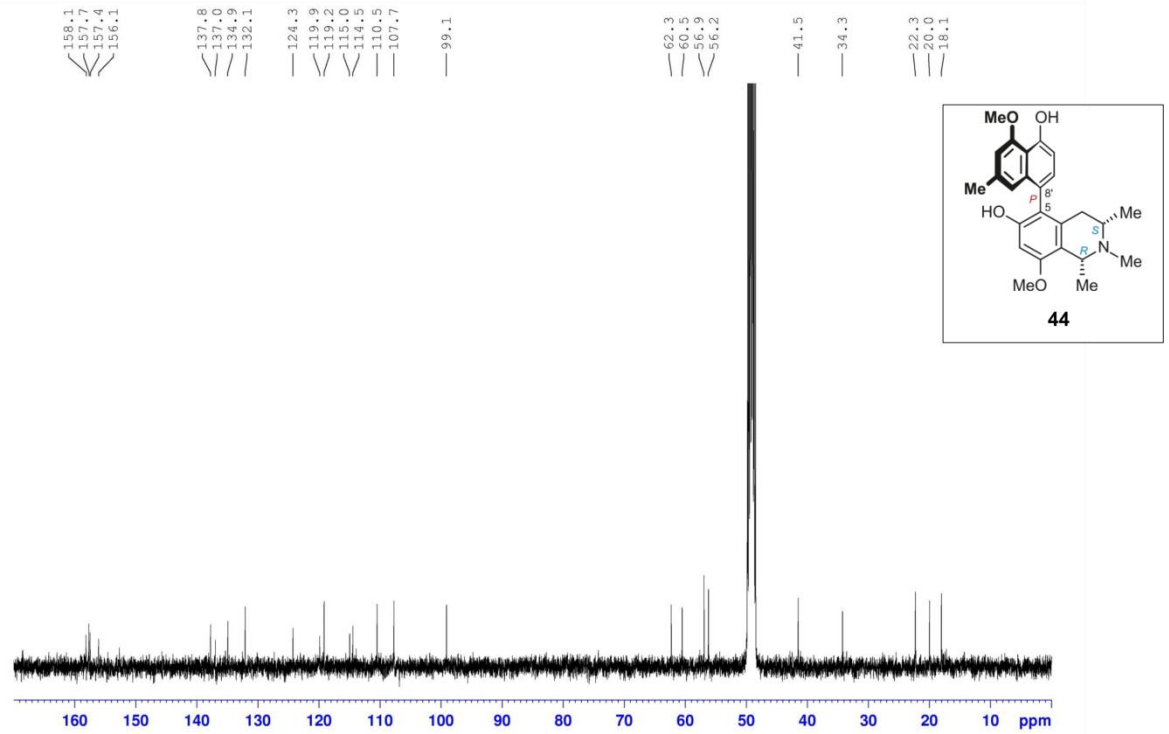

SI 13: *[13]C NMR spectrum of ancistroyafungine B (**44**) in CD_3OD*

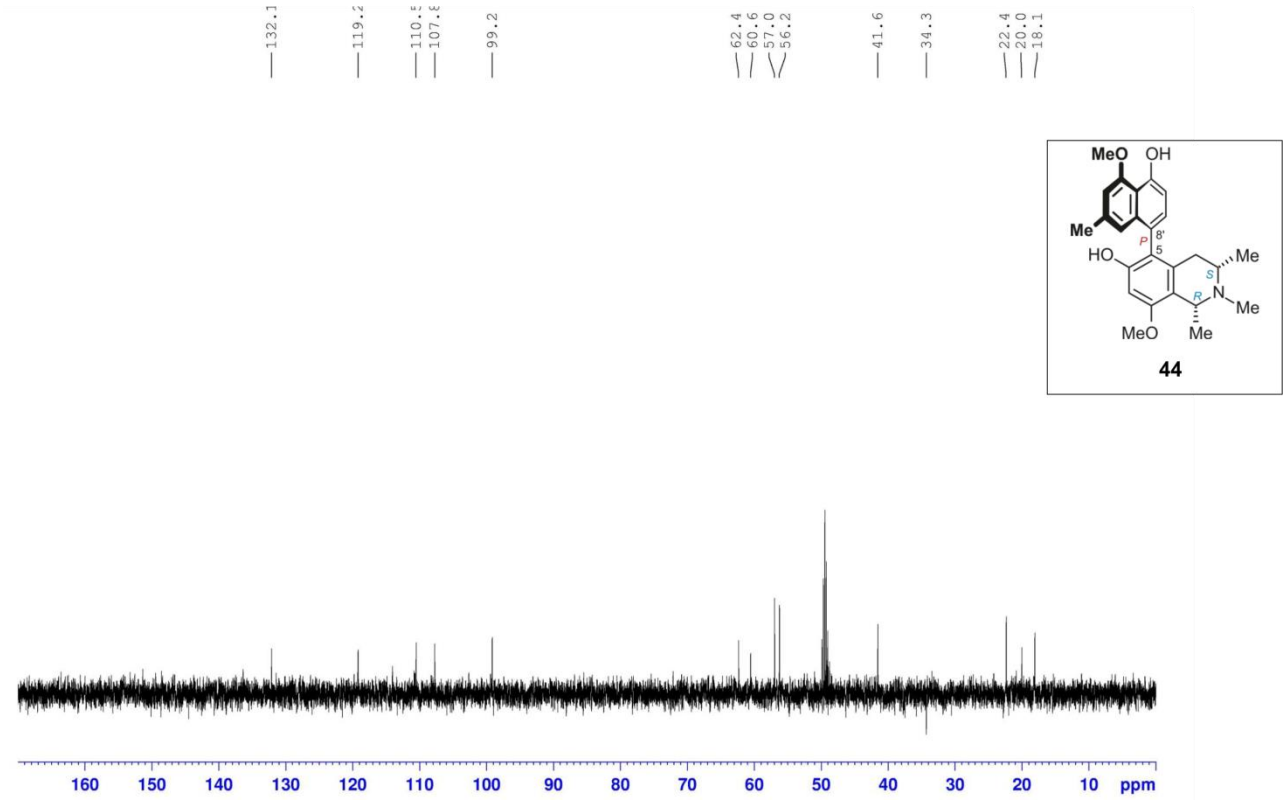

SI 14: *^{13}C DEPT-135 NMR spectrum of ancistroyafungine B (**44**) in CD_3OD*

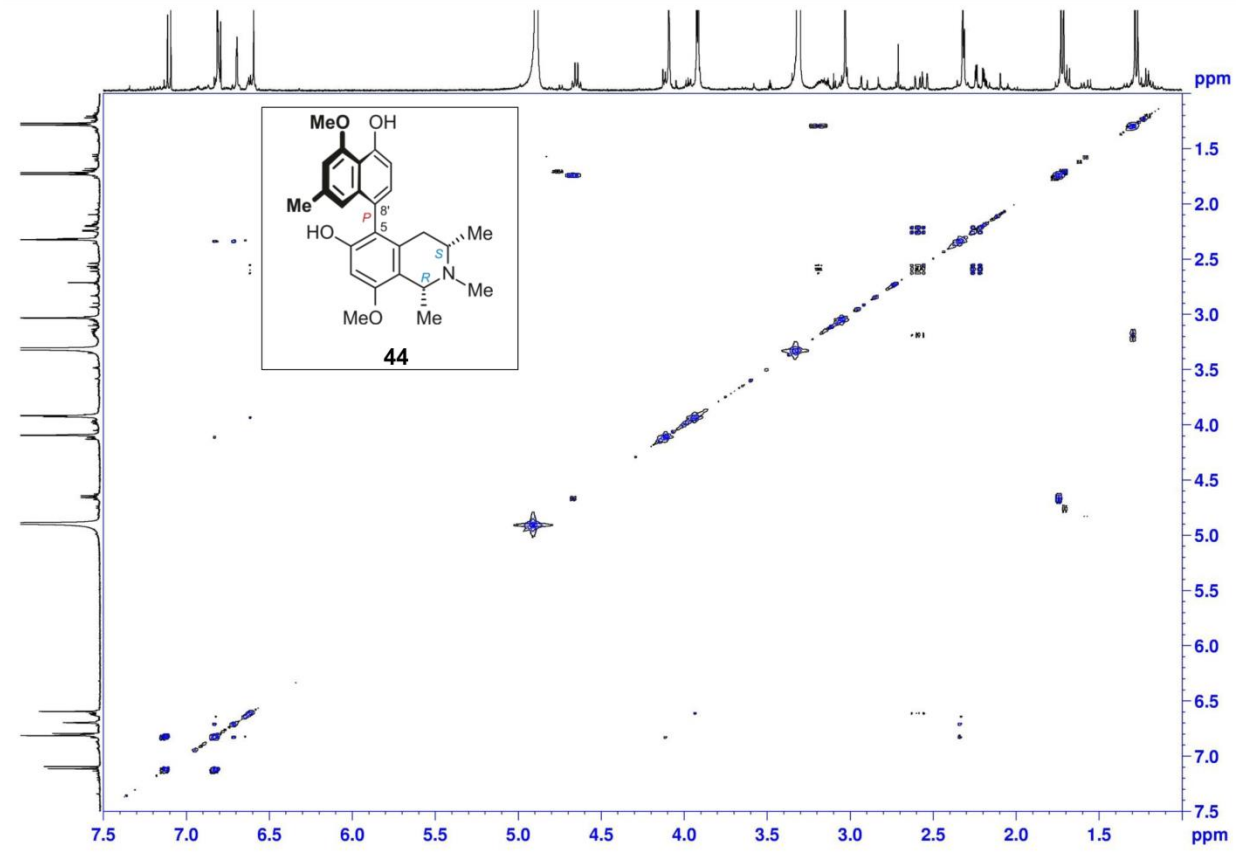

SI 15: *^{1}H-^{1}H COSY NMR spectrum of ancistroyafungine B (**44**) in CD_3OD*

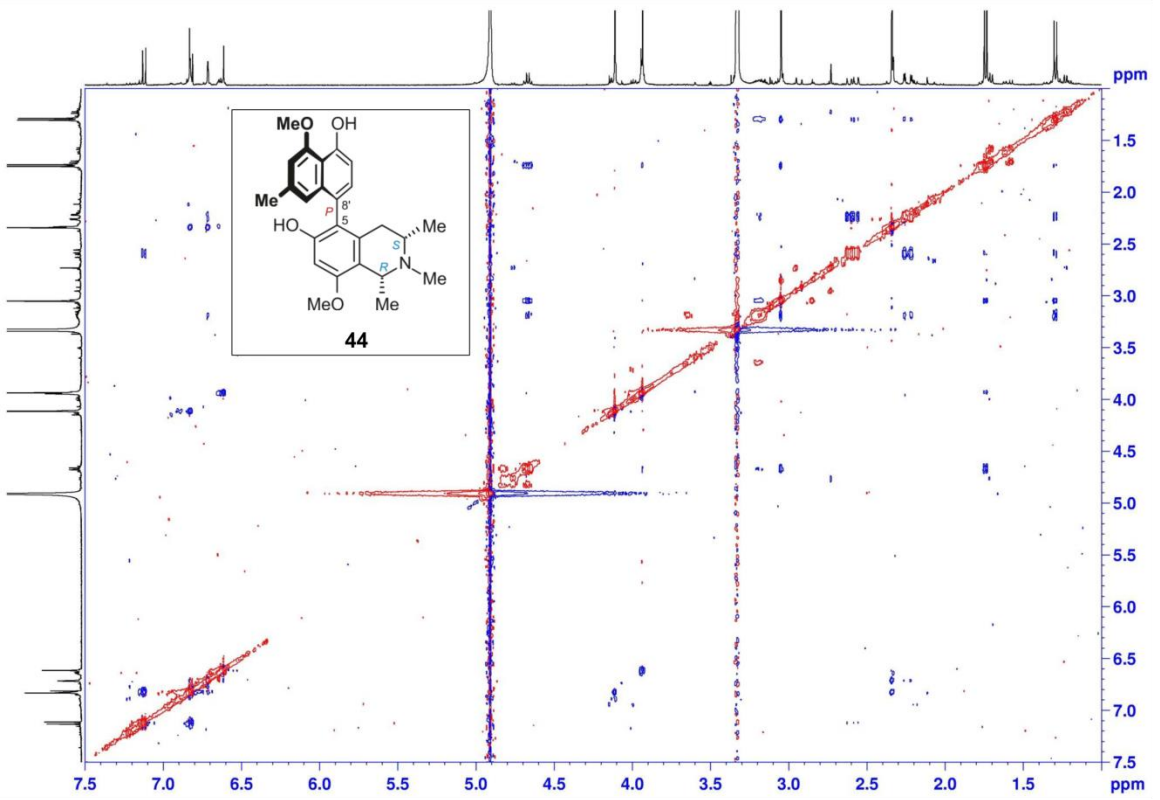

SI 16: *^{1}H-^{1}H NOESY NMR spectrum of ancistroyafungine B (**44**) in CD_3OD*

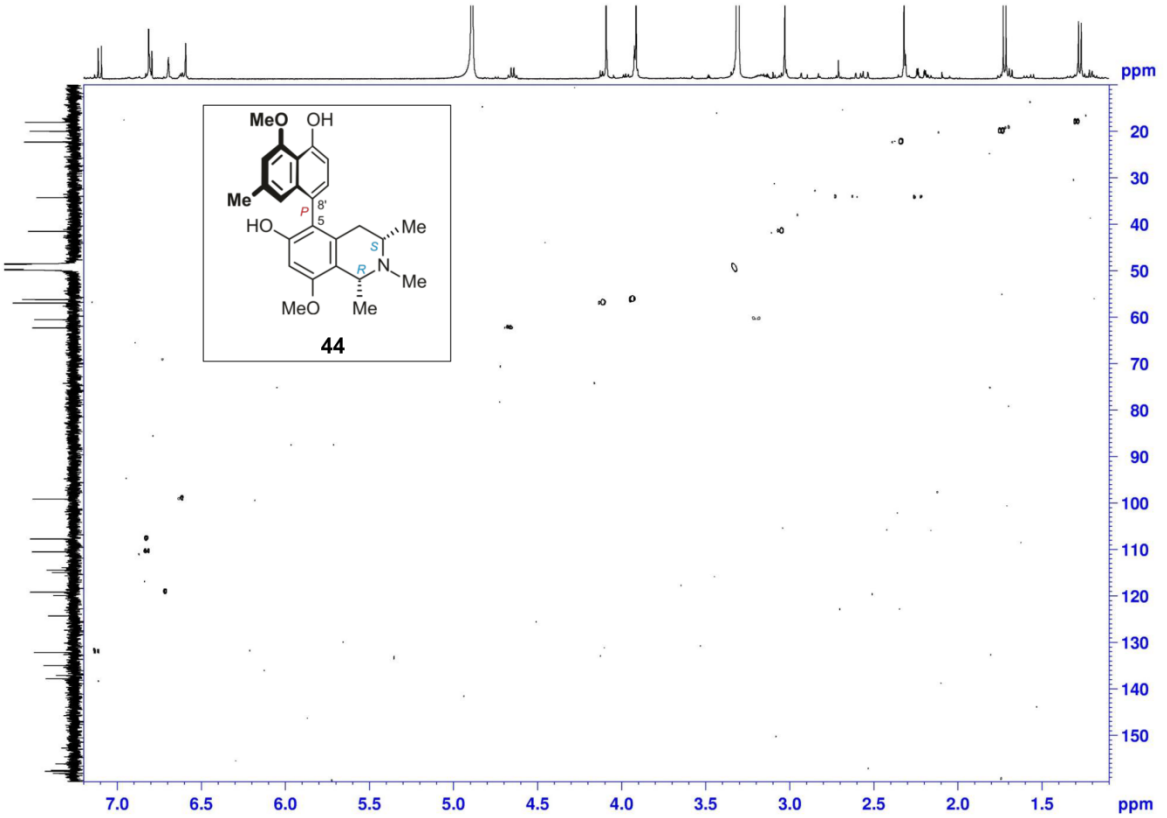

SI 17: *^{1}H-^{13}C HSQC NMR spectrum of ancistroyafungine B (**44**) in CD_3OD*

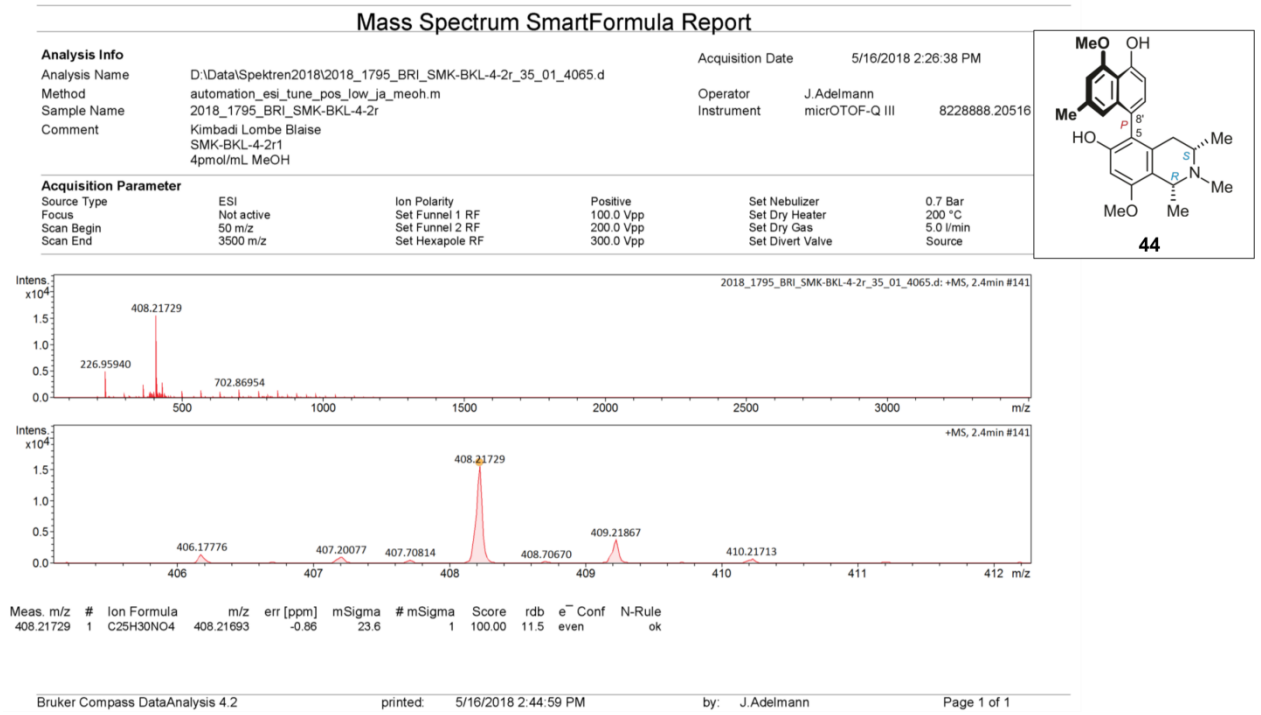

SI 18: *HRESIMS spectrum of ancistroyafungine B (**44**)*

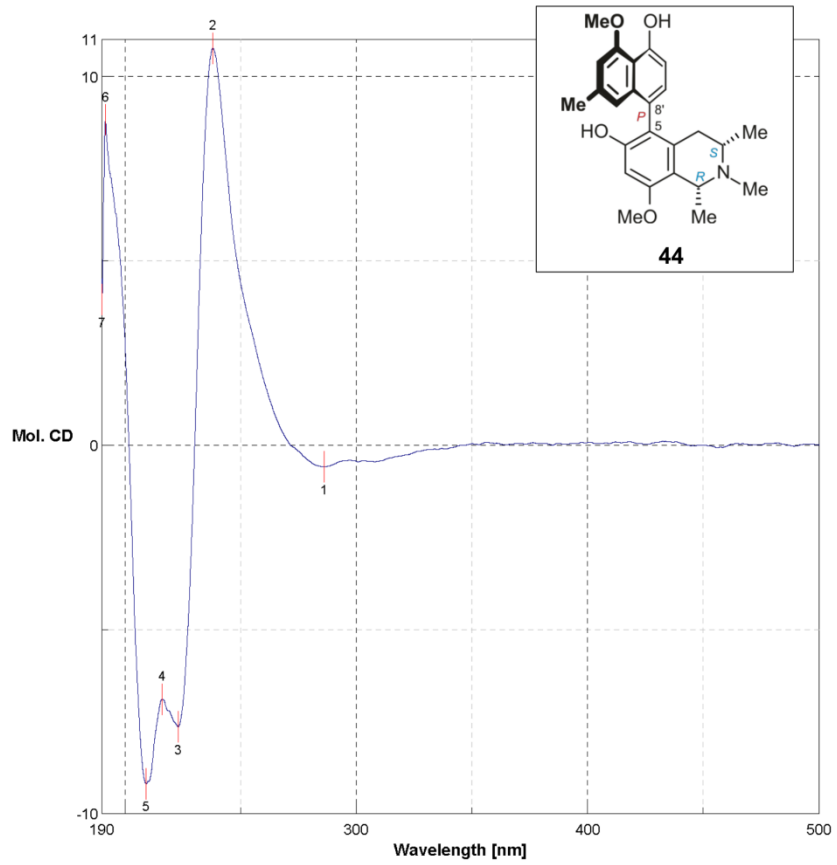

Date/Time	08.03.2018 12:40
Operator	Kimbadi
File Name	SMK-BKL-4-2-ok.jws
Sample Name	SMK-BKL-4-2
Comment	offline

No.	nm	Mol. CD	No.	nm	Mol. CD	No.	nm	Mol. CD
1	286.2	-0.590511	2	238	10.7705	3	223.1	-7.64418
4	216.1	-6.88753	5	209.1	-9.18463	6	191.6	8.81968
7	190.2	3.94518						

SI 19: *ECD spectrum of ancistroyafungine B (**44**) in methanol*

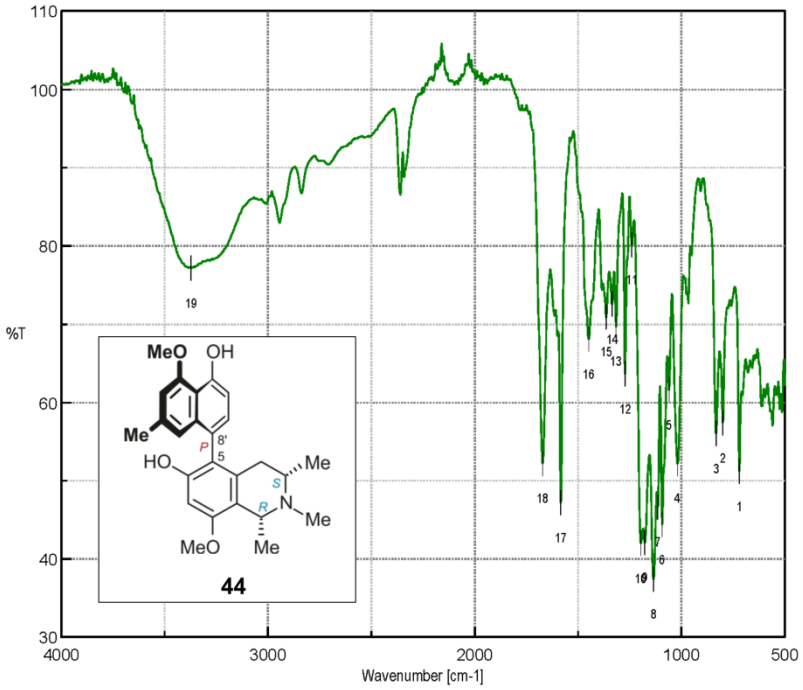

Results of Peak Find

No.	Position	Intensity	No.	Position	Intensity
1	720.282	51.2053	2	799.35	57.366
3	832.133	55.9912	4	1019.19	52.1644
5	1059.69	61.5783	6	1093.44	44.378
7	1113.69	46.5909	8	1134.9	37.4011
9	1177.33	42.0935	10	1195.65	41.9648
11	1240	80.0897	12	1272.79	63.5943
13	1316.18	69.6797	14	1336.43	72.5242
15	1364.39	70.8836	16	1448.28	68.0799
17	1583.27	47.1445	18	1671.02	52.1642
19	3371.92	77.1658			

[Comments]

Sample name	4-2
Comment	drop MeOH
User	Kimbadi
Division	AK Bringmann
Company	Uni Würzburg

[Measurement Information]

Model Name	FT/IR-4600typeA
Serial Number	D063461786
Accessory	ATR PRO ONE
Accessory S/N	A070661809
Incident angle	45 deg
Measurement Date	13.06.2018 14:15
Light Source	Standard
Detector	TGS
Accumulation	16
Resolution	4 cm-1
Zero Filling	On
Apodization	Cosine
Gain	Auto (4)
Aperture	Auto (7.1 mm)
Scanning Speed	Auto (2 mm/sec)
Filter	Auto (30000 Hz)

SI 20: *IR spectrum of ancistroyafungine B (**44**)*

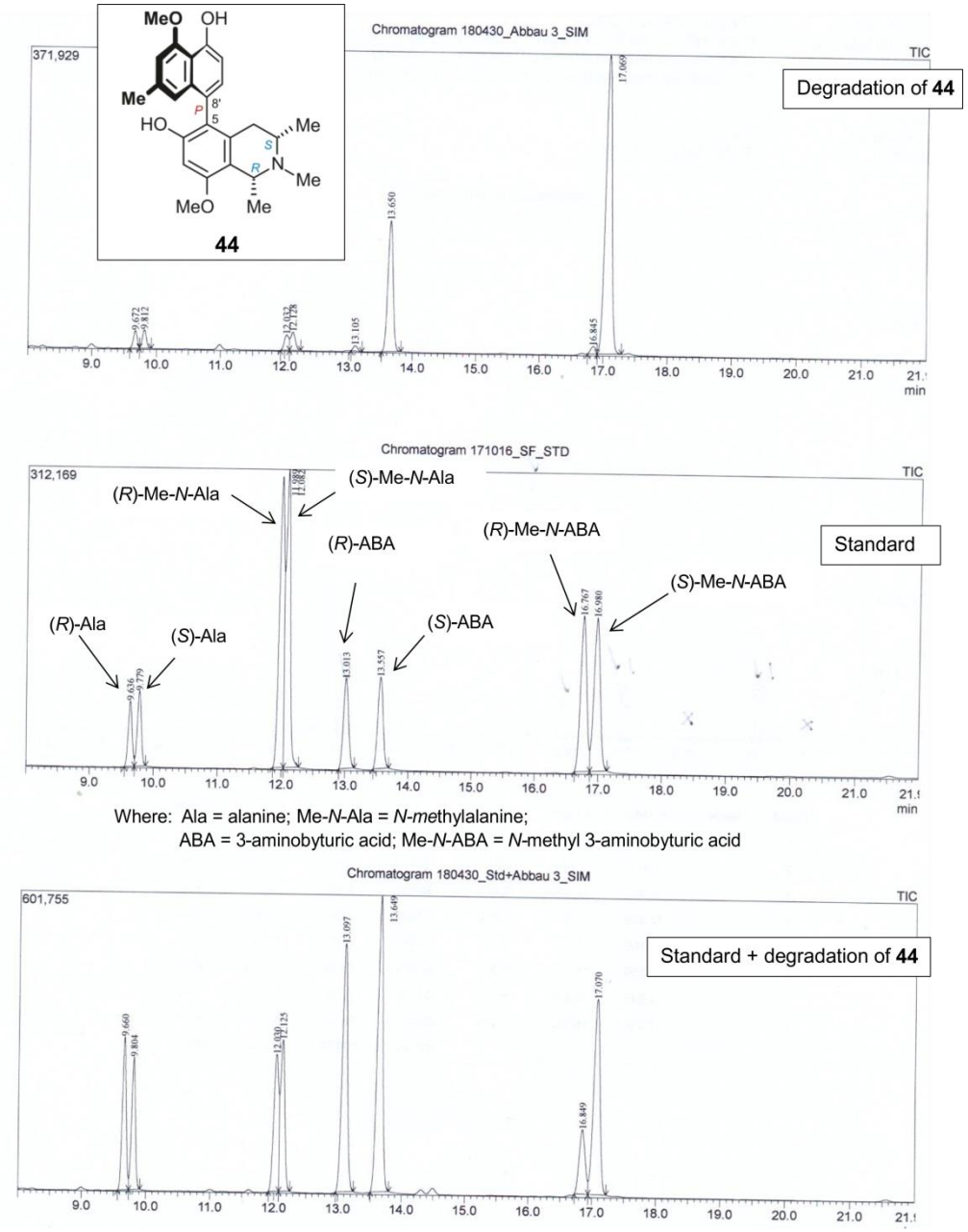

SI 21: *Oxidative degradation of ancistroyafungine B (**44**)*

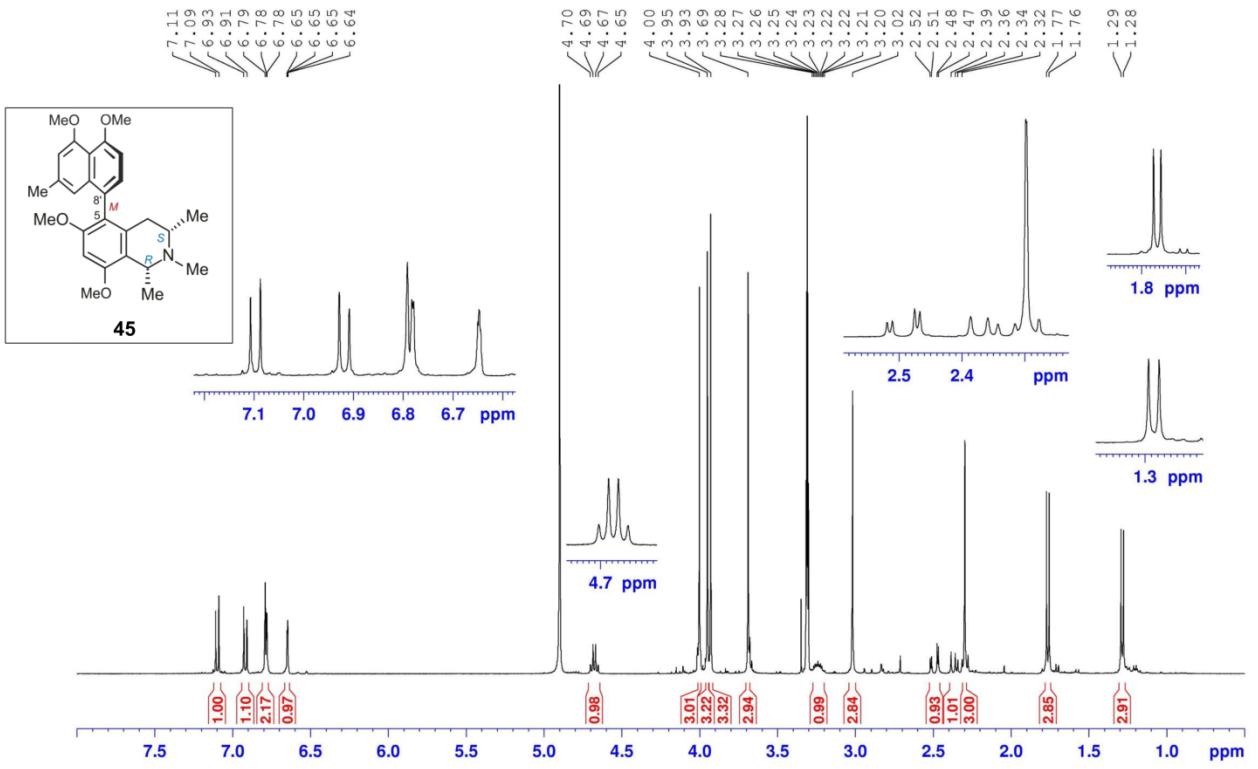

SI 22: *^{1}H NMR spectrum of ancistroyafungine C (**45**) in CD_3OD*

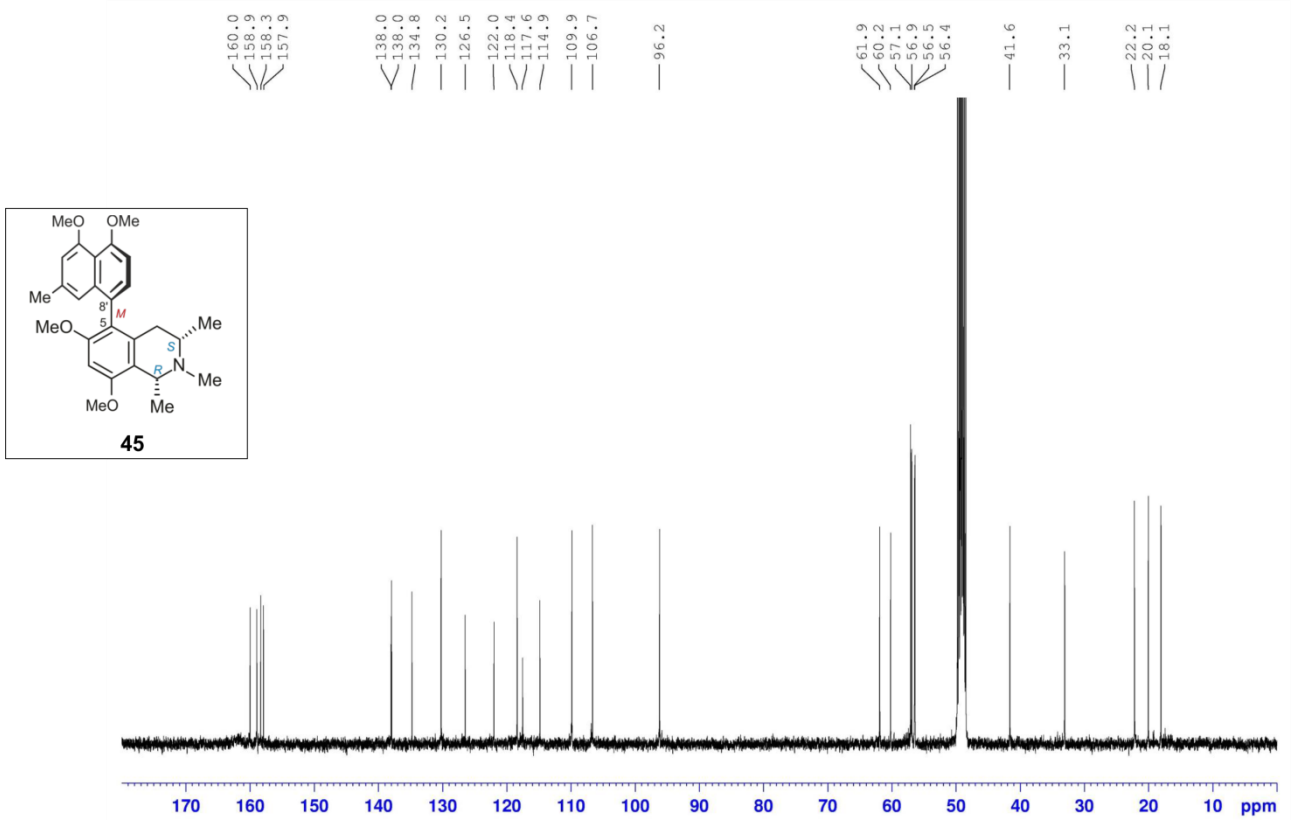

SI 23: *^{13}C NMR spectrum of ancistroyafungine C (**45**) in CD_3OD*

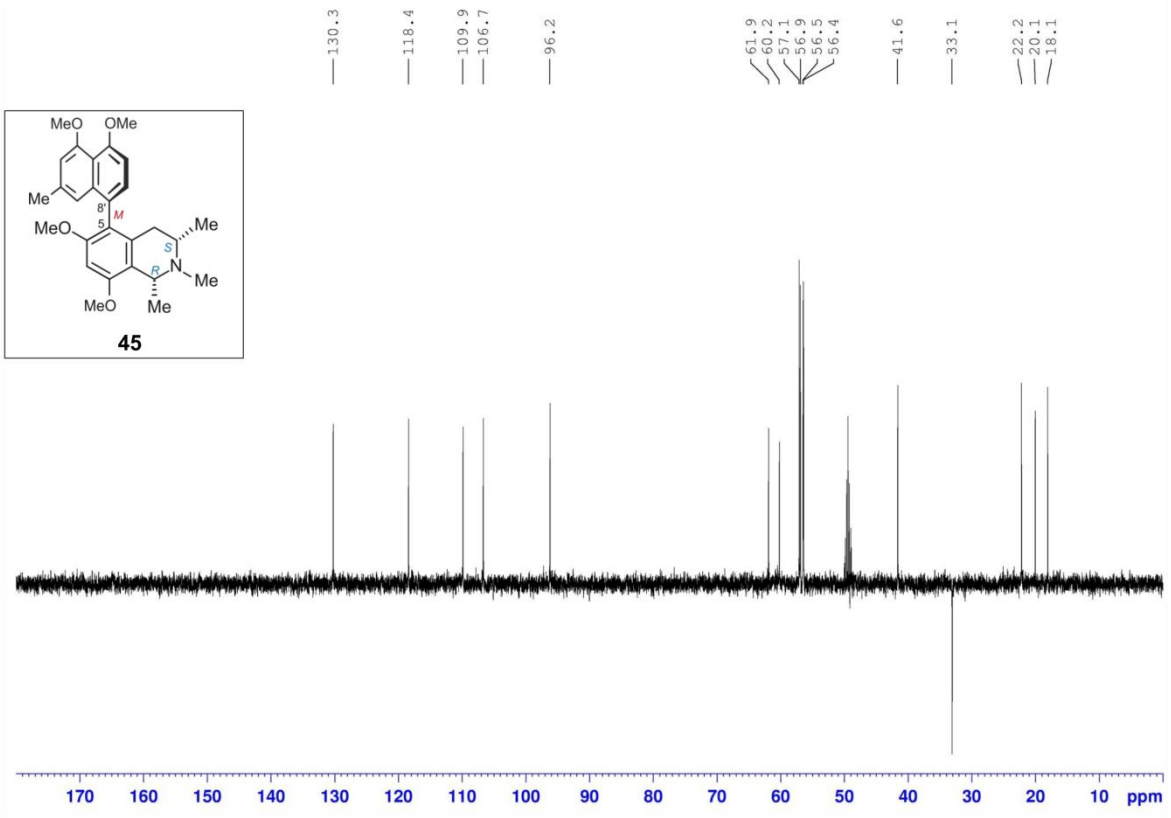

SI 24: *^{13}C DEPT-135 NMR spectrum of ancistroyafungine C (**45**) in CD_3OD*

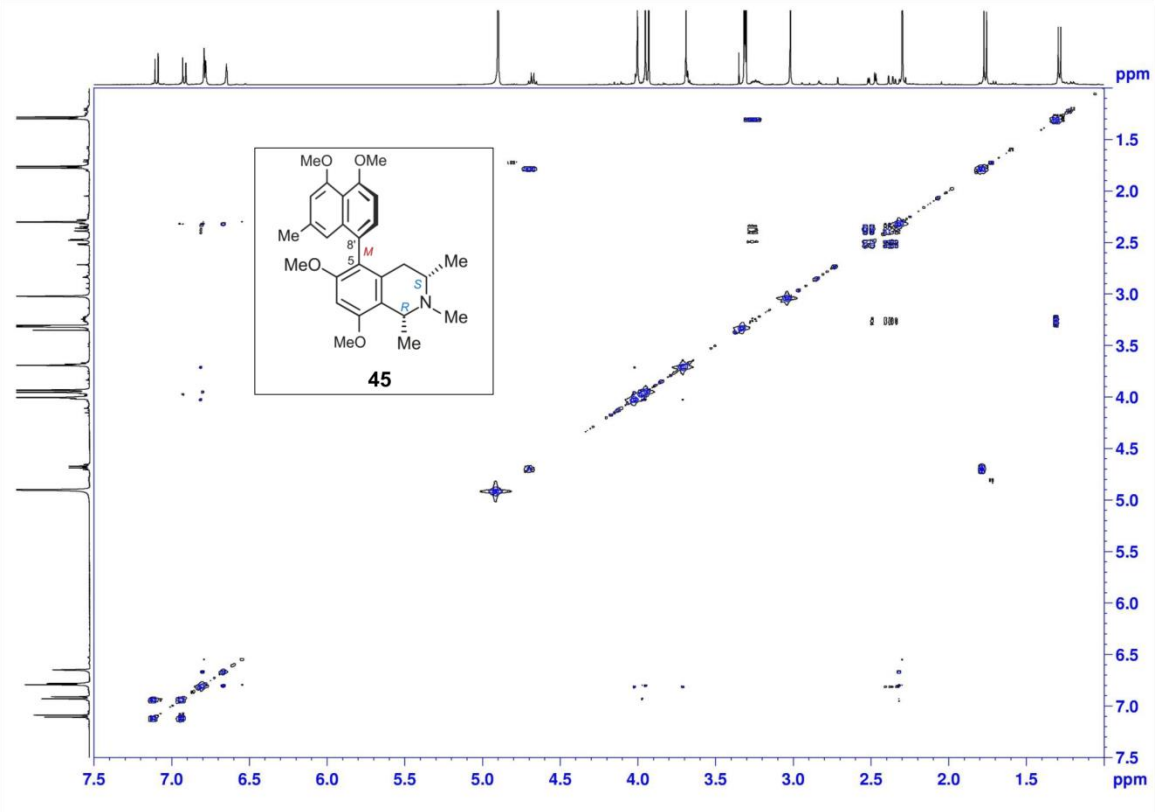

SI 25: *^{1}H-^{1}H COSY NMR spectrum of ancistroyafungine C (**45**) in CD_3OD*

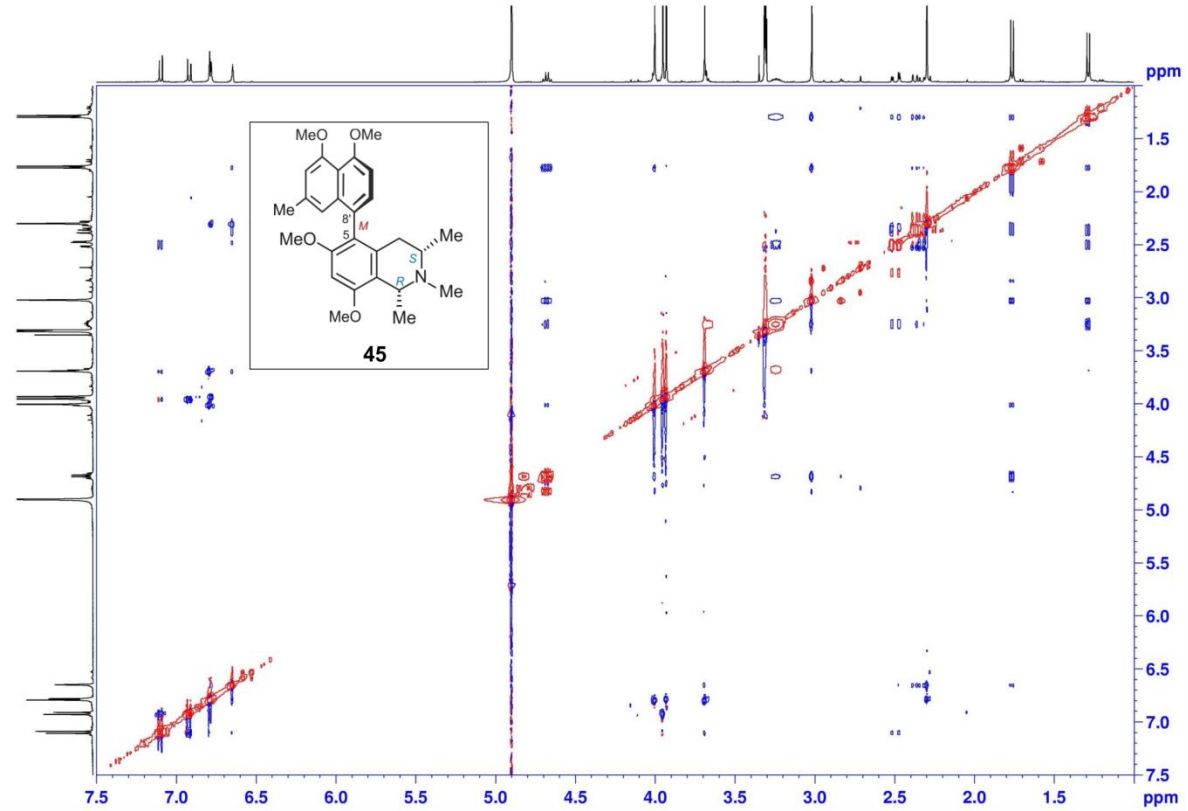

SI 26: *^{1}H-^{1}H NOESY NMR spectrum of ancistroyafungine C (**45**) in CD_3OD*

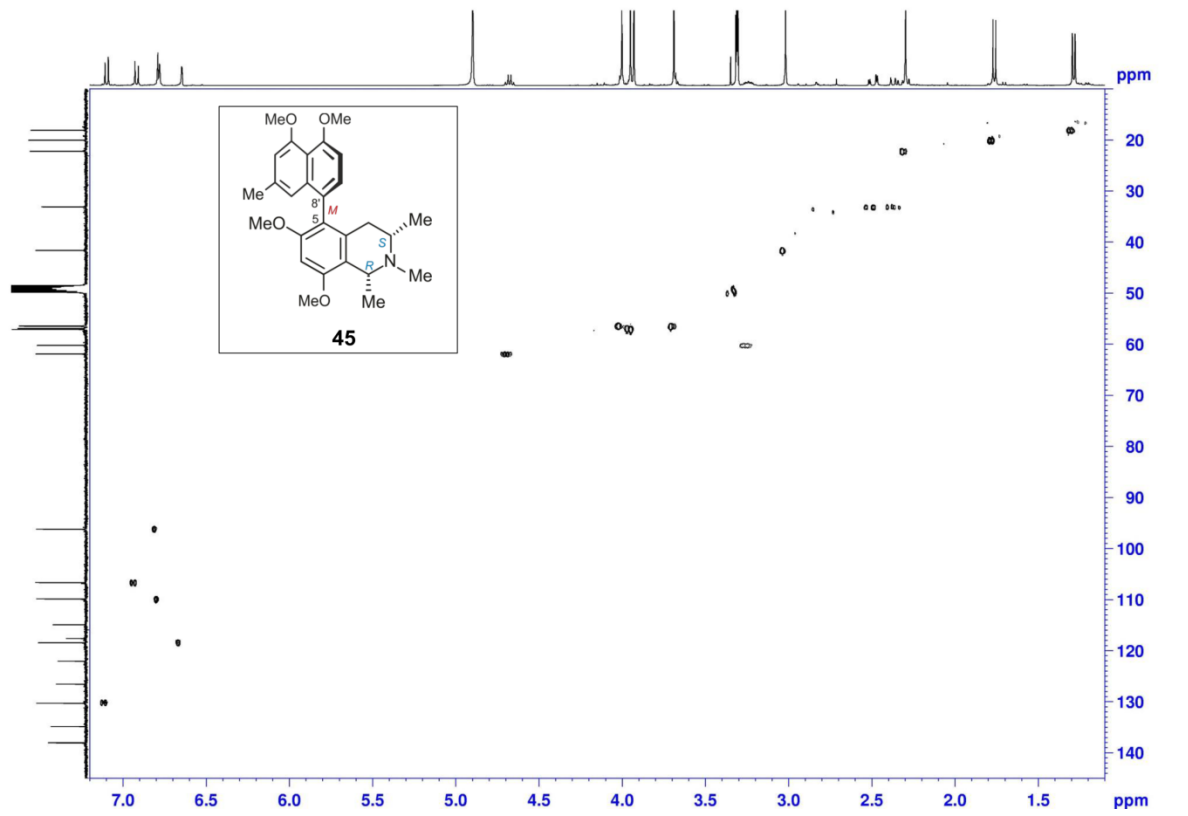

SI 27: *^{1}H-^{13}C HSQC NMR spectrum of ancistroyafungine C (**45**) in CD_3OD*

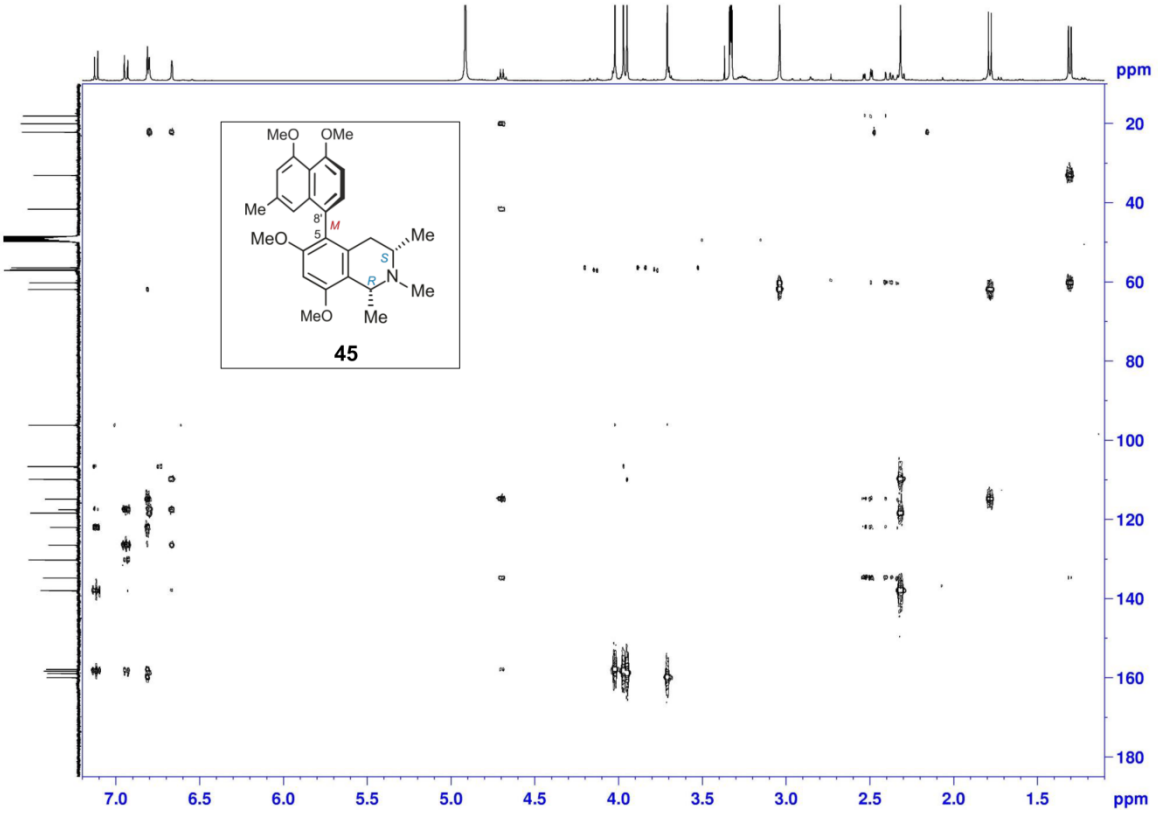

SI 28: *^{1}H-^{13}C HMBC NMR spectrum of ancistroyafungine C (**45**) in CD_3OD*

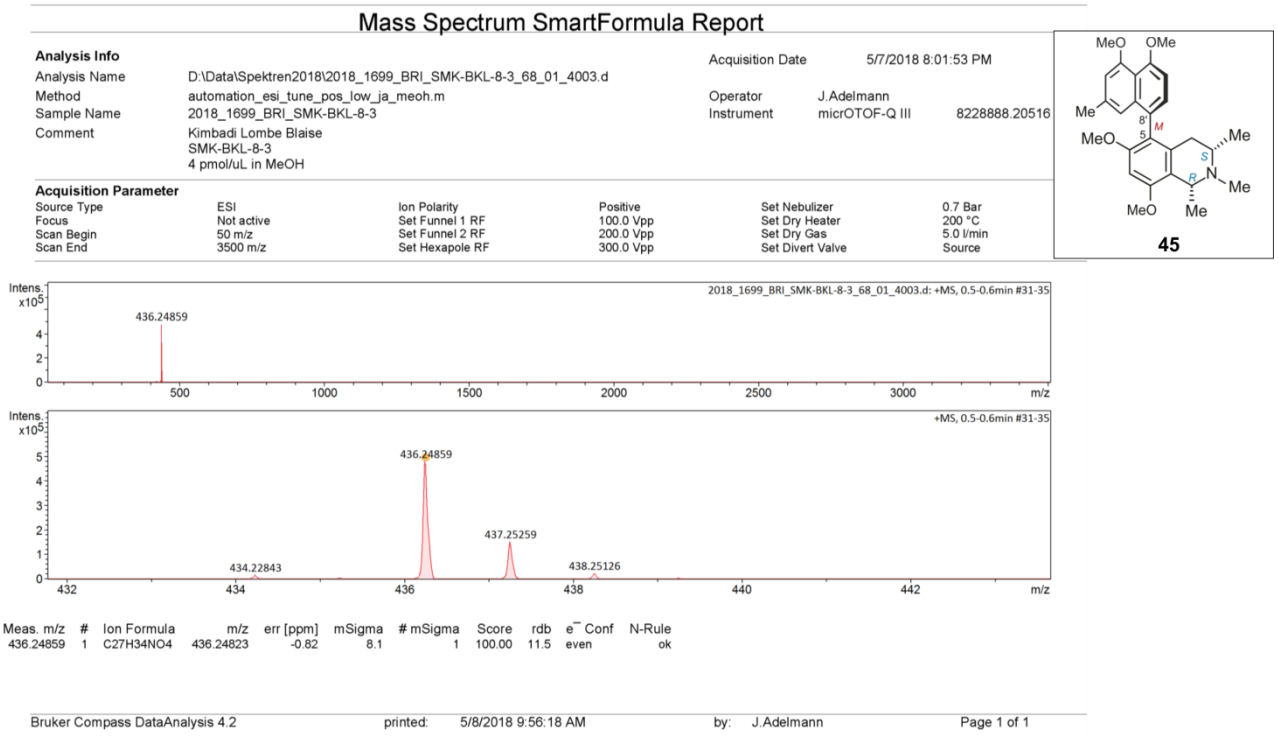

SI 29: *HRESIMS spectrum of ancistroyafungine C (**45**)*

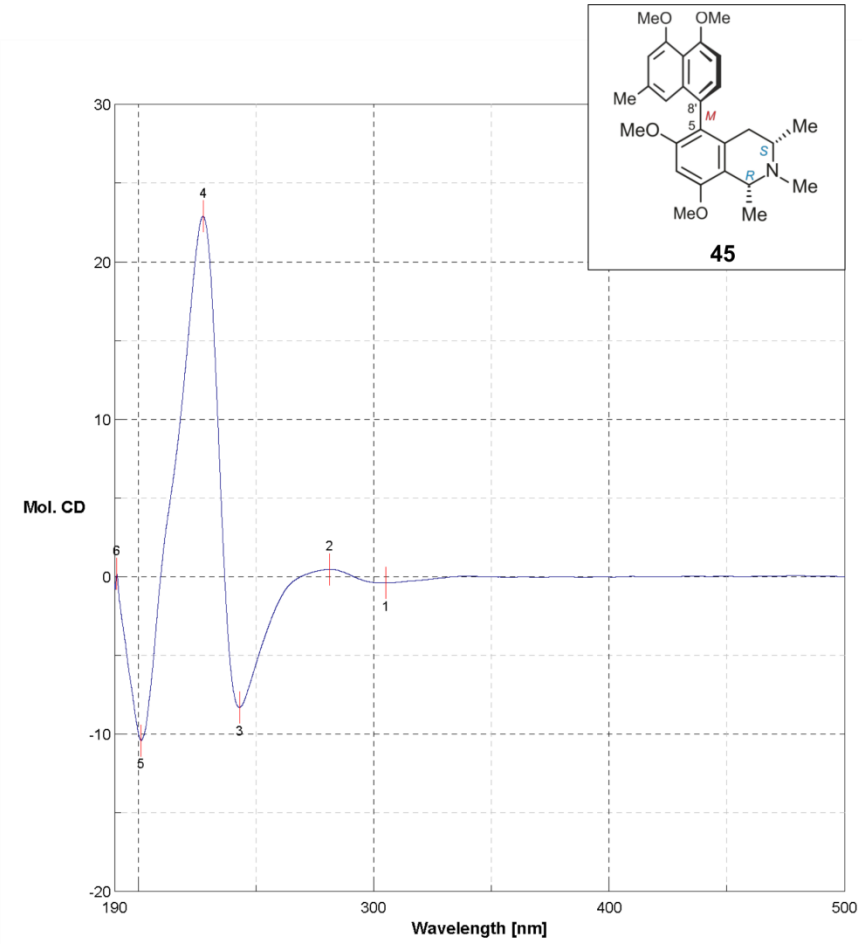

Date/Time	07.03.2018 14:37
Operator	Kimbadi
File Name	SMK-BKL-8-3-Ok.jws
Sample Name	SMK-BKL-8-3
Comment	offline

No.	nm	Mol. CD	No.	nm	Mol. CD	No.	nm	Mol. CD
1	305.2	-0.400637	2	281.2	0.471268	3	243.1	-8.3185
4	227.6	22.9011	5	201.2	-10.4047	6	190.9	0.176299

SI 30: *ECD spectrum of ancistroyafungine C (**45**) in methanol*

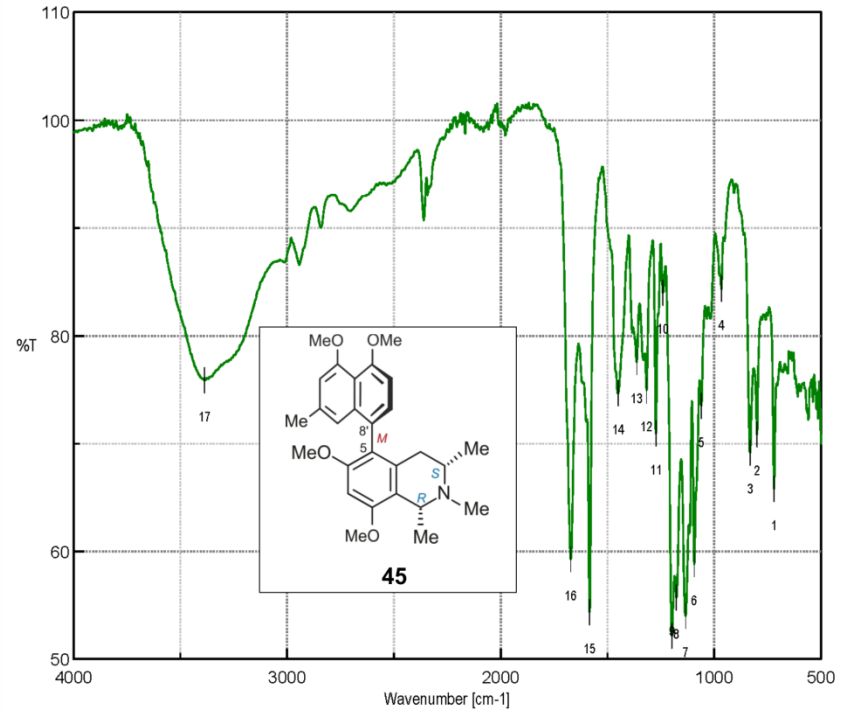

Results of Peak Find

No.	Position	Intensity	No.	Position	Intensity
1	720.282	65.7614	2	800.314	70.8219
3	832.133	69.1366	4	966.162	84.3278
5	1060.66	73.4742	6	1093.44	58.7921
7	1133.94	54.0076	8	1177.33	55.6987
9	1198.54	52.1641	10	1240	83.9623
11	1273.75	70.8869	12	1316.18	74.9134
13	1363.43	77.5307	14	1451.17	74.6323
15	1583.27	54.3343	16	1671.02	59.2389
17	3388.32	75.8631			

[Comments]

Sample name	8-3
Comment	drop MeOH
User	Kimbadi
Division	AK Bringmann
Company	Uni Würzburg

[Measurement Information]

Model Name	FT/IR-4600typeA
Serial Number	D063461786
Accessory	ATR PRO ONE
Accessory S/N	A070661809
Incident angle	45 deg
Measurement Date	13.06.2018 13:53
Light Source	Standard
Detector	TGS
Accumulation	16
Resolution	4 cm-1
Zero Filling	On
Apodization	Cosine
Gain	Auto (4)
Aperture	Auto (7.1 mm)
Scanning Speed	Auto (2 mm/sec)
Filter	Auto (30000 Hz)

SI 31: *IR spectrum of ancistroyafungine C (**45**)*

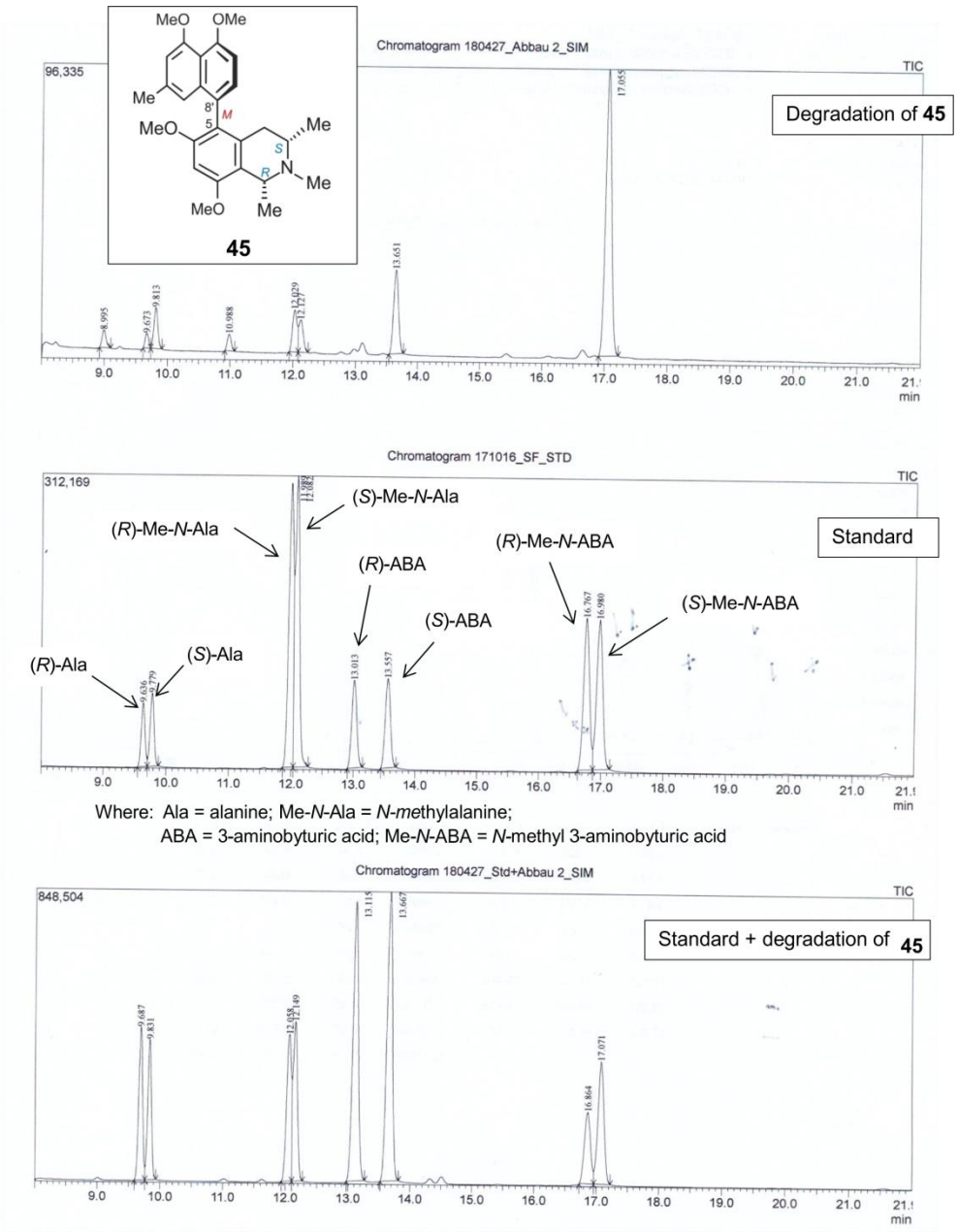

SI 32: *Oxidative degradation of ancistroyafungine C (**45**)*

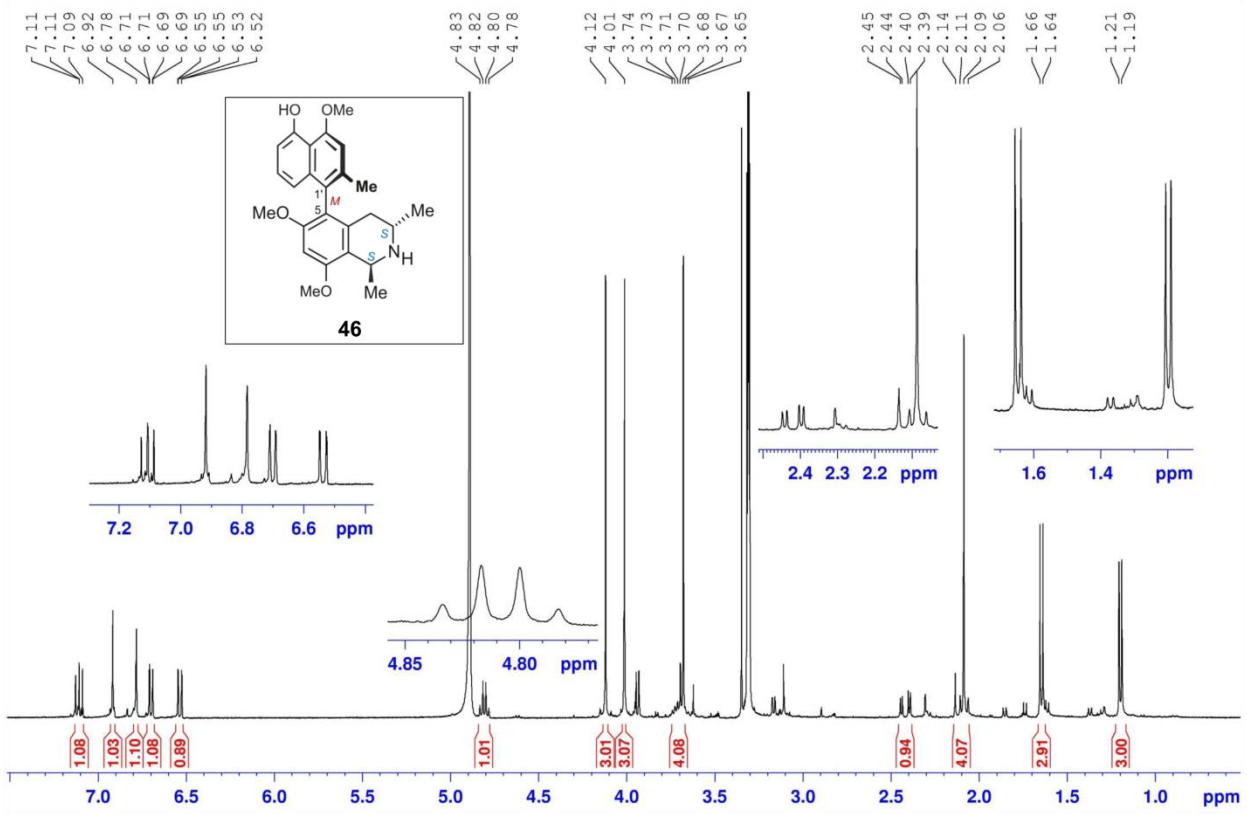

SI 33: *^{1}H NMR spectrum of ancistroyafungine D (**46**) in CD_3OD*

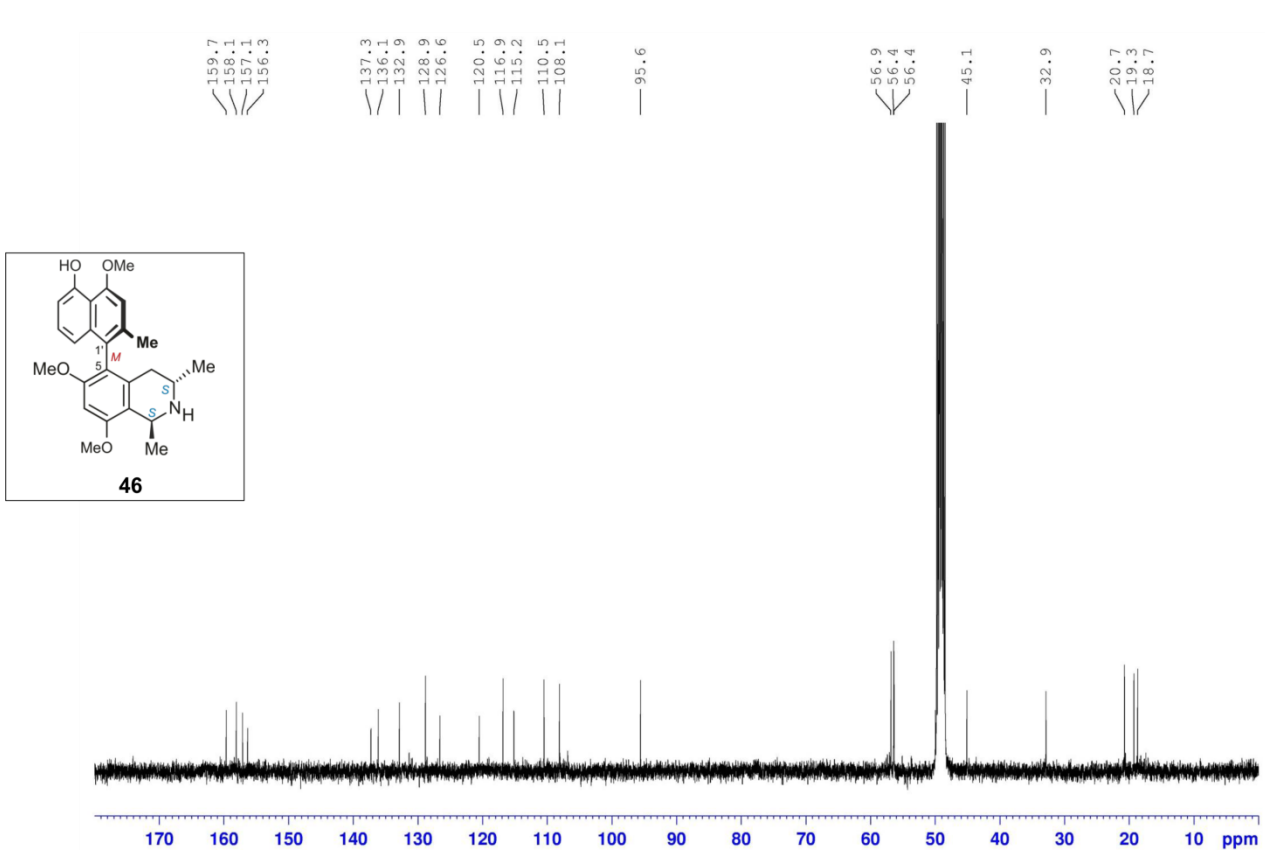

SI 34: *^{13}C NMR spectrum of ancistroyafungine D (**46**) in CD_3OD*

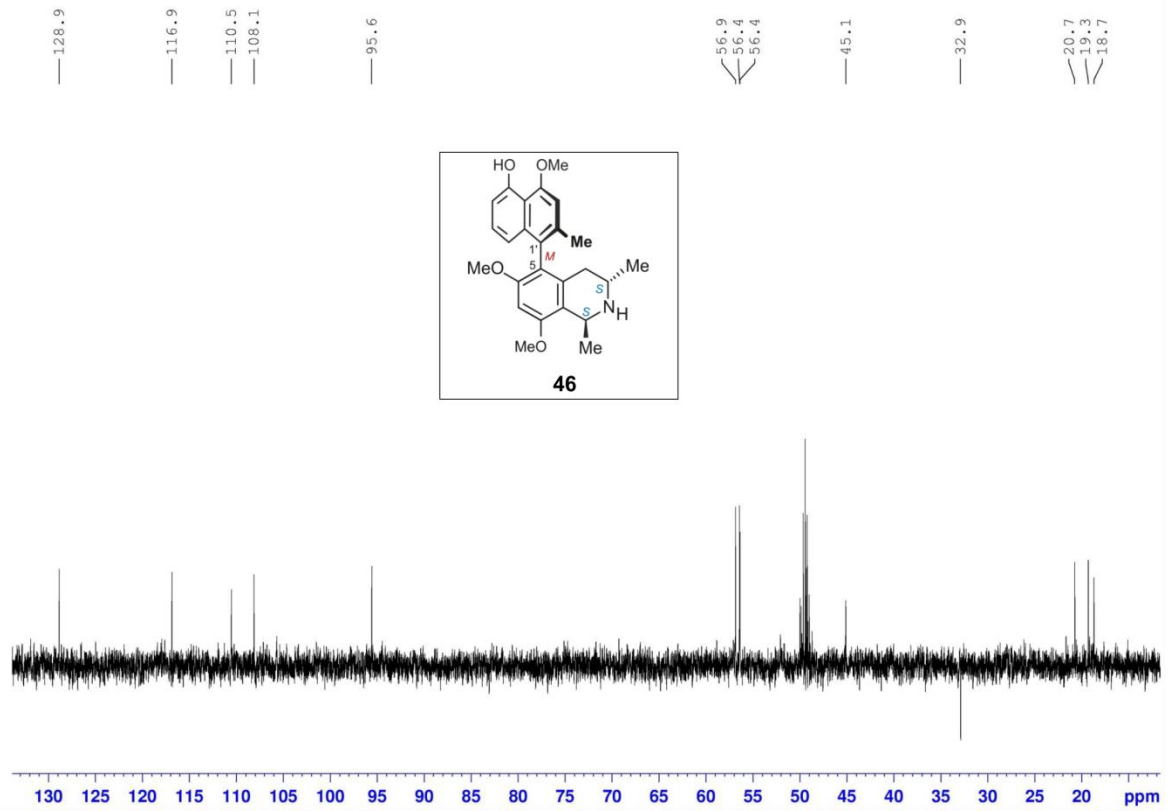

SI 35: *^{13}C DEPT-135 NMR spectrum of ancistroyafungine D (**46**) in CD_3OD*

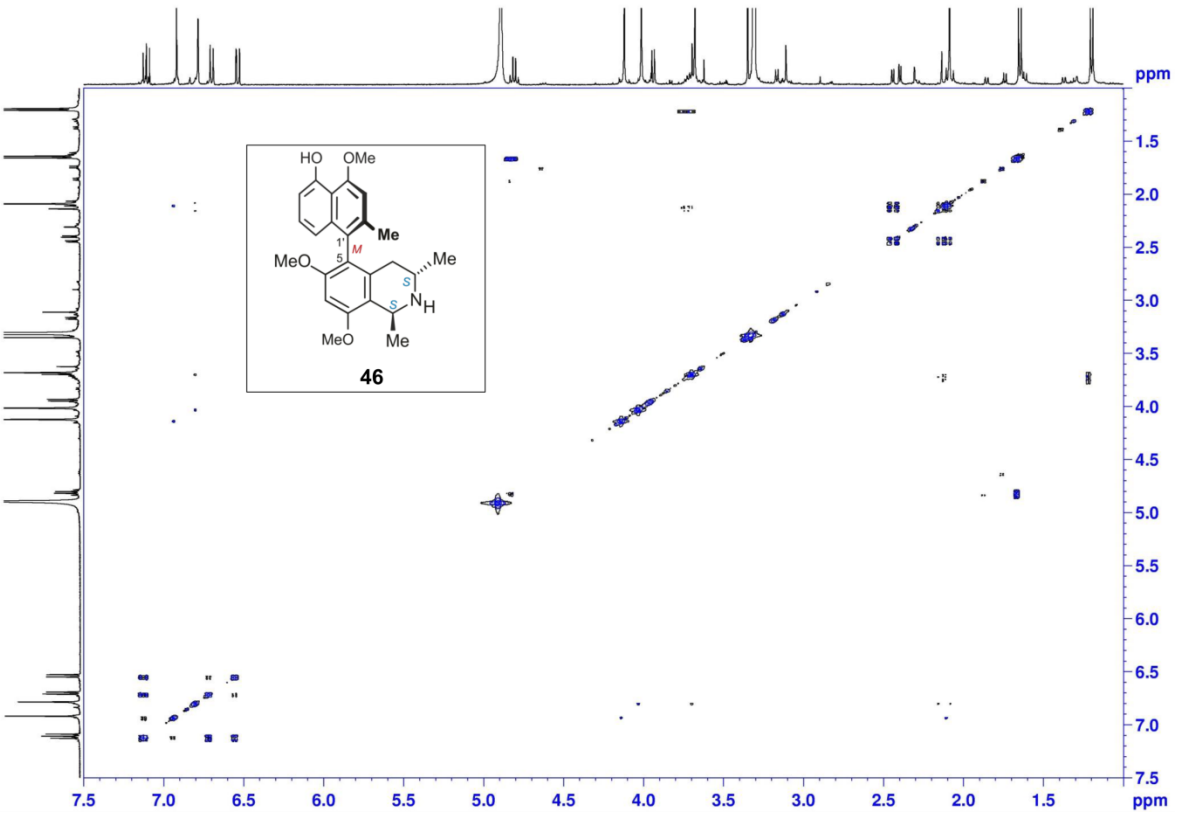

SI 36: *^{1}H-^{1}H COSY NMR spectrum of ancistroyafungine D (**46**) in CD_3OD*

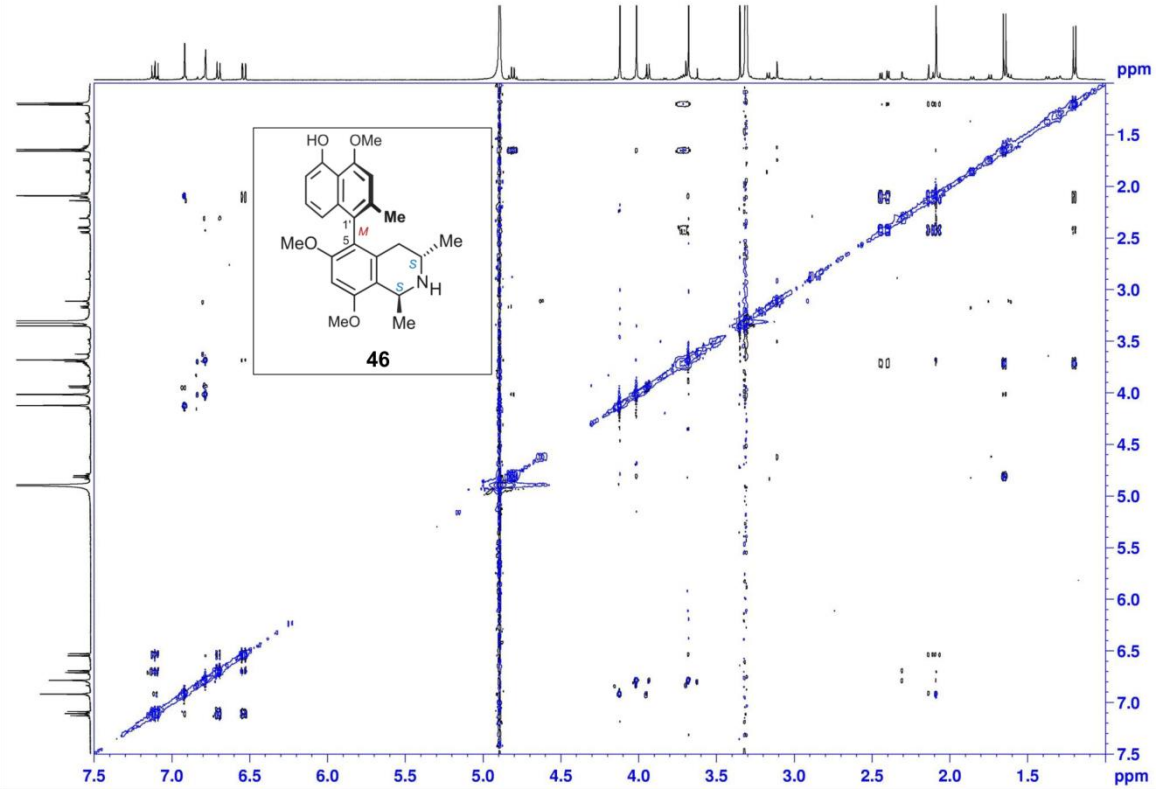

SI 37: *^{1}H-^{1}H NOESY NMR spectrum of ancistroyafungine D (**46**) in CD_3OD*

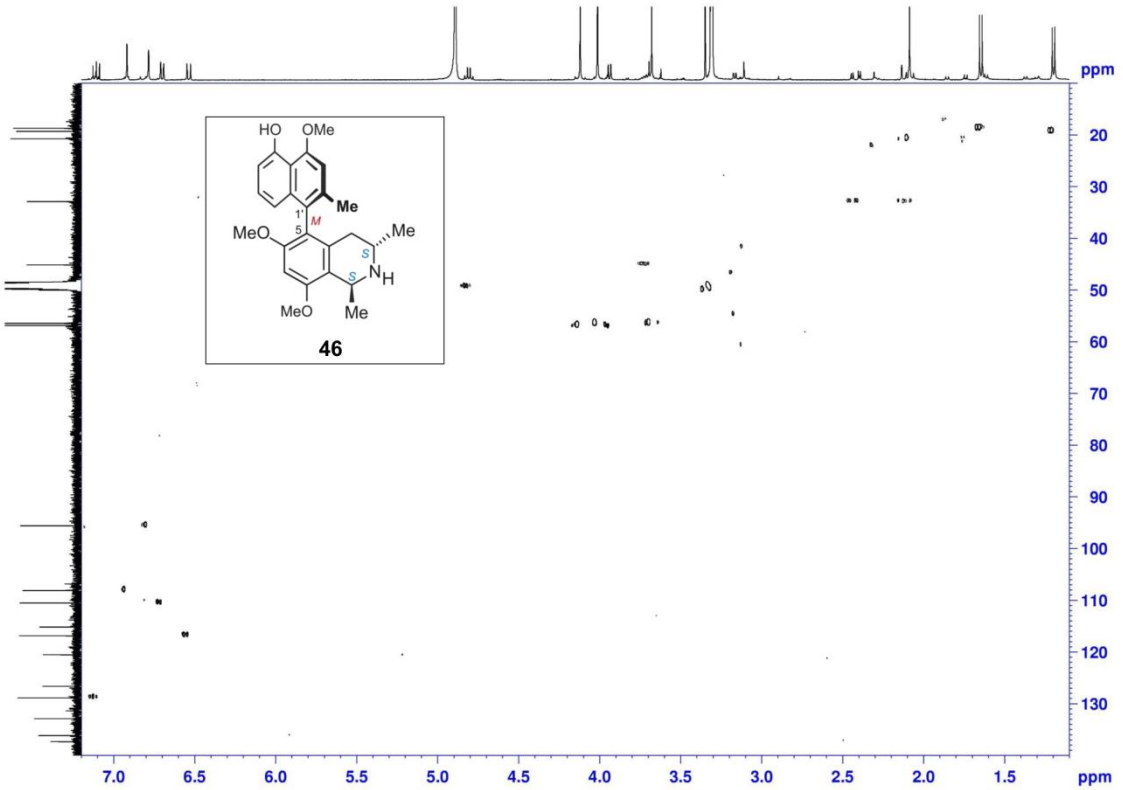

SI 38: *^{1}H-^{13}C HSQC NMR spectrum of ancistroyafungine D (**46**) in CD_3OD*

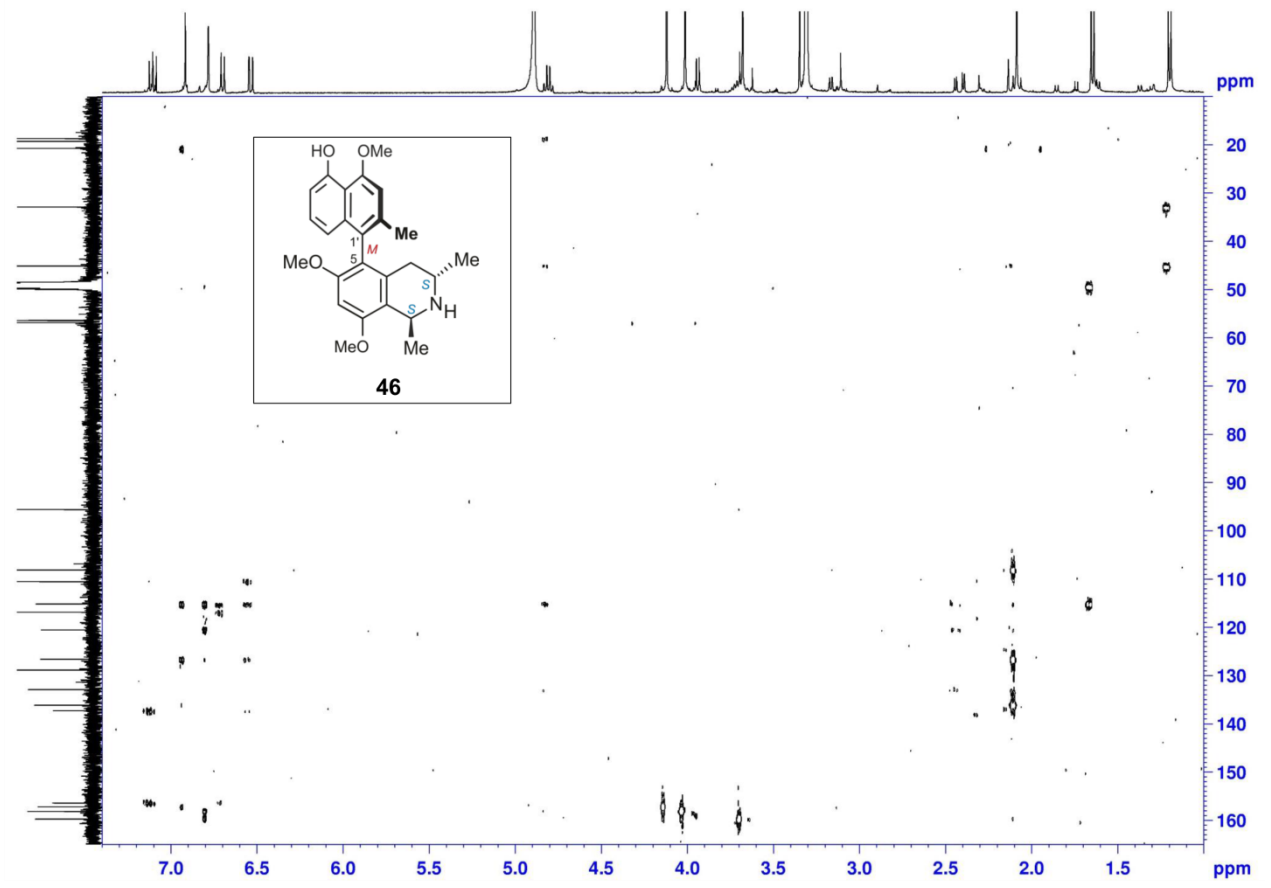

SI 39: *^{1}H-^{13}C HMBC NMR spectrum of ancistroyafungine D (**46**) in CD_3OD*

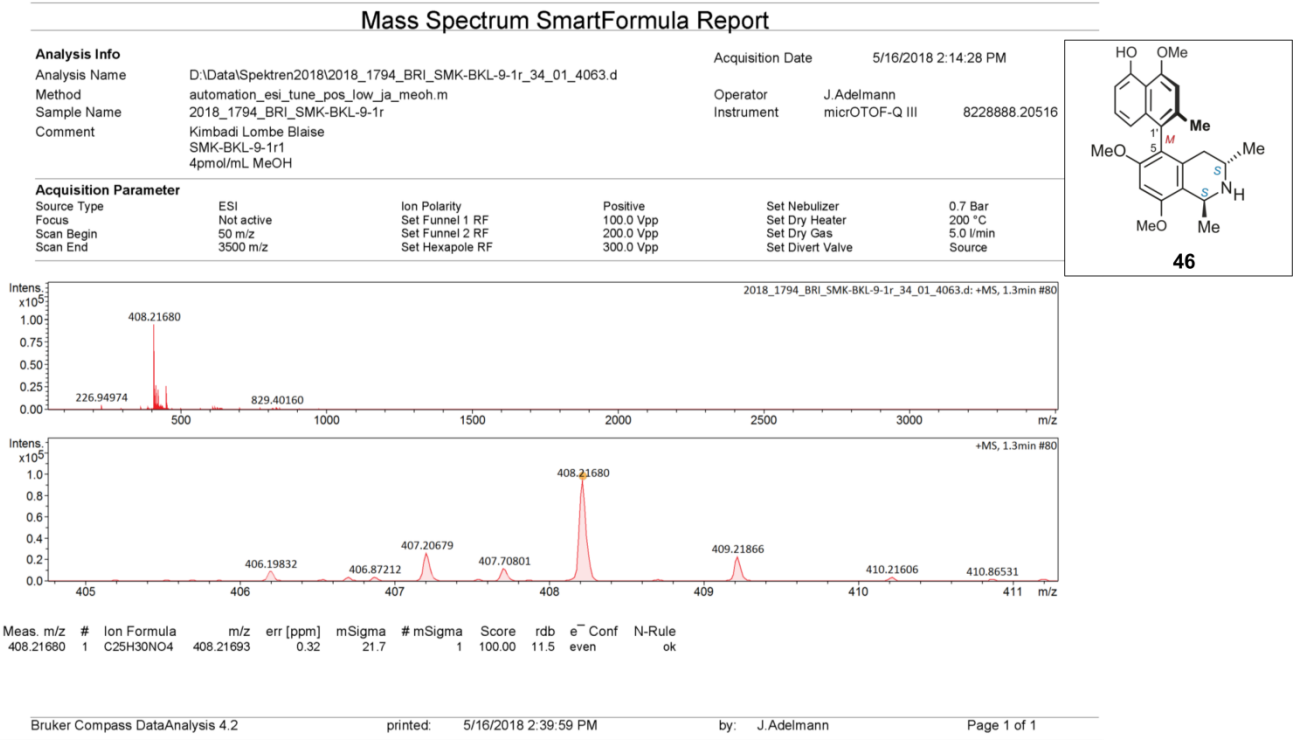

SI 40: *HRESIMS spectrum of ancistroyafungine D (**46**)*

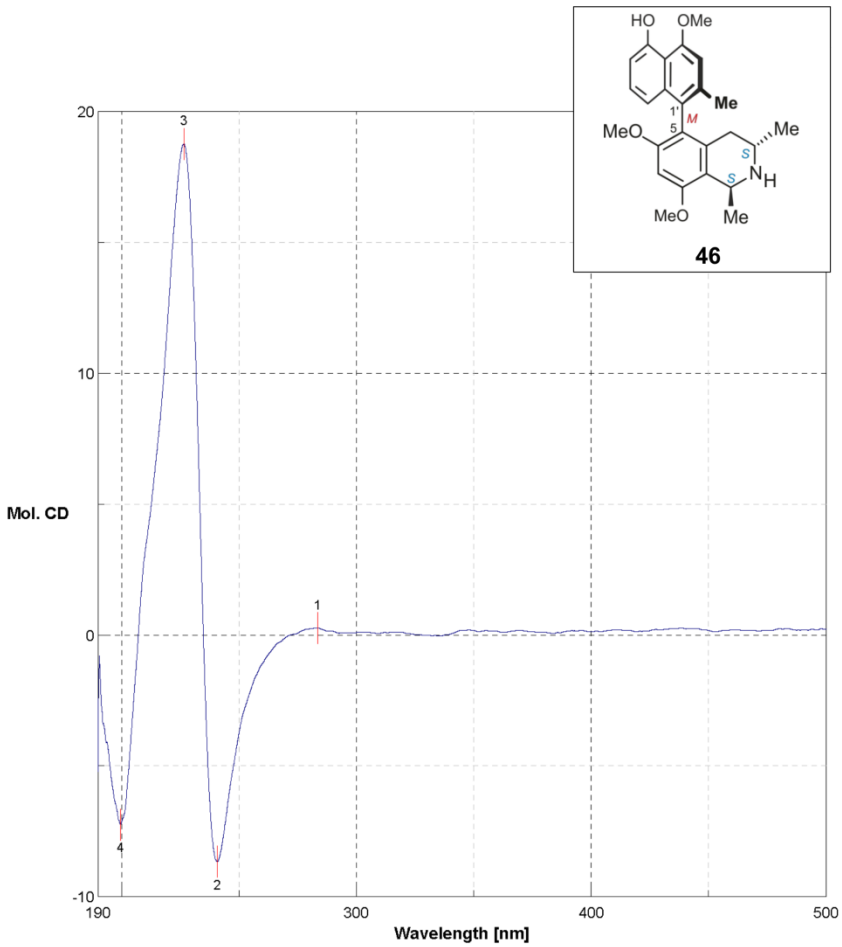

Date/Time	08.03.2018 15:48
Operator	Kimbadi
File Name	SMK-BKL-9-1-ok.jws
Sample Name	SMK-BKL-9-1
Comment	offline

No.	nm	Mol. CD	No.	nm	Mol. CD	No.	nm	Mol. CD
1	283.6	0.269555	2	240.8	-8.66036	3	226.6	18.7729
4	199.6	-7.2444						

SI 41: *ECD spectrum of ancistroyafungine D (**46**) in methanol*

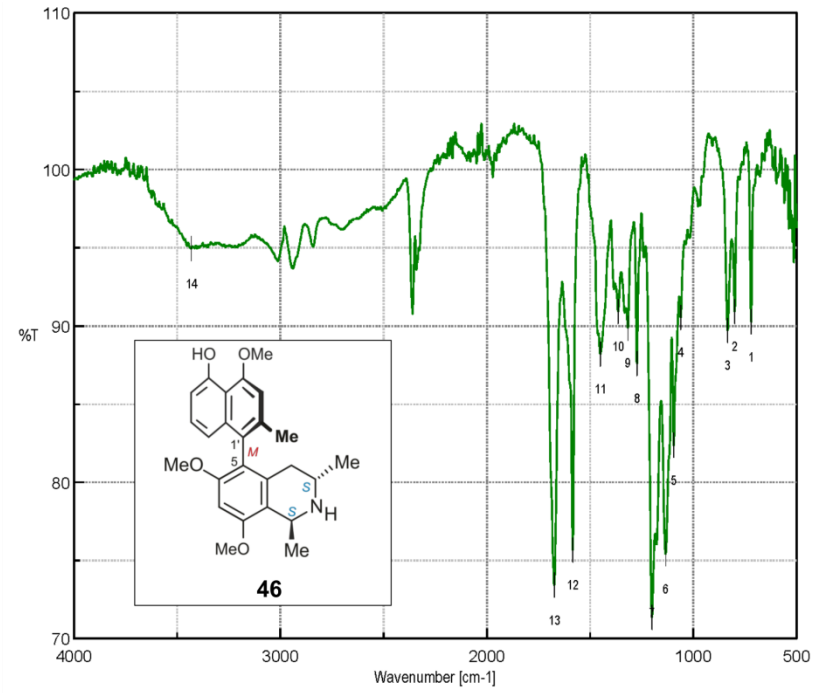

Results of Peak Find

No.	Position	Intensity	No.	Position	Intensity
1	720.282	90.2636	2	800.314	90.8948
3	834.062	89.6938	4	1061.62	90.5237
5	1095.37	82.3629	6	1133.94	75.4087
7	1200.47	71.3521	8	1273.75	87.5891
9	1316.18	89.8438	10	1364.39	90.8976
11	1450.21	88.1804	12	1584.24	75.6693
13	1672.95	73.4123	14	3431.71	94.9209

[Comments]

Sample name	9-1
Comment	drop MeOH
User	Kimbadi
Division	AK Bringmann
Company	Uni Würzburg

[Measurement Information]

Model Name	FT/IR-4600typeA
Serial Number	D063461786
Accessory	ATR PRO ONE
Accessory S/N	A070661809
Incident angle	45 deg
Measurement Date	13.06.2018 14:05
Light Source	Standard
Detector	TGS
Accumulation	16
Resolution	4 cm-1
Zero Filling	On
Apodization	Cosine
Gain	Auto (4)
Aperture	Auto (7.1 mm)
Scanning Speed	Auto (2 mm/sec)
Filter	Auto (30000 Hz)

SI 42: *IR spectrum of ancistroyafungine D (**46**)*

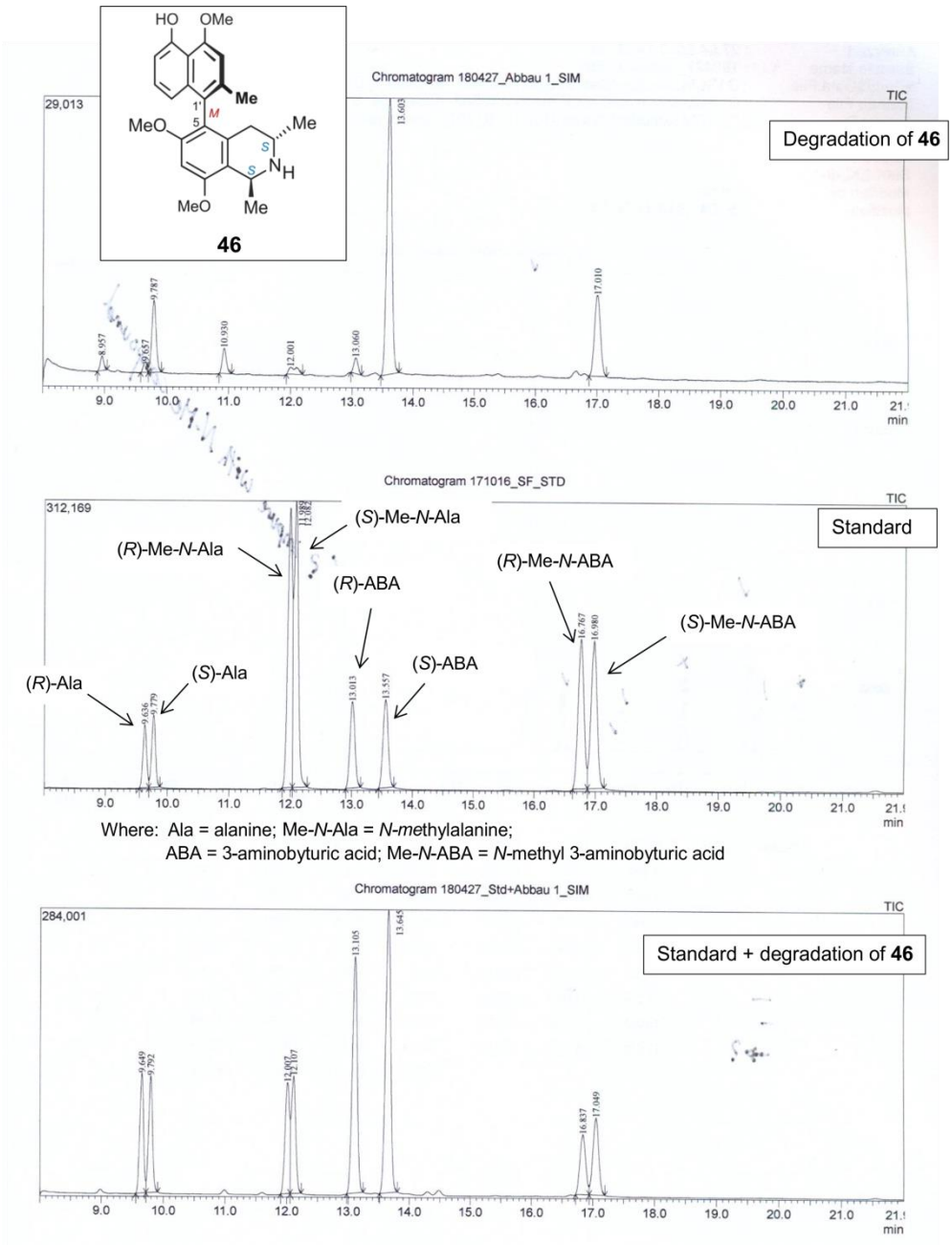

SI 43: *Oxidative degradation of ancistroyafungine D (**46**)*

SI 44: ^{1}H (400 MHz) and ^{13}C (100 MHz) NMR data of isolated 6-*O*-methylhamatine (**47**) in CD_3OD and the published data

Position	6-*O*-methylhamatine (**47**)		Data published for 6-*O*-methylhamatine in $CDCl_3$ (^{1}H, 400 MHz ^{13}C, 62.5 MHz) [1]	
	δ_H (*J* in Hz)	δ_C,	δ_H (*J* in Hz)	δ_C,
1	4.80, q (6.7)	49.1	4.82, q (6.8)	47.2
3	3.66, m	43.0	3.70, m	41.9
4ax	2.13, dd (16.9, 10.8)	37.8	2.11, dd (18.0, 11.3)	35.4
4eq	2.41, dd (16.9, 5.1)		2.39, dd (17.3, 4.8)	
5		121.8		120.7
6		150.9		151.9
7	6.74, s	97.0	6.78, s	96.2
8		157.3		156.5
9		116.5		115.6
10		136.0		135.0
1'		124.0		126.4
2'		134.9		136.3
3'	6.93, s	110.9	6.92, s	109.1
4'		156.0		157.3
5'		157.7		156.5
6'	6.70, d (8.0)	109.6	6.73, dd (8.0, 1.0)	110.9
7'	7.13, dd (8.0, 8.0)	127.8	7.12, dd (8.5, 8.0)	129.0
8'	6.58, d (8.0)	119.7	6.54, dd (8.5, 1.0)	117.3
9'		137.8		137.2
10'		115.0		115.3
1-Me	1.64, d (6.5)	20.4	1.65, d (6.9)	19.0
3-Me	1.21, d (6.5)	20.6	1.21, d (6.5)	19.9
2′-Me	2.06, s	20.9	2.08, s	20.8
6-OMe	3.65, s	55.7	3.67, s	56.7
8-OMe	3.99, s	55.7	4.02, s	56.9
4'-OMe	3.92, s	57.0	3.94, s	57.2
5'-OMe	4.09, s	57.0	4.09, s	56.8

SI 45: ^{1}H (400 MHz) and ^{13}C (100 MHz) NMR data of isolated 4'-*O*-demethylancistrocladine (**48**) in CD_3OD and the published data

Position	4'-*O*-demethylancistrocladine (**48**)		Data published for 4'-*O*-demethylancistrocladine in $CDCl_3$ (^{1}H, 400 MHz ^{13}C, 62.5 MHz) [1]	
	δ_H (*J* in Hz)	δ_C,	δ_H (*J* in Hz)	δ_C,
1	4.77, q (6.7)	50.1	4.30, q (6.5)	47.4
3	3.61, m	43.0	3.10, m	42.1
4ax	2.13, dd (16.9, 10.8)	37.8	1.75, dd (17.5, 11.0)	35.6
4eq	2.24, dd (16.9, 5.1)		1.95, dd (17.5, 4.5)	
5		121.8		120.3
6		150.9		152.4
7	6.60, s	98.0	6.45, s	96.0
8		157.3		156.8
9		116.5		115.8
10		137.0		135.2
1'		122.0		120.3
2'		140.9		139.7
3'	6.84, s	112.9	6.88, s	113.3
4'		156.0		154.7
5'		157.7		156.7
6'	6.86, d (8.0)	103.6	6.80, d (8.0)	103.9
7’	7.23, dd (8.0, 8.0)	127.8	7.20, dd (8.0, 8.0)	126.7
8'	6.89, d (8.0)	119.7	6.95, d (8.0)	118.9
9'		137.8		136.4
10'		115.0		114.2
1-Me	1.64, d (6.5)	22.4	1.42, d (6.5)	21.6
3-Me	1.21, d (6.5)	23.3	0.96, d (6.5)	22.5
2′-Me	2.06, s	20.9	2.08, s	20.8
8-OMe	3.92, s	55.7	3.82, s	55.3
5'-OMe	4.09, s	57.0	4.08, s	56.3

SI 46: ^{1}H (400 MHz) and ^{13}C (100 MHz) NMR data of isolated ancistroguineine A (**49**) in CD_3OD and the published data

Position	Ancistroguineine (**49**)		Data published for ancistroguineine A in $CDCl_3$ (^{1}H, 600 MHz ^{13}C, 150.9 MHz) [2]	
	δ_H (*J* in Hz)	δ_C,	δ_H (*J* in Hz)	δ_C,
1	4.76, q (6.5)	47.3	4.34, q (6.6)	47.2
3	3.65, m	45.2	3.09, m	42.0
4ax	2.26, dd (17.9, 7.6)	34.0	1.98, dd (17.6, 7.5)	36.0
4eq	2.42, dd (17.9, 5.1)		2.42, dd (17.6, 5.1)	
5		124.6		121.5
6		157.7		156.4
7	6.58, s	98.8	6.46, s	95.8
8		158.1		156.6
9		115.1		117.3
10		137.1		135.8
1'	6.81, s	119.0	6.83, s	117.9
2'		133.3		135.4
3'	6.75, s	107.8	6.67, s	106.8
4’		156.0		152.6
5'		157.4		155.0
6'	6.81, d (8.0)	110.5	6.88, d (7.9)	110.0
7'	7.03, d (8.0)	131.6	7.16, d (7.8)	131.7
8'		120.1		121.0
9'		137.8		136.8
10'		114.3		113.8
1-Me	1.65, d (6.8)	19.3	1.45, d (6.6)	21.5
3-Me	1.24, d (6.4)	18.8	0.97, d (6.2)	22.6
2′-Me	2.33, s	22.4	2.36, s	22.2
8-OMe	3.92, s	56.2	3.85, s	55.2
4'-OMe	4.09, s	56.9	4.08, s	56.2

SI 47: ^{1}H (400 MHz) and ^{13}C (100 MHz) NMR data of isolated ancistrobertsonine A (**50**) in *CD_3OD* and the published data

Position	Ancistrobertsonine A (**50**)		Data Published for ancistrobertsonine A in $CDCl_3$ (^{1}H, 600 MHz ^{13}C, 150.9 MHz) [3]	
	δ_H (*J* in Hz)	δ_C,	δ_H (*J* in Hz)	δ_C,
1	4.74, q (6.3)	60.4	3.90, q (6.3)	56.0
3	3.53, m	50.2	2.46, m	34.7
4ax	2.48, dd (18.6, 12.1)	29.9	2.42, dd (16.6, -)	29.5
4eq	2.22, dd (18.6, 5.1)		1.94, dd (16.6, 6.4)	
5		120.3		117.3
6		158.7		153.6
7	6.61, s	99.1	6.53, s	97.0
8		157.3		156.3
9		112.1		134.9
10		131.1		131.1
1′	6.74, s	118.5	6.72, s	108.9
2′		137.1		137.2
3′	6.80, s	110.2	6.67, s	116.3
4′		158.6		157.5
5′		155.6		157.9
6′	6.84, d (7.9)	107.0	6.84, d (8.0)	105.3
7′	7.15, d (7.9)	130.7	7.26, d (8.0)	131.0
8′		126.2		121.7
9′		138.1		135.9
10′		117.7		116.1
1-Me	1.71, d (6.8)	19.6	1.56, d (6.3)	20.3
3-Me	1.24, d (6.5)	16.9	1.10, d (5.4)	18.7
2′-Me	2.32, s	22.2	2.34, s	22.0
8-OMe	3.92, s	56.5	3.87, s	55.3
4′-OMe	3.93, s	57.7	3.94, s	56.2
5′-OMe	3.96, s	56.9	3.98, s	56.4
N-Me	2.76, s	34.8	2.54, s	41.1

SI 48: ^{1}H (400 MHz) and ^{13}C (100 MHz) NMR data of isolated ancistrobrevine B (**19**) in *CD_3OD* and the published data

Position	Ancistrobrevine B (**19**)		Data published for ancistrobrevine B in $CDCl_3$ (^{1}H, 250 MHz) [4]	
	δ_H (*J* in Hz)	δ_C,	δ_H (*J* in Hz)	δ_C,
1	4.78, q (6.6)	48.2	4.38, q (6.6)	na
3	3.20, m	45.4	3.20, m	na
4ax	2.10, dd (16.0, 9.8)	30.9	1.78, dd (17.0, 11.0)	na
4eq	2.65, dd (16.0, 4.2)		2.28, dd (17.0, 4.0)	
5		121.2		na
6		158.3		na
7	6.59, s	95.1	6.50, s	na
8		155.8		na
9		115.3		na
10		133.0		na
1′	6.78, s	118.2	6.72, s	na
2′		138.4		na
3′	6.66, s	110.5	6.68, s	na
4′		157.6		na
5′		157.1		na
6′	6.95, d (7.8)	105.3	6.85, d (8.0)	na
7′	7.17, d (7.8)	129.4	7.25, d (8.0)	na
8′		126.0		na
9′		136.7		na
10′		115.8		na
1-Me	1.62, d (6.8)	18.7	1.45, d (6.6)	na
3-Me	1.19, d (6.5)	18.7	0.95, d (6.2)	na
2′-Me	2.30, s	21.9	2.35, s	na
8-OMe	3.93, s	55.5	3.84, s	na
4′-OMe	3.93, s	56.7	3.97, s	na
5′-OMe	3.96, s	56.5	4.00, s	na

na: not available

SI 49: ^{1}H (400 MHz) and ^{13}C (100 MHz) NMR data of isolated ancistrotectoriline A (**51**) in CD_3OD and the published data

Position	Ancistrotectoriline A (**51**)		Data published for ancistrotectoriline A in $CDCl_3$ (^{1}H, 400 MHz ^{13}C, 100 MHz) [5].	
	δ_H (*J* in Hz)	δ_C,	δ_H (*J* in Hz)	δ_C,
1	4.82, q (6.2)	47.5	4.12, q (6.2)	47.5
3	3.30, m	44.5	3.30, m	44.5
4ax	210, dd (17.8, 12.0)	31.8	2.05, dd (17.8, 12.0)	31.8
4eq	2.66, dd (17.8, 4.2)		2.36, dd (17.8, 4.2)	
5		121.3		121.3
6		158.1		158.1
7	6.56, s	94.2	6.46, s	94.2
8		156.2		156.2
9		114.6		114.6
10		132.8		132.8
1′	6.76, s	117.8	6.64, s	117.8
2′		137.8		137.8
3′	6.76, s	109.2	6.68, s	109.2
4′		157.1		157.1
5′		156.8		156.8
6′	6.92, d (7.5)	105.0	6.82, d (7.5)	105.0
7′	7.09, d (7.5)	128.0	7.09, d (7.5)	128.0
8′		125.6		125.6
9′		136.2		136.2
10′		116.0		116.0
1-Me	1.65, d (6.6)	18.5	1.57, d (6.6)	18.5
3-Me	1.17, d (6.2)	18.5	1.14, d (6.2)	18.5
2′-Me	2.27, s	22.2	2.31, s	22.2
6-OMe	3.66, s	56.3	3.60, s	56.3
8-OMe	3.92, s	55.4	3.90, s	55.4
4′-OMe	3.94, s	56.6	3.94, s	56.6
5′-OMe	4.01, s	56.4	3.97, s	56.4

SI 50: ^{1}H (400 MHz) and ^{13}C (100 MHz) NMR data of isolated 6, 5′-*O*,*O*-didemethylancistroealaine A (**52**) in CD_3OD and published data

Position	6, 5′-*O*,*O*-didemethylancistroealaine A (**52**)		Data published for 6, 5′-*O*,*O*-didemethylancistroealaine A in CD_3OD (^{1}H, 400 MHz ^{13}C, 100 MHz) [6]	
	δ_H (*J* in Hz)	δ_C, type	δ_H (*J* in Hz)	δ_C, type
1		175.6		175.7
3	3.68, m	49.3	3.70, m	49.5
4ax	2.46, dd (17.6, 11.8)	33.8	2.48, dd (16.9, 11.2)	33.7
4eq	2.21, dd (17.3, 5.8)		2.41, dd (16.9, 5.9)	
5		120.3		122.6
6		168.1		168.1
7	6.66, s	99.3	6.67, s	99.4
8		165.9		165.9
9		109.1		108.7
10		142.9		142.8
1′	6.72, s	118.7	6.72, s	118.8
2′		138.1		138.2
3′	6.83, s	107.8	6.83, s	107.9
4′		158.3		158.2
5′		156.3		156.4
6′	6.80, d (7.7)	110.4	6.80, d (7.8)	110.4
7′	7.16, d (7.7)	131.5	7.05, d (7.8)	131.7
8′		123.1		123.1
9′		136.7		136.7
10′		114.9		115.0
1-Me	2.79, s	24.8	2.79, s	24.8
3-Me	1.26, d (6.5)	18.0	1.26, d (6.7)	22.3
2′-Me	2.34, s	22.5	2.34, s	22.2
8-OMe	4.04, s	56.2	4.04, s	56.8
4′-OMe	4.10, s	57.1	4.10, s	57.0

SI 51: ^{1}H (400 MHz) and ^{13}C (100 MHz) NMR data of isolated 6-*O*-demethylancistroealaine A (**53**) in CD_3OD and the published data

Position	6-*O*- demethylancistroealaine A (**53**)		Data published for 6-*O*-demethylancistroealaine A in CD_3OD [6]	
	δ_H (*J* in Hz)	δ_C, type	δ_H (*J* in Hz)	δ_C, type
1		175.8		175.8
3	3.69, m	49.5	3.70, m	49.5
4ax	2.49, dd (16.6, 10.9)	33.6	2.48, dd (16.9, 11.2)	33.6
4eq	2.39, dd (16.6, 6.0)		2.41, dd (16.9, 5.9)	
5		122.6		122.7
6		167.8		167.8
7	6.67, s	99.3	6.68, s	99.4
8		165.9		165.9
9		108.8		108.8
10		142.8		142.7
1′	6.71, s	118.0	6.71, s	118.1
2′		138.5		138.5
3′	6.81, s	110.2	6.82, s	110.3
4′		159.0		159.0
5′		159.0		159.0
6′	6.94, d (8.0)	106.5	6.94, d (8.1)	106.6
7′	7.09, d (8.0)	130.8	7.11, d (8.0)	130.8
8′		125.0		125.0
9′		137.3		137.3
10′		117.6		117.6
1-Me	2.79, s	24.8	2.80, s	24.8
3-Me	1.25, d (7.0)	18.2	1.25, d (6.7)	18.1
2′-Me	2.33, s	22.2	2.34, s	22.2
8-OMe	4.04, s	56.8	4.05, s	56.9
4′-OMe	3.96, s	57.1	3.96, s	57.1
5′-OMe	3.94, s	56.8	3.96, s	56.9

SI 52: ^{1}H (400 MHz) and ^{13}C (100 MHz) NMR data of isolated 7-*epi*-ancistrobrevine D (**54**) in CD_3OD and the published data

Position	7-*epi*-ancistrobrevine D (**54**)		Data published for 7-*epi*-ancistrobrevine D in $CDCl_3$ (^{1}H, 500 MHz ^{13}C, 75.5 MHz) [7]	
	δ_H (*J* in Hz)	δ_C,	δ_H (*J* in Hz)	δ_C,
1	4.63, q	58.3	3.74, q	57.3
3	3.50, m	55.7	2.65, m	55.0
4ax	3.11, dd (15.0, 7.8)	40.0	2.85, dd (15.2, 10.2)	39.4
4eq	3.07, dd (15.0, 3.2)		2.36, dd (15.2, 2.8)	
5	6.56, s	101.8	6.34, s	102.3
6		154.9		155.8
7		114.0		112.1
8		151.2		150.4
9		118.8		119.5
10		138.1		136.8
1′		117.9		119.8
2′		117.9		119.8
3′	6.95, s	109.7	6.81, s	108.9
4′		157.6		157.2
5′		157.2		157.4
6′	6.79, dd (7.3, 0.9)	105.3	6.75, dd (7.5, 0.9)	105.8
7′	7.15, dd (8.0, 7.3)	128.4	7.21, dd (8.4, 7.5)	127.9
8′	6.86, dd (8.0, 0.9)	119.0	6.92, dd (8.4, 0.9)	118.0
9′		136.7		136.9
10′		115.9		116.5
1-Me	1.77, d (6.6)	22.8	1.47, d (6.3)	22.8
3-Me	1.60, d (6.4)	21.7	1.30, d (6.3)	21.1
2′-Me	2.13, s	20.4	2.19, s	20.7
6-OMe	3.60, s	55.5	3.60, s	55.7
4′-OMe	3.97, s	56.0	3.97, s	56.2
5′-OMe	3.92, s	56.2	3.93, s	56.4
N-Me	3.11, s	40.9	2.52, s	41.1

SI 53: ^{1}H (400 MHz) and ^{13}C (100 MHz) NMR data of isolated ancistrocladinium A (**55**) in CD_3OD and the published data

Position	Ancistrocladinium A (**55**)		Data published for ancistrocladinium A in CD_3OD (^{1}H, 400 MHz ^{13}C, 100 MHz) [8]	
	δ_H (J in Hz)	δ_C,	δ_H (J in Hz)	δ_C,
1		179.6		179.6
3	4.25, m	59.2	4.25, m	61.3
4ax	3.84, dd (17.5, 6.5)	34.5	3.83, dd (17.4, 6.2)	36.7
4eq	3.13, dd (17.5, 2.7)		3.13, dd (17.4, 2.5)	
5	6.77, s	98.6	6.77, s	111.1
6		171.5		172.4
7	6.74, s	100.3	6.74, s	100.7
8		168.4		168.1
9		110.8		113.8
10		142.7		143.9
1′	7.10, s	112.8	7.03, s	114.8
2′		142.9		143.7
3′	6.98, s	109.0	6.98, s	112.9
4′		160.5		161.5
5′		162.0		162.7
6′	6.97, d (8.5)	104.4	6.97, d (8.5)	106.6
7′	7.47, d (8.5)	126.8	7.46, d (8.5)	128.9
8′		118.6		119.7
9′		13.1.9		133.8
10′		129.7		131.6
1-Me	2.52, s	24.6	2.52, s	26.5
3-Me	1.31, d (6.9)	15.2	1.30, d (7.1)	17.2
2′-Me	2.51, s	22.0	2.50, s	23.9
6-OMe	4.03, s	56.7	4.03, s	58.5
8-OMe	4.04, s	56.8	4.04, s	58.9
4′-OMe	3.97, s	59.2	3.97, s	58.9
5′-OMe	4.01, s	56.7	4.01, s	58.6

SI 54: ^{1}H (400 MHz) and ^{13}C (100 MHz) NMR data of isolated ancistrocladinium B (**56**) in CD_3OD and the published data

Position	Ancistrocladinium B (**56**)		Data published for ancistrocladinium A in DMSO-d_6 (^{1}H, 600 MHz ^{13}C, 150 MHz) [8]	
	δ_H (J in Hz)	δ_C,	δ_H (J in Hz)	δ_C,
1		176.9		174.5
3	4.48, m	61.2	4.49, m	59.0
4ax	3.66, dd (16.9, 6.4)	35.3	3.17, dd (16.9, 6.1)	33.3
4eq	3.06, dd (16.9, 2.1)		3.04, dd (16.9, 1.9)	
5	6.72, s	109.0	6.81, s	107.7
6		170.4		167.8
7	6.72, s	99.0	6.76, s	97.9
8		166.0		163.6
9		111.0		109.2
10		142.3		140.6
1′	7.35, s	121.8	7.36, s	120.0
2′		140.9		138.8
3′	6.99, s	109.5	6.99, s	108.2
4′		158.2		156.3
5′		149.8		147.7
6′		121.9		121.3
7′	7.47, d (9.0)	125.2	7.62, d (8.9)	124.5
8′	7.43, d (3.0)	121.9	7.51, d (8.9)	119.9
9′		138.7		136.5
10′		114.1		112.3
1-Me	2.66, s	23.8	2.56, s	22.9
3-Me	1.22, d (6.9)	14.8	1.11, d (6.9)	14.0
2′-Me	2.52, s	22.2	2.47, s	21.6
6-OMe	4.01, s	57.2	3.97, s	56.4
8-OMe	4.04, s	57.2	4.00, s	56.7
4′-OMe	4.12, s	57.2	4.04, s	56.3

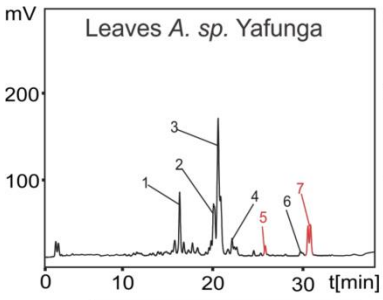

Peak	*m/z* = $[M+1]^+$
1	491.0
2	408.5
3	436.4
4	445.2
5	420.4
6	570.7
7	406.3

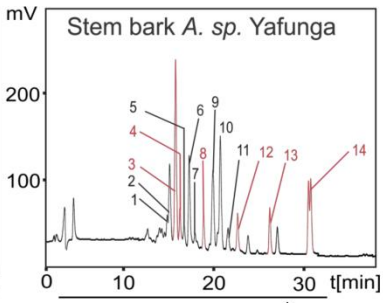

Peak	*m/z* = $[M+1]^+$
1	408.4
2	408.5
3	422.3
4	422.4
5	394.4
6	406.4
7	422.3
8	392.3
9	422.4
10	436.4
11	408.4
12	422.4
13	420.4
14	406.3

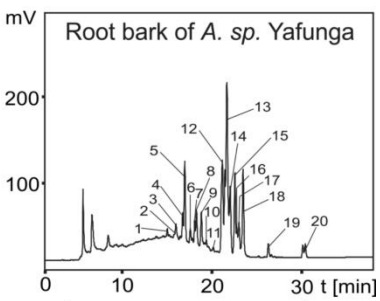

Peak	*m/z* = $[M+1]^+$
1	394.6
2	408.6
3	380.9
4	408.5
5	408.6
6	422.5
7	394.6
8	394.6
9	394.7
10	422.5
11	392.7
12	422.6
13	436.5
14	420.6
15	408.6
16	422.5
17	422.5
18	406.6
19	420.5
20	406.5

SI 55: *LC-MS chromatograms and tables of masses of leaves, stems and root barks of Ancistrocladus species investigated*

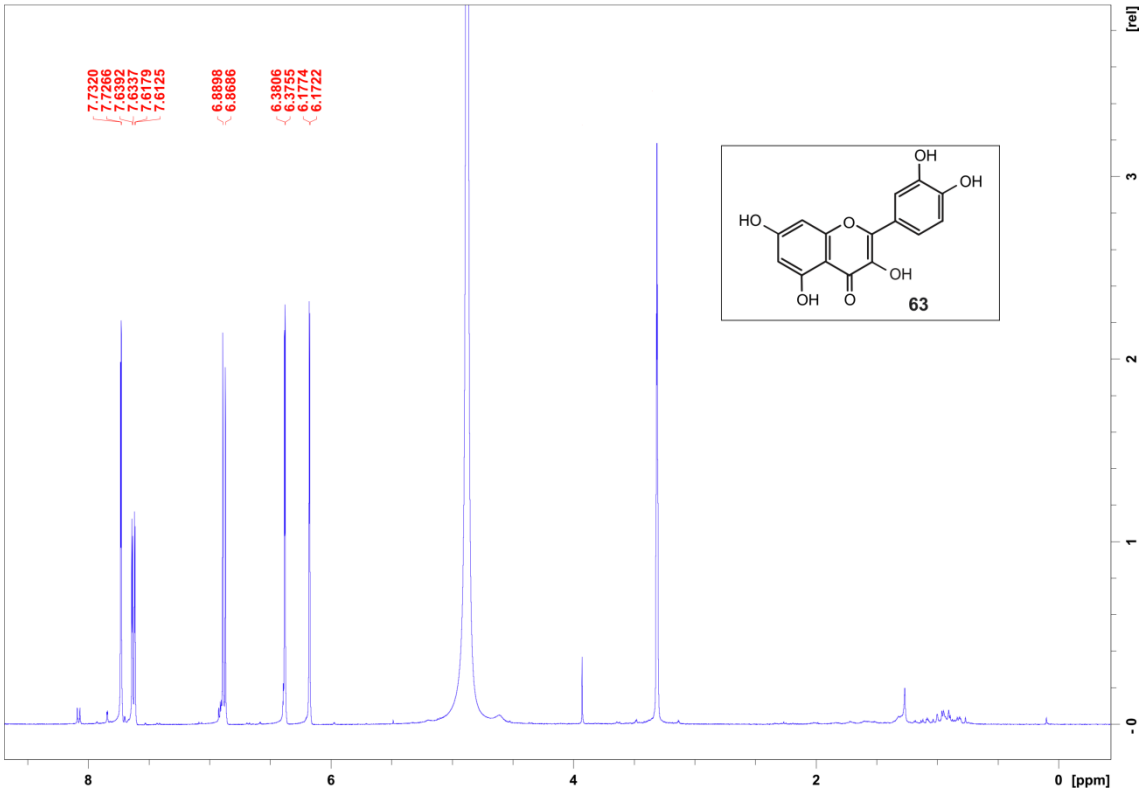

SI 56: *^{1}H NMR spectrum of quercetin (**63**) in CD_3OD*

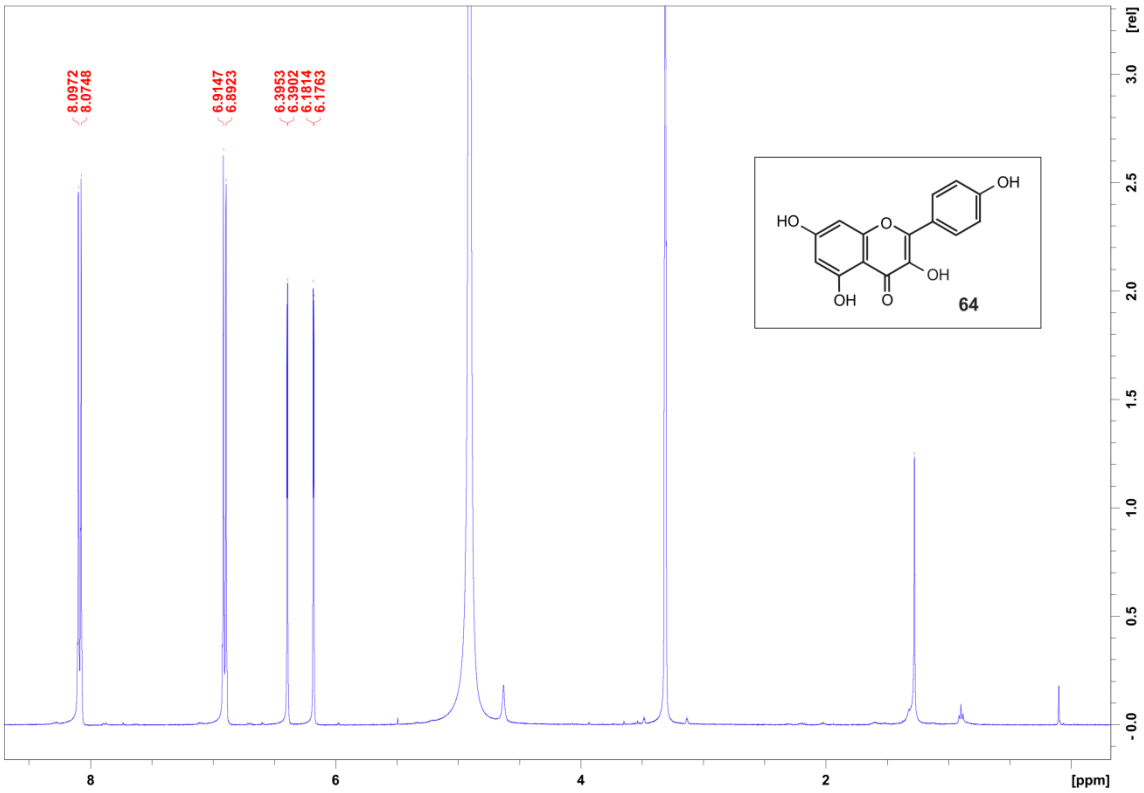

SI 57: *^{1}H NMR spectrum of kaempferol (**64**) in CD_3OD*

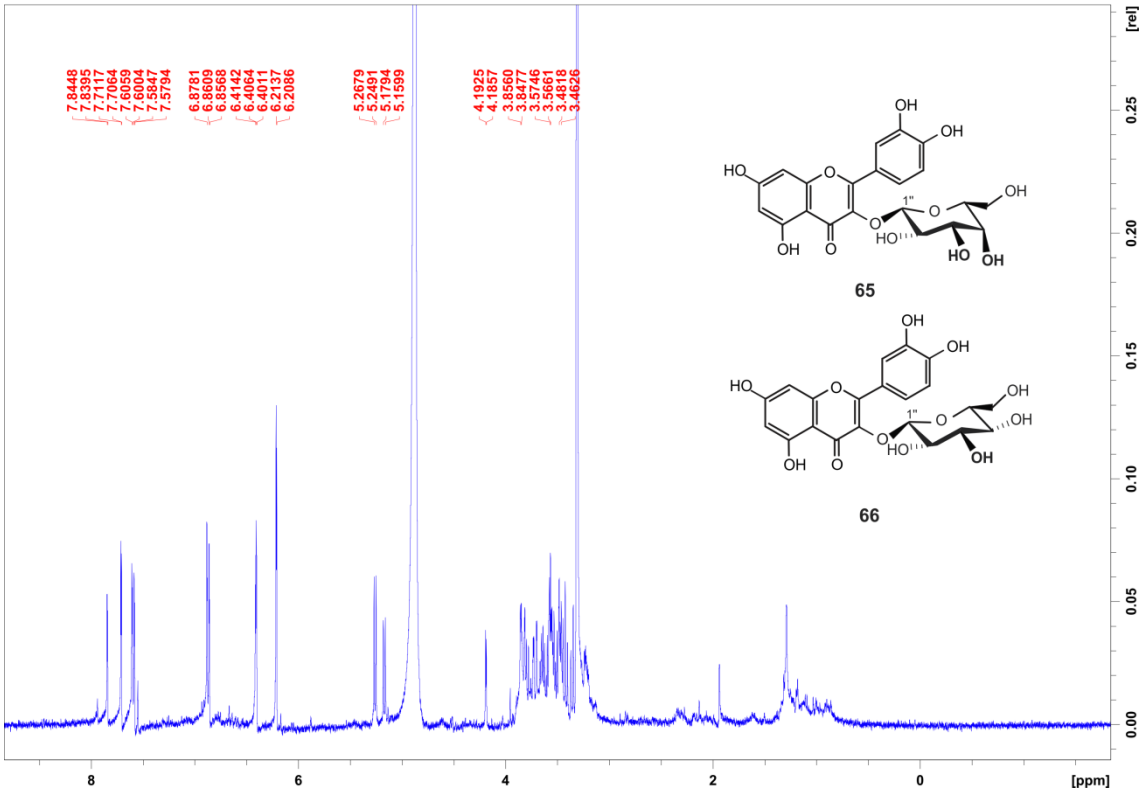

SI 58: *^{1}H NMR spectra of hyperoside (**64**) and isoquercetin (**65**) in CD_3OD*

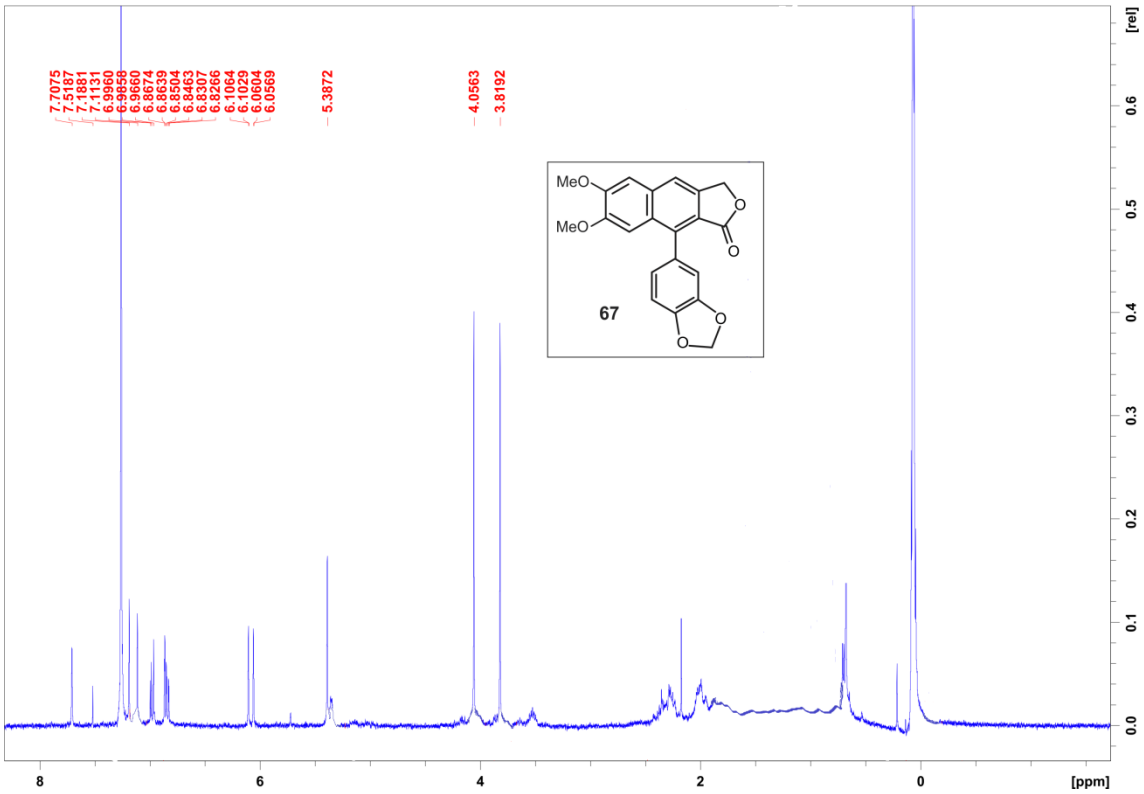

SI 59: *^{1}H NMR spectrum of justicidin B (**67**) in CD_3Cl*

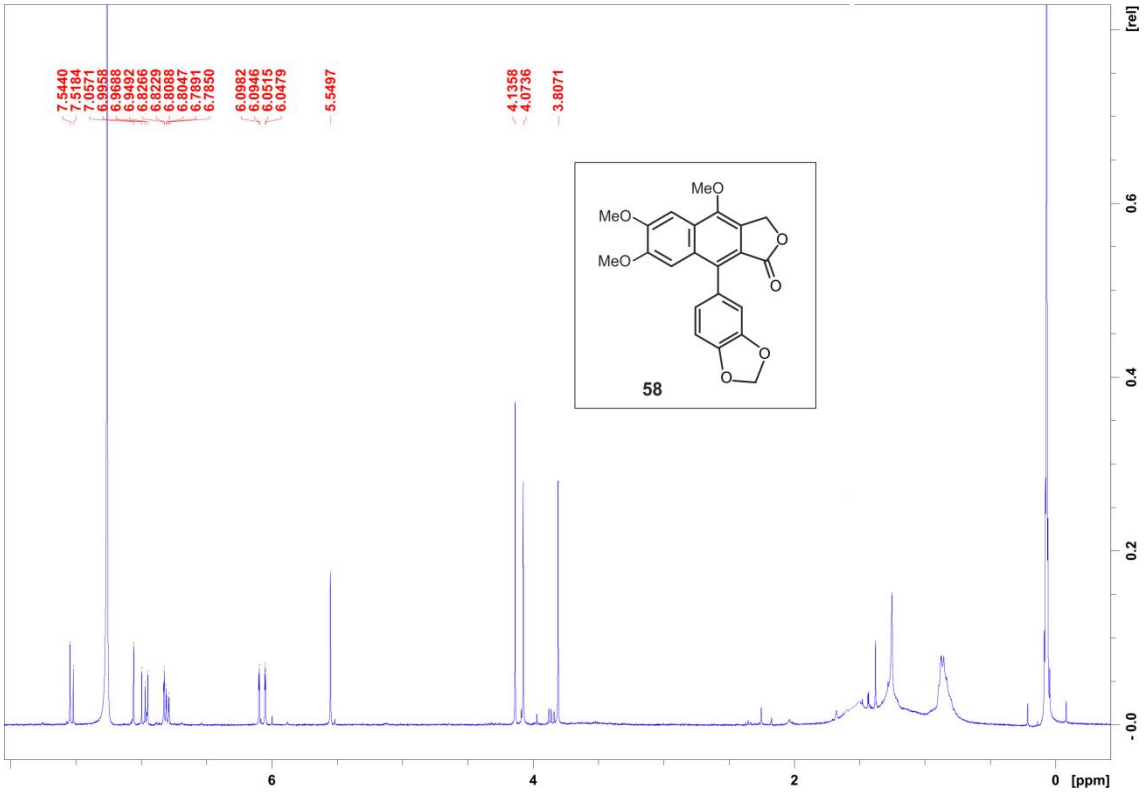

SI 60: *^{1}H NMR spectrum of justicidin A (**58**) in CD_3Cl*

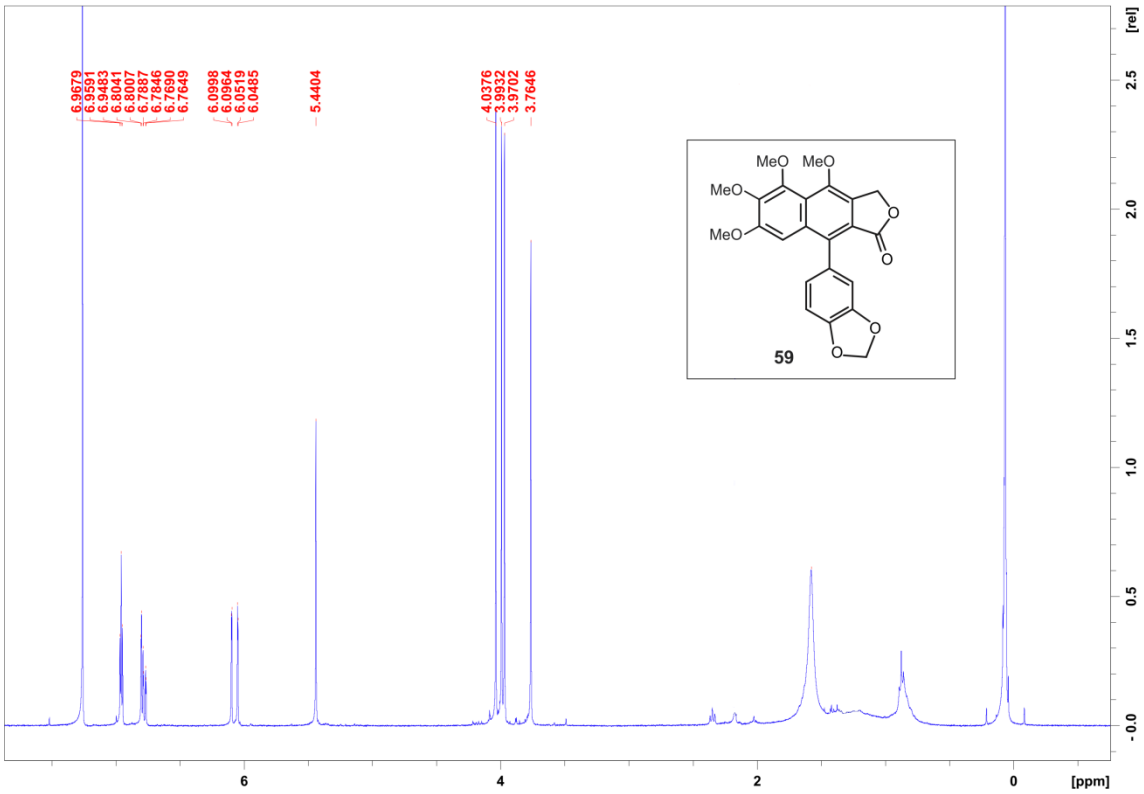

SI 61: *^{1}H NMR spectrum of 6-methoxyjusticidin A (**59**) in CD_3Cl*

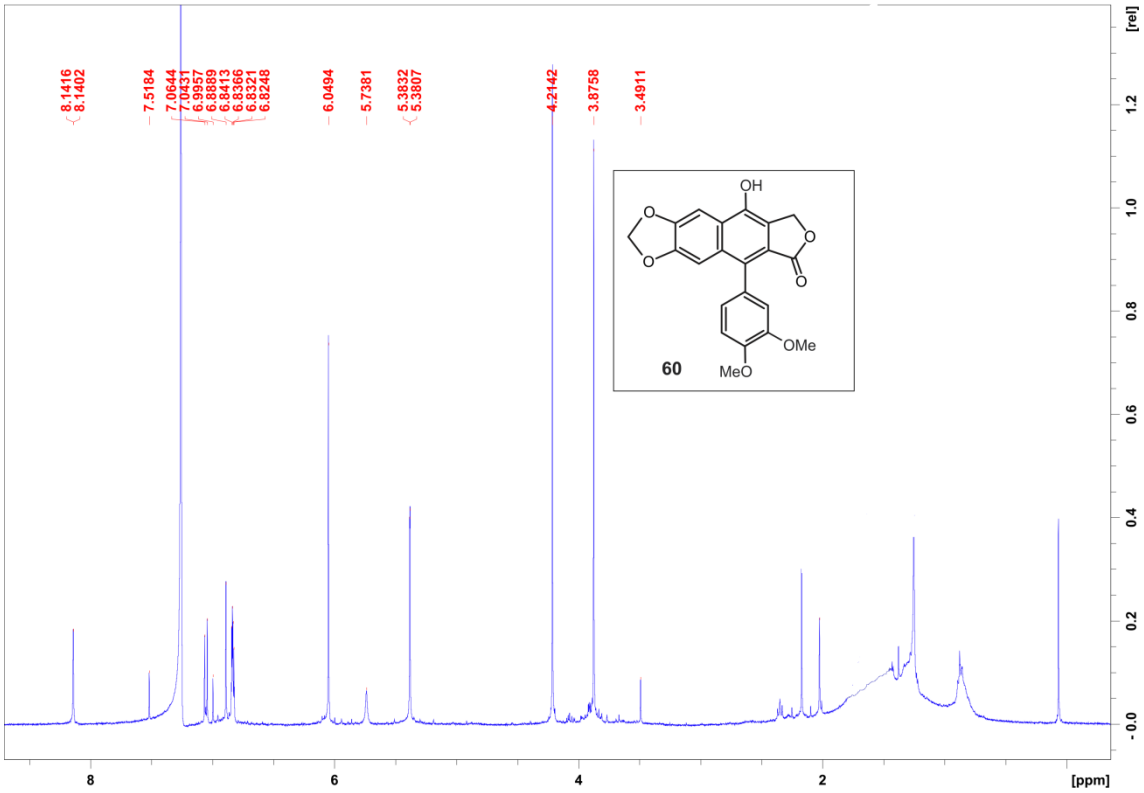

SI 62: *^{1}H NMR spectrum of chinensinaphthol (**60**) in CD_3Cl*

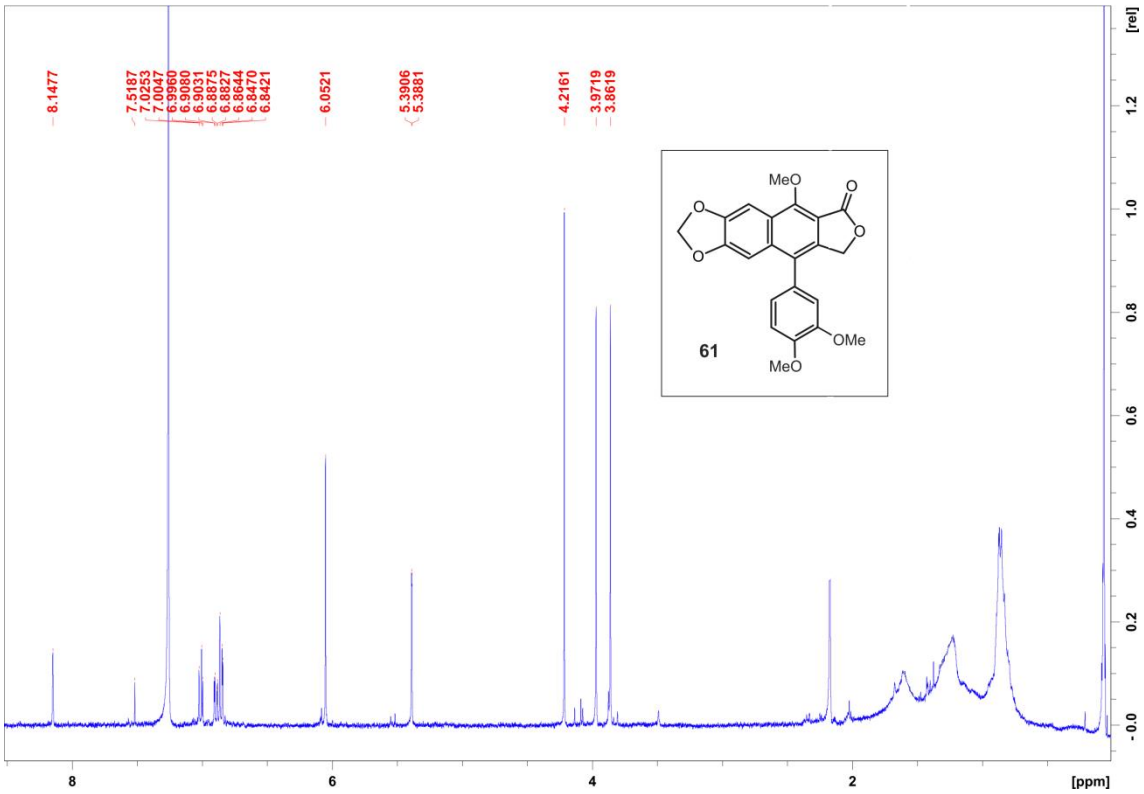

SI 63: *^{1}H NMR spectrum of retrochinensinaphthol methyl ether (**61**) in CD_3Cl*

References

1. Montagnac A, Hadi AAH, Remy F, Païs M: **Isoquinoline Alkaloids from *Ancistrocladus tectorius***. *Phytochemistry* 1995, **39**(3):701-704.
2. Bringmann G, Günther C, Busemann S, Schäffer M, Olowokudejo DJ, Alo BI: **Ancistroguineines A and B as well as Ancistrotectorine Naphthylisoquinoline Alkaloids from *Ancistrocladus guineënsis***. *Phytochemistry* 1998, **47**(1):37-43.
3. Bringmann G, Teltschik F, Schäffer M, Haller R, Bär S, Robertson SA, Isahakia AM: **Ancistrobertsonine A and Related Naphthylisoquinoline Alkaloids from *Ancistrocladus robertsoniorum***. *Phytochemistry* 1998, **47**(1):31-35.
4. Bringmann G, Zagst R, Reuscher H, Aké Assi L: **Ancistrobrevine B, the First Naphthylisoquinoline Alkaloid with A 5,8'-Coupling Site, and Related Compounds from *Ancistrocladus abbreviatus***. *Phytochemistry* 1992, **31**(11):4011-4014.
5. Tang C-P, Yang Y-P, Zhong Y, Zhong Q-X, Wu H-M, Ye Y: **Four New Naphthylisoquinoline Alkaloids from *Ancistrocladus tectorius***. *Journal of Natural Products* 2000, **63**(10):1384-1387.
6. Bringmann G, Spuziak J, Faber JH, Gulder T, Kajahn I, Dreyer M, Heubl G, Brun R, Mudogo V: **Six Naphthylisoquinoline Alkaloids and a Related Benzopyranone from a Congolese *Ancistrocladus* Species Related to *Ancistrocladus congolensis***. *Phytochemistry* 2008, **69**(4):1065-1075.
7. Nguyen HA, Porzel A, Ripperger H, Bringmann G, Schäffer M, God R, Van Sung T, Adam G: **Naphthylisoquinoline Alkaloids from *Ancistrocladus cochinchinensis***. *Phytochemistry* 1997, **45**(6):1287-1291.
8. Bringmann G, Kajahn I, Reichert M, Pedersen SEH, Faber JH, Gulder T, Brun R, Christensen SB, Ponte-Sucre A, Moll H, Heubl G, Mudogo V: **Ancistrocladinium A and B, the First *N,C*-Coupled Naphthyldihydroisoquinoline Alkaloids, from a Congolese**

***Ancistrocladus* Species**. *Journal of Organic Chemistry* 2006, **71**:9348-9356.